NASA CR-14568

Development of Fire Test Methods for Airplane Interior Materials

Everett A. Tustin

1979

Prepared for
Johnson Space Center
under contract NAS9-15168

Boeing Commercial Airplane Company
Seattle, Washington

PREFACE

Laboratory tests to evaluate airplane interior materials for combustion properties may not rank them by their performance in large fires. The lab test results, alone, do not provide direction for selection of materials where a choice between burning characteristics exists. The major objectives for this program have been to:

- Provide information to correlate flammability, smoke, and gaseous product-of-combustion data obtained under laboratory test conditions to data obtained in large scale tests of materials under airplane cabin fire conditions.

- Provide a procedure to assess possible trade-offs in flammability, smoke production, and gas evolution for selection of materials with optimum overall combustion properties.

Fire tests were conducted in a 737 airplane fuselage at the National Aeronautics and Space Administration, L. B. Johnson Space Center, (NASA-JSC), to study possible airplane fire conditions. Results from the tests characterized jet fuel fires in open steel pans (simulating post-crash fire sources and a ruptured airplane fuselage) and characterized fires in some common combustibles (simulating in-flight fire sources). "Design" post-crash and in-flight fire source selections were based on these data. The program scope did not permit examination of all the many possible locations and positions of fire exposure for airplane interior materials. The vertical sidewall location was selected as a near-maximum thermal exposure position. Large panels of airplane interior materials were exposed to closely-controlled large scale heating simulations of the sidewall threat by the two design fire sources. These tests were conducted in a Boeing fire test facility using a surplused 707 fuselage section. Small samples of the same airplane materials were tested by several laboratory fire test methods. Test methods which are now relatively common in evaluating airplane materials and methods which appeared promising for data correlation to large scale fire results of the sidewall panels were employed.

Large scale and laboratory scale data were reduced to express specific material combustion properties in the same form wherever possible; then, the results were examined for correlative factors. Published data for dangerous hazard levels in a fire environment were used as the basis for developing a method to select the most desirable material where trade-offs in heat, smoke and gaseous toxicant evolution must be considered.

It was concluded that several individual laboratory test methods could rank interior materials by their heat and/or smoke release rates. It appears that a currently used test method could be revised to predict the magnitude of heat and smoke release by materials subjected to large scale airplane fires. The method for assessing gas release was found to give inconsistent results as compared to large scale test data. A relatively simple analytical tool may be developed to evaluate trade-off in combustion products, once the laboratory fire test methods have been refined, to more accurately predict large scale combustion products release.

It is recommended that further laboratory and large scale testing be conducted to refine the most promising laboratory test method for heat and smoke release assessment, and to extend data correlation to consideration of overhead horizontal material positions in aircraft. Further search is needed for a laboratory method to predict material gas release in a large scale fire.

CONTENTS

CONTENTS (CONCLUDED)

FIGURES

FIGURES (Continued)

FIGURES (Continued)

FIGURES (Concluded)

TABLES

SYMBOLS AND ABBREVIATIONS

ASTM	American Society for Testing of Materials
Btu	British thermal unit
°C	degrees Celcius
cm	centimeter(s)
CO	carbon monoxide
CO_2	carbon dioxide
D_s	specific optical density
E	theoretical escape index
E_D	escape index for design post-crash fire source
E_m	escape index for a specific material
ΔE	escape index decrement
ΔE_g	escape index decrement from gaseous toxicants
ΔE_h	escape index decrement from heat
ΔE_s	escape index decrement from smoke
°F	degrees Fahrenheit
$°F_{abs}$	degrees Fahrenheit absolute
F_s	flame spread factor
ft	foot, feet
fwd	forward
HCL	hydrogen chloride
HF	hydrogen fluoride
IRAD	Independent Research and Development
I_s	flame spread index
J	joules

K.	degrees Kelvin
kg	kilogram(s)
lb	pound(s)
LOI	limiting oxygen index
m	meter(s)
min	minute(s)
NASA-JSC	National Aeronautics and Space Administration Johnson Space Center
NBS Chamber	National Bureau of Standards smoke density chamber
NO_x	oxides of nitrogen
OSU apparatus	Ohio State University release rate apparatus
O_2	oxygen
Pa	Pascal(s)
psf	pounds per square foot
psi	pounds per square inch
ppm	parts per million by volume
Q	heat evolution factor
r	escape rate factor
sec	second(s)
SO_2	sulphur dioxide
$t_{(g)}$	time at which the predicted cabin gas concentration at head level exceeds the established incapacitation limit for that gas
$t_{(1\%)}$	time at which the predicted cabin smoke density reduces light transmission to 1% over a 0.92 m (3 ft) distance at head level
$t_{(204°C)}$	time at which the predicted cabin air temperature exceeds 204°C (400°F) at head level
W	watt(s)

INTRODUCTION

This program consisted of four study phases to develop fire test methods, ranking airplane interior materials by their probable performance during in-flight and post-crash fires. A fifth phase evaluated some experimental materials, using the laboratory and large scale fire test methods employed in the test methods study.

The first of the four development stages utilized large scale tests of possible fire sources in a fire-inert 737 airplane fuselage to define "design fire sources." Baseline (current) airplane materials were then tested in an airplane fuselage section, to simulations of the sidewall heating by the design fire sources. In the third stage, the same baseline materials were subjected to selected laboratory fire test methods. The final step analyzed the laboratory and large scale test results on the baseline materials for possible correlation. An examination of published fire hazard limits provided a possible procedure to be used with test results for material trade-offs in heat, smoke, and gas evolution.

ACKNOWLEDGEMENT

This report is based upon the data from literally hundreds of laboratory and large scale fire tests that have been directed, conducted, and analyzed by a large number of Boeing, NASA-JSC, and support personnel. The author also gratefully acknowledges the direct contributions of Susan P. Allen, Gailerd L. Korver and Steven R. Nemeth to the technical content of this report.

INTRODUCTION

This program consisted of four study phases to develop fire test methods, ranking airplane interior materials by their probable performance during in-flight and post-crash fires. A fifth phase evaluated some experimental materials, using the laboratory and large scale fire test methods employed in the test methods study.

The first of the four development stages utilized large scale tests of possible fire sources in a fire-inert 737 airplane fuselage to define "design fire sources." Baseline (current) airplane materials were then tested in an airplane fuselage section, to simulations of the sidewall heating by the design fire sources. In the third stage, the same baseline materials were subjected to selected laboratory fire test methods. The final step analyzed the laboratory and large scale test results on the baseline materials for possible correlation. An examination of published fire hazard limits provided a possible procedure to be used with test results for material trade-offs in heat, smoke, and gas evolution.

ACKNOWLEDGEMENT

This report is based upon the data from literally hundreds of laboratory and large scale fire tests that have been directed, conducted, and analyzed by a large number of Boeing, NASA-JSC, and support personnel. The author also gratefully acknowledges the direct contribution of Susan P. Allen, Galiera L. Korver and Steven R. Nemeth to the technical content of this report.

1.0 DESIGN FIRE SOURCE DEFINITION

Studies of past transport airplane accidents and fires have shown there is no typical airplane fire. Fires have varied in size from small cabin in-flight fires, readily controlled by hand-held extinguishers to extensive post-crash, fuel-fed fires which have reduced airplanes to ashes in a matter of minutes. It was the objective of this project to find laboratory test methods which would rank interior materials by their probable performance in airplane fires. Laboratory testing has shown that most materials behave differently when exposed to different heating rates and ignition sources. It was not feasible in this project to attempt correlation of the complete range of fire sources to laboratory results. Consequently, it was established that two "design" fire sources would be defined. The post-crash design fire source and the in-flight design fire source would be selected, using full-scale fire testing data and considering possible fire hazard limits and reasonable fire sizes.

1.1 NASA-JSC FIRE TEST FUSELAGE

Tests were conducted to characterize cabin fire sources in a salvaged 737 fuselage at the National Aeronautics and Space Administration, Johnson Space Center (NASA-JSC), Figure 1. Boeing designed the test configuration. NASA-JSC technical personnel directed the test facility build-up, conducted the tests, and reduced test data to a form compatible with Boeing computer-augmented analysis procedures. NASA also provided all operation and instrumentation personnel for the testing in the 737 fuselage. Boeing provided on-site technical support during test phases requiring coordinated decisions. The airplane fuselage was insulated, "fire-proofed", and instrumented to become a large calorimeter with heat transfer characteristics, ventilating capabilities, and an interior cross-section like those of current jet transports. Production airplane insulation was installed in the upper lobe for most of the fuselage length. The center 4.6 meters (15 feet) of the cabin was insulated with a heat resistant material and lined with stainless steel sheet. The rest was lined with aluminum sheet. The midpoint of the more fire-hardened section was established as the test fire location.

The cabin was instrumented with thermocouples to monitor cabin air temperatures, and with light transmission instrumentation for determining smoke obscuration. Provisions were made for automatically sampling the cabin atmosphere from two locations, at predetermined times during a test. Movable forward and aft bulkheads were installed such that the test section length could be varied from a maximum of 17.07 meters (56 feet) down to 6.10 meters (20 feet). The cabin cross-section area is approximately 6.5m^2 (70 ft^2); therefore, the limits of test section volume were 111 m^3 (3920 ft^3) and 39.7 m^3 (1400 ft^3). Figure 2 shows the interior of the test section. Smoke "meters" and exit signs for subjective evaluation of smoke obscuration are not shown in Figure 2. Figures 3 through 7 show complete cabin environment instrumentation for the 17.07 m (56 ft) and 6.10 m (20 ft) test configurations.

A forced air ventilation system was installed to simulate both post-crash natural convection and in-flight ventilation. A controlled air flow of 17.0 kg/min (37.5 lb/min) entering at the forward bulkhead was established for all post-crash testing. Exhaust was in the aft bulkhead. Ventilating air for simulated in-flight fire tests entered from a continuous, perforated inlet

down the longitudinal cabin ceiling centerline. Air was exhausted into the lower lobe at the junctions of the cabin sidewalls and the floor. Simulated in-flight air flow was adjusted to be typical for the length of the test section, at approximately 3.0 kg/min-meter (2.0 lb/min-ft).

Test fires were conducted adjacent to an extensively instrumented panel, installed in the airplane sidewall position (Figure 8). An array of eight calorimeters, one radiometer, and eleven thermocouples are exposed on the inboard surface of the panel. Six thermocouples were attached to the outboard face of the panel to monitor panel temperatures for an indication of total heat absorption of the panel. Figure 9 locates the panel's thermal instrumentation. This calibration panel was used to characterize the direct threat to a sidewall panel from adjacent fires.

Auxiliary instrumentation was installed for some or all of the tests to measure ventilating air temperature, exhaust temperature and flow, cabin air wet bulb temperature, ceiling heat flux, and radiant heating at a specified distance from test fires. These data were not used directly in test analysis to meet the program objectives, but were taken to confirm calculated parameters and to use in possible future studies of fire properties.

1.2 POST-CRASH FIRE SOURCE SELECTION

Shallow open steel pans containing burning Jet A fuel and resting on the cabin floor were used in tests to simulate post-crash fuel-fed flames entering a ruptured fuselage, adjacent to the sidewall thermal calibration panel. To promote rapid ignition and consistent burning, the fuel was preheated to 32°C (90°F), then floated on water heated to approximately 49°C (120°F) and poured to a depth of about 2.5 cm (1 in.) in the pans. Test fire size and duration were varied by changes in pan size (burning surface area) and fuel volume, respectively.

The post-crash design fire source was selected to represent a realistically high thermal exposure from a post-crash fuel-fed fire, but was limited in size such that the fire source, alone, would not produce a lethal environment in an airplane fuselage in an unacceptably short escape time. Obviously, such constraints would produce different sizes of "design" fire sources for different sizes of airplane cabins. The "design" fuselage size was established as the 17.07 m (56 ft) long 737 test section at NASA-JSC, because it permitted a great amount of testing with an existing facility without the scaling of results. Also because the smaller cabin environment (as compared to longer standard body airplanes or wide-body cabins) should suffer the most rapid degradation for any given fire size. Interior material contribution to the hazard level could be more significant in the smaller jet transports.

The incapacitation levels for expected hazards at head level at airplane centerline were established as:

- 204°C (400°F) air temperature
- 8000 ppm carbon monoxide
- 100 ppm hydrogen cyanide

If concentrations of above 50,000 ppm carbon dioxide or 30 ppm sulfur dioxide were encountered, some consideration of the effect on escape would be given. Also, oxygen levels below 17% would be considered to affect toxicant intake. The air temperature limit was based on Reference 1, and the toxicant limits on Reference 2.

Fire tests were run with Jet A fuel in four sizes of steel pans:

- 30.5 x 30.5 cm (12 x 12 in.)
- 45.7 x 45.7 cm (18 x 18 in.)
- 61.0 x 61.0 cm (24 x 24 in.)
- 76.2 x 76.2 cm (30 x 30 in.)

For calibration, the fuel fires had to burn near their maximum heating rate for at least five minutes or until 204°C (400°F) was exceeded at head level down the cabin centerline. Preliminary tests were run in each pan until the required fuel quantity was determined.

Tests run with full thermal instrumentation showed that with the 61 x 61 cm (24 x 24 in.) pan with 4.5 liters (4.76 qt), the average centerline head level temperature (average of thermocouples 3, 7, 11, 15, 19, 23 and 27) approached the limit at four minutes, but did not exceed it during the five minute test (Figure 10). Gas samples taken during tests with the 61 x 61 cm (24 x 24 in.) pan showed that none of the toxic gas limits were approached. Carbon monoxide was the only toxicant found in a significant quantity (Figure 11). Carbon dioxide and oxygen measurements did not show levels which (theoretically) should significantly affect respiration (Figure 12). Methods for gas sampling and analysis were described in Appendix A.

The 61.0 x 61.0 cm (24 x 24 in.) fuel pan with 4.5 liters (4.76 qt) of Jet A fuel was established as the design post-crash fire source.

The cabin temperature curve for the design post-crash fire flattens at approximately four minutes. This is partly due to the approaching of a steady state air temperature, but occurs primarily because the heat release rate has started to decrease. This decrease may be explained by the early burning of the more volatile fuel fractions and the less easily-ignited, lower vapor pressure portions later. Experimentation with different fuel pan sizes and fuel quantities may have produced a fuel pan fire, meeting the desired temperature criterion more exactly. However, the tests were not run at any standard conditions of ambient temperature or pressure, but were conducted under the prevailing conditions. A change in the test conditions can significantly change the resulting cabin temperatures. Furthermore, the limiting temperature of 204°C (400°F) is by no means exact, nor can a definite time of exposure for incapacitation be established. The purpose of the tests was to establish a design point (condition), approximating an incapacitating environment in about five minutes. The selected fire source was deemed acceptable for that purpose.

The 61 x 61 cm (24 x 24 in.) fuel pan fire, representing the design post-crash fire source, was tested in two other fuselage section lengths [9.73 meter (32 foot) and 6.10 meter (20 foot)]. The cabin's average centerline temperature and gas data at head level are shown in Figures 13 through 16. The average light transmission data over a 0.92 meter (3 ft) light path at head level are shown in Figure 17. The prevailing test conditions are listed in Figure 13.

1.3 INFLIGHT FIRE SOURCE SELECTION

Six different fuels were tested as possible interior fire sources. They were considered to be near the maximum size sources likely to be found in an airplane cabin, excluding materials used for an arson attempt. The sources tested were:

- 2.27 kg (5.0 lb) shredded newspaper (Figure 18)
- 2.27 kg (5.0 lb) cabin and lavatory trash (Figure 19)
- 1.135 kg (2.5 lb) polyster/acrylic cloth
- 2.27 kg (5.0 lb) polyvinylchloride, polycarbonate, and acetone-soaked paper (simulated under-seat baggage) (Figure 20)
- 0.91 kg (2.0 lb) polyester filled airline pillows (4) (Figure 21)
- 0.76 kg (1.67 lb) wool/acrylic airline blankets (2)

The polyester/acrylic cloth and the wool/acrylic blankets were hung over a metal frame adjacent to the calibration panel for testing, to simulate draping over a seat.

The centerline thermocouple and the calibration panel data showed the trash bag fire was probably the greatest threat of the sources tested. It was selected as the design in-flight fire source.

The other candidate sources produced appreciably lower centerline temperatures, as shown in Figure 22. The concentrations of fixed gases for the design in-flight fire source are shown in Figures 23 and 24. The simulated under-seat baggage produced the only significant measured acid gas concentration, with a maximum of 300 ppm of hydrogen chloride.

As tested, the design in-flight fire source consisted of two polyethylene bags filled with a total of 2.27 kg (5.0 lb) of trash made up as follows:

1.81 kg (4 lb) paper towels
0.136 kg (0.3 lb) paper cups
0.316 kg (0.7 lb) polystyrene glasses

Ignition was made near the bottom of one bag, adjacent to the calibration panel. The wire cage prevented the contents spilling away from the sidewall during the tests.

The design in-flight fire source was tested in two smaller fuselage sections. Results of the cabin environment data are shown in Figures 25 through 29.

1.4 CHARACTERISTICS OF THE DESIGN FIRE SOURCES

Two major characteristics were defined in order to adequately describe the design fire sources for the remainder of the program:

- Products-of-combustion release rates
- Thermal threat to the sidewall

The first characteristic is not complete without an assessment of the probable effects on cabin environment under selected standard conditions. Such an evaluation is included in the following text.

1.4.1 PRODUCTS-OF-COMBUSTION RELEASE RATES

Most laboratory and large scale fire tests use instrumentation to measure physical properties of the air around, or passing by, the burning material. If all fires are conducted in the same chamber and under the same conditions, these measurements may be sufficient to rank the fires by the release of products-of-combustion. If comparing data collected from different test apparatus at different conditions is required, some method must be used to "normalize" the data or reduce the environment data to product-of-combustion release rates. Such data reduction is desirable to develop a correlation between laboratory and large scale material tests and to judge the relative contribution of the material and its fire source to the hazard levels produced in a real fire situation.

Equations to reduce large scale fire test data to heat, smoke, and gas release rates have been developed by Boeing during an IRAD project, concurrent with this effort. Although relatively simple and based on rather wide assumptions, use has shown them to be valuable analytical tools. Appendix B describes the equations and summarizes the method for their use. Reversal of the equations permits the prediction of temperature, light transmission, and gas concentrations under ventilation and volume conditions other than those for which the release rates were obtained. Care must be taken to make sure the conditions do not differ to the extent that disparities in oxygen availability and temperature could significantly change the burning of the fire studied. Details of the development of the equations may be found in Reference 3.

The apparent (calculated) release rates for the design post-crash and in-flight fire sources are graphed in Figures 30 and 31, respectively. The rates are calculated as constant over finite time periods. Because the initial data were taken at specific instrumentation points in the fuselage, a negative value (or one much lower than the preceding value) probably indicates a settling or dispersal of the combustion product after an active period of production. Figures 32 and 33 show the predicted 17.07 meter (56 ft) fuselage section hazard levels at head level for the design fire sources under "standardized" conditions. For all environment predictions in the 17.07 meter (56 ft) fuselage section, the standardized conditions are:

- ambient air and ventilating air temperature – 294 K ($530°F_{abs}$)

- ambient air and cabin air pressure -- 1.013 x 10^5 Pa (2110.29 psf)
- ventilating air flow in (post-crash) -- 17.04 kg/min (37.5 lb/min)
- ventilating air flow in (in-flight) -- 50.82 kg/min (112 lb/min)

1.4.2 THERMAL THREAT TO THE SIDEWALL

The sidewall calibration panel data provides a history of the incident heat flux and adjacent air temperatures during exposure to the design fire sources. Figures 34 and 35 characterize the design post-crash fire source heat threat to the sidewall, while Figures 36 and 37 provide the same data for the design in-flight fire source.

2.0 BASELINE MATERIAL TESTS WITH SIMULATED DESIGN FIRE SOURCES

Ideally, large samples of the baseline materials could be tested against the actual design fire sources and the total hazardous products release rates calculated. Then the differences between these rates and those of the design fire sources, alone, could be taken as the material contribution. This method is impractical because the burning of the design fire sources is difficult to reproduce within an acceptable tolerance. The fire sources produce such large amounts of heat and smoke that the combustion products produced by the same materials, even in large samples, may be hidden by variations in the fire source from test to test. For these reasons, large samples of the baseline materials were tested against controlled simulations of the sidewall thermal threat from design fire sources defined in the tests conducted in the NASA-JSC fire test fuselage.

2.1 BOEING 707 FIRE TEST SECTION

The Boeing 707 cabin section, (Figure 38), modified for large scale fire testing, has the same cabin cross-section as the NASA-JSC 737 fuselage. The interior lines of both test vehicles are representative of the new interior lines in the Boeing standard body airplanes. The 707 section has been insulated with production airplane insulation and lined with stainless sheeting, the full 6.10 meter (20 foot) test length (Figure 39).

The cabin environment instrumentation was located the same as in the NASA-JSC 737 fuselage in the 6.10 meter (20 ft) long test mode (Figures 3, 5, 6, and 7), except the exit signs which were oriented for viewing from the aft end of the test section, rather than from the forward end. The sidewall thermal calibration panels in both facilities were designed and fabricated at Boeing for conformity. Quartz lamps were selected to provide the major portion of the energy to simulate the sidewall exposure to the design fire sources (Figure 40). A propane burner may be adjusted to produce the desired flame and impinging air temperatures.

2.2 BASELINE MATERIALS

It was specified for this program that two baseline (current) interior materials would be tested in large scale and laboratory test to collect data for correlation efforts. These data are supplemented with results of tests on other baseline materials from a parallel Boeing IRAD project. Table 1 – Baseline Materials lists materials by sample number, descriptive-title, and type of material. The materials are fully described in Appendix C. Two numbers are assigned to each material because specimens for laboratory and large scale tests may differ in thickness, in order to be accommodated in the laboratory text fixture. Differences are described in Appendix C. With this numbering system, displayed results can be readily identified as based upon laboratory or large scale data.

Table 1.—Baseline Materials

Material number*	Description	Use or type
N00/N01	Polyurethane foam	Seat cushion
N02/N03	Fabric-backed vinyl	Covering material
402/403	Polyvinylfluoride/ Epoxy-fiberglass/ Polyamide-phenolic Honeycomb sandwich	Sidewall panel
412/413	Polycarbonate	Thermoplastic
416/417	Polyvinylfluoride/ Polyvinylchloride/ Aluminum laminate	Sidewall panel

*Large scale sample/laboratory sample

2.3 DESIGN POST-CRASH FIRE SOURCE TESTS

2.3.1 SIMULATION DEVELOPMENT

Figures 34 and 35 display the calorimeter readings from the sidewall calibration panel for the design post-crash fire source. A very accurate simulation of the thermal exposure would require simulation of each trace for the five minute test period. Such an exact simulation was not considered justifiable because of the variance in the original test data from test to test. Instead, the graphs of data from the calorimeters measuring the higher heat fluxes (calorimeters 1, 3 and 6) were examined for the period of maximum heat release. This period occurred between test time 30 seconds and 210 seconds. It was decided that for each calorimeter on the panel, the average heat flux during this period would be established as the design post-crash fire source flux. Since the intensity of the fuel pan fire subsided during later portions of the test, the simulated design fire heat flux would be removed from the material specimens when the total heat applied corresponded to the area under the design fire heat flux calorimeter curves. This time of exposure is approximately 4.5 minutes for a 5 minute test. Heat exposure is terminated by removing the panel from its position in front of the fire simulation. Figures 41 and 42 graphically show the described analysis for calorimeter 1. Figure 43 is a sketch of the calibration panel, showing the approximate lines of constant heat flux calculated for the design post-crash fire by the method just discussed. For simulation, the corresponding lateral calorimeter readings were averaged to produce the symmetrical thermal map of Figure 44. Experimentation with the fire simulation equipment showed that with a simple propane burner, it was not possible to approximate the distribution of the post-crash design fire source air temperatures along the calibration panel. Therefore, in the simulation the flame was made approximately the same as the height of the fuel pan fire as observed during testing and a 600°C (1112°F) flame temperature maintained near the bottom-center of the test panels to assure adequate ignition temperature. The average temperatures experienced during the design post-crash fire source are shown in Figure 45, while the simulation temperatures are plotted in Figure 46. To confirm the adequacy of simulation, four materials were tested in the 6.10 meter (20 ft) 707 test section fire simulation and then tested against the 61.0 x 61.0 cm (24 x 24 in.) fuel pan in the 17.07 meter (56 ft) 737 test section. It was not expected that differences between materials would be evident in the light transmission or temperature data in the fuel pan fire tests. However, it was thought that the material weight loss and acid gas release could be compared for the simulated fire source test and the fuel pan fire tests on the same material. The comparison is shown in Figure 47. Two of the materials, N00 and N02, were almost totally consumed by both fire conditions. The other two materials were more fire resistant and there was a discrepancy in the resulting damage. There were major differences in the total toxicant release, as calculated for the tests using the data reduction equations of Appendix B.

The simulation test procedures and gas analysis methods were examined for possible explanations for the discrepancies with the fuel pan fire test data. The simulation was established and the steady state environment achieved. The calibration panel was removed from the heat exposure and allowed to cool. Then the calibration panel was replaced in the material testing position. It was found that the incident heat on the calibration panel increased rapidly to approximately 83% of the stabilization value, then climbed slowly to the full value over the next 5 minutes (Figure 48). This climb is apparently caused by increased heating of the panel and heating equipment by mutual re-radiation. This does not occur

when a test material is placed in front of the heat source. Consequently, the test procedure was changed to elevate the heating by the simulation equipment until the desired heating rate was measured during the first minute of calibration panel exposure. Furthermore, during the early part of one of the fuel pan fire tests of the design fire source, significantly higher fluxes were experienced at calorimeters 1 and 3. These higher fluxes occurred during test time 30 seconds to 90 seconds. The average flux was 8.86 W/cm^2 (7.81 Btu/ft^2-sec) and 7.37 W/cm^2 (6.49 Btu/ft^2-sec) at calorimeters 1 and 3, respectively. To assure maximum thermal exposure to the material test panels, the heat flux was raised at these two calorimeters to the higher values for the first minute of test, then returned to the lower level established by the averaging of 30 seconds to 210 second data. Figure 49 shows the modified heating schedule for calorimeter 1. The total exposure time for the panel was shortened slightly, to maintain the same area (total heat) under the curve. All four materials were retested to the modified heating schedule. Results are summarized in Figure 50 and compared to the fuel pan fire tests and original simulated test data. The weight loss now compared more favorably. The second testing of the N02 material showed a measurable quantity of hydrogen cyanide, which by interference causes incorrect determination of hydrogen chloride by the analysis method used. A change in procedure was made (see Appendix A) to alleviate this interference, resulting in the lower value of hydrogen chloride shown.

On the basis of the post-test appearance of the 402 and 416 panels (Figures 51 through 54) and the weight loss data, the NASA and Boeing technical personnel concluded that the simulated testing should continue, using the described modifications.

Tests with calibrated toxicant concentrations, run in both test facilities, showed that the sampling systems and analysis methods gave accurate, repeatable and comparable data. The discrepancies between the test data have not been explained; however, it appears that for fire safety evaluations, the simulated fire tests gave conservative results (higher toxicant release) except in the case of hydrogen chloride (HCL).

2.3.2 BASELINE MATERIAL TESTS

Each of the five baseline materials (Table 1) were tested with the simulated post-crash fire source. Materials 402, 412, 416, and N02 were tested in a steel frame backed by an 0.030 cm (0.012 in.) thick stainless steel sheet. The total exposed surface area was 2.08 m^2 (22.3 ft^2), 122 x 170 cm (48 x 67 in.). The N00 foam sample was arranged in a recessed 61 x 61 cm (24 x 24 in.) by 5.08 cm (2 in.) dish in a stainless steel panel with the bottom edge 30.5 cm (12 in.) from the floor (Figure 55). Thermoplastic material 412 was partly supported by screen and metal strips to prevent post-test interference with test equipment (Figure 56). Tests were repeated when obvious anomalies occurred. The initial data was reduced to the form in Figure 57. The material did not contribute to the data collected until the fire simulation had operated sufficiently for cabin environment stabilization. After the 40 minute stabilization period, the material sample replaced the calibration panel in front of the simulated fire and the five minute test period began. As explained in the previous discussion, the specimen was removed from the exposure position (but was left in the cabin) at approximately 270 seconds, when the desired total heat exposure had been accumulated.

Data from the tests were reduced by computer, using the equations of Appendix B to develop heat, smoke and gas release rates. The results are in Appendix C.

2.4 DESIGN IN-FLIGHT FIRE SOURCE TESTS

2.4.1 SIMULATION DEVELOPMENT

The simulation of the sidewall fire threat from the design in-flight fire source was developed with the same methods and rationale used in development of the simulated post-crash fire source. However, the heat flux varied so much from the first of the test to the last that a single flux distribution would not accurately simulate the sidewall threat. Figure 58 shows the design fire heat flux at calorimeter 1 (the most intensely heated instrumentation point). The other calorimeters recorded similar trends at lower heating levels. The simulated test was established for a total of fifteen minutes. The average heat flux was found for each of the stages shown for each calorimeter. Stage II and Stage III were established as shown for 150 seconds and 300 seconds, respectively. Stage I was established at 116 seconds to provide the same total heat (area under the curve) shown from 0 to 150 seconds on Figure 58. The simulation heat flux for calorimeter 1 is then the "stepped" heating schedule shown in Figure 59. The lines of constant flux on the calibration panel for the simulated fire are shown in Figures 60, 61 and 62 for Stages I, II, and III, respectively. The required heating rates for Stage IV are so low that at 566 seconds the heating equipment is turned off and the panel exposed to only the residual heat in the fixture.

The average flame (air) temperatures on the calibration panel for the design fire during Stage I (Figure 63) were lower than could be simulated while maintaining the desired heating rate. Therefore, as with the simulated post-crash condition, the simulated in-flight fire source approximated the actual flame height and provided an igniting flame temperature 538°C (1000°F) at the base of the panel during Stage I (Figure 64). The calibration panel air temperatures for the other stages fell as the heating rate was reduced. This was similar to the design in-flight fire source tests with the trash bags.

No confirmation fire tests with material samples and the trash bags were run in the NASA 737 fuselage because the thermal exposure by the source was found to be unrepeatable. However, the simulated in-flight fire source was calibrated during the first minute of calibration panel exposure as found desirable for the simulated post-crash condition.

2.4.2 BASELINE MATERIAL TESTS

The baseline materials were tested using the same specimen fixtures as described for the simulated design post-crash fire source testing. Data acquisition and reduction were also the same and the results are contained in Appendix C.

3.0 LABORATORY FIRE TESTS ON BASELINE MATERIALS

3.1 LABORATORY TEST METHODS

Existing laboratory test methods were selected to obtain the combustion properties of the baseline materials for comparison to the properties as measured in large scale testing. Figure 65 shows the five test apparatus selected in approximately increasing order of complexity along with the properties evaluated by each during this program. A more complete description of each method is contained in Appendix D.

3.2 BASELINE MATERIAL TESTS

Each of the five baseline materials were tested by each of the five laboratory test methods. The data are included in Appendix C and evaluated in the following report discussion, "Laboratory and Large Scale Fire Test Data Correlation."

4.0 LABORATORY AND LARGE SCALE FIRE TEST DATA CORRELATION

The correlation of large scale fire test data and laboratory data was conducted in two phases:

- The results were compared directly to observe the consistency of ranking order, and
- A simple means of approximating large scale test results from laboratory test data was studied.

In the attempt to obtain correlation, two basic assumptions were made:

- The primary combustion properties of the materials are heat release, smoke release and gas release because they can be related to the selected cabin fire scenarios, and
- The release rates (and total released products) calculated from the large scale tests are the correct and desired result of the laboratory test data analysis.

The above imply that the release rates are all functions of flame spread, decomposition temperatures, decomposition rates, etc., and act as the integrating characteristics for all these individual material properties. This analysis also assumes that the large scale test specimens are extensive enough that the fire would not have progressed further laterally if the samples had been larger. Test results showed that this was true of most samples tested. The seat foam (N00) test was an obvious exception; however, the specimen was sized to approximate a foam item expected to be exposed upon the initiation of a post-crash or in-flight fire source. Material N00 data will not be discussed for correlation purposes because of the disparity in thicknesses between the large scale sample and the laboratory sample. All data are included in Appendix C.

4.1 DIRECT COMPARISON

4.1.1 POST-CRASH FIRE SOURCE

Examination of the predicted cabin environment at standardized conditions for the design post-crash fire source (Figure 32) provides an estimate of time period for which the release of the products of combustion are most critical. The predicted cabin temperature does not exceed our established limit of 204°C (400°F) until 300 seconds. However, during the last 85 seconds, the temperature hovered above 193°C (390°F) without exceeding the limit. This plateau was described during the examination of data for the design fire selection as due to test setup constraints rather than actual fire characteristics. Since the temperature limit cannot be considered exact, it was decided arbitrarily to extend the slope of the initial temperature curve to the point at which it would cross the limit. This time was found to be approximately 215 seconds. Figure 121, shows graphically the definition of the 215 second limit. The definition of the design fire required the temperature to limit escape at 300 seconds. Based on the predicted temperatures and this discussion, the limit now becomes 85 seconds (300-215 seconds) at an air temperature above 204°C (400°F). Therefore, heat release by the material is critical in the first 215 seconds in the post-crash design fire condition.

The matching of observed visual loss of the production exit signs (apparent total obscuration of light) with the measured light transmission showed that the observers reported sign obscuration at approximately 1% light transmission. Escape is seriously hampered when smoke obscuration occurs. Figure 32 shows that light transmission over 0.92 meter (3 ft) nears 1% at 90 seconds. Extrapolation shows that light transmission drops below 1% for distances greater than 1.52 meters (5 ft) in less than 60 seconds. Based on these observations, the critical time period for smoke production was established as the first 90 seconds. With passengers seated as much as 6.10 meters (20 feet) from exit signs, it probably is not warranted to consider material smoke production beyond the 90 seconds in the design post-crash fire condition.

The only toxicant measured during the design post-crash fire source tests relevant to material properties was carbon monoxide. The level of carbon monoxide found was far below an incapacitation level; therefore, material toxicant production must be considered for the full five minute evaluation period.

Heat release was the first property examined. Several of the laboratory tests give values which cannot be directly related to time. Figure 66 and 67 compare the indices from these tests with the heat release from the baseline materials in the large scale tests for the first 215 seconds. The tabular form of Figure 66 presents the data but the specific relationship of the values cannot be easily visualized. Figure 67 compares the data with the bar of the material having the greatest heat release or flammability value given a rating of 100. Other materials are given ratings proportional to the values obtained from the tests. Ideally, the lab tests would produce bars corresponding to those of the large scale heat results. The Ohio State University (OSU) release rate apparatus produces time based data. Figures 68 and 69 compare OSU heat release for 215 seconds obtained at different heating levels to the large scale data at the same time.

Smoke release data are obtained from the National Bureau of Standards (NBS) smoke chamber and the OSU apparatus. Both give time-based values which are compared for the first 90 seconds with that of the large scale tests in Figures 70 through 73. The NBS chamber as modified at Boeing, provides gas release data which is compared to the full scale results in Figures 74 through 77. There is no apparent relationship between the values found for hydrogen cyanide in the large scale tests and in the NBS chambers, so no bar chart was made.

4.1.2 IN-FLIGHT FIRE SOURCE

The same data comparison procedure was used for the in-flight condition. However, the release rates are important for the whole test because the design in-flight fire source does not produce theoretically limiting levels of combustion products. Most materials have completed burning by 300 seconds in the large scale testing. Three-hundred seconds was selected as the time to compare large scale and laboratory scale release data for the in-flight condition. Figures 78 and 79 compare OSU heat release data to the large scale results. Figure 80 compares the large scale test heat release to laboratory tests which give only indices. The large scale values of Figure 78 and the laboratory data from Figure 66 are not repeated in a separate figure. Figures 81 through 87 compare smoke and toxicant release data for large scale and laboratory tests.

4.1.3 RESULTS OF DIRECT DATA COMPARISON

The post-crash condition will be considered first. Based on the limited data base (four materials) the following is concluded:

- The ASTM E-162 heat evolution factor (Q) and the OSU apparatus heat release obtained at 2.5 W/cm^2 (2.20 Btu/ft^2-sec) (flaming mode, bottom-center ignition) placed the materials in correct order of heat release. None of laboratory test data correctly ranked the materials in proportion to heat release in the large scale tests. Bunsen burner "length-burned" did not relate well to the heat contribution by the materials.

- The NBS chamber (flaming mode) and the OSU apparatus (flaming mode, bottom-center ignition) at 2.5 W/cm^2 (2.20 Btu/ft^2-sec) correctly ranked the materials in order of smoke release in large scale testing. Neither test showed the materials producing smoke in the same relative proportions as shown in the large scale tests.

- The NBS chamber testing showed good relative, proportionate ranking of the two materials producing hydrogen fluoride at both 2.5 W/cm^2 (2.20 Btu/ft^2-sec) and 5.0 W/cm^2 (4.41 Btu/ft^2-sec) heating rates. No relationship between NBS chamber data and large scale test results could be found for hydrogen cynaide, hydrogen chloride or carbon monoxide production.

The in-flight condition showed different tests more applicable:

- None of the laboratory methods correctly ranked all four materials for large scale heat release. If the thermoplastic (412/413) were excluded, the ASTM E-162 heat evolution factor (Q) correctly ranked the remaining three materials in good proportion to their large scale test heat release. The OSU heat release data from 1.5 W/cm^2 (1.32 Btu/ft^2-sec) tests correctly ranked the same three materials but not in the same proportion of heat release as the large scale tests. The Bunsen burner test (burn length) showed poor correlation to the large scale results.

- Again, no method properly ranked the materials for smoke production if thermoplastic (412/413) were considered. The OSU data 2.5 W/cm^2 (2.20 Btu/ft^2-sec) and the NBS data at both 2.5 W/cm^2 (2.20 Btu/ft^2-sec) and 5.0 W/cm^2 (4.41 Btu/ft^2-sec) correctly ranked the other three materials. The NBS data at 5.0 W/cm^2 provided the best proportionate correlation.

- NBS chamber data at both 2.5 W/cm^2 (2.20 Btu/ft^2-sec) and 5.0 W/cm^2 (4.41 Btu/ft^2-sec) correctly ranked the three non-thermoplastic materials for hydrogen chloride production; although, the proportions produced were not predictable from the data. No relation to large scale results was evident for hydrogen fluoride, hydrogen cyanide, and carbon monoxide production.

Based on this direct comparison of data for the small sample studied, only limited knowledge of the material contribution to cabin fire hazards may be gained from the direct laboratory data on the relatively fire-retardant airplane interior materials. If screening tests are needed for order ranking of heat and smoke production of thermosetting organic materials under both post-crash and in-flight fire conditions, the ASTM E-162 heat evolution factor (Q), OSU

apparatus heat and smoke release data taken at 2.5 W/cm^2 (2.20 Btu/ft^2-sec), and NBS chamber smoke data at 2.5 W/cm^2 (2.20 Btu/ft^2-sec) show the greatest reliability for single tests. Thermoplastic materials can be evaluated by the same tests for the post-crash environment for heat production at 215 seconds and smoke production at 90 seconds. However, the one sample tested could not be ranked for in-flight fire performance by these methods. The large sample always softened and ran before sustained ignition was achieved in the large scale in-flight fire source test and, consequently, produced less heat and smoke than predicted by testing better retained samples in laboratory apparatus. The material was burned more predictably by the higher heating rates in the simulated post-crash testing.

Only one laboratory method of assessing toxicant production was studied. Results generally were not related to the large scale data and, therefore the NBS chamber as used, cannot be considered an acceptable method of determining toxicant production.

4.2 CORRELATION DEVELOPMENT

A complete evaluation of materials for fire hazard contribution requires not only that the release rates be established proportionately in proper ranking order but also that the magnitude of the large scale test results be predicted with reasonable accuracy by the laboratory test methodology. Only this information can help determine if differences in the material properties are truly significant in the real fire condition. The OSU release rate apparatus was the most versatile test equipment utilized in this program, since ventilation rate and heating rate could be readily adjusted (only heating rate was varied in this project). Therefore, an effort was made to obtain large scale quantitative correlation of smoke and heat release with OSU data.

4.2.1 POST-CRASH FIRE SOURCE

The heat flux map of Figure 44 was examined to define areas of heating which might be exposed to approximately the four fluxes tested in the OSU apparatus. The result was Figure 88. Next, the same total area was apportioned to only two levels of heating, 2.5 W/cm^2 (2.20 Btu/ft^2-sec) and 5.0 W/cm^2 (4.41 Btu/ft^2-sec), as in Figure 89. Using the equations shown on these two figures, total heat and smoke were calculated for the 300 second test period and plotted (Figures 91, 92, 95 and 96) for comparison to those results calculated from large scale test data in Figures 90 and 94. Study showed that use of only the two heating rates produced nearly as good correlation to the large scale data as the more complex calculation with the four heating rates. Further refinement using the two heating rates was attempted by using materials 402/403 and 416/417 as a base and multiplying all calculated data from OSU results by the average ratio of large scale release to the laboratory test-based release for those two materials. The results are shown in Figures 93 and 97 for heat and smoke respectively. Correlation with the large scale results is not good but the methodology does show some promise.

4.2.2 IN-FLIGHT FIRE SOURCE

The same analysis steps were taken with the first 300 seconds of the simulated in-flight fire source test data. Figures 98 through 101 reflect the assumed areas of large scale heating rates for Stages I and II of the testing. Figures 102 and 106 show heat and smoke release, respectively, from large scale test data. Figures 103 through 105 and Figures 107 through 109

show successive attempts at laboratory test data refinement for heat and smoke release, respectively. Again, the methodology shows promise, except for the previously discussed (direct comparison results) poor correlation of the thermoplastic (material 412/413).

4.2.3 RESULTS OF CORRELATION DEVELOPMENT

It appears possible to develop a reasonably good prediction of the large scale test results from the OSU apparatus data if the reason(s) for the disproportionate release rates for some materials can be found and corrected. Two possible sources for these apparent errors may already have been discovered and are under study. The first is the selection of the calibration "dummy" used in the specimen holder for the pretest. As shown in Figure 110, the pretest is run with the dummy in place to determine the effect of specimen and holder heat absorption upon the stack air temperature. In our tests, the pretest dummy was a 1.27 cm (0.5 in.) thick cement-asbestos board while the specimen backup panel during the actual test was a 0.64 cm (0.250 in.) panel of the same material. Preliminary analysis indicates that changing of both panels to a thinner material with less heat capacity and greater thermal conductivity could improve the heat release correlation because of the method of calculation as shown in Figure 110. Such a change of the backup panel will also affect the burning (and thus the smoke release) of the thinner materials. This change would make a mounting more representative of most airplane material installations.

The apparent heat release from the OSU apparatus is affected also by the "thermal lag" inherent in burning such a small sample in close proximity to the relatively large heat sink of the apparatus and specimen holder. This phenomena is described by Figure 111. Methods of correction have been studied by Boeing and other investigators.

In the previous discussion, an attempt was made to obtain closer correlation to large scale test results with a "correction factor." This may be possible with materials of similar density, thermal conductivity, and specific heat. However, dissimilar materials would require different "correction" factors. This can be seen by comparing the values for material N02/N03 in Figures 90 and 93. Since the proportional correction factor was based on materials 402/403 and 416/417, its use does not bring close correlation for material N02/N03. Therefore, an improvement in correlation between the laboratory and large scale fire test results will require an understanding and elimination of the factors contributing to the disparities rather than development of an empirical correction factor.

4.3 EVALUATION OF NEW MATERIALS

NASA-JSC has actively promoted the development of airplane materials with improved fire properties for more than a decade. NASA-JSC participation with suppliers and manufacturers has included evaluation of the fire properties of proposed and experimental materials. In this role, NASA-JSC submitted eleven new materials for evaluation by large scale and laboratory fire tests. Table 2 – NEW MATERIALS – is a summary list of the materials submitted. All of these materials are in some stage of development; they were not submitted as ready for airplane use. Many of them have structural limitations which make them unacceptable; others are impracticable for other reasons. Some show promising characteristics and their continued development is being promoted by NASA-JSC. To evaluate the combustion characteristics of the possible new materials, all were tested regardless of feasibility of use. The detailed material descriptions along with laboratory and large scale fire test data are in Appendix E.

Table 2.—New Materials

Material number*	Description	Proposed use or type
N04/N05	Polyimide foam	Seat foam
N06/N07	Phenolic-fiberglass/polymide foam sandwich panel	Floor or structural partition
N08/N09	Polyvinylidene fluoride film/phenolic-fiberglass/polyimide foam sandwich panel	Sidewall panel
N10/N11	Polyimide-coated fiberglass	Covering material
N12/N13	Polyimide moldable material	Thermoplastic replacement
N14/N15	Phenolic-fiberglass/polyimide foam sandwich panel	Floor panel
N16/N17	Polyvinylidene fluoride film/phenolic-fiberglass laminate	Ceiling panel
N18/N19	FX resin/fiberglass laminate	Air ducting
N20/N21	Flexible polyimide foam	Thermal/acoustical insulation
N22/N23	Monsanto E200-3Z	Thermoplastic
N24/N25	Inorganic resin system—fiberglass panel	Thermoplastic replacement

*Large scale sample/laboratory sample

Experience has shown the post-crash condition to be the most severe. Therefore, the heat and smoke release of the new materials will be compared to the baseline materials heat and smoke release at test times 215 seconds and 90 seconds, respectively. In general, the gas emission of the new materials was very low. Because of the poor correlation of gas results demonstrated in the analysis of the baseline materials data, no comparison of the toxicant release was made. Gas analysis data are included in Appendix E.

The new materials were divided into four categories for comparison: panels, covering material and laminates, foams, and thermoplastics (and proposed thermoplastic replacements). Figures 112 through 119 compare the materials by apparent heat and smoke release from the simulated design post-crash fire source tests and by laboratory data found most valid during the fire test methods study. The five baseline materials are included in appropriate categories for comparison.

5.0 LABORATORY FIRE TEST METHODS FOR MATERIAL EVALUATION

Based upon the data collected from large scale fire tests of materials in a vertical position (sidewall orientation), certain laboratory test methods can determine some of the burning properties of airplane interior materials. Only four currently used and eleven experimental materials were studied. The design post-crash fire source subjected the materials to the greatest thermal threat. Therefore, the results of testing materials to this thermal exposure were taken as the base for developing laboratory test correlation.

5.1 METHODS SELECTED

Current materials used in similar construction (i.e., laminates, sandwich panels or foams) may be ranked in order of critical heat release under post-crash conditions by the ASTM E-162 heat evolution factor, Q, and by the heat release from the OSU release rate apparatus at 215 seconds from testing at 2.5 W/cm^2 (2.20 Btu/ft^2-sec) with bottom-center ignition. Correct magnitude of heat released (particularly with more fire resistant materials) cannot be compared without testing in the OSU at 5.0 W/cm^2 (4.41 Btu/ft^2-sec) as well. If testing is conducted by the method described in Appendix C, using 1.27 cm (0.5 in.) thick and 0.64 cm (0.250 in.) thick asbestos/cement board for the dummy and the backup plate respectively, it appears the total heat release in a large scale sidewall test by current sidewall panels may be crudely approximated by:

$$\text{release at 215 seconds in joules} =$$

$$0.38 \left[8289 \text{ cm}^2 \, (\text{OSU}_{2.5 \text{ W/cm}^2}) + \right.$$

$$\left. 5587 \text{ cm}^2 \, (\text{OSU}_{5.0 \text{ W/cm}^2}) \right] \qquad (\text{---})$$

where OSU is heat release in joules/cm^2 at 215 seconds.

If customary units are desired, the areas above, respectively, are 8.92 ft^2 and 6.01 ft^2, while the heat release in Btu/ft^2 would be found for 2.20 Btu/ft^2-sec and 4.41 Btu/ft^2-sec conditions.

Smoke release ranking may be made for post-crash exposure using 90 second data from the NBS chamber or the OSU apparatus at 2.5 W/cm^2 (2.20 Btu/ft^2-sec). Correct magnitude of release for current sidewall panel constructions can be approximated for many materials using a combination of the OSU data at 2.5 W/cm^2 (2.20 Btu/ft^2-sec) and 5.0 W/cm^2 (4.41 Btu/ft^2-sec) data as with heat release, except the correction factor is 0.97 instead of 0.38. The correction factors cannot be assumed applicable for panel constructions varying greatly from those tested.

Only one method of obtaining gaseous toxicant release by laboratory testing was investigated. No correlation to large scale data could be determined. It is concluded at this time that sampling of gases released in the NBS chamber testing can only indicate the type of gases which might be expected from the burning of a material.

5.2 LIMITATIONS

Primarily, panel and laminated materials were tested in this program; however, a thermoplastic and a foam were among the baseline materials. The foam laboratory data was not correlative directly to the large scale results because the thickness of the laboratory sample was much less than the large sample to meet fixture constraints. The thermoplastic material behavior was predictable for the post-crash condition. It contributed much less in the simulated in-flight test than expected from laboratory testing because at the lower heating rate it melted and pulled away from the igniting flame before a burning front could be established.

Correlation of OSU data to large scale results can probably be enhanced by some procedure and analysis changes discussed in the data correlation development. Ideally, the need for a "correction factor" would be removed completely.

6.0 POSSIBLE TRADE-OFFS AMONG PRODUCTS-OF-COMBUSTION

Selection of a material for "best" fire properties from several choices may require a decision as to whether a relatively high smoke production, high heat generation or high toxicant evolution is preferable if all cannot be avoided. A sound judgement would require that three more pieces of information be available:

- The release of the products-of-combustion under large scale conditions,
- The effect of each product-of-combustion on passenger escape or survivability, and
- Any synergistic or antagonistic effects of two or more products-of-combustion.

An attempt was made to define a procedure which might be used with some success to provide the first two data. An understanding of the third item was beyond the scope of this project. First, from the previous discussion on data correlation, it appears possible that refinements in the OSU release rate apparatus and procedures may produce relatively good approximations of heat and smoke release from a sidewall panel exposed to simulated design fire sources. At this time, a method for the estimate of gaseous toxicant production cannot be established.

The trade-off of combustion products study was based upon the simulated design post-crash condition as being the most severe. As with the correlation effort, the 17.07 meter (56 ft) standard body fuselage section was selected as the design condition. The heat production prior to 215 seconds was established as the evaluation factor. At this time, the average head level predicted air temperature in the aisle approaches 204°C (400°F) with the design post-crash fire source alone. This limit was based upon Reference 1. As in the earlier correlation discussion, it was arbitrarily set that 85 seconds at temperatures above 204°C (400°F) would be incapacitating. Therefore, from heat alone, theoretical escape would be limited to 5 minutes.

In the correlation development, smoke release prior to 90 seconds was set as the criteria. At that time, it is predicted that visibility of exit signs, etc., at distances of 0.92 meter (3 ft) would be obscured by the smoke from the design post-crash fire source.

The limits for individual toxicants could be established in the same fashion as for temperature. That is, when a certain predicted concentration was reached before 300 seconds, it is assumed incapacitation would result. Reference 2 was used to define the limits for some toxicants for design post-crash fire source selection and it could be used for other toxicants. This project was not able to develop a laboratory method for prediction of large scale test toxicant release rates, but the study considered trade-offs for gas evolution.

First, to develop a trade-off method, several concepts must be defined. If it is assumed that escape from a post-crash environment is unimpeded for 300 seconds by the products of combustion within the cabin, the escape index E, may be considered as unity. This escape index can be thought of as the product of a constant escape rate factor r, and time, t.

$$E = rt,$$

If it is desired to protect an evacuation time of 300 seconds, $r = \frac{E}{t} = \frac{1}{300}$ sec^{-1}.

With only heat considered and with a usable evacuation time of 300 seconds, the design post-crash fire source escape index would still be unity since, by definition, the heat limit of the design fire is not reached until 300 seconds.

A reduction in the escape index must be developed for the effect of smoke. Reference 4 describes airplane evacuation tests conducted under various lighting conditions. Examination of the data shows that under dark cabin and very low outside illumination conditions, the evacuation rate was approximately one-fourth of that found under emergency lighting conditions. Arbitrarily assuming one-third of the loss in rate due to the darkened outside conditions, it was estimated that the rate for evacuation from a smoke-filled cabin might be one-half that with no smoke. Therefore, the design fire source escape index (E_D) considering both heat and smoke can be calculated:

$$E_D = r\ 90\ (\text{seconds}) + \frac{r}{2}\ (300\text{–}90)\ (\text{seconds})$$

or $$E_D = \frac{90}{300} + \frac{210}{600} = 0.65$$

Another concept, ΔE, or escape index decrement was developed. If the heat release rate for a material exposed to the design post-crash fire source as a function of time is known, it may be added to that of the design fire source as shown in Figure 120, using material 416 exposed in the sidewall position as an example. Using the cabin temperature prediction equation of Appendix B, the temperature for the combined heat release is predicted (Figure 121). Now a heat escape decrement, ΔE_h, can be calculated.

$$\Delta E_h = \frac{215 - t_{(204°C)}}{600}$$

Where $t_{(204°C)}$ is the time at which the predicted cabin temperature exceeds 204°C (400°F). If $t_{(204°C)} > 215$ seconds, it is assumed to be 215, i.e., $\Delta E_h = 0$. Toxicant escape decrements could also be established for individual gases when release rates can be successfully measured and design fire test concentrations predicted. A gas escape decrement ΔE_g, can be calculated as:

$$\Delta E_g = \frac{300 - t_{(g)}}{600}$$

Where $t_{(g)}$ is the time in seconds at which the predicted gaseous toxicant concentration exceeds the incapacitation limit for that gas (time must be less than 300 seconds or $\Delta E_g = 0$).

The smoke escape decrement, ΔE_S, would be calculated as:

$$\Delta E_S = \frac{90 - t_{(1\%)}}{600}$$

Where $t_{(1\%)}$ is the time when the predicted 0.92 meter (3 ft) light transmission for the design post-crash fire source plus material exposed drops below 1%. For our example material, Figure 122 shows the predicted transmission and the resulting $t_{(1\%)}$.

From this discussion, a material can be said to have an escape index, E_M, calculated as:

$$E_M = E_D - \Delta E_S - (\text{either } \Delta E_h \text{ or } \Delta E_g)$$

The either/or term is necessary since both temperature and gas decrements operate from an assumed 300 second limit and are not considered additive. The larger of the gas or heat decrements is used. For our example material, gas was not considered because the accuracy of any gas concentration prediction is in question. The escape index is:

$$\begin{aligned} E_{416} &= E_D - \Delta E_S - \Delta E_h \\ &= .65 - \left[\frac{90 - t_{(1\%)}}{600}\right] - \left[\frac{215 - t_{(204°C}}{600}\right] \\ &= .65 - \left[\frac{90 - 58}{600}\right] - \left[\frac{215 - 204}{600}\right] \\ &= .578 \end{aligned}$$

The escape index may be calculated for several materials in this manner (if temperature and light transmission predictions in the "standard" fuselage section for design post-crash conditions can be made) and the higher index would indicate the better material. Thus trade-offs in combustion products can be considered.

One obvious over-simplification is the assumption that escape rate is not degraded until the 1% level at 0.92 meter (3 ft) is reached and then suddenly is reduced by 50%. A gradual reduction formula would provide better rating of smoke effect, but would require further research to develop.

7.0 NEW TECHNOLOGY

No inventions or new technologies were developed during this program.

8.0 CONCLUSIONS

Five current and eleven experimental materials were tested by simulated large scale fire exposure and by selected laboratory tests. Laboratory tests were found which apparently can rank, in order, materials in a sidewall position for heat and smoke production in two defined "design" fires. The laboratory method investigated for measuring toxicant production did not consistently produce results which could be related to large scale fire test data. Therefore, no laboratory method for assessing toxicant release was defined.

Direct correlation of laboratory results to the magnitude of the large scale test heat and smoke data was sought. Data from the Ohio State University release rate apparatus holds promise for being adopted to this purpose, but changes in the test method and analysis procedures will be required.

A method for trade-off of combustion products for material selection was developed using an analytical method to predict temperature, light transmission and gas concentrations in a "standard" airplane cabin based on the heat, smoke and gas release rates for the materials under consideration. For effective utilization, the method requires that a satisfactory gas release test be developed and that the Ohio State University apparatus be further evaluated to refine the prediction of heat and smoke release in large scale fires.

9.0 RECOMMENDATIONS

It is recommended that further large scale and laboratory testing of materials be accomplished to:

- Extend laboratory and large scale fire test data correlation to foams and to materials burned in an overhead, horizontal position.
- Refine the direct correlation of Ohio State University (OSU) apparatus heat and smoke release to the large scale test release of the same combustion products.
- Develop a laboratory test method capable of predicting the magnitude of the gaseous combustion products released in a large scale fire (a modified OSU apparatus should receive consideration).

APPENDIX A
GAS SAMPLING AND ANALYSIS PROCEDURES

DESIGN FIRE SOURCE TESTS IN NASA-JSC 737 FUSELAGE

The exposure of aircraft cabin interior materials to a fire results in the production of a variety of gaseous combustion products. It is mandatory that these gases be collected quantitatively and measured accurately. The hydrolyzable, acid gases, such as hydrogen cyanide (HCN), hydrogen fluoride (HF), and hydrogen chloride (HCL) are collected and analyzed differently from the non-hydrolyzable gases, such as oxygen (O_2), carbon monoxide (CO), and carbon dioxide (CO_2). In the former case the gases are collected in 0.1 Molar NaOH by "bubbler" systems (microimpingers) and analyzed via specific ion electrode techniques. In the latter case, the gases are collected in stainless steel bottles and analyzed via gas chromatographic techniques.

Gases are removed from the 737 fuselage at two different locations. One collection site is 8 feet forward of the ignition source and the second is 5 feet aft of the ignition source. Heated Teflon lines [66° ± 14°C (150° ± 25°F)], are used to transport the hydrolyzable, acid gases to glass microimpinger bubblers which contain the 0.1 Molar NaOH. Stainless steel lines connected to evacuated 32-liter stainless steel bottles collect the nonhydrolyzable gases.

The bubbler systems consist of 4 racks of 11 bubblers, each bubbler filled with 10 ml of 0.1 Molar NaOH. Systems A and B comprise 2 racks of 11 bubblers each which collect gas samples 8 feet forward of the ignition source. Systems C and D comprise 2 racks of 11 bubblers each which collect gas samples 5 feet aft of the ignition source. Each rack of 11 bubblers has 5 sets of 2 bubblers (types "a" and "b") for 5 time intervals during the fire, plus a background bubbler.

The 32-liter stainless steel bottle systems consist of 12 evacuated bottles for the collection of nonhydrolyzable gases. System E consists of 6 bottles which remove gases 8 feet forward of the ignition source and System F performs the same function 5 feet aft of the ignition source. This permits the collection of gases at the same frequency as for the bubbler systems. The bottles are pumped down to 5 torr just prior to the test.

The 0.1 Molar NaOH is prepared fresh every week. The solution is prepared by dissolving 16.4 grams of reagent grade NaOH in 4 liters of deionized water. This solution is stored in a gallon plastic bottle.

Prior to an actual test, verify that the heated Teflon lines are 66 ± 14°C (150°F ± 25°F). In addition, the bubblers are filled with 10 ml of 0.1 Molar NaOH and installed in the appropriate rack positions.

Background samples for all 6 systems (4 bubblers and 2 stainless steel bottles) are taken just before fire source ignition. During the background sequence, verify that the flow meter needle values are providing flow rates of 400 ml/min through all 4 bubbler systems. Continue to maintain the proper flow throughout the remainder of the test.

The 5 bubbler pairs in each of the 4 bubbler systems are activated consecutively (1 minute each for a 5 minute burn). The 32-liter bottles are each activated 30 seconds in the middle of each bubbler interval.

After the test, disconnect the bubblers from the sampling lines. With the aid of a clean pipette bulb, carefully draw the 0.1 Molar NaOH solution up into the bubbler inlet tube 2-3 times. Shake and tilt each bubbler so as to wet all internal surfaces and then transfer the contents of each to appropriately labeled 50 ml beakers. Cover the beakers until the solutions can be analyzed.

The meter used in the analysis of the bubbler solutions is the Orion Model 801 digital pH/millivolt meter. The electrodes used are Orion solid state cyanide, fluoride, and chloride specific ion electrodes. The Orion Model 605 electrode switch is also recommended, as it saves a significant amount of time in analyzing the bubbler solutions. The common reference jack on the back of the Model 605 permits the insertion and use of 3 electrodes (the reference, the specific ion, and the pH electrode) all at the same time.

Since electrode response is sensitive to temperature and stirring rate of the solutions, the following recommendations are made. Place a piece of insulating material between the 50 ml beaker and the magnetic stirrer to prevent heating of the solution by the stirrer motor. Both standard and test solutions are to be stirred at the same speed and with the same type of stirring motion. A fairly high speed just below the creation of a visible vortex is recommended. Also, a small diameter, .32 cm (1/8 in.) or less, magnetic Teflon-coated stirring bar is recommended.

The cyanide, fluoride, and chloride standard solutions are prepared in the following manner and at the suggested frequency. The 10^{-2}M cyanide stock solution is prepared fresh every 2 weeks by placing 0.500 gram of reagent grade sodium cyanide (NaCN) in a 1 liter plastic volumetric flask and filling with 0.1M NaOH. The 10^{-3}, 10^{-4} and 10^{-5}M standards are prepared by serial dilution of the stock solution with 0.1M NaOH in 100 ml plastic volumetric flasks. The 10^{-3} and 10^{-4}M solutions should be prepared fresh every 2 days and the 10^{-5}M solution daily.

The 10^{-2}M fluoride stock solution is prepared every 2 months by placing 0.420 gram of reagent grade sodium fluoride (NaF) in a 1 liter plastic volumetric flask and filling with 0.1M NaOH solution. The 10^{-3}, 10^{-4} and 10^{-5}M standards are prepared by serial dilution of the stock solution with 0.1M NaOH in 100 ml plastic volumetric flasks. The 10^{-3} and 10^{-4}M solutions should be prepared monthly and the 10^{-5}M solution weekly.

The 10^{-1}M chloride stock solution is prepared every 2 months by placing 5.844 grams of reagent grade sodium chloride (NaCL) in a 1 liter plastic volumetric flask and filling with 0.1M NaOH solution. The 10^{-2}, 10^{-3}, 10^{-4} and 2×10^{-5}M standards are prepared by serial dilution of the stock solution with 0.1M NaOH solution in 100 ml plastic volumetric flasks. The 10^{-2}, 10^{-3} and 10^{-4}M standards are prepared monthly and the 2×10^{-5}M standard weekly. The reason for using 2×10^{-5}M instead of 10^{-5}M as the minimum chloride standard is that the chloride electrode "bottoms out" at concentrations less than 10^{-5} Molar. There are very few millivolts of potential difference between 10^{-5}M chloride and pure water.

The order of specific ion electrode analysis is cyanide, followed by fluoride, and lastly, chloride. Prior to starting the analysis it is recommended that a preliminary calibration be made to verify that the 3 electrodes respond similarly as for the previous calibration. Only the 10^{-5} and 10^{-4} molar standards are needed for the preliminary calibration. Use 10 ml of each standard and add 80 microliters of reagent grade glacial acetic acid to the fluoride and chloride standards to lower the pH between 5.0 and 5.5. The cyanide standards are run as is (pH 12-13). After making these adjustments, insert the Orion double junction reference, pH, and applicable specific ion electrodes into the stirred standards and record the millivolt (MV) reading, after it has stabilized to less than 0.5MV change/minute. Verify that the response of each electrode is as expected.

In analyzing the test solutions it is important to check for the 3 ions even if none is expected. Spot check the bubblers which would be expected to give maximum concentrations if acid gases were produced in the combustion process. If an ion is found at a level much greater than 10^{-5} Molar, then analyze all test solutions for that ion. When checking for cyanide, be certain that the pH of the solution is in the 12-13 range. If the pH is less than 12, add sufficient 6M NaOH to bring the pH into the required range.

If the b-type bubblers were used, spot check at least 3 "b" bubblers expected to contain maximum concentrations of cyanide after completing analysis of the a-type bublers. If the "b" bubbler solutions contain less than 10% of the cyanide concentration in the "a" bubbler solutions, then it is not necessary to analyze any additional "b" bubblers. If they contain greater than 10% of the "a" bubbler concentration, then analyze the remaining "b" bubblers.

Fluoride analysis is performed after completing the analysis for cyanide. Before beginning the analysis, bring the pH of the solutions down to the 5.0 to 5.5 range with 80 microliters of glacial acetic acid.

If cyanide was detected at greater than an estimated trace concentration of 10^{-6} Molar, then it is necessary to lower the pH of the test solutions to minimize interference of cyanide when analyzing for chloride. This is accomplished by lowering the pH to the 1.0-1.5 range with concentrated nitric acid (HNO_3) (usually 8-10 drops). This addition must be performed before inserting the chloride electrode into the solutions. If the electrode is inserted prematurely, its response will be extremely sluggish and it will not give a stable reading. If this should happen, the chloride electrode must be polished with Orion 94-82-01 or equivalent polishing paper.

The data for the calibration curves for each ion are obtained immediately after analyzing the test solutions for that ion. Calibrate only with the standard solution needed to cover the range of the test sample concentrations. Start with the 10^{-5}M standard and continue in order of increasing concentration. Since cyanide ions will gradually dissolve the membrane of the cyanide electrode, avoid using a cyanide standard greater than 10^{-3} Molar. However, if it becomes necessary, do not leave the cyanide electrode exposed to greater than 10^{-3} Molar cyanide for more than 1 or 2 minutes. If HNO_3 acid was added to the chloride test solutions, then the chloride calibration data must also be obtained at 1.0-1.5 pH. The calibration curves are produced by plotting millivolt readings vs molar concentration on semi-log graph paper (concentration on logarithmic scale).

To calculate the concentrations of each ion in the bubbler solutions, convert the millivolt readings to molar concentrations from the calibration curves for each ion. Convert the molar concentrations to parts per million (ppm) as shown:

$$ppm = \frac{C_m \times V_a \times V_m \times 10^6}{V_s}$$

where
- C_m = concentration in moles/liter
- V_a = volume of bubbler solution = 0.01 liter
- V_m = molar gas volume, approximately 24 liters/mole at sea level and 25°C
- V_s = volume sampled = F x T where F is the flow rate (0.4 liter/min) and T is the sampling time

For a 1 minute sampling time, this equation becomes

$$ppm = C_m \times 6 \times 10^5$$

If the type-b bubblers have more than 10% of the amounts found in the type-a bubblers, then these amounts are added to give a total concentration.

For each sampling period, duplicate determinations are available. The results obtained for rack A and rack B bubblers are averaged and reported as the concentrations measured for each time interval at a point 8 feet forward of the fire. The results obtained for rack C and rack D bubblers are averaged and reported as the concentrations measured for each time interval at a point 5 feet aft of the fire.

Concentrations of the 3 nonhydrolyzable gases (oxygen, carbon dioxide, and carbon monoxide) are determined by gas chromatographic analysis of the contents of the 32-liter stainless steel bottles. A dual column, dual detector (thermal conductivity and flame ionization) gas chromatograph is used for the analysis. Test gas samples are injected into the chromatograph at a known pressure. The sample is split (approximately 50/50) in such a manner that one portion flows through a molecular sieve (13X) column and the other through a porapak P column. Oxygen and carbon dioxide are detected with the thermal conductivity detector while carbon monoxide is converted to methane in a nickel catalyst bed and subsequently detected by the flame ionization detector.

A standard gas blend containing the 3 gases is used to obtain peak height data for known concentrations. Peak heights for oxygen, carbon dioxide, and carbon monoxide are computed for both the test samples and calibration standards by multiplying the recorded peak height by the amplifier attenuation. The individual gas concentration is calculated using the following equation:

$$C = \frac{C_{std} \times H}{H_{std}}$$

where C = concentration of sample gas component (ppm)

C_{std} = concentration of standard gas component (ppm)

H = peak height of sample gas component

H_{std} = peak height of standard gas component

The values determined for System E are reported as the concentration of gas measured for each time interval at a point 8 feet forward of the fire. The values determined for System F are reported as the concentration of gas measured for each time interval at a point 5 feet aft of the fire.

MATERIAL TESTS WITH SIMULATED DESIGN FIRE SOURCES IN BOEING 707 FUSELAGE SECTION

The procedures used for the collection and measurement of hydrolyzable acid gases produced via a simulated design fire source combustion of interior materials in a 707 fuselage section are essentially identical to those used in the design fire source tests. However, for the case of the nonhydrolyzable gases (oxygen, carbon monoxide, and carbon dioxide), different procedures are followed.

In the former case, the procedural changes are minor, while in the latter case a totally different approach is taken. The modifications in the specific ion electrode techniques involve use of pH paper instead of a pH electrode and the preparation of fluoride and chloride standards in 0.1M NaOAc instead of 0.1M sodium hydroxide (NaOH). Since an Orion Model 605 electrode switch was not available the decision was made to use pH paper to measure pH of the test solutions. The paper used is pHydrion (0-9 range and 9-13 range) produced by Micro Essential Laboratory, Brooklyn, New York.

The other change involves the preparation of chloride and fluoride standards in 0.1M NaOAc instead of 0.1M NaOH. Thus, the 10^{-1} stock solutions are prepared by placing 0.5844g NaCL or 0.42g NaF in 100 ml volumetric flasks and filling with 0.1M NaOAc. The 10^{-2}, 10^{-3}, 10^{-4}, and 10^{-5} standards are prepared by serial dilution of the stock solutions with 0.1M NaOAc. Because of this change in procedure, the fluoride and chloride standards require only 25 microliters of glacial acetic acid to lower their pH to 5.0-5.5 rather than 80 microliters when they are prepared in 0.1M NaOH.

Continuous gas analyzers are used to measure the concentrations of oxygen, carbon monoxide, and carbon dioxide. A Beckman Process Oxygen (O_2) monitor, Model 751, is used to continuously measure the concentration of oxygen during combustion of aircraft interior materials with simulated design fire sources. An Infrared Industries Model IR702 Gas Analyzer is used to monitor the concentrations of carbon monoxide and carbon dioxide. A stainless steel tube is used to transport the gases from a point 8 feet forward of the fire to each analyzer.

MATERIAL TESTS IN NBS SMOKE CHAMBER

A National Bureau of Standards smoke density chamber is utilized in laboratory testing of aircraft cabin interior materials to monitor gaseous combustion products. The smoke chamber is modified to allow for removal of combustion products for subsequent measurement of concentrations. As in the case of large scale testing, the hydrolyzable acid gases are collected with microimpingers (bubblers) located in the geometric center of the chamber. Since 1 liter of air is passed through the bubbler (400 ml/min for 2.5 minutes) the equation for calculating the concentration of acid gas becomes the following:

$$ppm = C_M \times 2.5 \times 10^5$$

Draeger specific gas analysis tubes are used to determine the concentrations of sulfur dioxide and nitrogen dioxide. They are also used as backup methods for the acid gases. An NDIR analyzer is utilized to continuously measure the concentration of carbon monoxide.

Concentrations of oxygen and carbon dioxide are not recorded. Oxygen concentrations are not measured because there is no significant depletion of the chamber oxygen. Carbon dioxide is not monitored because the lethal gas concentration (120,000 ppm) is so high compared to the lethal levels of the other combustion products.

APPENDIX B
FIRE TEST DATA ANALYSIS EQUATIONS

Fire tests of furnishing materials conducted in large scale fixtures generally are compared directly by enclosure temperature, smoke density (light transmission), toxicant concentrations, and fixed gas levels. This method is acceptable if all ambient conditions (temperature, ventilating flow, pressure, lighting level, etc., are carefully reproduced for each test and if the large chamber can be used indefinitely for material evaluations. If these two conditions cannot be met, then methods must be developed to reduce large scale data to some "standardized" conditions and to obtain data which might be correlated to small scale laboratory testing of the materials. Several laboratory test methods, including the National Bureau of Standards (NBS) smoke chamber and the Ohio State University (OSU) release rate apparatus, reduce data to forms defining total release and/or release rates of combustion products. The Boeing 707 fire test section may be considered a large scale moderately insulated release rate apparatus. Therefore, the development of applicable release rate equations appeared to be a feasible step in analysis of the large scale test results.

The thermodynamic, heat transfer, smoke accumulation, and gas generation principles operating in the fire test section were defined as much as possible. Equations were written to calculate the apparent release rates (heat, smoke, toxicants) from a material burning in the test section. The section was defined as shown in Figure B-1. All symbols are defined in Table B-1 at the end of this appendix.

Analysis produced the equations shown in Figure B-2 using the general assumptions listed. Solving the equations for temperature, light transmission and gas concentrations provided the equations in Figure B-3 and permits a prediction of cabin environment if the release rates are assumed or known. The temperature prediction must be made first to obtain the data by which M_X is calculated:

$$M_X = M_i + \frac{P_c V_c C_p}{R\Delta t} \left(\frac{T_c - T_{co}}{T_c \; T_{co}} \right)$$

The development of these equations is detailed in Boeing Document D6-46952, "Airplane Interior Materials Fire Test Methodology", Allen, Nemeth, Peterson and Tustin, 1978. Experience has shown them sufficiently accurate for comparisons of materials which are relatively fire retardant (such as airplane interior materials) such that very early flashover, extremely rapid flame spread, etc., need not be considered a factor.

Table B-1.—Nomenclature

C_g	–	Gas concentration at end of time interval
C_{go}	–	Gas concentration at start of time interval
C_p	–	Specific heat of air for standard atmospheric pressure, 1.0045 J/gm – K, (0.24 Btu/lb_m –$^{\circ}F_{abs}$)
e	–	Base (2.718) of natural system of logarithms
L	–	Length of light path for transmission measurement, meter (feet)
m_i	–	Mass of forced airflow into cabin (test section), kg/sec (lb_m/sec)
m_x	–	Mass of airflow from cabin (test section), kg/sec (lb_m/sec)
P_c	–	Air pressure in cabin (test section), Pa (lb/ft^2)
R	–	Gas constant for air, 267.89 J/kg – K (53.34 ft-lb_f/lb_m – $^{\circ}F_{abs}$)
$\overline{R}_g$	–	Apparent gas release rate, kg/sec (lb_m/sec)
$\overline{R}_h$	–	Apparent heat release rate, J/sec (Btu/sec)
$\overline{R}_s$	–	Apparent smoke release rate, kg/sec (lb_m/sec)
t	–	Time interval, seconds
T_c	–	Cabin (test section) air temperature at end of time interval, K ($^{\circ}F_{abs}$)
T_{co}	–	Cabin (test section) air temperature at start of time interval, K ($^{\circ}F_{abs}$)
T_i	–	Temperature of entering air flow, K ($^{\circ}F_{abs}$)
%T	–	Light transmission over length, L, at end of time interval
$\%T_o$	–	Light transmission over length, L, at start of time interval
V_c	–	Volume of cabin (test section), cubic meters (cubic feet)
α	–	Factor to convert optical density of smoke to mass of smoke per unit volume when the length of view, L, is known, 2.05×10^{-4} m^2/kg (3905.94 ft^2/lb_m)
γ_g	–	Specific volume of gas at the air temperature of the cabin, m^3/kg (ft^3/lb_m)
ρ	–	Air density at the cabin air temperature kg/m^3 (lb_m/ft^3)

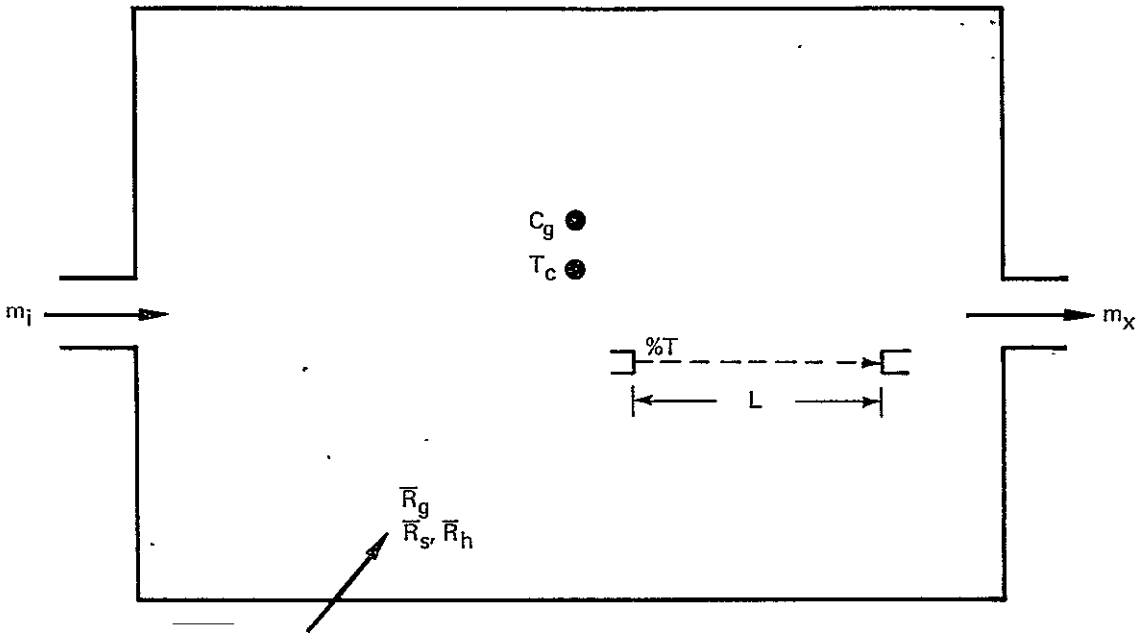

Figure B1.—Simplified Schematic of Boeing 707 Fire Test Section

Heat Release Rate

$$\bar{R}_h = \frac{P_c V_c C_P}{R\Delta t}\left(1n\frac{T_c}{T_{co}}\right) + C_P\left[m_i + \frac{P_c V_c}{R\Delta t}\left(\frac{T_c - T_{co}}{T_c T_{co}}\right)\right]\left[\frac{T_c + T_{co}}{2} - T_i\right]$$

Smoke Release Rate

$$\bar{R}_s = \frac{m_x}{\rho}\frac{1}{\alpha L}\left\{\log\frac{100}{\%T} \cdot \left[e^{\left(m_x \Delta t/\rho V_c\right)}\right] - \log\frac{100}{\%T_o}\right\} \div \left\{e^{\left(m_x \Delta t/\rho V_c\right)} - 1\right\}$$

Gas Release Rate

$$\bar{R}_g = \frac{m_x}{\rho}\frac{1}{\gamma_g}\left\{C_g\left[e^{\left(m_x \Delta t/\rho V_c\right)}\right] - C_{go}\right\} \div \left\{e^{\left(m_x \Delta t/\rho V_c\right)} - 1\right\}$$

Equations based on:

- Instantaneous distributions; instrumentation at avg points
- Perfect gas laws; basic thermodynamic and heat transfer theory
- Past studies on smoke particles affecting transmission by other individuals and organizations

Figure B-2.—Data Analysis Equations

Temperature

$$\bar{R}_h - \frac{P_c V_c C_p}{R\Delta t}\left(1n\frac{T_c}{T_{co}}\right) = C_P\left[m_i + \frac{P_c V_c}{R\Delta t}\left(\frac{T_c - T_{co}}{T_c T_{co}}\right)\right]\left[\frac{T_c + T_{co}}{2} - T_i\right]$$

Substitute values of T_c and solve by trial and error solution

Transmission

$$\%T = 10^{2 + \left[e^{\left(-\Delta t m_x/\rho V_c\right)}\left(\alpha L \rho R_s/m_x - \log 100/\%T_o\right) - \left(\alpha L \rho \bar{R}_s/m_x\right)\right]}$$

Gas Concentration

$$C_g = \left[C_{go} - \frac{\rho \bar{R}_g \gamma_g}{m_x}\right]\left[e^{\left(-\Delta t m_x/\rho V_c\right)}\right] + \frac{\rho \bar{R}_g \gamma_g}{m_x}$$

Equations based on:

- Instantaneous distributions; instrumentation at avg points
- Perfect gas laws; basic thermodynamic and heat transfer theory
- Past studies on smoke particles affecting transmission by other individuals and organizations

Figure B-3.—Equations for Prediction and Correlation

APPENDIX C
BASELINE MATERIALS DESCRIPTIONS, LABORATORY TEST DATA, AND LARGE SCALE TEST RESULTS

This appendix defines the baseline materials specimens and summarizes the results from the large scale and laboratory fire tests conducted on these materials. Laboratory data is displayed in the following order:

Table C-1	Materials Descriptions, Mettler Thermogravimetric Analysis Data, and the Limiting Oxygen Index
Table C-2	Federal Aviation Regulations (FAR) 25.853 Bunsen Burner Test Data
Table C-3	Radiant Panel Test ASTM E162-67 Data
Table C-4	NBS Chamber Toxicant Concentrations
Figures C-1—C-5	Heat Release in the OSU Apparatus in the Vertical Bottom-Center Ignition Mode
Figures C-6—C-10	Smoke Release in the OSU Apparatus in the Vertical Bottom-Center Ignition Mode
Figures C-11—C-15	Smoke Release in the NBS Chamber in the Flaming Mode

The large scale fire test results are related for both post-crash and in-flight simulated design fire source conditions:

Figures C-16—C-21	Apparent Heat, Smoke, and Toxicant Release from Simulated Design Post-Crash Fire Source Tests—Baseline Materials
Figures C-22—C-27	Apparent Heat, Smoke, and Toxicant Release from Simulated Design In-flight Fire Source Tests—Baseline Materials

Table C-1.—Materials Descriptions and Data From Mettler Thermal Balance and Limiting Oxygen Index (LOI)

402/403 — Sidewall panel — Area density = 0.1507 g/cm^2 (0.0021 lb/in.^{2})

0.0114 cm (0.0045 in.) 2 plies, type 120 fiberglass epoxy prepreg BMS*8-151

Polyamide honeycomb core 0.3175 cm (1/8 in.) cell, 0.6350 cm (1/4 in.) thick, 48.06 kg/m^3 (3 lb/ft^3) BMS 8-124

0.0114 cm (0.0045 in.) Type 120 fiberglass epoxy prepreg BMS 8-151

0.0203 cm (0.008 in.) Type 181 fiberglass prepreg BMS 8-143**

0.0051 cm (0.002 in.) White polyvinylfluoride film

Ink overprint

0.0025 cm (0.001 in.) Clear polyvinylfluoride film

1. Mettler — BMS 8-151, type 120, sample wt - 37.43 mg; wt loss started - 280°C

W_1	W_2	W_3
18.3% (485°C)	78.1% (860°C)	3.6% residue

LOI = 35.22

2. Mettler — BMS 8-124, sample wt - 37.87 mg; wt loss started - 330°C

W_1	W_2	W_3
20.3% (495°C)	79.3% (895°C)	0.4% residue

LOI = 30.76

3. Mettler — BMS 8-151, type 120, sample wt - 37.43 mg; wt loss started - 280°C

W_1	W_2	W_3
18.3% (485°C)	78.1% (860°C)	3.6% residue

LOI = 35.22

4. Mettler — BMS 8-143 , sample wt - 6.68 mg; wt loss started - 315°C

W_1	W_2	W_3
22.3% (440°C)	16.9% (695°C)	60.8% residue

LOI = 37.23

5. Mettler — White polyvinylfluoride film, sample wt - 35.42 mg, wt loss started - 275°C

W_1	W_2	W_2	W_4	W_5
27.6% (300°C)	1.4% (340°C)	21.3% (520°C)	21.6% (720°C)	28.1% residue

LOI = 30.01

Table C-1.—(Continued)

6. Mettler — Ink overprint - acrylic, sample wt - 45.83 mg, wt loss started - 80°C

W_1	W_2	W_3
15.9% (315°C)	24.7% (670°C)	54.4% residue

LOI = 21.62

7. Mettler — Clear polyvinylfluoride film, sample wt - 11.49 mg, wt loss started - 310°C

W_1	W_2	W_3	W_4	W_5
50.4% (435°C)	10.4% (465°C)	8.7% (520°C)	27.9% (660°C)	2.6% residue

LOI = 46.70

412/413 — Thermoplastic - area density = 0.2695 g/cm^2 (0.0038 lb/in.^{2})

———— Sheet polycarbonate 0.2286 cm (0.090 in.) thick

1. Mettler — Sheet polycarbonate, sample wt - 25.94 mg; wt loss started - 410°C

W_1	W_2	W_3	W_4
15.2% (455°C)	51.7% (545°C)	30.3% (685°C)	2.8% residue

LOI = 28.25

416/417 — Sidewall panel — area density = 0.2411 g/cm^2 (0.0034 lb/in.^{2})

———— 0.0813 cm (0.032 in.) aluminum
———— 0.0178 cm (0.007 in.) polyvinylchloride
— — — — Polyvinylchloride ink
———— 0.0025 cm (0.001 in.) clear polyvinylfluoride film

1. Mettler — Aluminum, sample wt - (not tested)

2. Mettler — Polyvinylchloride, sample wt - 23.32 mg; wt loss started - 245°C

W_1	W_2	W_3	W_4
44.3% (360°C)	12.0% (510°C)	14.4% (650°C)	29.3% residue

1 -2 LOI = 60.20

3. Mettler — Polyvinylchloride ink, sample wt - 53.54 mg; wt loss started - 85°C

W_1	W_2	W_3	W_4
32.2% (373°C)	4.6% (500°C)	10.2% (750°C)	53.0% residue

LOI = 25.29

Table C-1.—(Concluded)

4. Mettler — Clear polyvinylfluoride film; sample wt - 16.07 mg; wt loss started - 300°C				
W_1	W_2	W_3	W_4	W_5
46.8% (428°C)	20.5% (450°C)	4.7% (510°C)	25.2% (655°C)	2.8% residue
		LOI = 46.70		
N01 — Polyurethane seat foam (CPR 9700 SE) — area density = 0.0883 g/cm^2 (0.0013 lb/in.^{2})***				
Mettler — Flexible polyurethane foam 2.54 cm (1.0 in.) thick, 28.83 kg/m^3 (1.8 #/ft^3) density; sample weight 15.12 mg; weight loss started 195°C.				
W_1	W_2	W_3	W_4	
7% (280°C)	63% (420°C)	24% (705°C)	6% residue	
		LOI = 23.35		
N02/N03 — Fabric-backed vinyl — area density = 0.0913 g/cm^2 (0.0013 lb/in.^{2})				
Mettler — Fabric-backed flexible polyvinylchloride, 8.14 kg/m^2 (24 oz/yd^2); sample weight 24.08 mg; weight loss started 180°C.				
W_1	W_2	W_3	W_4	
66% (400°C)	22% (615°C)	3% (750°C)	9% residue	
		LOI = 26.98		

*BMS - Boeing material specification

**BMS 8-143, type 181, is currently the same material as BMS 8-132, type 181

***N00 had a thickness 2x that of the lab sample, therefore its area density = 0.1776 g/cm^2 (0.0025 lb/in.^{2})

Table C-2.—Federal Aviation Regulations FAR 25.853 Bunsen Burner Test Data

	12 second test—vertical	60 second test—vertical	15 second test—horizontal
403 Sidewall panel	Burn length = 9.65 cm (3.8 in.) Extinguishing time = 1.1 sec	Burn length = 9.91 cm (3.9 in.) Extinguishing time = 1.5 sec	Burn length = 3.05 cm (1.2 in.) Extinguishing time = 3.4 sec
413 Thermo-plastic	Burn length = 9.06 cm (3.6 in.) Extinguishing time = 4.6 sec	Burn length = 8.47 cm (3.3 in.) Extinguishing time = 6.0 sec	Burn length = 1.61 cm (0.6 in.) Extinguishing time = 1.8 sec
417 Sidewall	Burn length = 3.73 cm (1.5 in.) Extinguishing time = 1.0 sec	Burn length = 3.13 cm (1 2 in.) Extinguishing time,= 1.0 sec	Burn length = 1.78 cm (0.7 in.) Extinguishing time = 0.9 sec
N01 Polyurethane seat foam	Burn length = 11.94 cm (4.7 in.) Extinguishing time = 0 sec	Burn length = 13.21 cm (5.2 in.) Extinguishing time = 1.4 sec	Burn length 1.27 cm (0.50 in.) Extinguishing time = 0.80 sec
N03 Fabric-backed vinyl	Burn length = 10.24 cm (4.03 in.) Extinguishing time = 0.80 sec	Burn length = 7.37 cm (2.9 in.) Extinguishing time = 2.4 sec	Burn length = 1.44 cm (0.57 in.) Extinguishing time = 3.7 sec

Table C-3.—Radiant Panel Test ASTM E 162-67 Data

	Flame spread (F_s)	Heat evolution factor (Q)	Index ($I_s = F_s \times Q$)
403 Sidewall panel	24.86	1.88	49.62
413 Thermoplastic	4.92	4.82	23.90
417 Sidewall panel	9.39	3.02	28.10
N01 Polyurethane seat foam	52.47	15.79	798.82
N03 Fabric-backed vinyl	33.45	10.75	346.10

Table C-4.—NBS Chamber Toxicant Concentrations

The gas collection initiated times are listed. Where bubblers were used the collection period was for 150 seconds. NO_x was always sampled using a Drager tube whose collection period was 100 seconds. CO was determined with an NDIR meter.

	HCN	HCL	HF	NO_x	CO	HBR
403 (402)						
2.5 w/fl*	—	—	—	—	—	—
4.0 min	2.0	60	64	—	276	—
10.0 min	—	149	44	5	540	—
2.5 w/smol**	—	—	—	—	—	—
4.0 min	0.90	47	60	0	0	
10.0 min	1.4	59	46	—	0	—
5.0 w/fl*	—	—	—	—	—	—
1.5 min	0	50	149	1	204	—
4.0 min	7	44	141	2	370	—
413 (412)						
2.5 w/fl*	—	—	—	—	—	—
4.0 min	—	42	—	—	280	—
10.0 min	trace	3	—	3	863	—
2.5 w/smol**	—	—	—	—	—	—
4.0 min	—	3	—	—	0	—
10.0 min	—	3	—	—	0	—
5.0 w/fl**	—	—	—	—	—	—
1.5 min	—	458	—	2	216	—
4.0 min	—	946	—	5	800	—
417 (416)						
2.5 w/fl*	—	—	—	—	—	—
4.0 min	trace	342	30	—	102	—
10.0 min	—	242	39	1	222	—
2.5 w/smol**	—	—	—	—	—	—
4.0 min	0.5	265	7	—	0	—
10.0 min	0.3	745	13	—	0	—
5.0 w/fl*	—	—	—	—	—	—
1.5 min	—	312	30	0	37	—
4.0 min	—	656	53	2	67	—

Table C-4.—NBS Chamber Toxicant Concentrations (Concluded)

	HCN	HCL	HF	NO_x	CO	HBR
N01						
2.5 w/fl*	—	—	—	—	—	—
4.0 min	25	1379	—	33	—	—
10.0 min	—	2514	—	—	—	—
2.5 w/smol**	—	—	—	—	—	—
4.0 min	5	0	—	0	83	—
10.0 min	—	—	—	—	340	—
5.0 w/fl*	—	—	—	—	—	—
1.5 min	57	1574	—	50	303	—
4.0 min	69	1506	—	60	405	—
N03 (N02)						
2.5 w/fl*	—	—	—	—	—	—
4.0 min	trace	2578	15***	2	62	—
2.5 w/smol**	—	—	—	—	—	—
4.0 min	trace	1542	60***	2	10	—
5.0 w/fl*	—	—	—	—	—	—
1.5 min	2	736	5***	2	687	—
4.0 min	4	992	15***	5	785	—

*W/cm^2 — flaming mode
**W/cm^2 — smoldering mode
*** — derived from Drager tube data

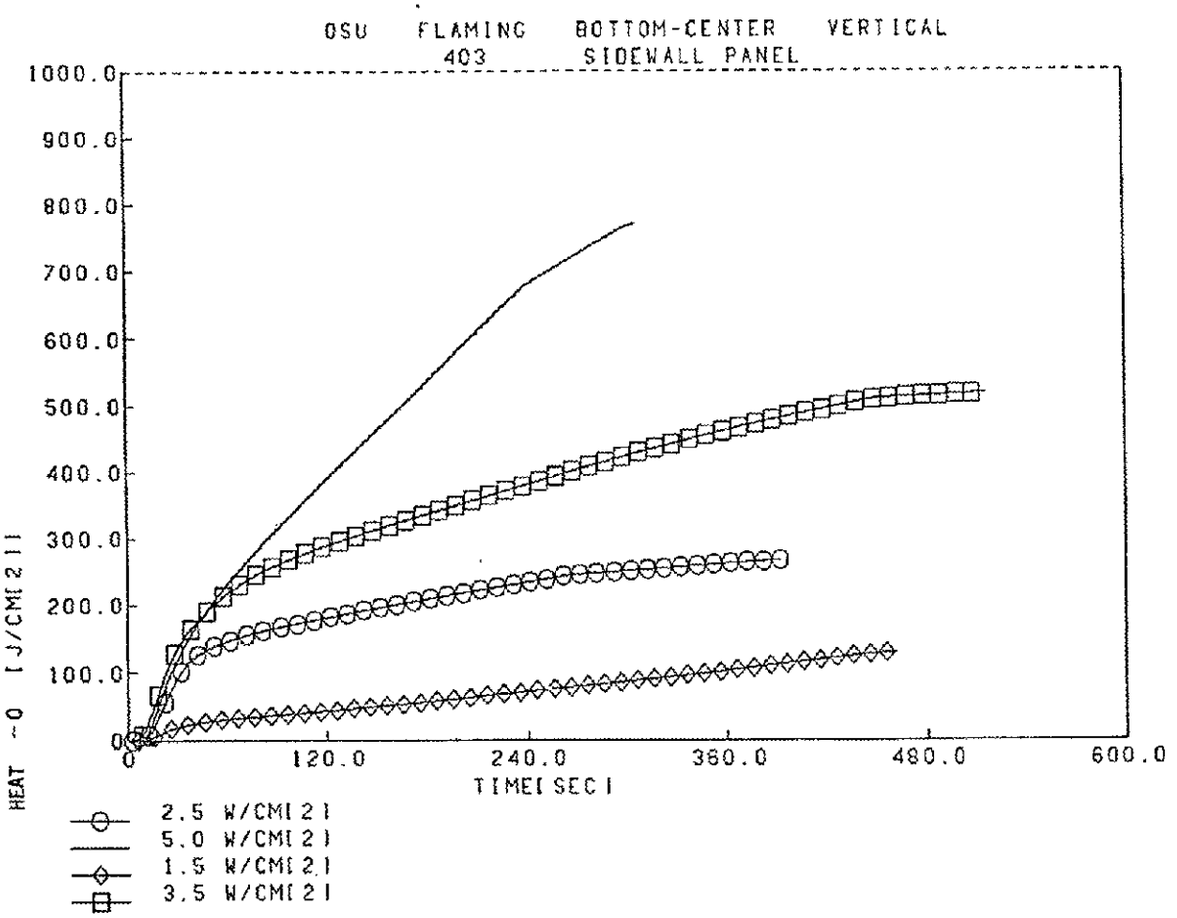

Figure C-1.—Heat Release in the OSU Apparatus in the Vertical Bottom-Center Ignition Mode—402/403

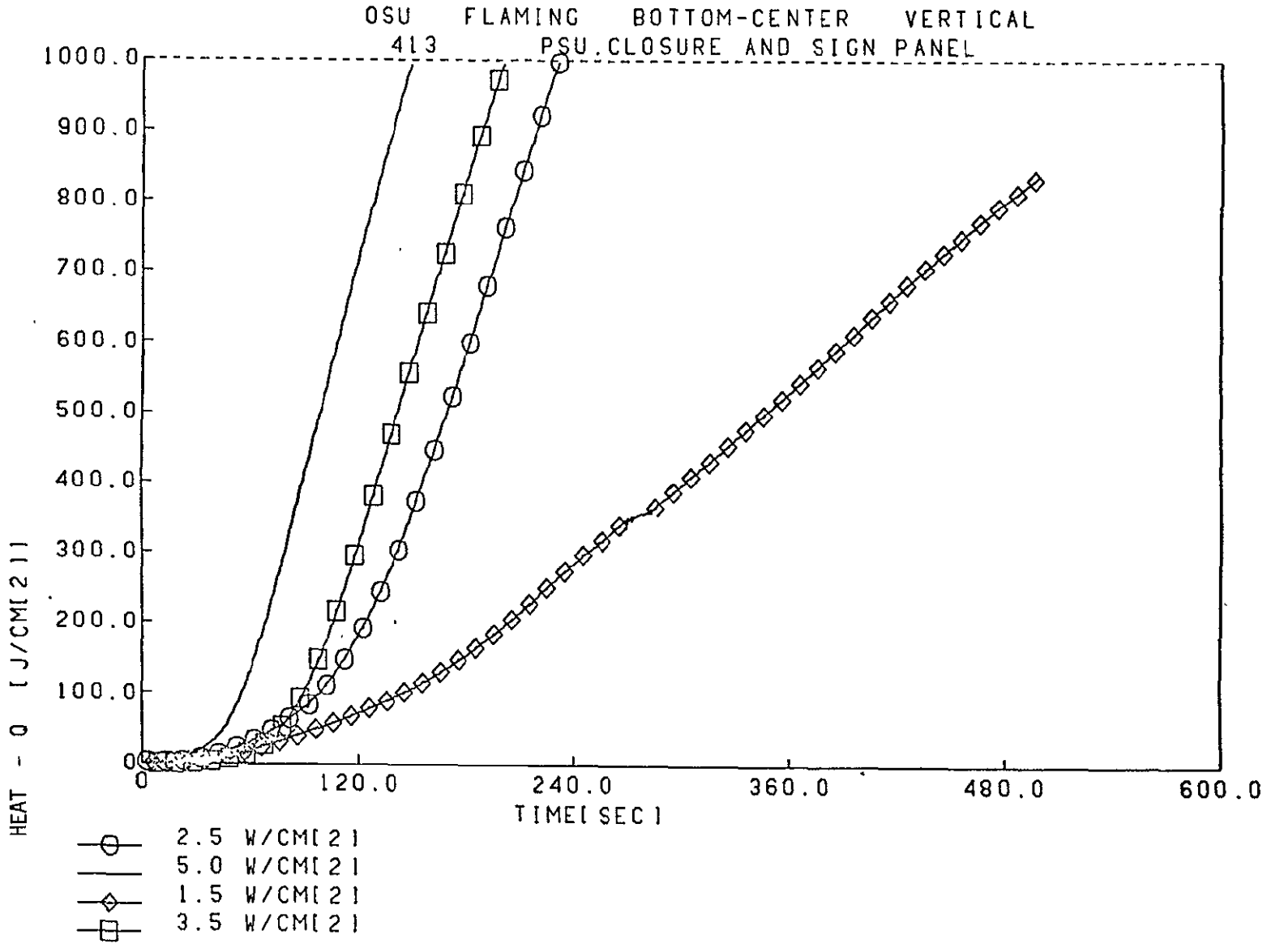

Figure C-2.—Heat Release in the OSU Apparatus in the Vertical Bottom-Center Ignition Mode—412/413

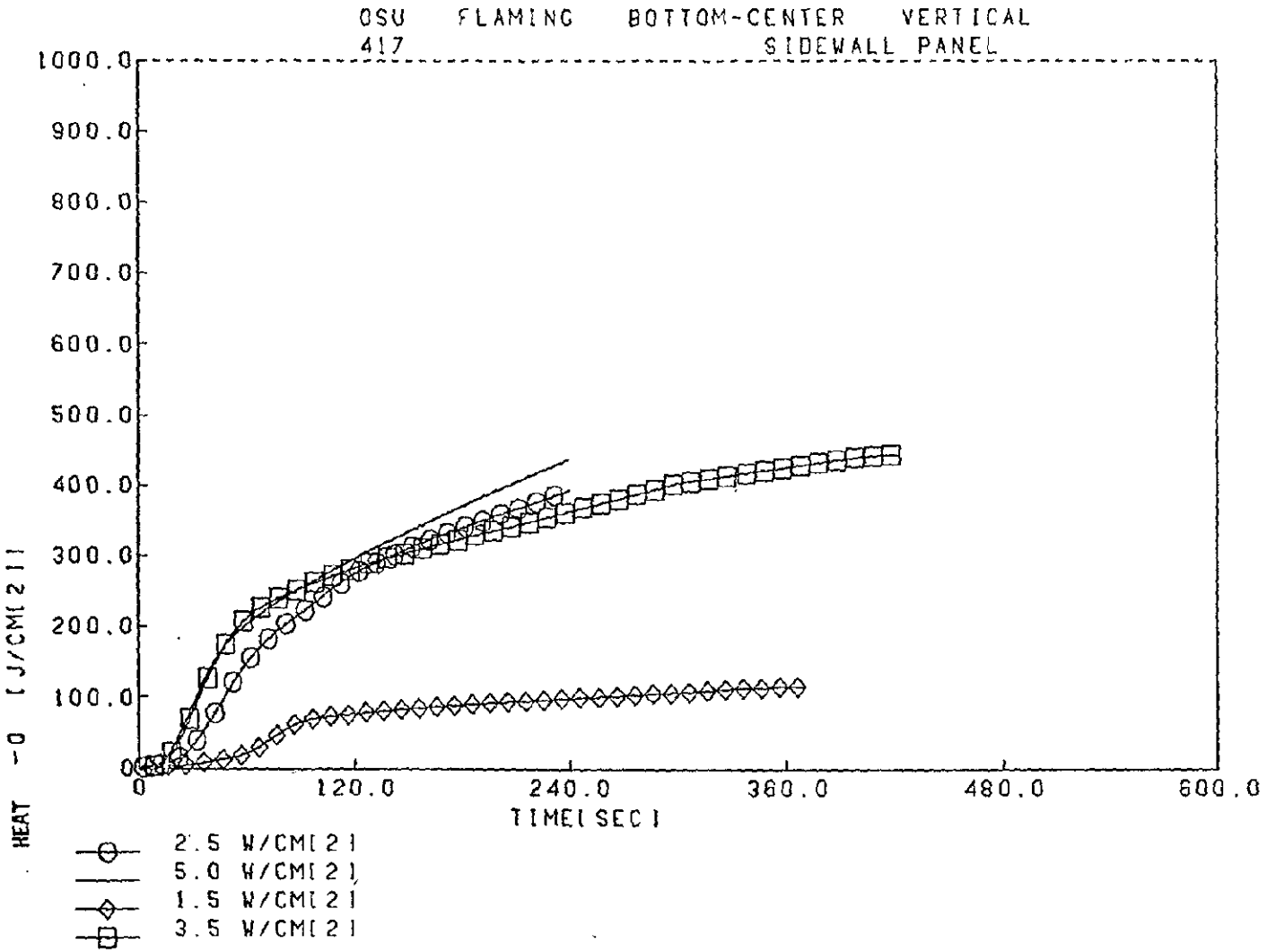

Figure C-3.—Heat Release in the OSU Apparatus in the Vertical Bottom-Center Ignition Mode—416/417

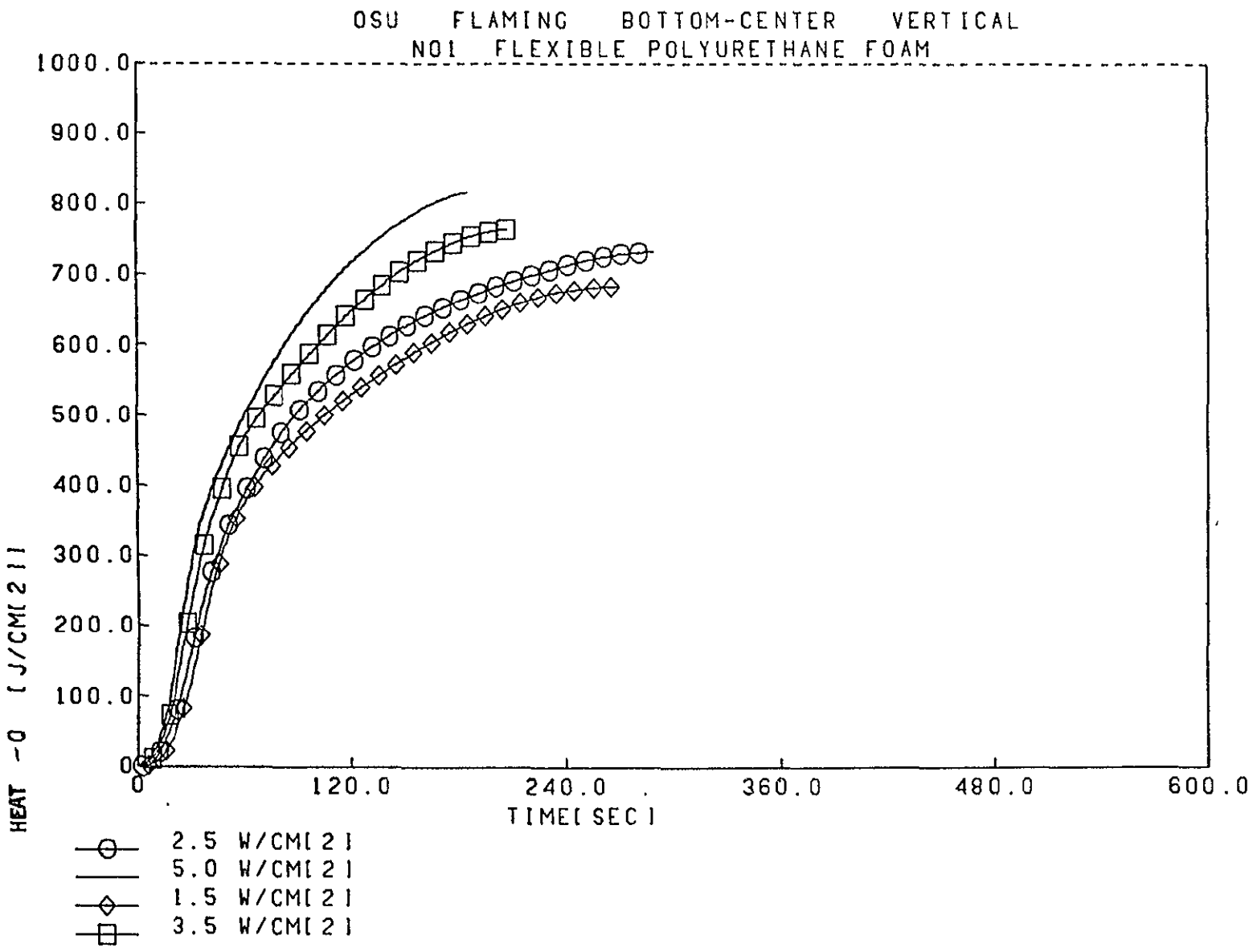

Figure C-4.—Heat Release in the OSU Apparatus in the Vertical Bottom-Center Ignition Mode—N01

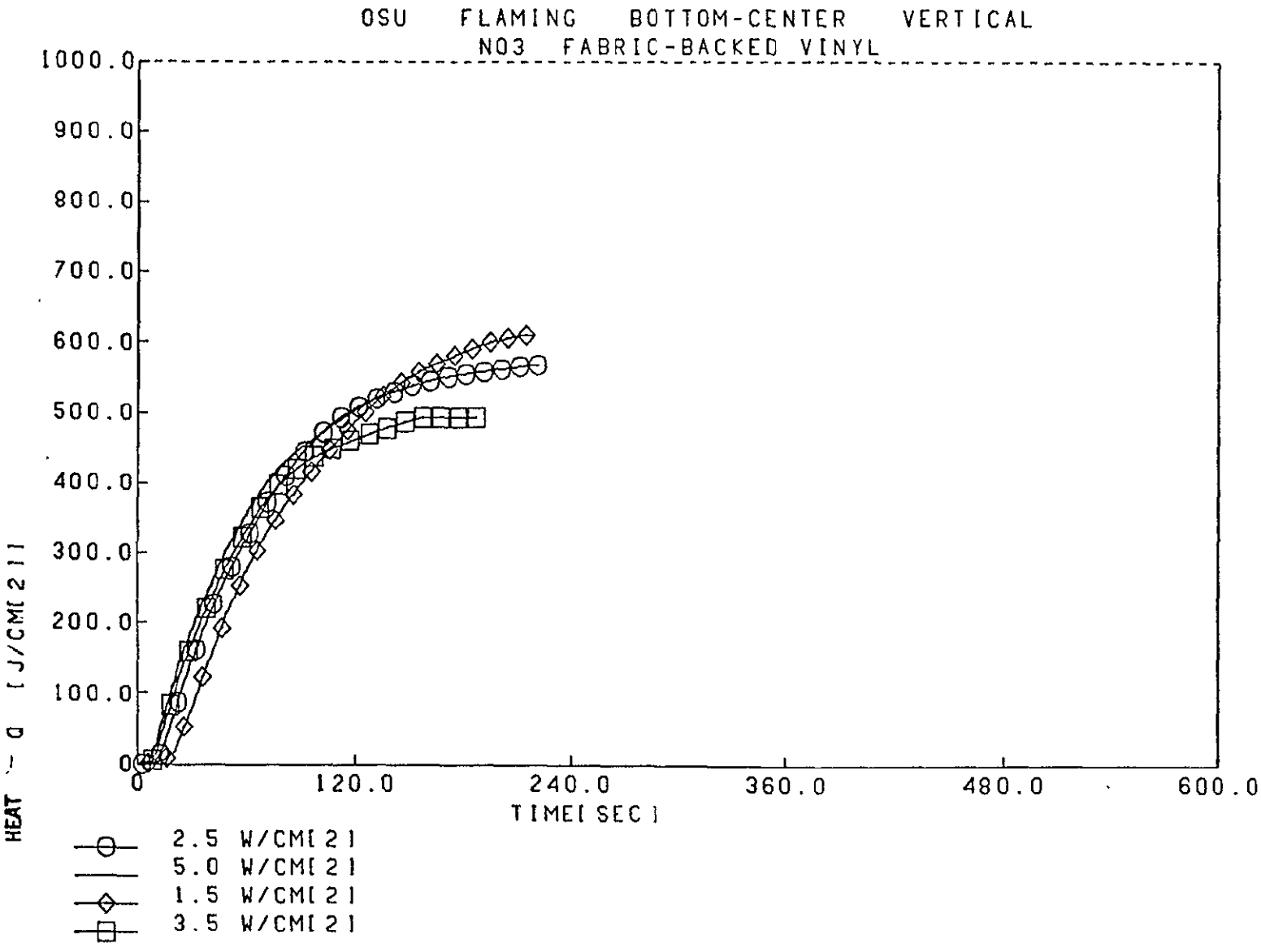

Figure C-5.—Heat Release in the OSU Apparatus in the Vertical Bottom-Center Ignition Mode—N02/N03

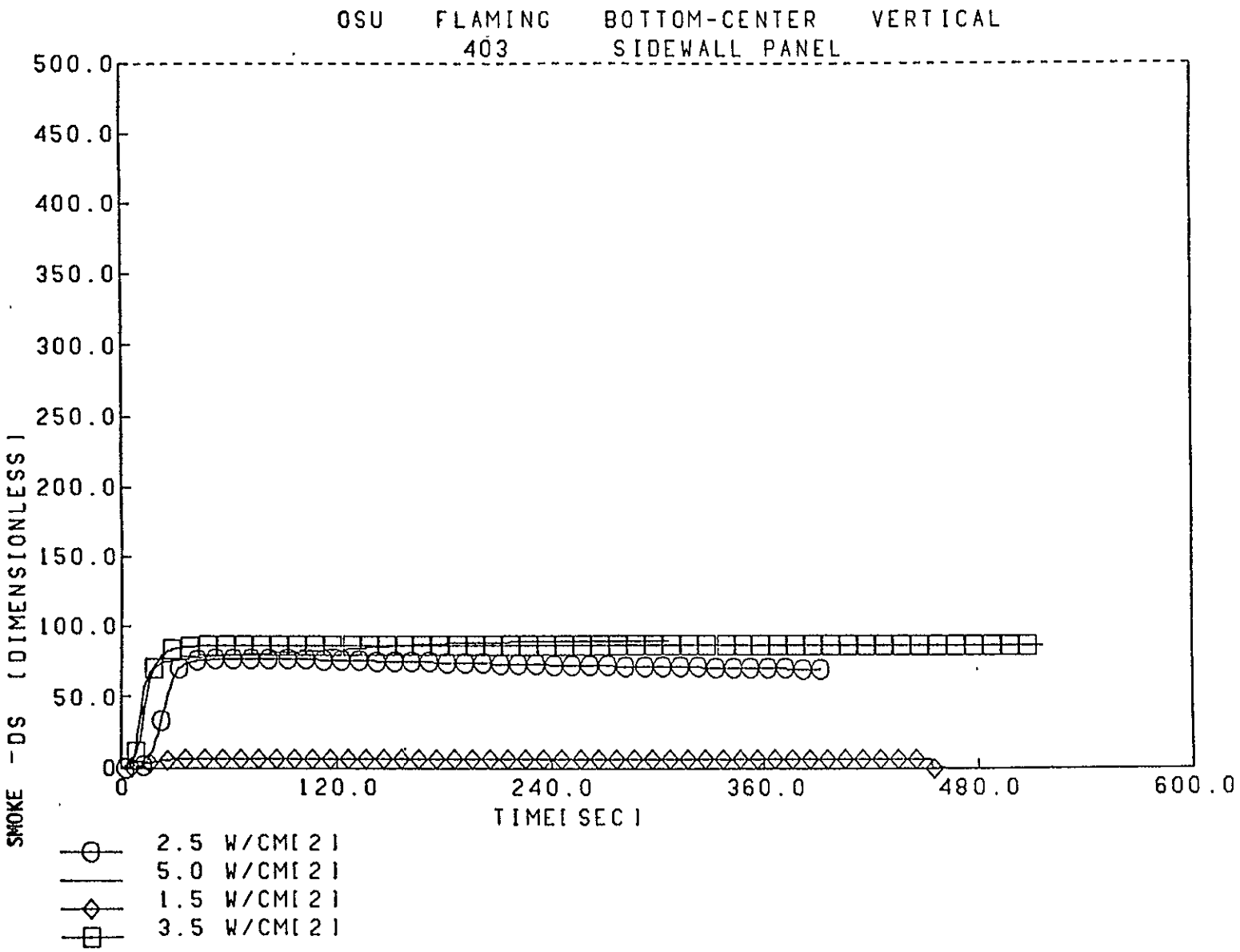

Figure C-6.—Smoke Release in the OSU Apparatus in the Vertical Bottom-Center Ignition Mode—402/403

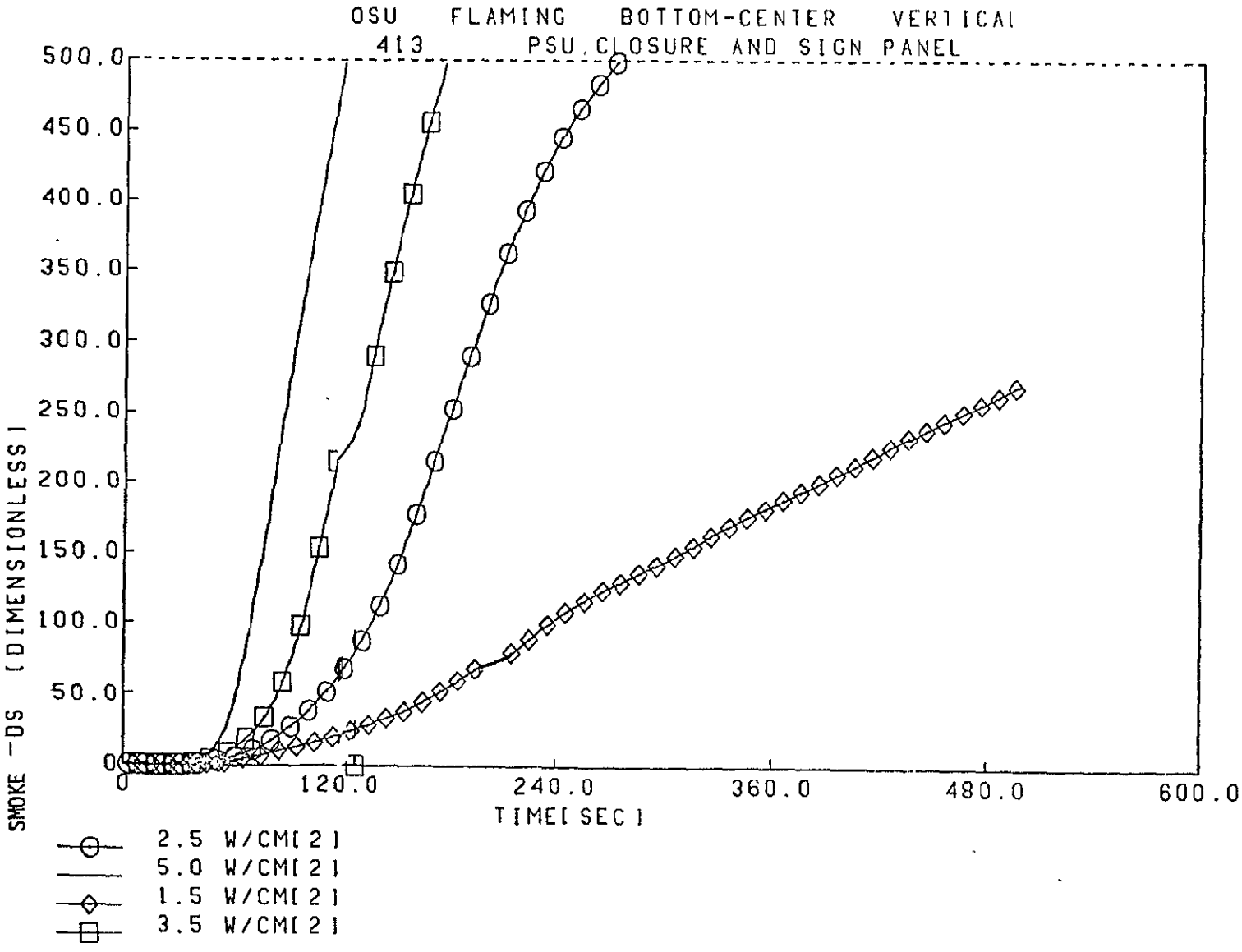

Figure C-7.—Smoke Release in the OSU Apparatus in the Vertical Bottom-Center Ignition Mode—412/413

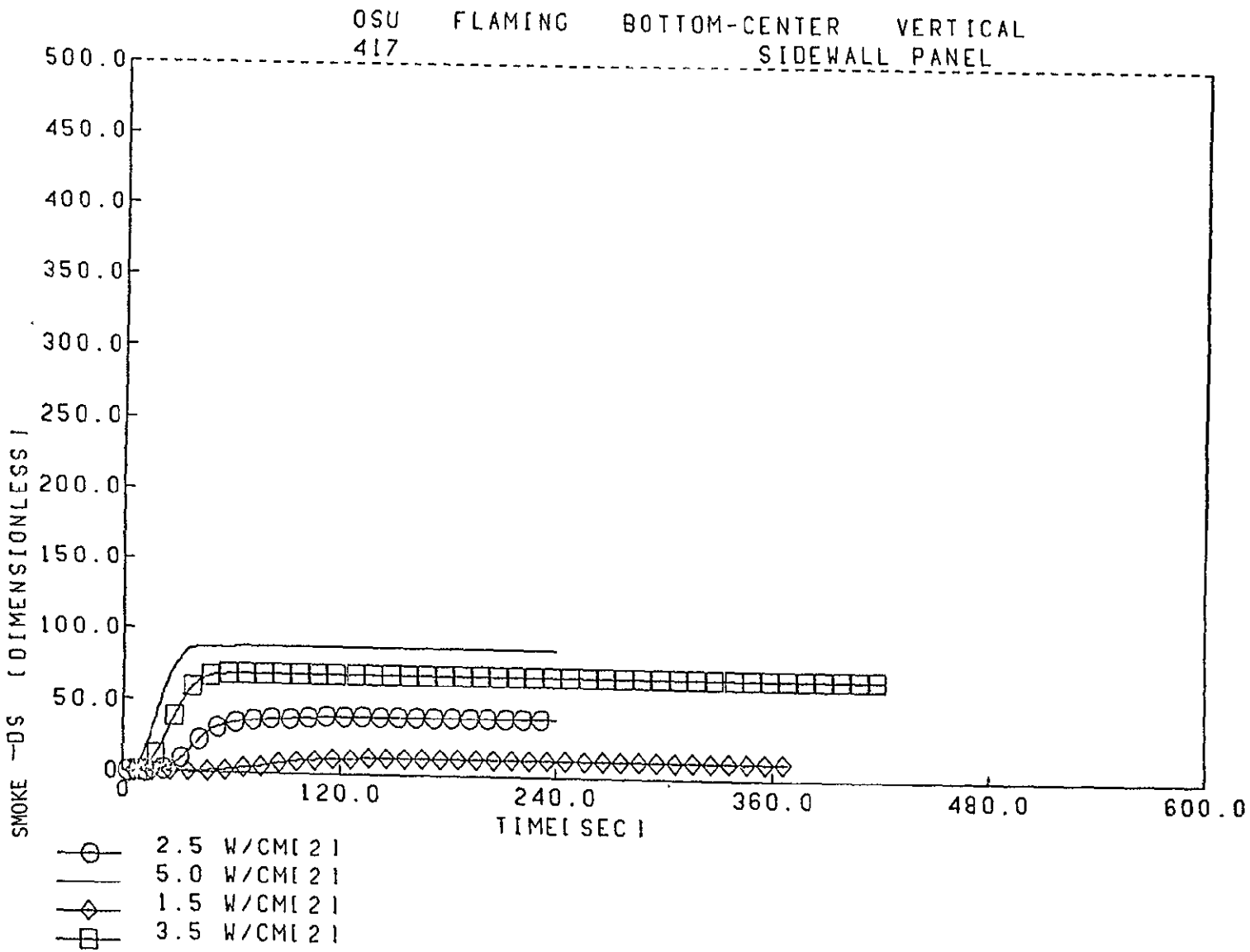

Figure C-8.—Smoke Release in the OSU Apparatus in the Vertical Bottom-Center Ignition Mode—416/417

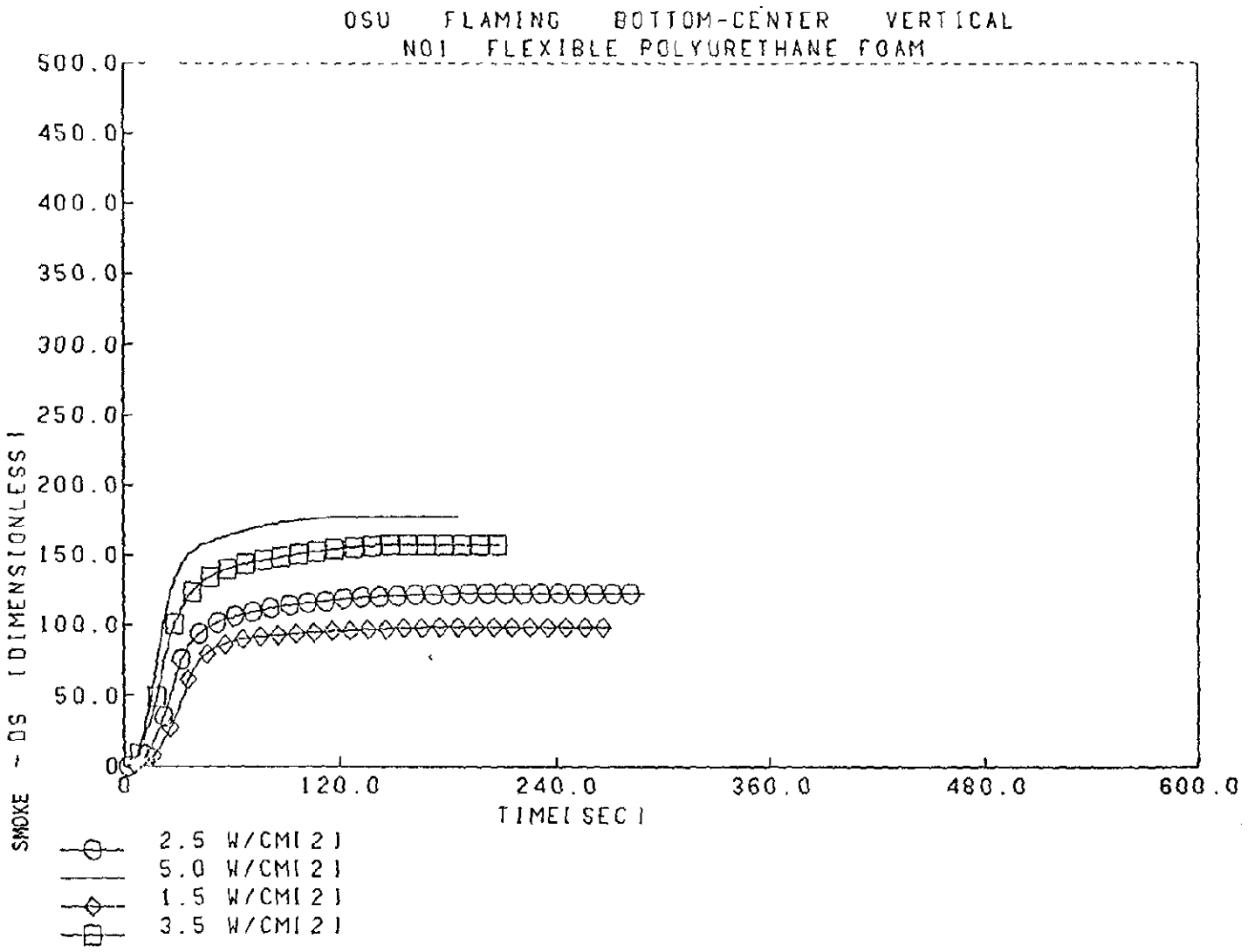

Figure C-9.—Smoke Release in the OSU Apparatus in the Vertical Bottom-Center Ignition Mode—N01

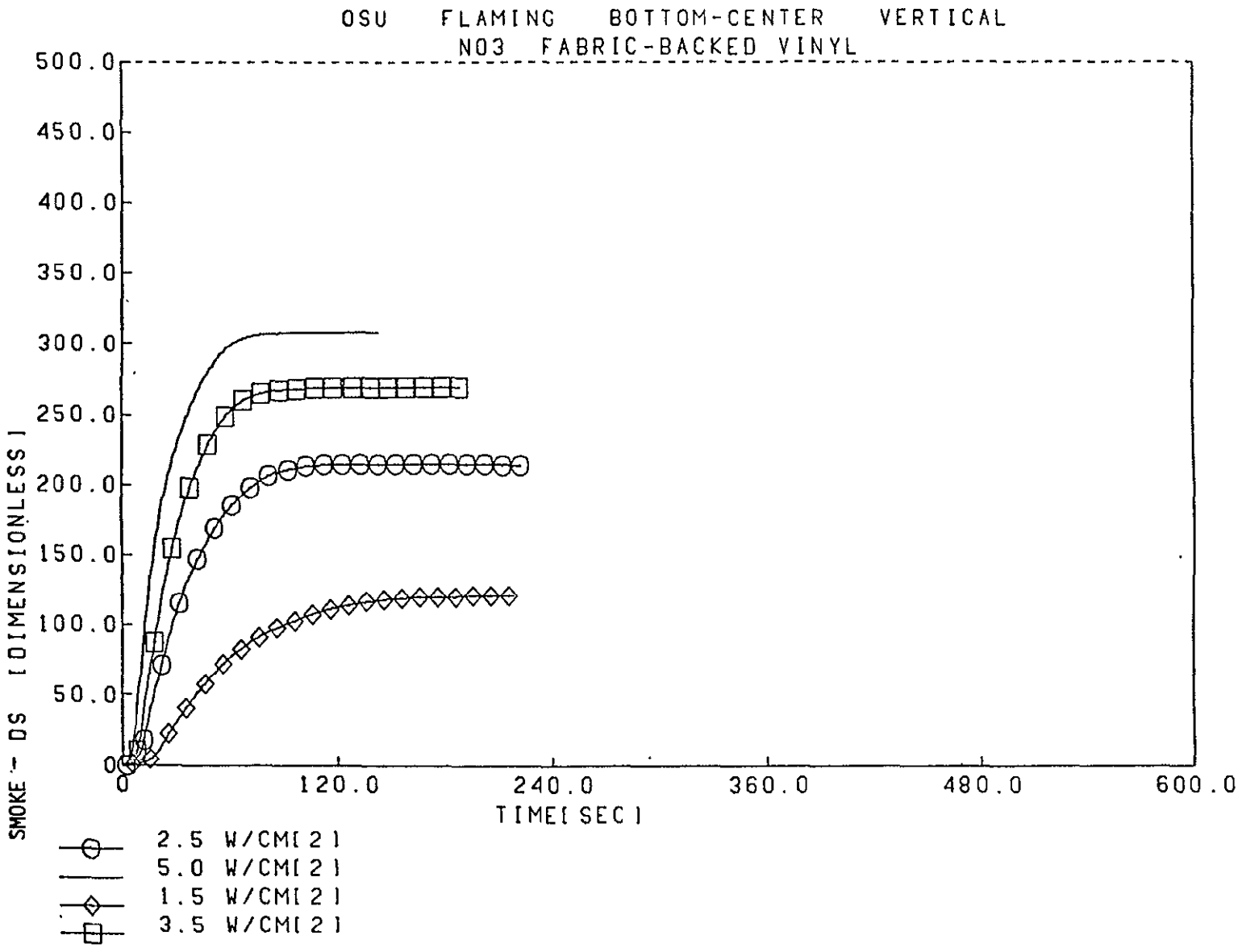

Figure C-10.–Smoke Release in the OSU Apparatus in the Vertical Bottom-Center Ignition Mode–N02/N03

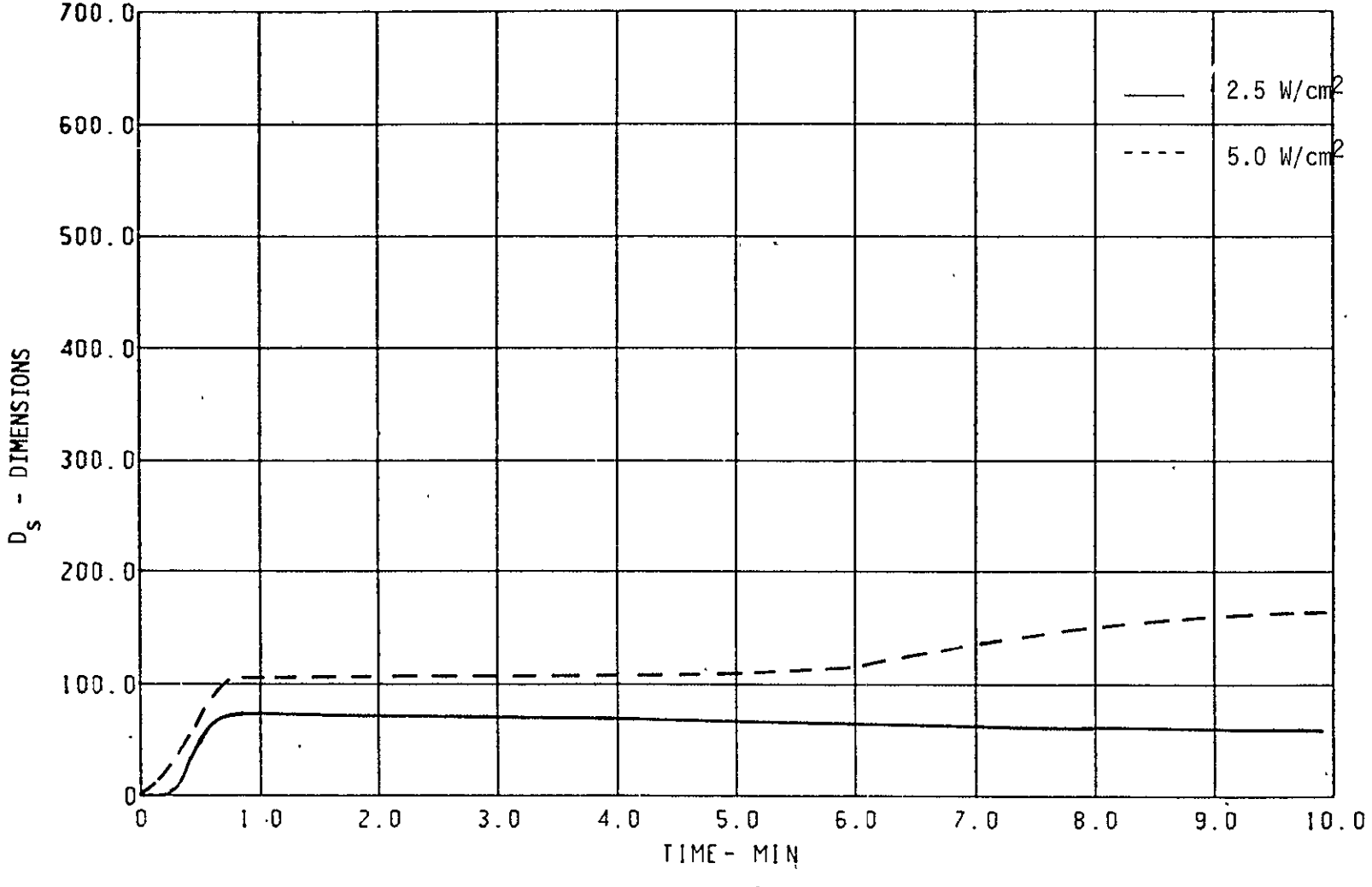

Figure C-11.—Smoke Release in the NBS Chamber in the Flaming Mode—402/403

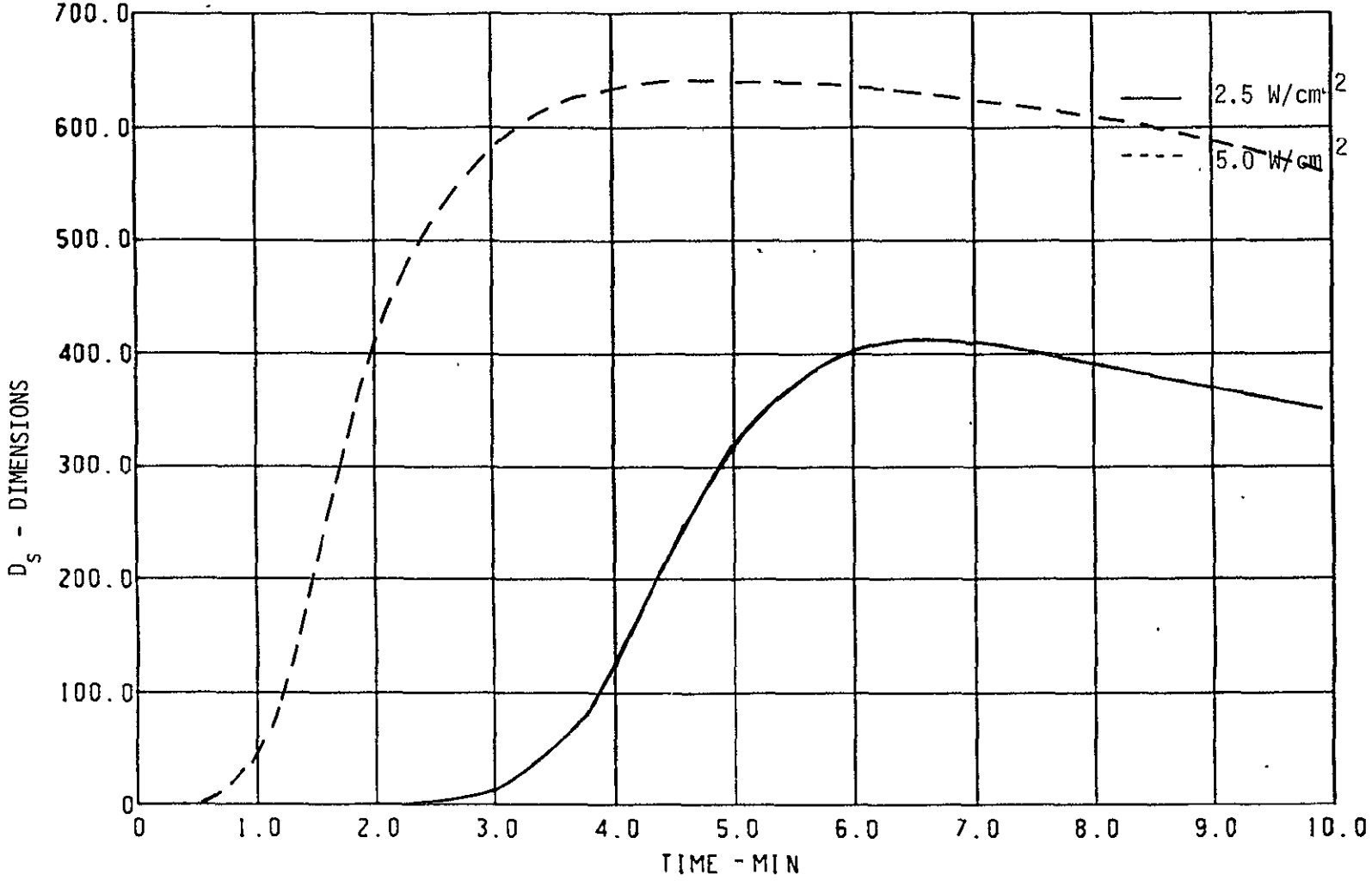

Figure C-12.—Smoke Release in the NBS Chamber in the Flaming Mode—412/413

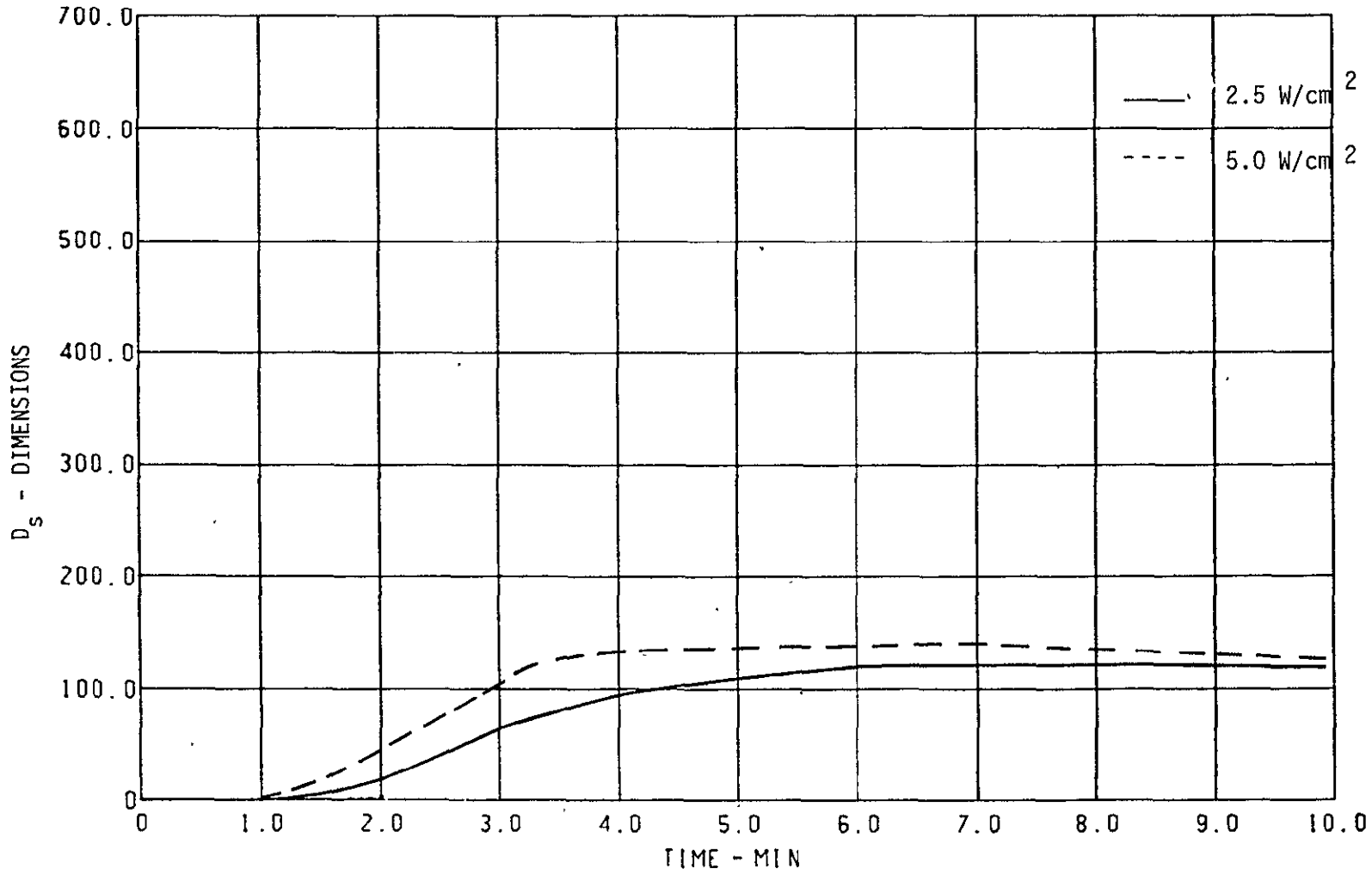

Figure C-13.--Smoke Release in the NBS Chamber in the Flaming Mode--416/417

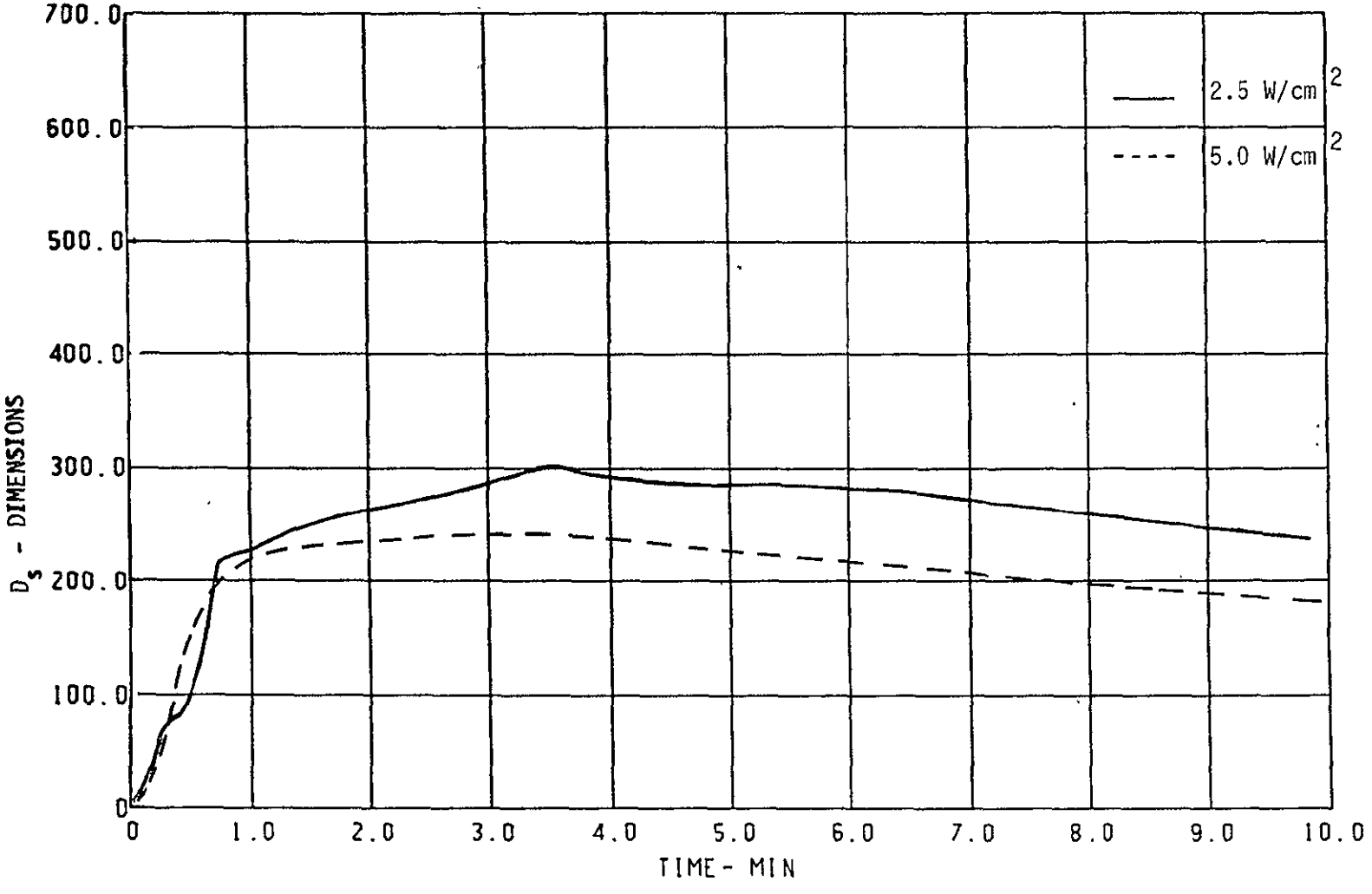

Figure C-14.—Smoke Release in the NBS Chamber in the Flaming Mode—NO1

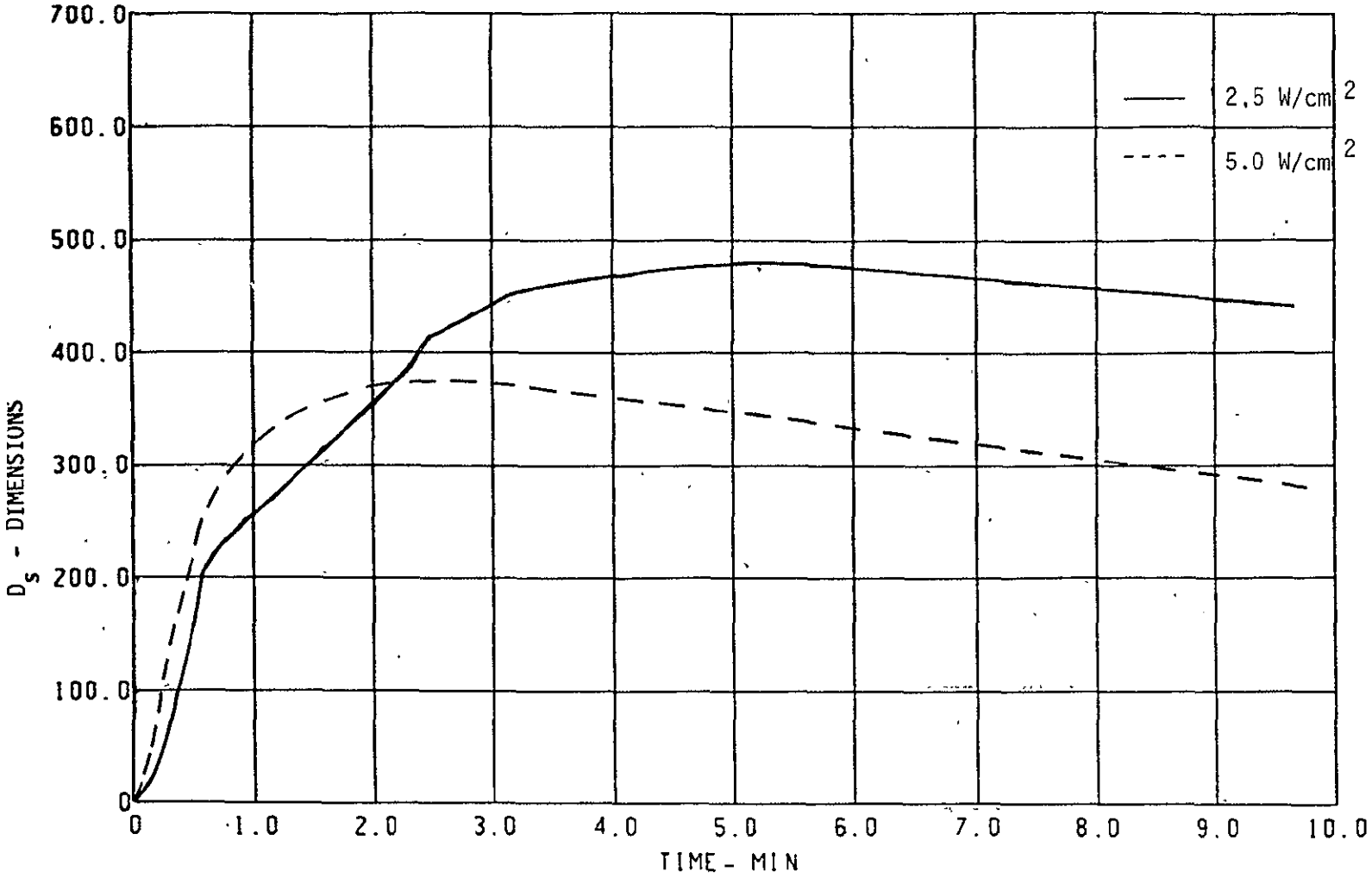

Figure C-15.—Smoke Release in the NBS Chamber in the Flaming Mode—N02/N03

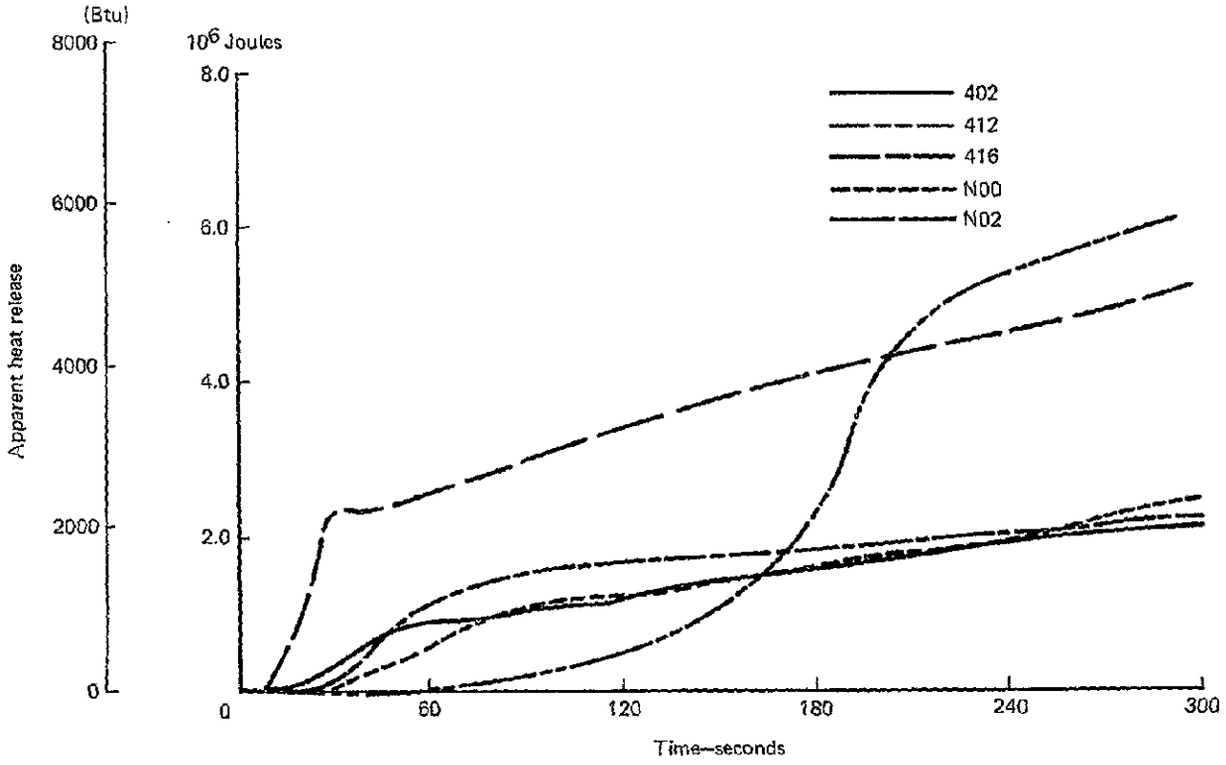

Figure C-16.—Apparent Heat Release from Simulated Design Post-crash Fire Source Tests—Baseline Materials

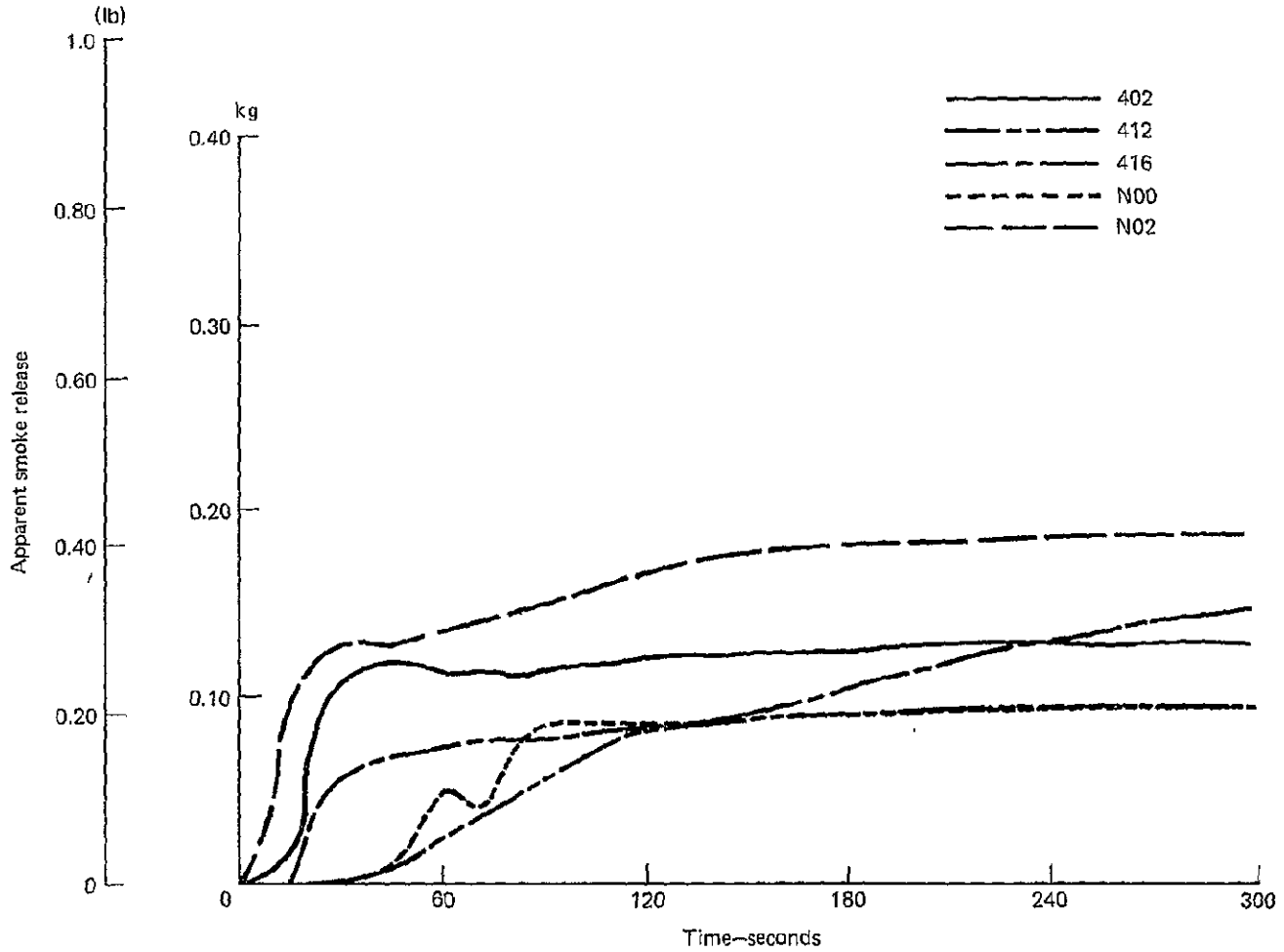

Figure C-17.—Apparent Smoke Release from Simulated Design Post-crash Fire Source Tests—Baseline Materials

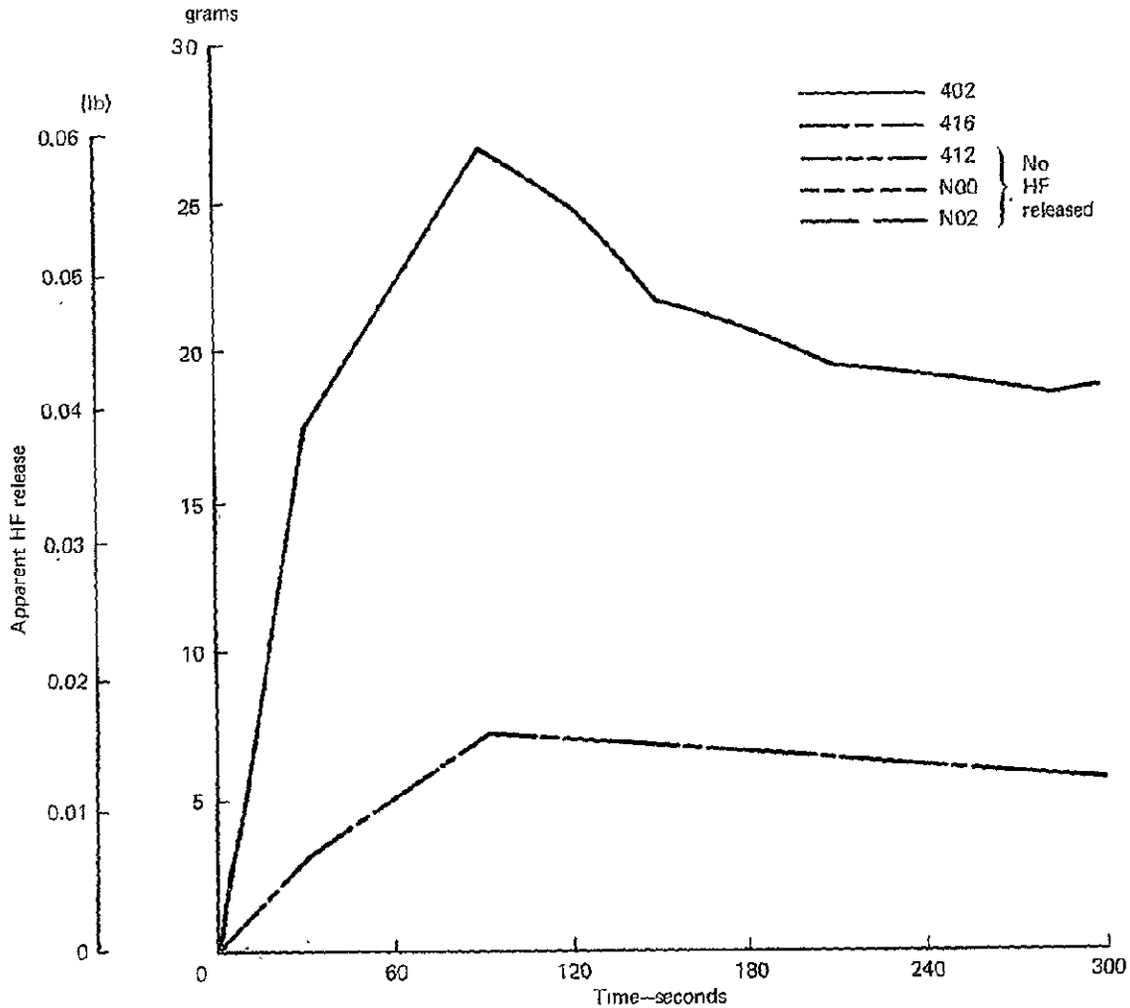

Figure C-18.—Apparent Hydrogen Fluoride (HF) Release from Simulated Design Post-crash Fire Source Tests—Baseline Materials

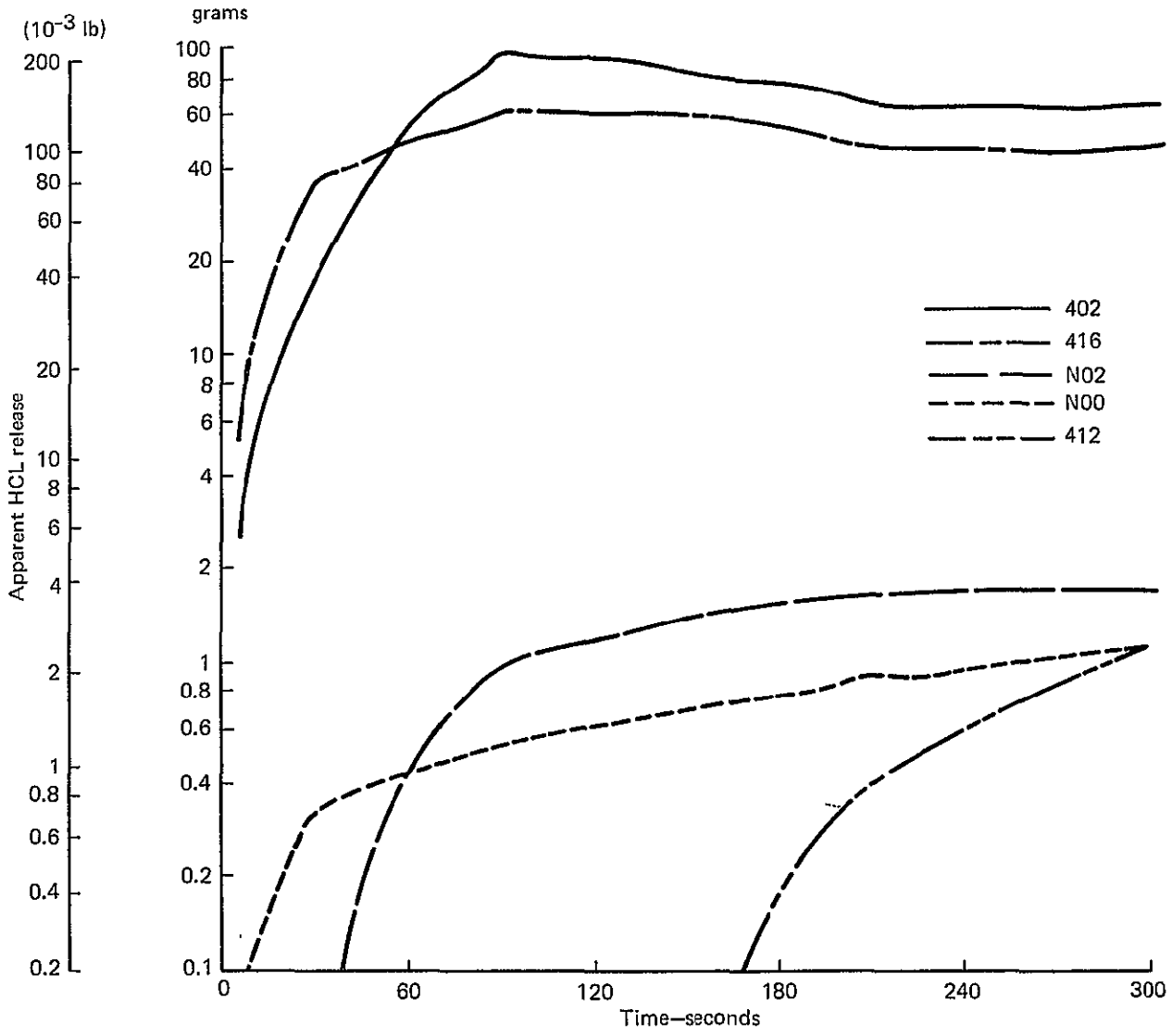

Figure C-19.—Apparent Hydrogen Chloride (HCL) Release from the Simulated Design Post-crash Fire Source Tests—Baseline Materials

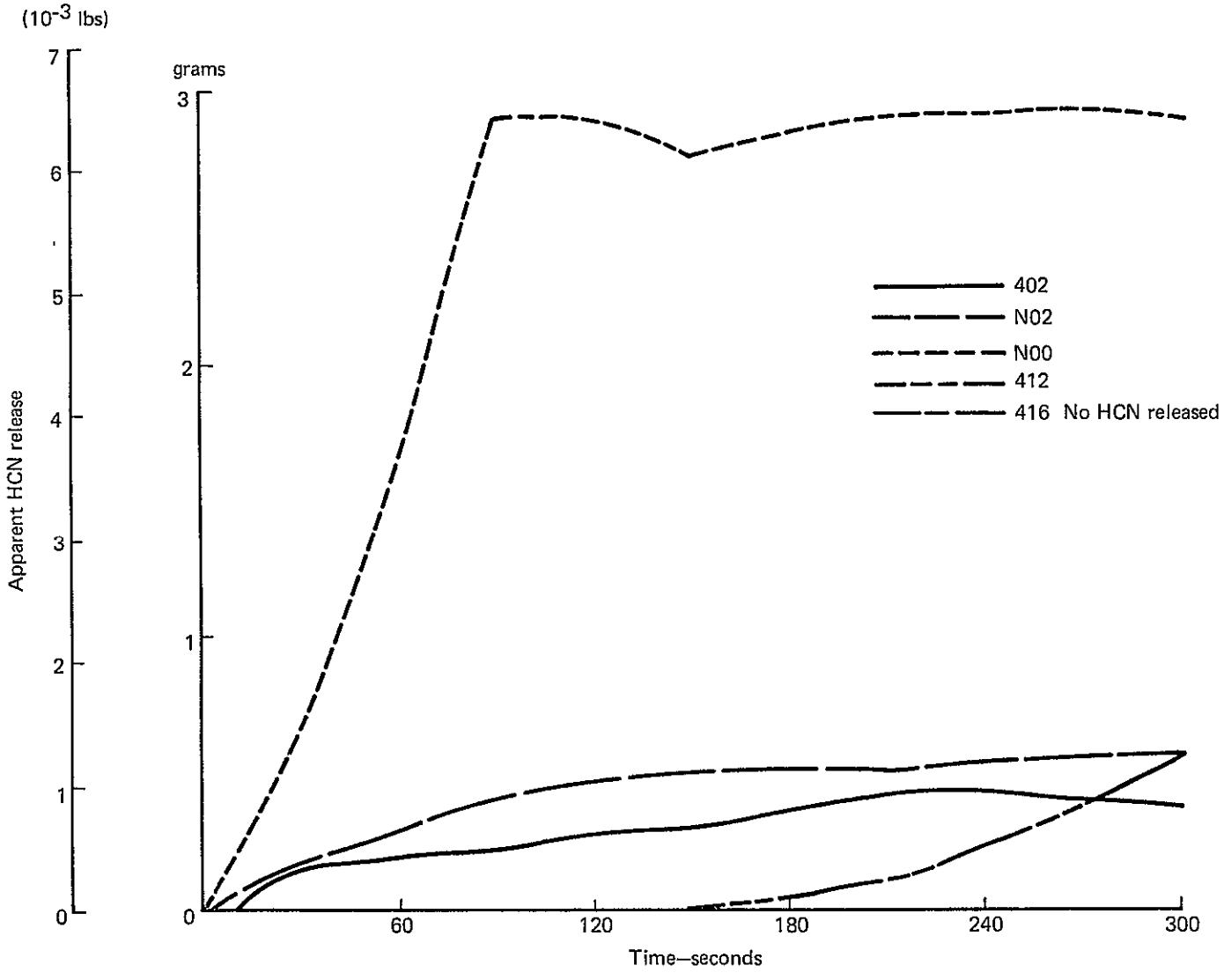

Figure C-20.—Apparent Hydrogen Cyanide (HCN) Release from the Simulated Post-crash Fire Source Tests—Baseline Materials

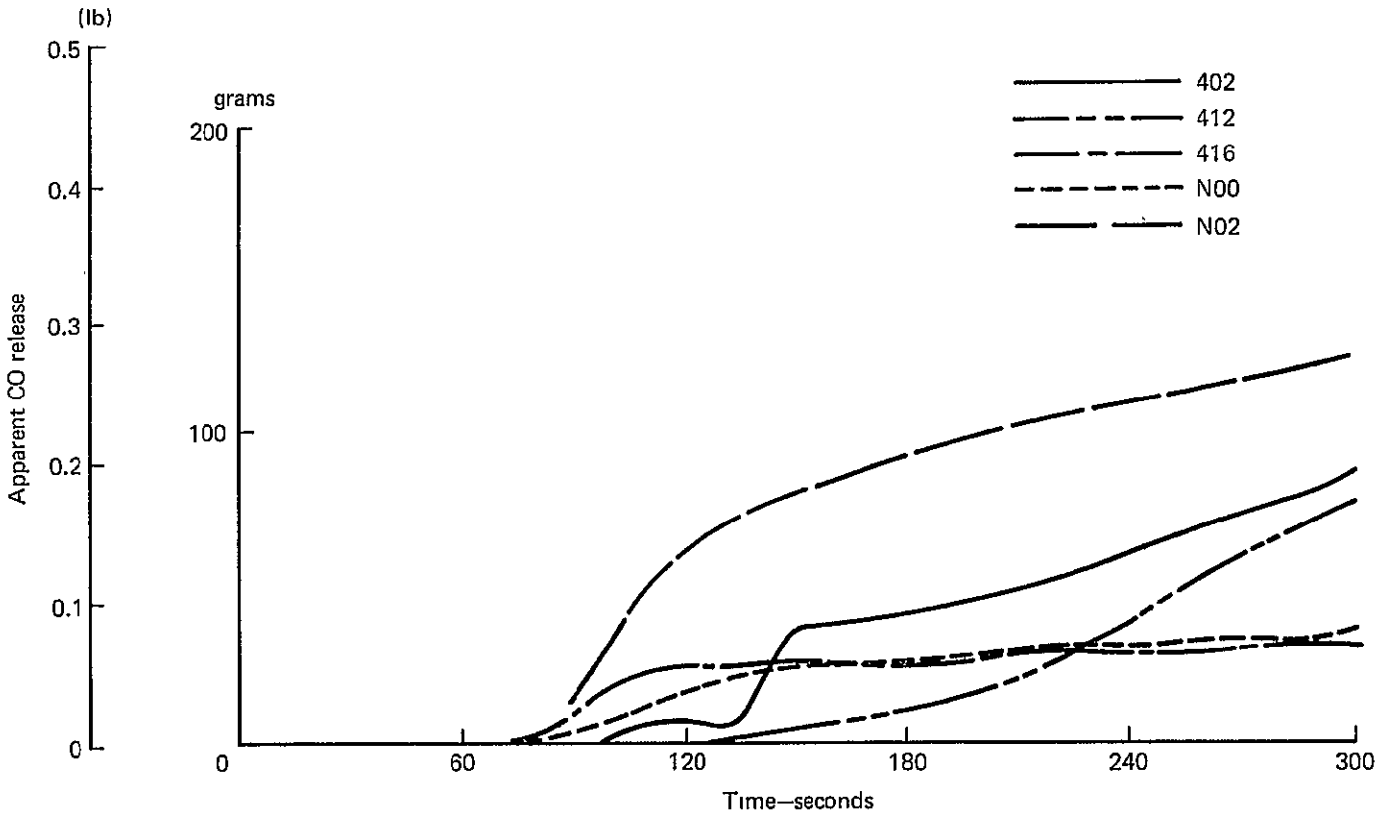

Figure C-21.—Apparent Carbon Monoxide (CO) Release from the Simulated Design Post-crash Fire Source Tests—Baseline Materials

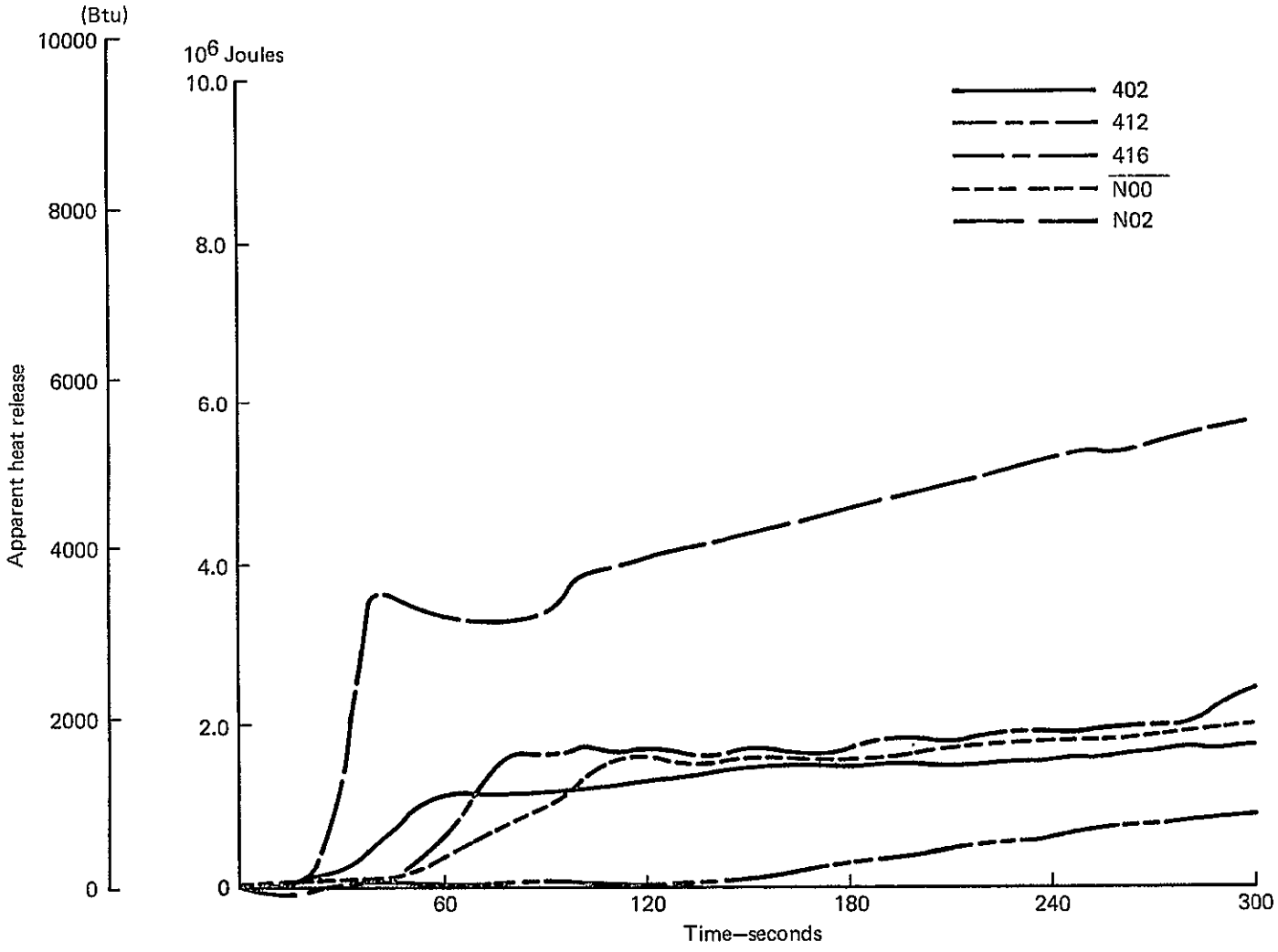

Figure C-22.—Apparent Heat Release from Simulated Design In-flight Fire Source Tests—Baseline Materials

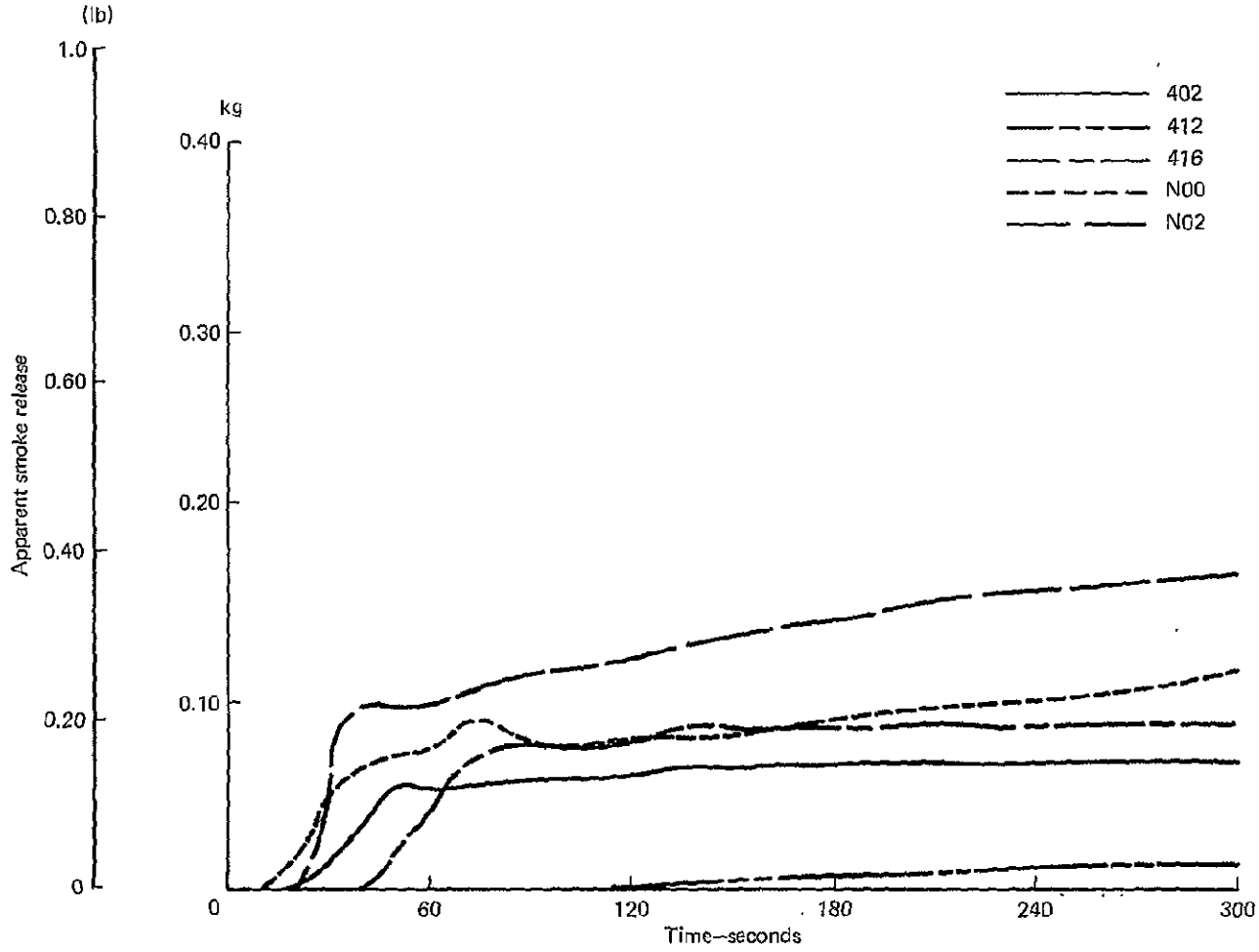

Figure C-23.—Apparent Smoke Release from Simulated Design In-flight Fire Source Tests—Baseline Materials

Figure C-24.—Apparent Hydrogen Fluoride (HF) Release from Simulated Design In-flight Fire Source Tests—Baseline Materials

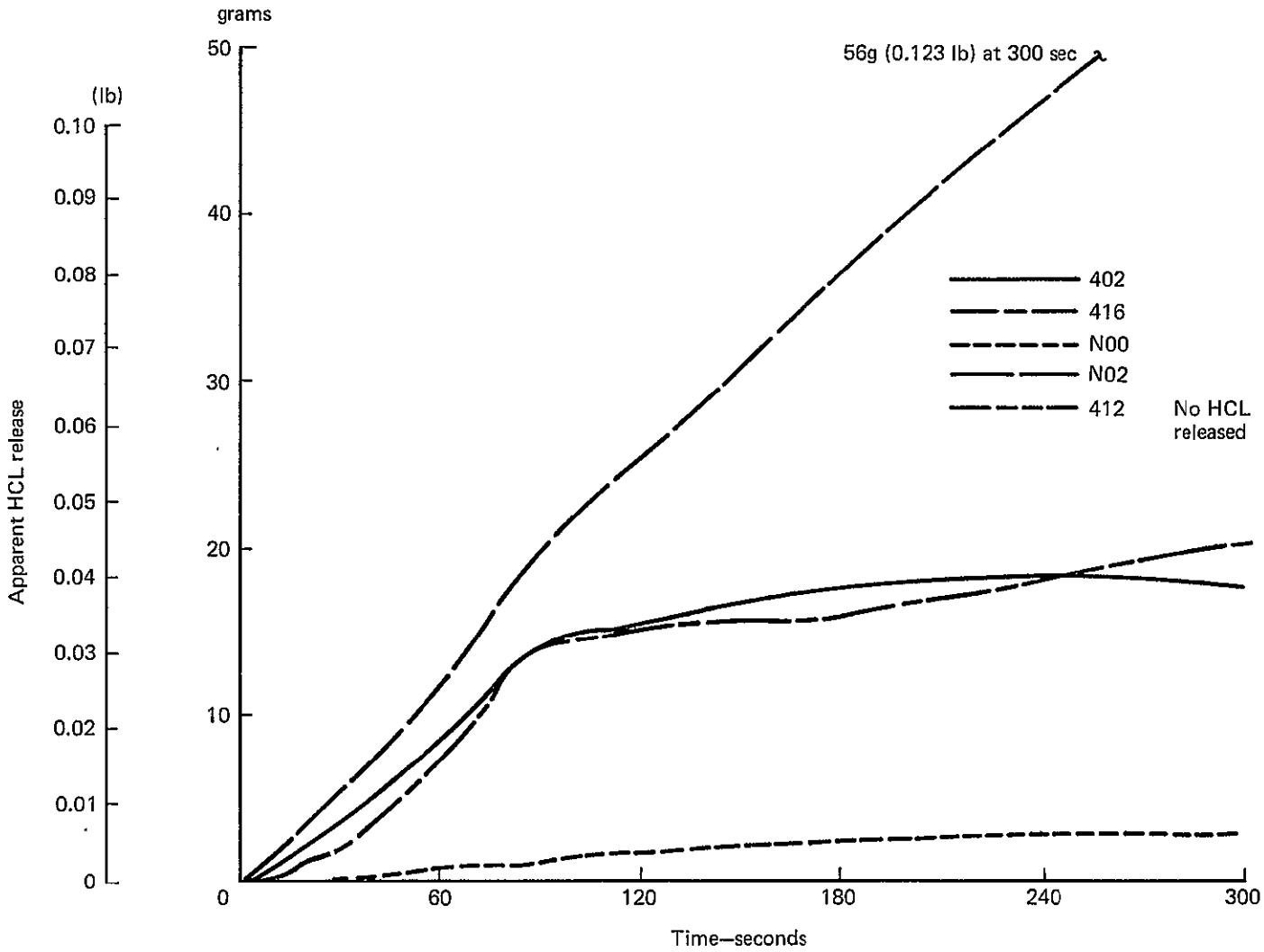

Figure C-25.—Apparent Hydrogen Chloride (HCL) Release from Simulated Design In-flight Fire Source Tests—Baseline Materials

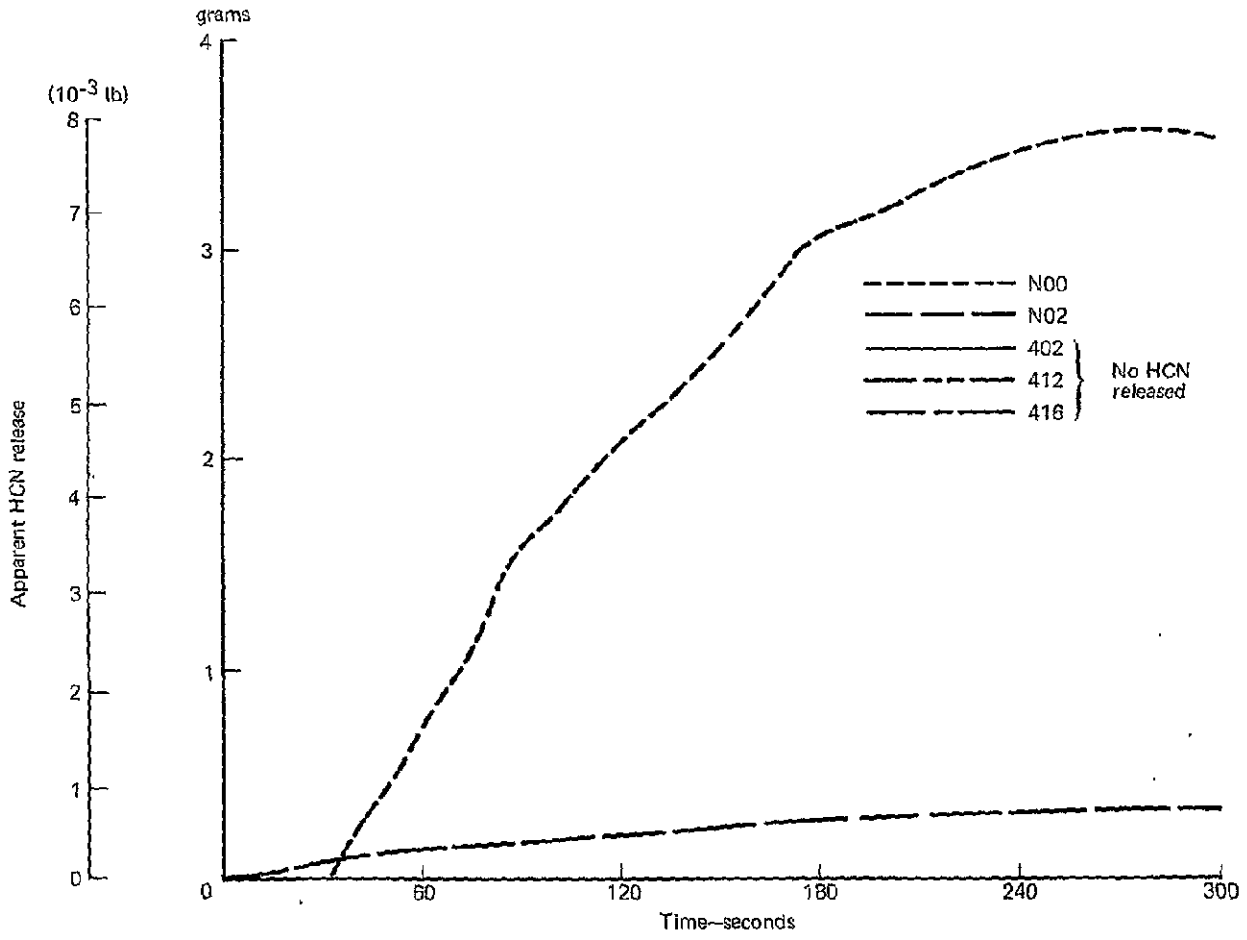

Figure C-26.—Apparent Hydrogen Cyanide (HCN) Release from Simulated Design In-flight Fire Source Tests—Baseline Materials

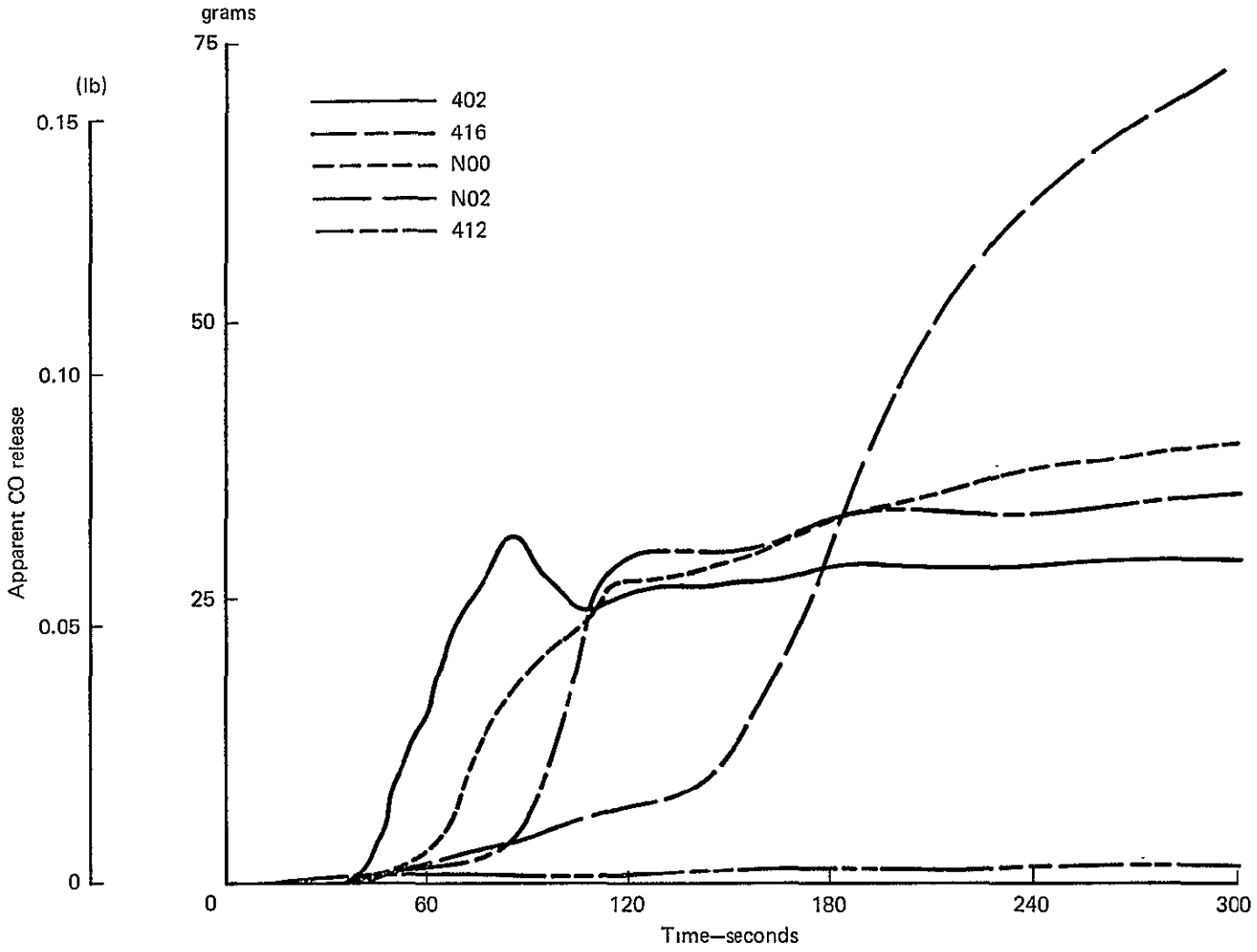

Figure C-27.—Apparent Carbon Monoxide (CO) Release from Simulated Design In-flight Fire Source Tests—Baseline Materials

APPENDIX D
LABORATORY TEST METHODS

This appendix describes the laboratory test methods used for this contract. Included are basic test procedures and results. The tests described are: Mettler Thermal Balance, Federal Aviation Regulation (FAR) 25.853, American Society for Testing of Materials (ASTM) E162-67, Limiting Oxygen Index (LOI), Ohio State University (OSU) Release Rate Apparatus, and the National Bureau of Standards (NBS) Smoke Density Chamber.

METTLER THERMAL BALANCE

The Mettler Thermal Balance (Figure D-1) is used to determine weight and enthalphy changes of materials in relation to temperature, pressure and time. The instrument recorded: (a) Thermogravimetric Analysis (TGA) - mg,- weight loss, (b) an expanded TGA - an increased sensitivity scale of weight loss, (c) Derivated Weight Curve (DTG) - the weight change per time and (d) Differential Thermal Analysis (DTA) - records whether an endothermic or exothermic reaction took place.

The tests were done in an ambient air environment, with an air flow rate of 177 cm^3/min (6.25×10^{-3} ft^3/min). The chamber was heated to a maximum of 1000°C (1832°F) in 10°C/min (18°F/min) increments. If the material reactions stopped before 1000°C (1832F) was reached, the test was terminated. For these tests, the materials were separated into their constituents (i.e., prepreg, decorative film, etc.) and the constituents were tested individually.

For this program only the TGA was recorded.

FAR 25.853 BUNSEN BURNER TEST

The FAR 25.853 Bunsen Burner Test (Figure D-2) is run in compliance with FAA requirements stated in FAR Part 25.853 (Amendments 25-15 and 25-32). The Bunsen burner flame height was adjusted until it was 3.81 cm (1.5 in.) in height and had a temperature of 843°C ($1550°F \pm {}^{100}_{0}$). The middle of the 7.62 cm (3 in.) edge of the 7.62 cm x 30.48 cm (3 in. . x 12 in.) specimens was set at 1.91 cm (0.75 in.) above the tip of the Bunsen burner. The baseline materials were tested with 3 horizontally oriented specimens for 15 seconds and 3 vertically oriented specimens for 60 seconds. The eleven proposed new NASA-JSC materials were tested with the ignition source applied to a minimum of 3 vertically oriented specimens for 60 seconds, and/or 3 vertically oriented specimens for 12 seconds, depending on which vertical test satisfies the FAR test requirements for the type and orientation of the material when used in-service. Measurements taken included burn length – cm (in.), self-extinguishing time – sec, and a visual observation of whether or not the specimen drips.

RADIANT PANEL TEST–AMERICAN SOCIETY FOR TESTING OF MATERIALS (ASTM) E162-67

The ASTM E162-67 (Figure D-3) is used to measure surface flammability of materials. A horizontally mounted gas and air pilot burner ignites the 15.24 cm x 45.72 cm (6 in. x 18 in.)

specimens by coming into contact with, or 1.27 cm (0.50 in.) above, the top of the specimen. The radiant energy source for surface flammability is a radiant energy panel that is gas and air supplied and set at 670°C ± 4 (1238°F ± 7). The orientation of the specimen is such that after the upper edge ignites, the flame front moves down the specimen surface. Four test runs are made for each type of material.

The tests were completed when the flame progressed the full length of the specimen, or after an exposure of 15 minutes. Measurements taken during the test included: the rate of progress of the flame front, or time of arrival of the flame front at 7.62 cm (3 in.) interval markers scribed on the specimen holder, and the temperature variations of the stack thermocouples.

The Flame Spread Index, I_S was the product of the flame spread factor, F_S, and the heat evolution factor, Q.

$$I_S = F_S Q$$

LIMITING OXYGEN INDEX (LOI)

The LOI (Figure D-4) is used to rank the relative flammability of materials by measuring the minimum concentration of oxygen (expressed as volume percent), in a slowly rising mixture of oxygen and nitrogen that will just support combustion. The 0.64 cm x 15.24 cm (0.25 x 6 in.) test specimens are contained in a heat resistant glass tube, and ignited at the upper edge by a natural gas igniter. Evolved gases, soot and heat are vented through a hood.

For this test the materials were separated into their constituents (i.e., prepreg, decorative film, etc.) and the constituents were tested individually.

The oxygen index, n, of the material was calculated by:

$$n \text{ (percent} = (100 \times O_2)/(O_2 + N_2)$$

OHIO STATE UNIVERSITY (OSU) RELEASE RATE APPARATUS

The Ohio State University (OSU) Release Rate Apparatus (Figure D-5) is used to determine the release rates of heat and smoke. A pilot flame provides the ignition source and an electrically heated radiant energy panel provides the heat fluxes. The heat flux is calibrated to the desired setting at the geometric center of the specimen.

For the baseline materials, nine specimens, 15.24 cm x 15.24 cm (6 in. x 6 in.), were tested in a vertical orientation. Six of these were tested in a flaming mode and three were tested in a non-flaming mode. Half of the specimens tested in a flaming mode were ignited in the center of the panel and the other half were ignited at the bottom center of the panel. Six specimens, 10.16 cm x 25.40 cm (4 in. x 10 in.) were tested in a horizontal position. Three were tested in a non-flaming mode. Thus, a set of 15 specimens per material was run at each heat flux. The heat fluxes for the baseline materials were 1.5 watts/cm^2 (1.32 Btu/ft^2-sec), 2.5 watts/cm^2 (2.20 Btu/ft^2-sec), 3.5 watts/cm^2 (3.08 Btu/ft^2-sec) and 5.0 watts/cm^2

(4.41 Btu/ft^2-sec). Tests on the eleven proposed new materials were conducted at 2.5 and 5.0 watts/cm^2 (2.20 and 4.41 Btu/ft^2-sec).

Measurements included: heat - temperature difference across the environmental chamber, and, smoke - change in voltage in the photocell absorbing a light source beamed across the stack. The rate of flame spread was observed periodically through the test.

Calculations made were:

A. Heat Release Rate (HRR) = Specific heat of air (C) X Mass Flow Rate of Air (M)

B. Smoke Release Rate (SRR) = Concentration (C_S) X Volumetric Flow Rate of Air (V)

The heat release rate was integrated over time to produce total heat release. The Smoke release rate was operated upon by the National Bureau of Standards (NBS) Smoke Density Chamber equation to produce specific optical density (D_S).

NATIONAL BUREAU OF STANDARDS (NBS) SMOKE DENSITY CHAMBER

The NBS chamber (Figure D-6) measures the increase of opacification due to smoke accumulation. For the baseline materials, a minimum of 3 specimens under flaming exposure and 3 specimens under non-flaming (smoldering) exposure were tested at 2.5 watts/cm^2 (2.20 Btu/ft^2-sec). A minimum of 3 specimens under flaming exposure were tested at 5.0 watts/cm^2 (4.41 Btu/ft^2-sec). All testing was done in accordance with the NBS chamber requirements. The 0.0042 m^2 (0.0456 ft^2)* samples are ignited by a propane gas jet and exposed to a radiant energy panel. The proposed eleven new NASA-JSC materials were tested at 2.5 watts/cm^2 (2.20 Btu/ft^2-sec) and 5.0 watts/cm^2 (4.41 Btu/ft^2-sec) flaming exposure.

Measurements included: the percent change in light transmission, which was continually monitored by a photocell and recorder, and gas sampling with subsequent toxicant analysis. Calculations were made for the specific optical density (D_S):

$$D_S = (V/AL) \text{ Log}_{10} 100/T$$

where V is chamber volume, A is specimen area and L is the light path length.

D_S is a measure of opacification due to smoke accumulation, and can be compared for different materials on a unit area basis.

Toxic gas analysis included: (A) Drager specific gas analysis tubes, (b) specific ion electrode and colorimetric analysis with samples collected by microimpingers.

* This is the area of the exposed sample. The actual sample area is 0.0058m^2 (0.0625 ft^2).

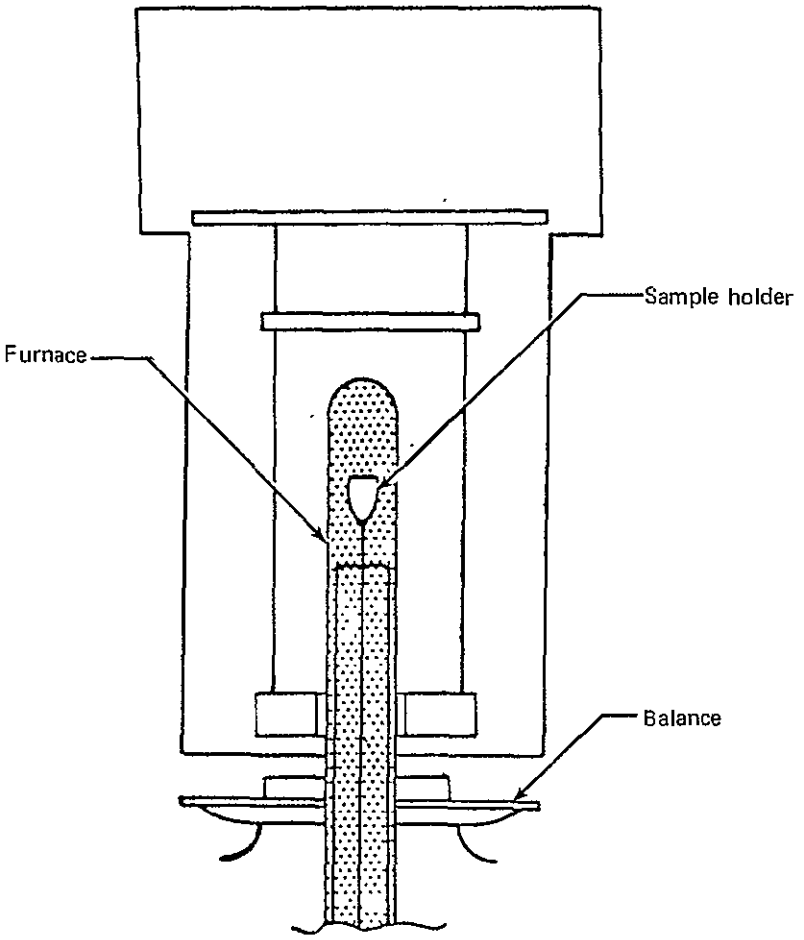

Figure D-1.—Mettler Thermal Balance

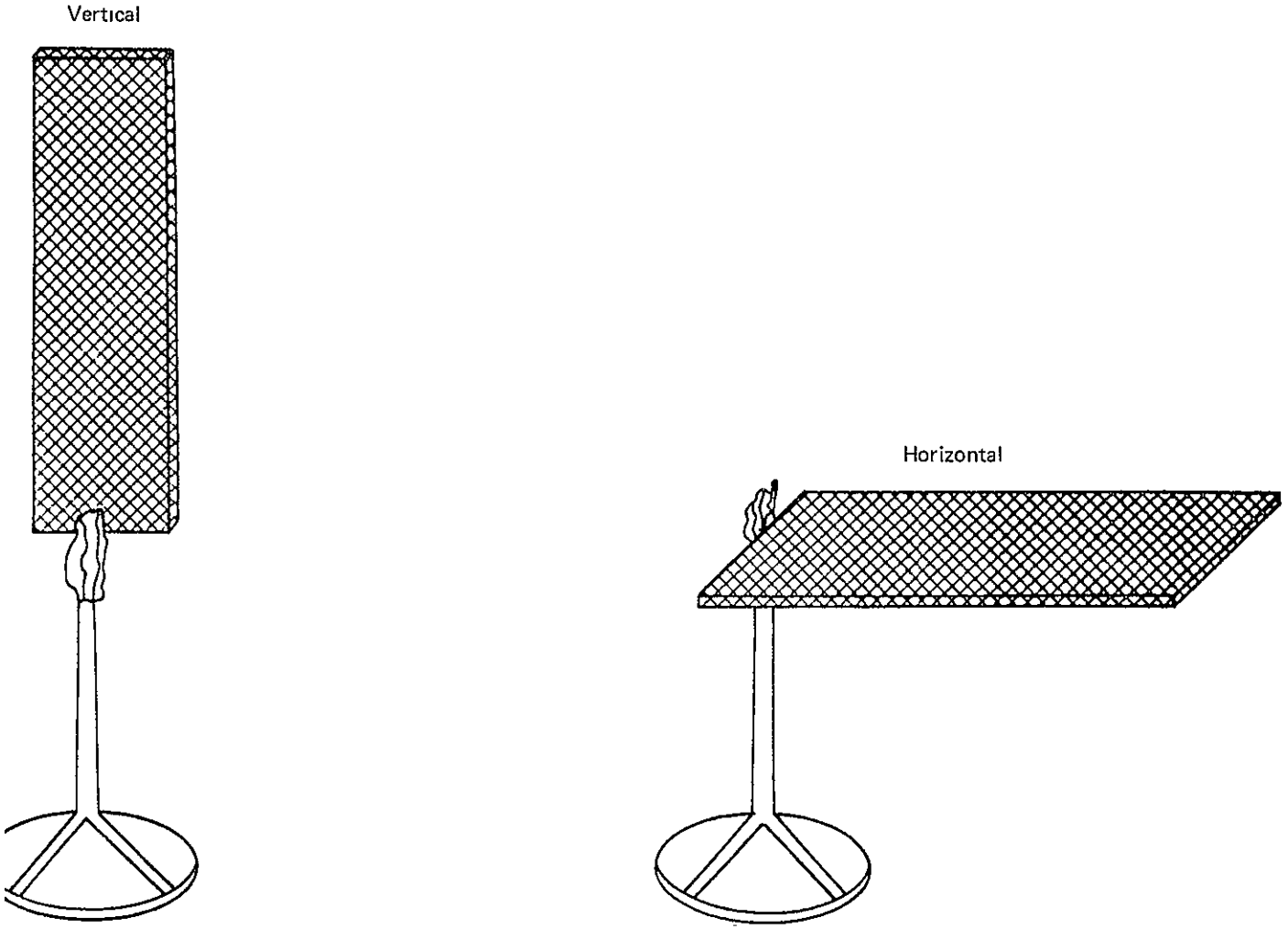

Figure D-2. FAR 25.853 Bunsen Burner Test

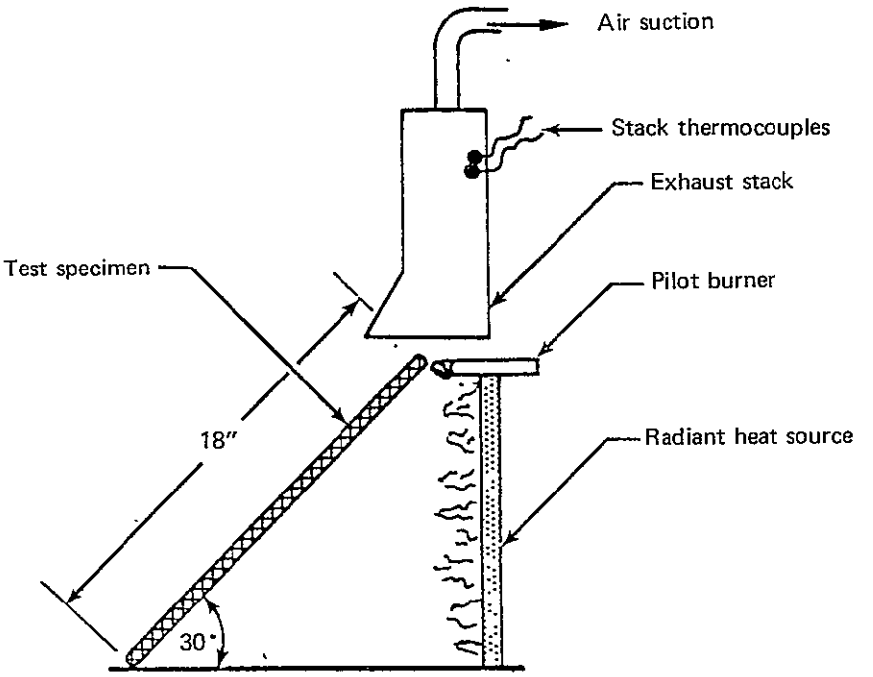

Figure D-3.—ASTM E162-67

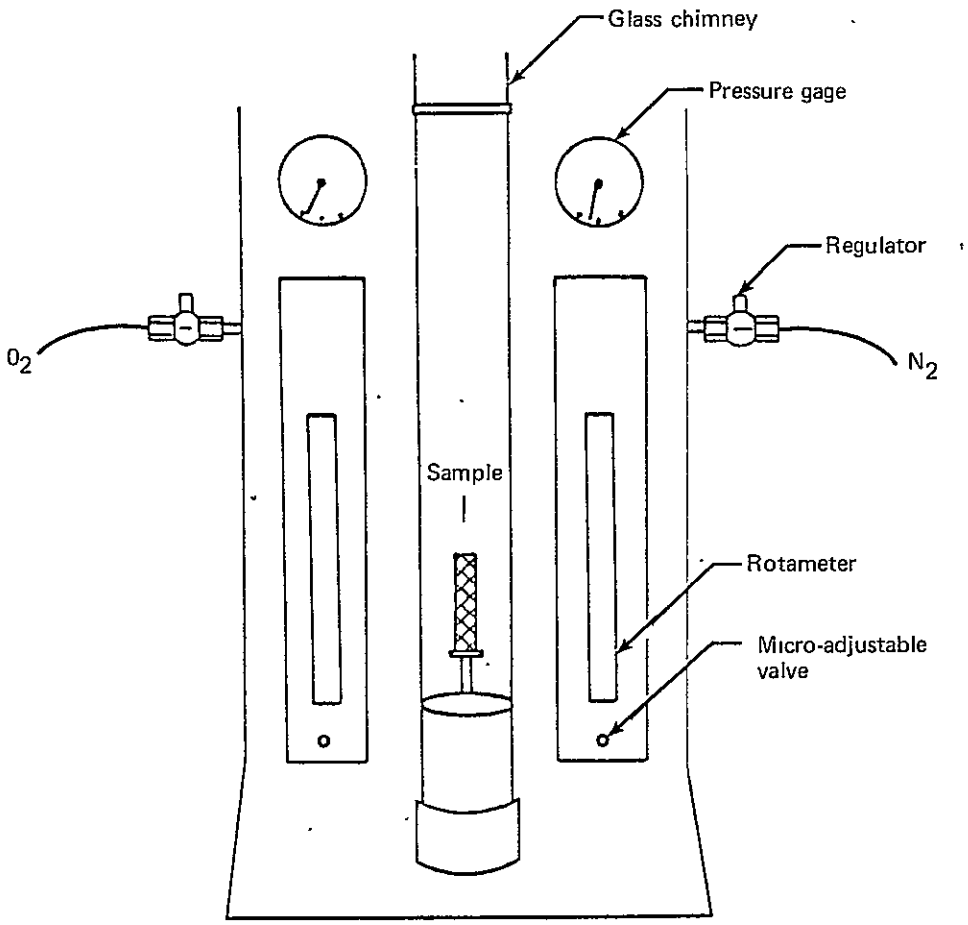

Figure D-4.—LOI Apparatus

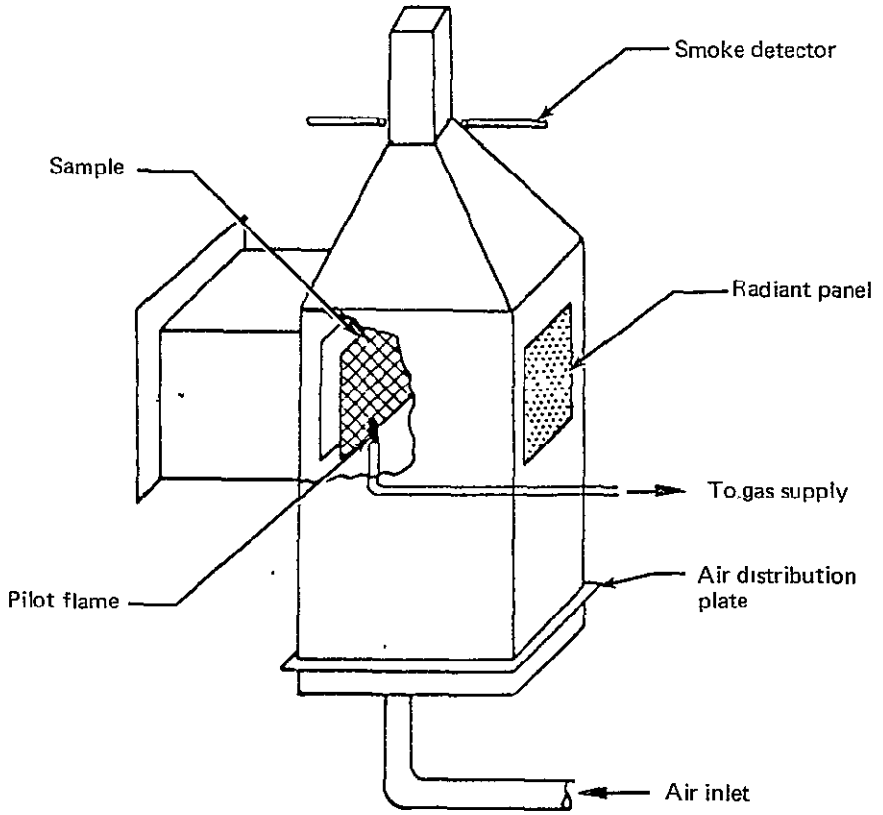

Figure D-5.—OSU Release Rate Apparatus

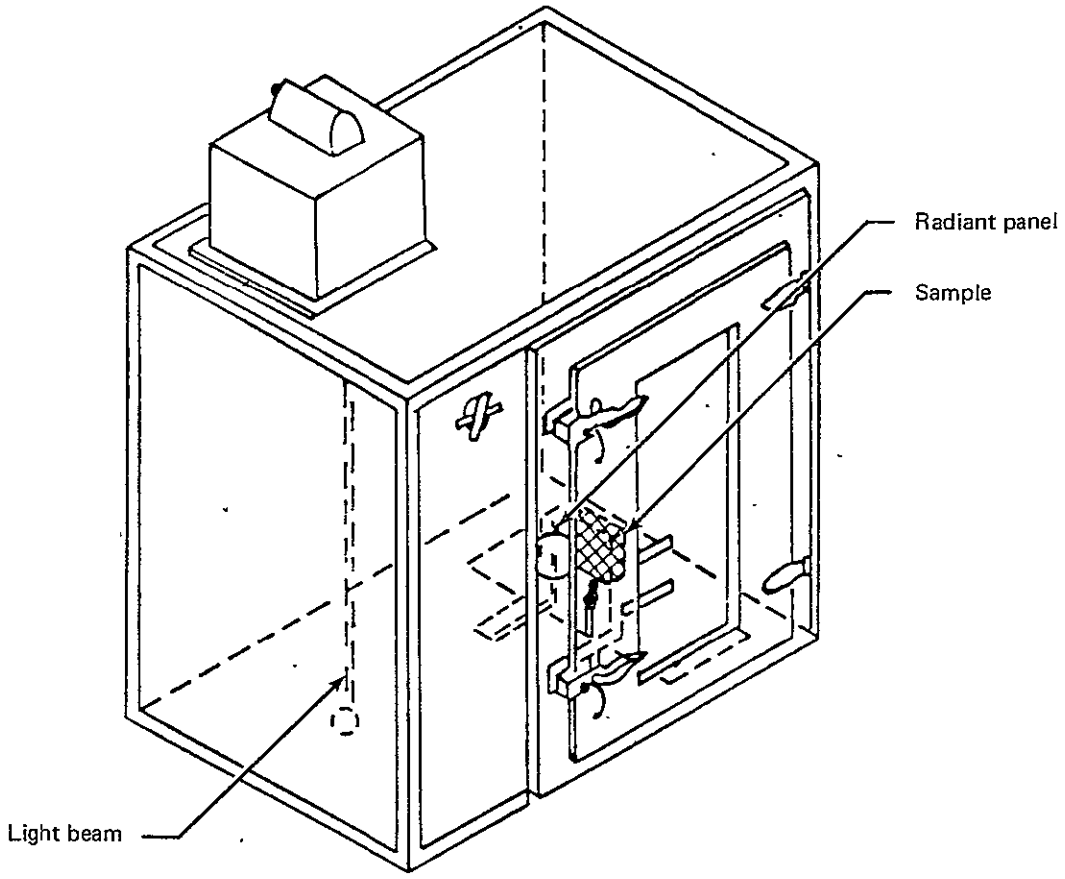

Figure D-6.—NBS Smoke Density Chamber

APPENDIX E
NEW MATERIALS DESCRIPTIONS, LABORATORY TEST DATA, AND LARGE SCALE TEST RESULTS

This appendix defines the new materials specimens and summarizes the results from the large scale and laboratory fire tests conducted on these materials. Laboratory data is displayed in the following order:

Table E-1	Materials Descriptions, Mettler Thermogravimetric Analysis Data, and Limiting Oxygen Index
Table E-2	Federal Aviation Regulations (FAR) 25.853 Bunsen Burner Test Data
Table E-3	Radiant Panel Test ASTM E162-67 Data
Table E-4	NBS Chamber Toxicant Concentrations
Figures E-1—E-11	Heat Release in the OSU Apparatus in the Vertical Bottom-Center Ignition Mode
Figures E-12—E-22	Smoke Release in the OSU Apparatus in the Vertical Bottom-Center Ignition Mode
Figures E-23—E-33	Smoke Release in the NBS Chamber in the Flaming Mode

The large scale fire test results are related for both post-crash and in-flight simulated design fire source conditions:

Figures E-34—E-55	Apparent Heat, Smoke, and Toxicant Release from Simulated Design Post-Crash Fire Source Tests—New Materials
Figures E-56—E-74	Apparent Heat, Smoke, and Toxicant Release from Simulated Design In-flight Fire Source Tests—New Materials

Table E-1.—Materials Descriptions, Mettler Thermogravimetric Analysis Data and Limiting Oxygen Index

N05 — Polyimide seat foam area density = 0.0141 g/cm^2 (0.0002 lb/in.^{2})*

Mettler — Flexible polyimide foam 2.54 cm (1 in.) thick, sample weight 6.00 mg, weight loss started 455°C.

W_1	W_2
93% (685°C)	7% residue

LOI = 37.26

N06/N07 — Floor/structural partition area density = 0.2463 g/cm^2 (0.0035 lb/in.^{2})

- Phenolic/unidirectional fiberglass skin, 0.0318 cm (0.0125 in.) thick
- FX resin adhesive
- Polyimide rigid foam, 0.953 cm (0.375 in.) thick, 80.09 kg/m^3 (5#/ft^3)
- FX resin adhesive
- Phenolic/unidirectional fiberglass skin, 0.0318 cm (0.0125 in.) thick

1. Mettler — Phenolic/fiberglass skin; sample wt 38.17 mg, wt loss started 120°C

W_1	W_2	W_3	W_4	W_5
2.4% (295°C)	2.2% (465°C)	16.8% (700°C)	2.7% (800°C)	75.9% residue

LOI = 100 (does not burn)

2. Mettler — Polyimide foam core; sample wt 6.15 mg, wt loss started 415°C

W_1	W_2
93.5% (800°C)	6.5% residue

LOI = 53.56

N08/N09 — Sidewall panel — area density = 0.1722 g/cm^2 (0.0024 lb/in.^{2})

- Polyvinylidene fluoride film
- Phenolic/unidirectional fiberglass skin, 0.0318 cm (0.0125 in.) thick
- FX resin adhesive
- Polyimide rigid foam, 0.6350 cm (0.25 in.) thick, 48.06 kg/m^3 (3#/ft^3)
- FX resin adhesive
- Phenolic/unidirectional fiberglass skin, 0.0229 cm (0.009 in.) thick

*N04 had a thickness 2x that of the lab sample, therefore its area density = 0.0282 g/cm^2 (0.0004 lb/in.^{2})

Table E-1.—(Continued)

1. Mettler — Polyvinylidene fluoride film (white), sample wt 13.22 mg, wt loss started 340°C				
W_1		W_2		W_3
50.8% (435°C)		44.6% (620°C)		4.6% residue
2. Mettler — Phenolic/fiberglass skin - 0.0318 cm thick; sample wt 38.17 mg, wt loss started 120°C.				
W_1	W_2	W_3	W_4	W_5
2.4% (295°C)	2.2% (465°C)	16.8% (700°C)	2.7% (800°C)	75.9% residue
LOI = 100 (XMP 100 skin only)				
LOI = 88.96 (XMP 100 skin + polyvinylidene film)				
3. Mettler — Polyimide rigid foam 48.06 kg/m^3; specimen wt 6.97 mg; wt loss start 395°C				
W_1		W_2		
42.8% (790°C)		57.2% (residue)		
LOI = 49.52				
4. Mettler — Phenolic/fiberglass skin 0.0229 cm thick; specimen wt 35.26 mg; wt loss start 60°C				
W_1		W_2		W_3
7.7% (460°C)		30.0% (750°C)		62.3% (residue)
LOI = 74.62				
N10/N11 — "Naugahyde" replacement — area density = 0.0127 g/cm^2 (0.0002 lb/in.^{2})				
1. Mettler — Polyimide coated fiberglass 0.2392 gm/m^2 (3.2 oz/yd^2); specimen wt 14.77 mg, wt loss start 280°C				
W_1		W_2		
19.8% (640°C)		80.2% (residue)		
LOI = 100 (will not burn)				
N12/N13 — Polyimide thermoplastic replacement — area density = 0.2756 g/cm^2 (0.0039 lb/in.^{2})				
1. Mettler — Polyimide moldable material 0.2286 cm thick; specimen wt 16.62 mg; wt loss start 410°C				
W_1		W_2		
60.7% (745°C)		39.3% (residue)		
LOI = 64.76				

Table E-1.—(Continued)

N14/N15 — Floor board — area density = 0.3617 g/cm^2 (0.0051 lb/in.^{2})
——— Phenolic/unidirectional fiberglass skin 0.0318 cm (0.0125 in.) thick ∪∪∪∪ Phenolic resin adhesive (Narmco 9251)  Polyimide foam filled polyamide/phenolic honeycomb core, 0.9525 cm (0.3750 in.) thick, 144.17 kg/m^3 (9 #ft^3) ∪∪∪∪ Phenolic resin adhesive (Narmco 9251) ——— Phenolic/unidirectional fiberglass skin 0.0318 cm (0.0125 in.) thick
1. Mettler — Phenolic/fiberglass skin with phenolic resin adhesive; specimen wt 18.70 mg, wt loss start 275°C W_1 W_2 W_3 W_4 11.3% (420°C) 15.8% (535°C) 56.3% (685°C) 16.6% (residue) LOI = 100 (Phenolic/fiberglass skin only)
2. Mettler — Polyimide foam filled polyamide/phenolic honeycomb; specimen wt 24.79 mg; wt loss start 50°C W_1 W_2 W_3 W_4 3.5% (290°C) 7.5% (450°C) 87.9% (910°C) 1.1% (residue) LOI = 45.15
3. Mettler — Phenolic/fiberglass skin with phenolic resin adhesive; specimen wt 18.70 mg, wt loss start 275°C W_1 W_2 W_3 W_4 11.3% (420°C) 15.8% (535°C) 56.3% (685°C) 16.6% (residue) LOI = 100 (Phenolic/fiberglass skin only)
N16/N17 — Ceiling panel laminate — area density = 0.1636 g/cm^2 (0.0023 lb/in^2)
——— Phenolic/fiberglass laminate 0.1016 cm (0.040 in.) thick ——— Polyvinylidene fluoride film
1. Mettler — Phenolic/fiberglass laminate; specimen wt 46.60 mg; wt loss start 205°C W_1 W_2 W_3 0 7% (300°C) 25.8% (720°C) 73.5% (residue) LOI = 58.31

Table E-1.–(Concluded)

2. Mettler – Polyvinylidene film (clear); specimen wt 13.89 mg; wt loss start 290°C W_1 W_2 W_3 W_4 4.1% (350°C) 59.2% (500°C) 35.0% (645°C) 1.7% (residue) LOI = 51.13
N18/N19 – Air ducting – area density = 0.1257 g/cm^2 (0.0018 lb/in.^{2})
1. Mettler – FX resin fiberglass laminate 0.0711 cm (0.028 in.) thick; specimen wt 27.75 mg, wt loss start 70°C W_1 W_2 41.6% (700°C) 58.4% (residue) LOI = 53.79
N21 – Thermal/acoustical insulation – area density = 0.0129 g/cm^2 (0.0002 lb/in.^{2}) **
1. Mettler – Flexible polyimide foam 2.54 cm (1 in.) thick; specimen wt 6.12 mg; wt loss start 410°C W_1 W_2 93.5% (695°C) 6.5% (residue) LOI = 37.56
N22/N23 – Thermoplastic replacement – Monsanto – area density = 0.2971 g/cm^2 (0.0042 lb/in.^{2})
1. Mettler – Monsanto E200-3Z, 0.2286 cm (0.090 in.) thick; specimen wt 16.04 mg, wt loss start 370°C) W_1 W_2 W_3 64.5% (530°C) 31.9% (665°C) 3.6% (residue) LOI = 35.94
N24/N25 – Thermoplastic replacement – area density = 0.3014 g/cm^2 (0.0043 lb/in.^{2})
1. Mettler – Inorganic resin system (IRS)/glass fiber panels, 0.2286 cm (0.90 in.) thick, specimen wt 34.48 mg ; wt loss start 60° C) W_1 W_2 W_3 W_4 16.8% (325°C) 18.0% (545°C) 5.6% (780°C) 59.6% (residue) LOI = 100 (will not burn)

**N20 had a thickness 3x that of the lab sample, therefore its area density = 0.0387 g/cm^2 (0.0006 lb/in.^{2})

Table E-2.—Federal Aviation Regulations FAR 25.853 Bunsen Burner Test Data

Description	12 second vertical	60 second vertical
N05 Polyimide seat foam	Burn length = 2.12 cm (0.83 in.) Extinguishing time = 0 sec	
N07 Floor/structural partition		Burn length = 1.61 cm (0.63 in.) Extinguishing time = 0 sec
N09 Sidewall panel		Burn length = 1.78 cm (0.70 in.) Extinguishing time = 0 sec
N11 "Naugahyde" replacement	Burn length = 3.39 cm (1.33 in.) Extinguishing time = 0 sec	Burn length = 4.83 cm (1.9 in.) Extinguishing time = 0 sec
N13 Polyimide thermoplastic replacement		Burn length = 1.86 cm (0.73 in.) Extinguishing time = 0 sec
N15 Floor board		Burn length = 3.22 cm (1.27 in.) Extinguishing time = 0.1 sec
N17 Ceiling panel laminate	Burn length = 1.20 cm (0.47 in.) Extinguishing time = 0 sec	Burn length = 4.49 cm (1.8 in.) Extinguishing time = 0 sec
N19 Air ducting	Burn length = 3.47 cm (1.37 in.) Extinguishing time = 0 sec	
N21 Thermal/ acoustical insulation	Burn length = 3.64 cm (1.43 in.) Extinguishing time = 0 sec	
N23 Thermoplastic replacement— Monsanto		Burn length = 5.33 cm (2.1 in.) Extinguishing time = 0.70 sec
N25 Thermoplastic replacement		Burn length = 0 cm (0 in.) Extinguishing time = 0 sec

Table E-3.—Radiant Panel Test ASTM E162-67 Data

Description	Flame spread factor (F_s)	Heat evolution factor (Q)	Index ($I_s = F_s \times Q$)
N05 Polyimide seat foam	1.00	1.64	1.64
N07 Floor/ structural partition	1.00	1.76	1.76
N09 Sidewall panel	1.89	1.67	3.19
N11 "Naugahyde" replacement	1.00	1.50	1.50
N13 Polyimide thermoplastic replacement	1.00	1.72	1.72
N15 Floor board	1.00	1.64	1.64
N17 Ceiling panel laminate	1.00	2.32	2.32
N19 Air ducting	1.00	2.68	2.68
N21 Thermal/ acoustical insulation	1.00	1.71	1.71
N23 Thermoplastic replacement— Monsanto	9.56	26.11	246.21
N25 Thermoplastic replacement	1.00	2.11	2.11

Note: Data is an average of 4 specimens

Table E-4.—NBS Chamber Toxicant Concentrations

The gas collection initiated times are listed. Where bubblers were used the collection period was for 150 seconds. NO_x was always sampled using a Drager tube whose collection period was for 100 seconds. CO was tested for using an NDIR meter.

	HCN	HCL	HF	NO_x	CO	HBR
N05						
2.5 w/fl*	—	—	—	—	—	—
1.5 min	0	15	0	trace	25	—
4.0 min	0	27	0	trace	46	—
5.0 w/fl*	—	—	—	—	—	—
1.5 min	32	5	5	5	188	—
4.0 min	30	7	4	10	670	—
N07 (N06)						
2.5 w/fl*	—	—	—	—	—	—
1.5 min	3	34	0	2	20	—
4.0 min	3	33	0	3	59	—
5.0 w/fl*	—	—	—	—	—	—
1.5 min	14	20	0	2	81	—
4.0 min	17	—	0	10	303	—
N09 (N08)						
2.5 w/fl*	—	—	—	—	—	—
1.5 min	trace	55	0	3.0	32	—
4.0 min	3.0	96	0	trace	111	—
5 w/fl*	—	—	—	—	—	—
1.5 min	18	32	216	4	176	—
4.0 min	22	39	124	5	410	—
N11 (N10)						
2.5 w/fl*	—	—	—	—	—	—
1.5 min	0	4	0	trace	12	—
4.0 min	0	5	0	trace	18	—
5.0 w/fl*	—	—	—	—	—	—
1.5 min	0	8	5	trace	17	—
4.0 min	0	7	0	1.0	30	—
N13 (N12)						
2.5 w/fl*	—	—	—	—	—	—
1.5 min	0	21	0	0	11	—
4.0 min	0	54	0	2	29	—
5.0 w/fl*	—	—	—	—	—	—
1.5 min	24	11	0	4	5	—
4.0 min	28	8	0	1	152	—

Table E-4.—NBS Chamber Toxicant Concentrations (Concluded)

	HCN	HCL	HF	NOx	CO	HBR
N15 (N14)						
2.5 w/fl*	—	—	—	—	—	—
1.5 min	—	—	—	—	—	—
4.0 min	trace	27	—	5	19	0
5.0 w/fl*	—	—	—	—	—	—
1.5 min	15	0	—	18	76	0
4.0 min	33	0	—	30	310	0
N17 (N16)						
2.5 w/fl*	—	—	—	—	—	—
1.5 min	0	8	42	trace	16	—
4.0 min	0	25	41	trace	54	—
5.0 w/fl*	—	—	—	—	—	—
1.5 min	0	20	176	2	36	—
4.0 min	4	19	164	2	128	—
N19 (N18)						
2.5 w/fl*	—	—	—	—	—	—
1.5 min	0	6	0	0	11	—
4.0 min	0	8	0	0	68	—
5.0 w/fl*	—	—	—	—	—	—
1.5 min	0	8	1	0	53	—
4.0 min	0	4	0	1	215	—
N21						
2.5 w/fl*	—	—	—	—	—	—
1.5 min	0	8	0	trace	14	—
4.0 min	2	20	0	trace	39	—
5.0 w/fl*	—	—	—	—	—	—
1.5 min	32	11	1	trace	87	—
4.0 min	34	5	2	3	423	—
N23 (N22)						
2.5 w/fl*	—	—	—	—	—	—
1.5 min	0	9	0	0	11	—
4.0 min	2	10	0	trace	133	—
5.0 w/fl*	—	—	—	—	—	—
1.5 min	0	5	0	trace	70	—
4.0 min	0	5	0	trace	293	—
N25 (N24)						
2.5 w/fl*	—	—	—	—	—	—
1.5 min	0	37	0	trace	10	—
4.0 min	0	38	0	trace	15	—
5.0 w/fl*	—	—	—	—	—	—
1.5 min	0	103	6	0	4	—
4.0 min	0	253	9	0	23	—

*W/cm^2 — flaming mode

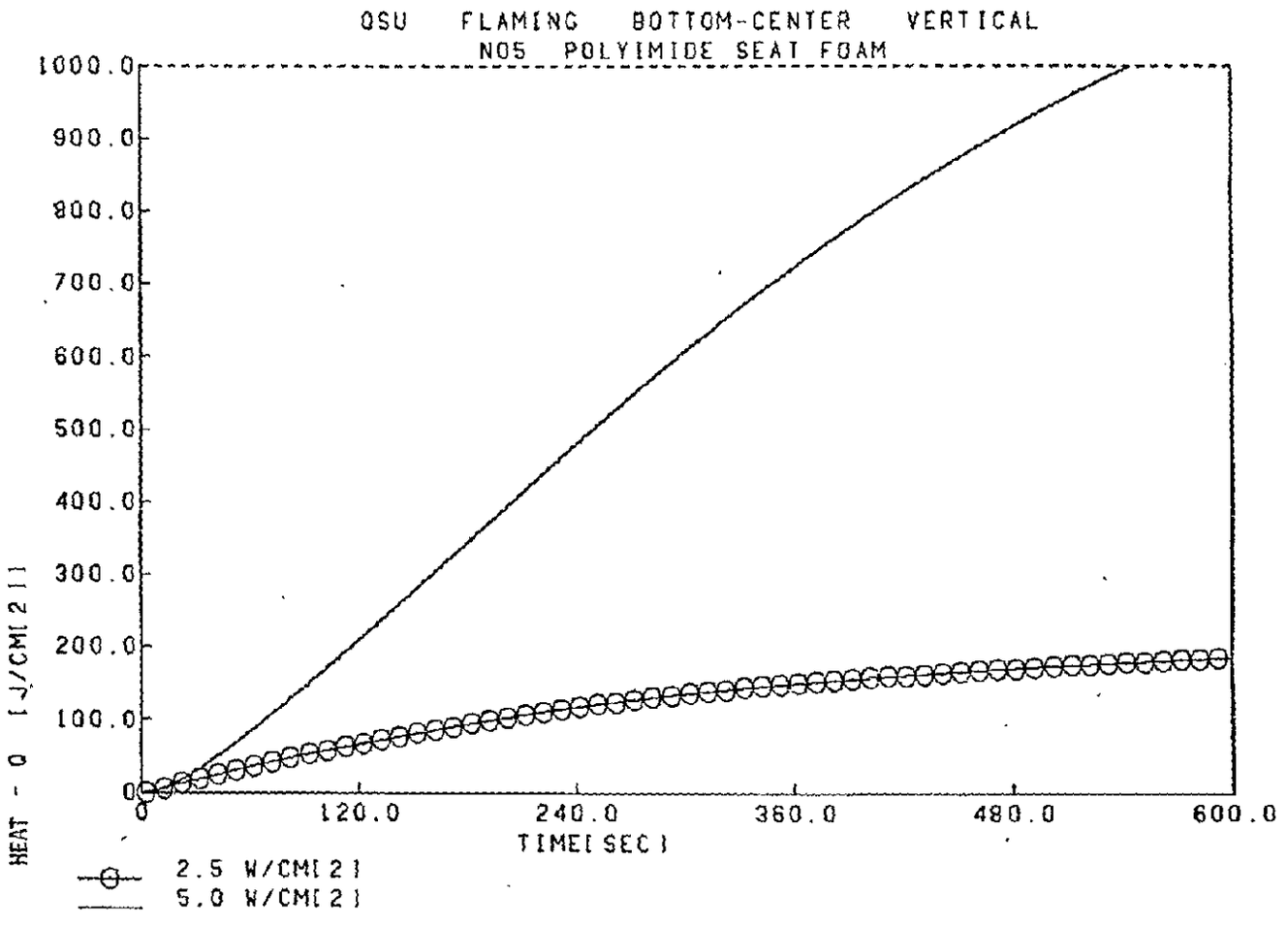

Figure E-1.—Heat Release in the OSU Apparatus in the Vertical Bottom-Center Ignition Mode—N05

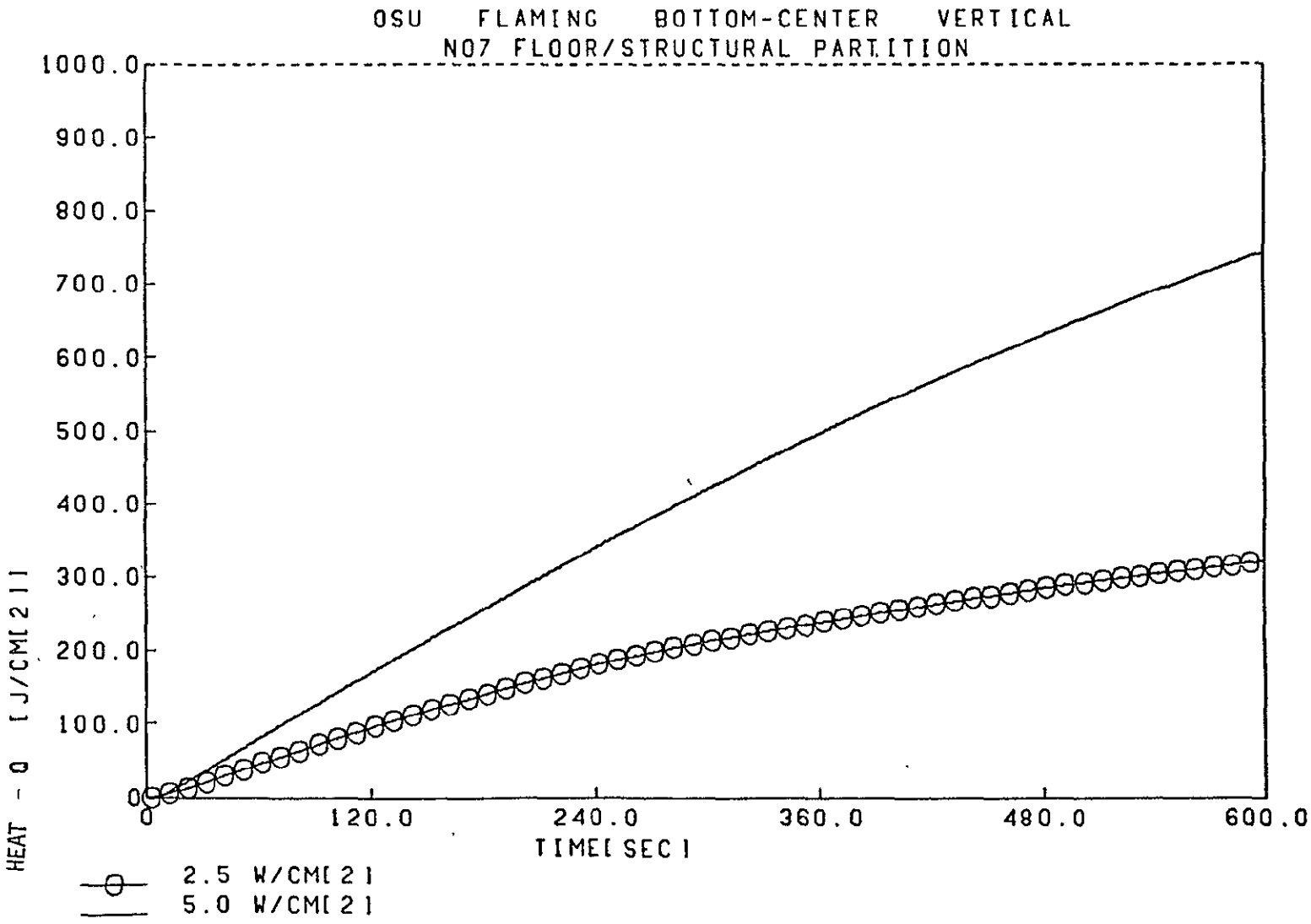

Figure E-2.—Heat Release in the OSU Apparatus in the Vertical Bottom-Center Ignition Mode—N06/N07

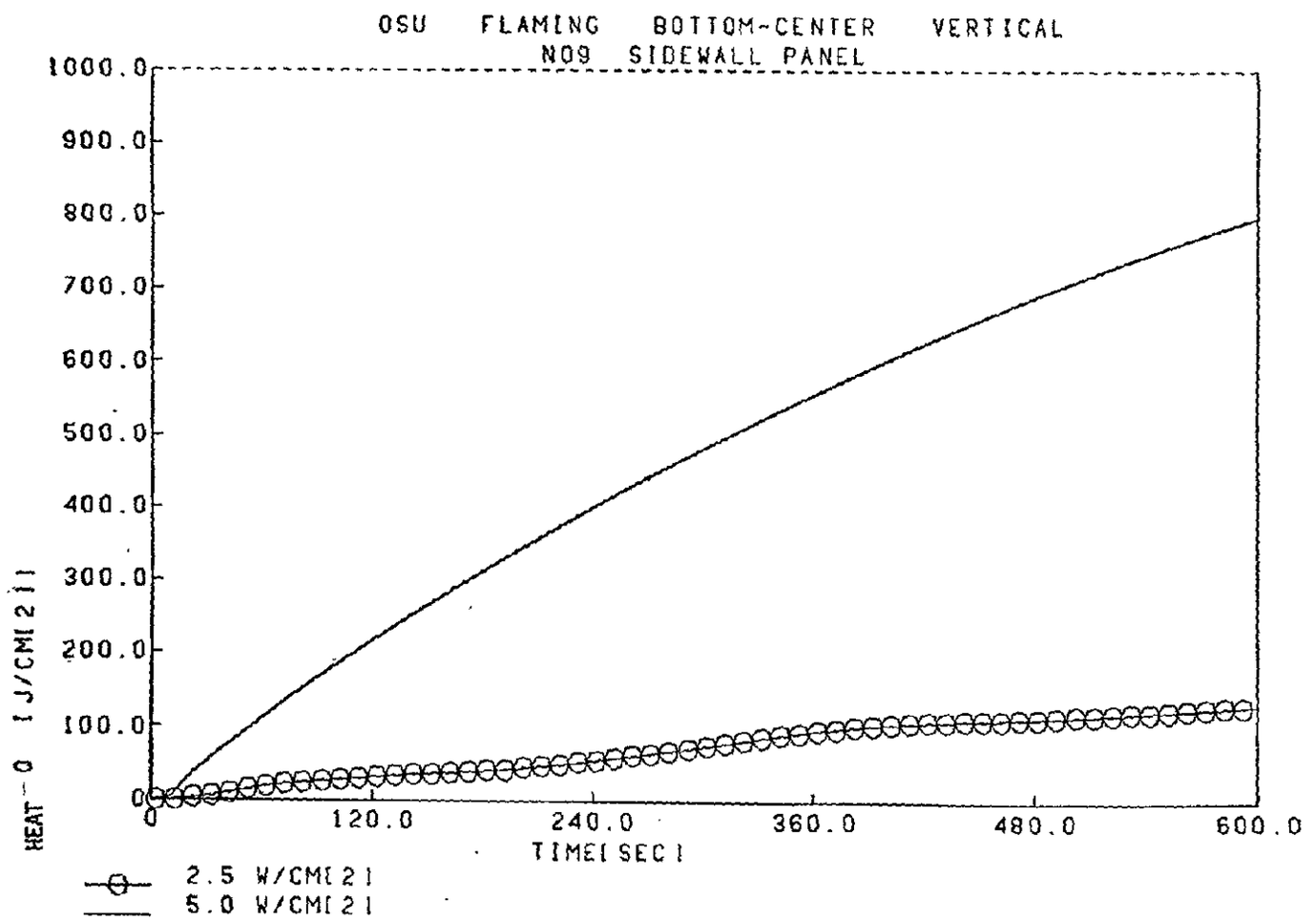

Figure E-3.—Heat Release in the OSU Apparatus in the Vertical Bottom-Center Ignition Mode—N08/N09

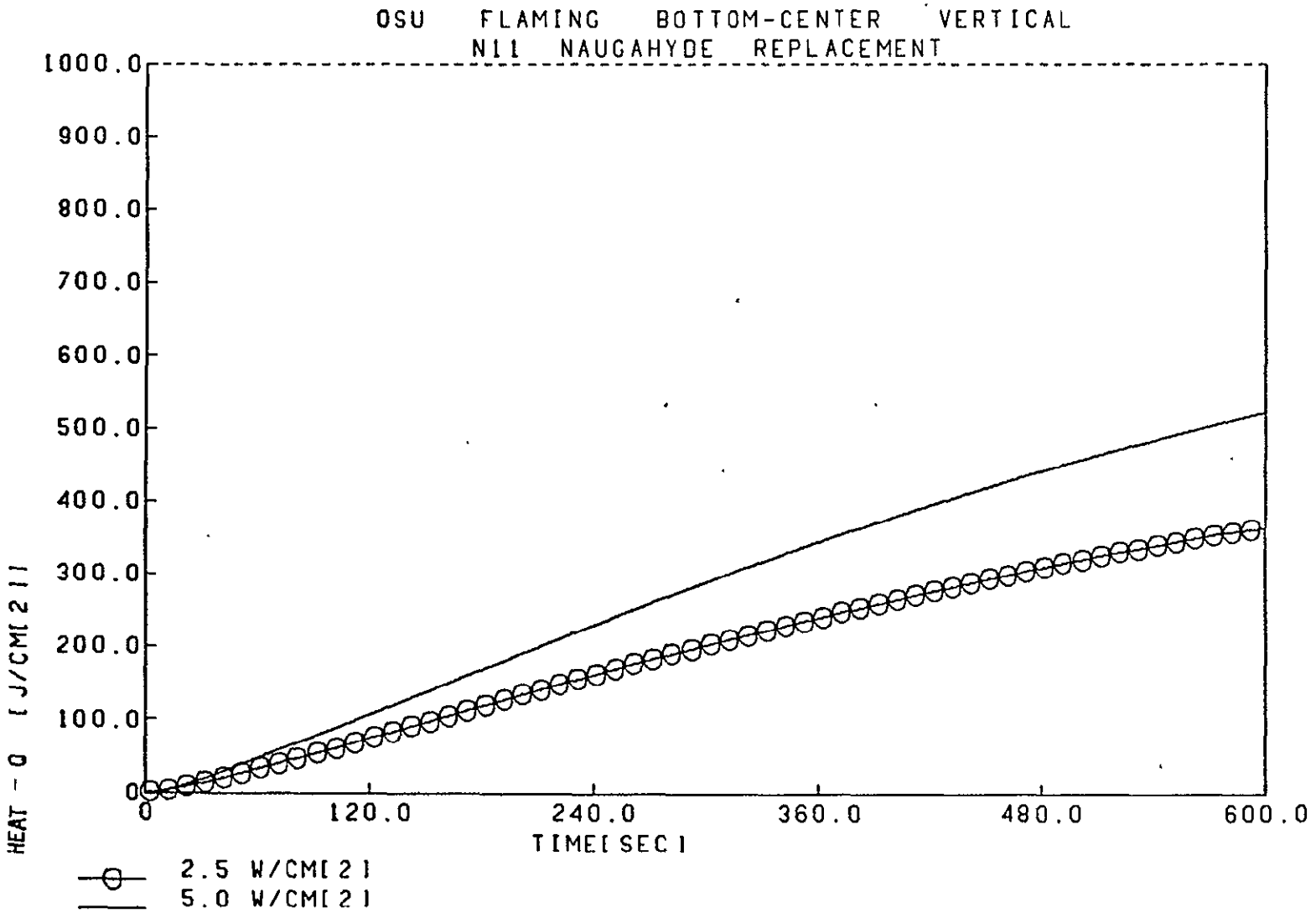

Figure E-4.—Heat Release in the OSU Apparatus in the Vertical Bottom-Center Ignition Mode—N10/N11

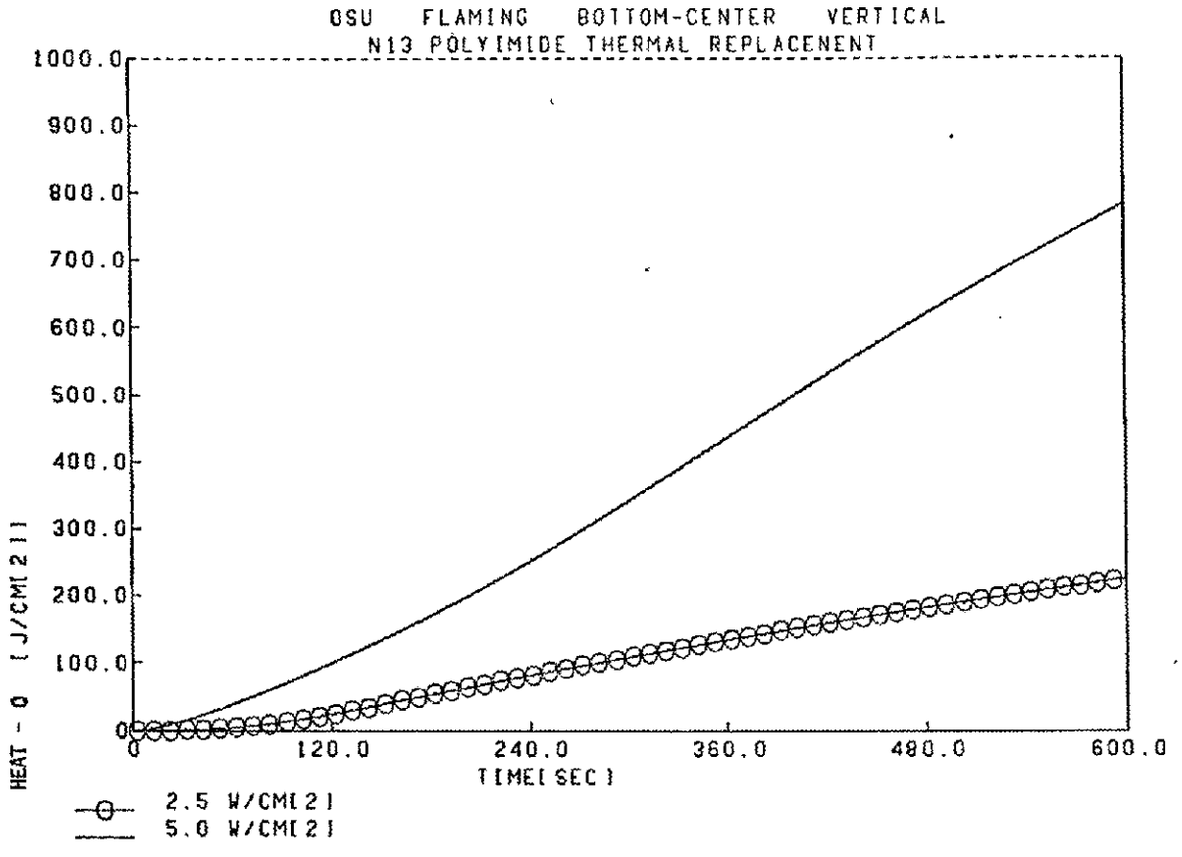

Figure E-5.—Heat Release in the OSU Apparatus in the Vertical Bottom-Center Ignition Mode—N12/N13

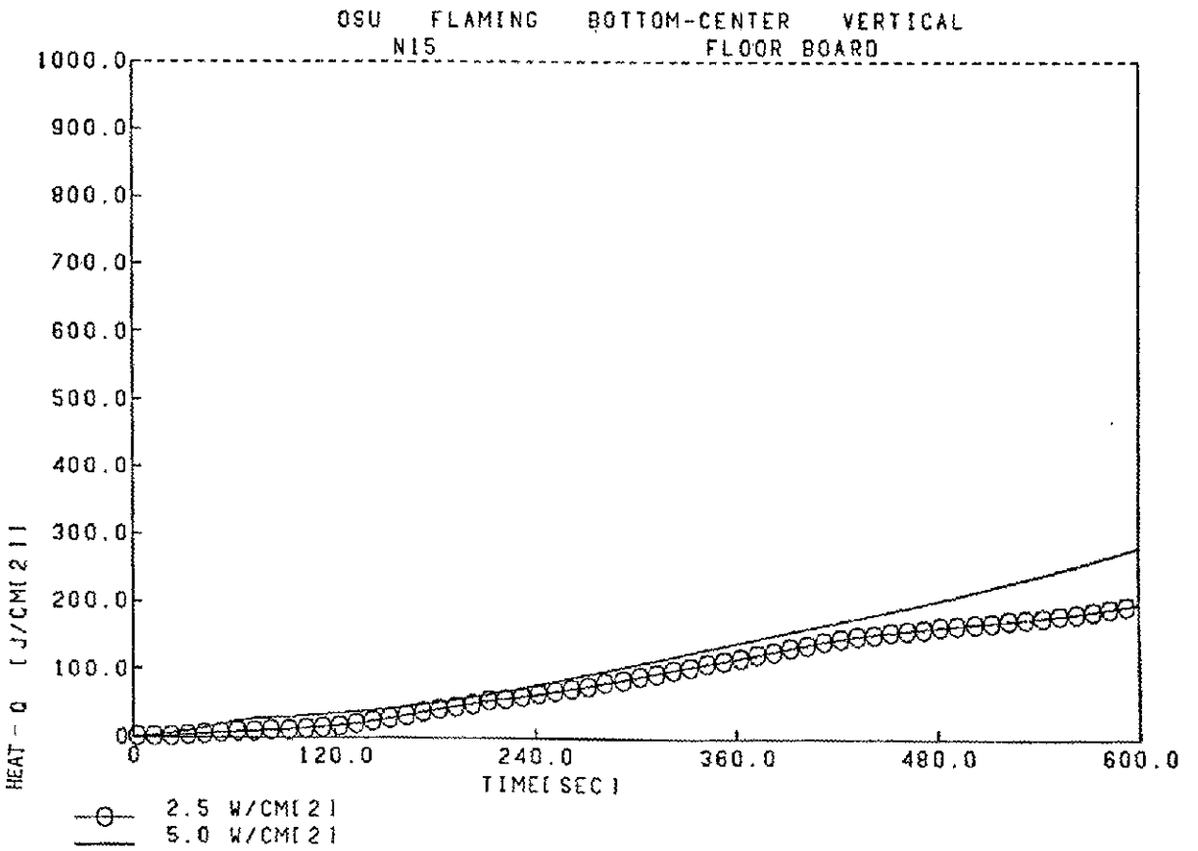

Figure E-6.—Heat Release in the OSU Apparatus in the Vertical Bottom-Center Ignition Mode—N14/N15

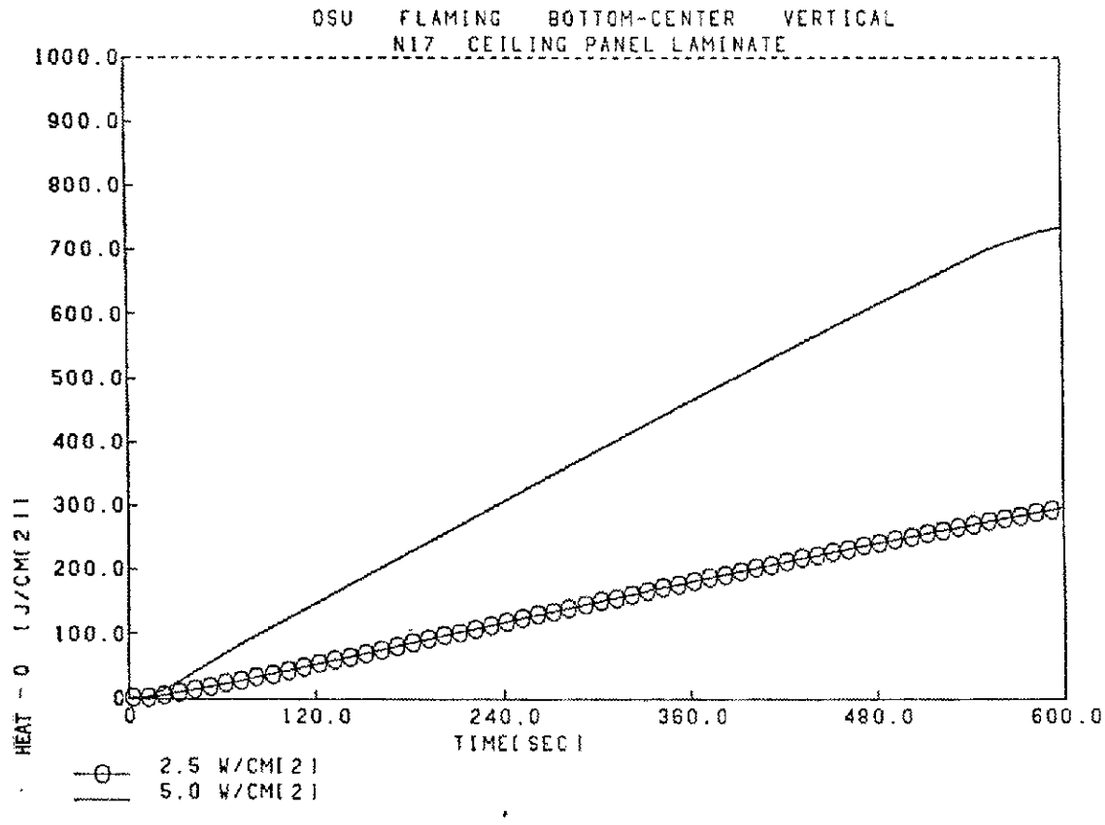

Figure E-7.—Heat Release in the OSU Apparatus in the Vertical Bottom-Center Ignition Mode—N16/N17

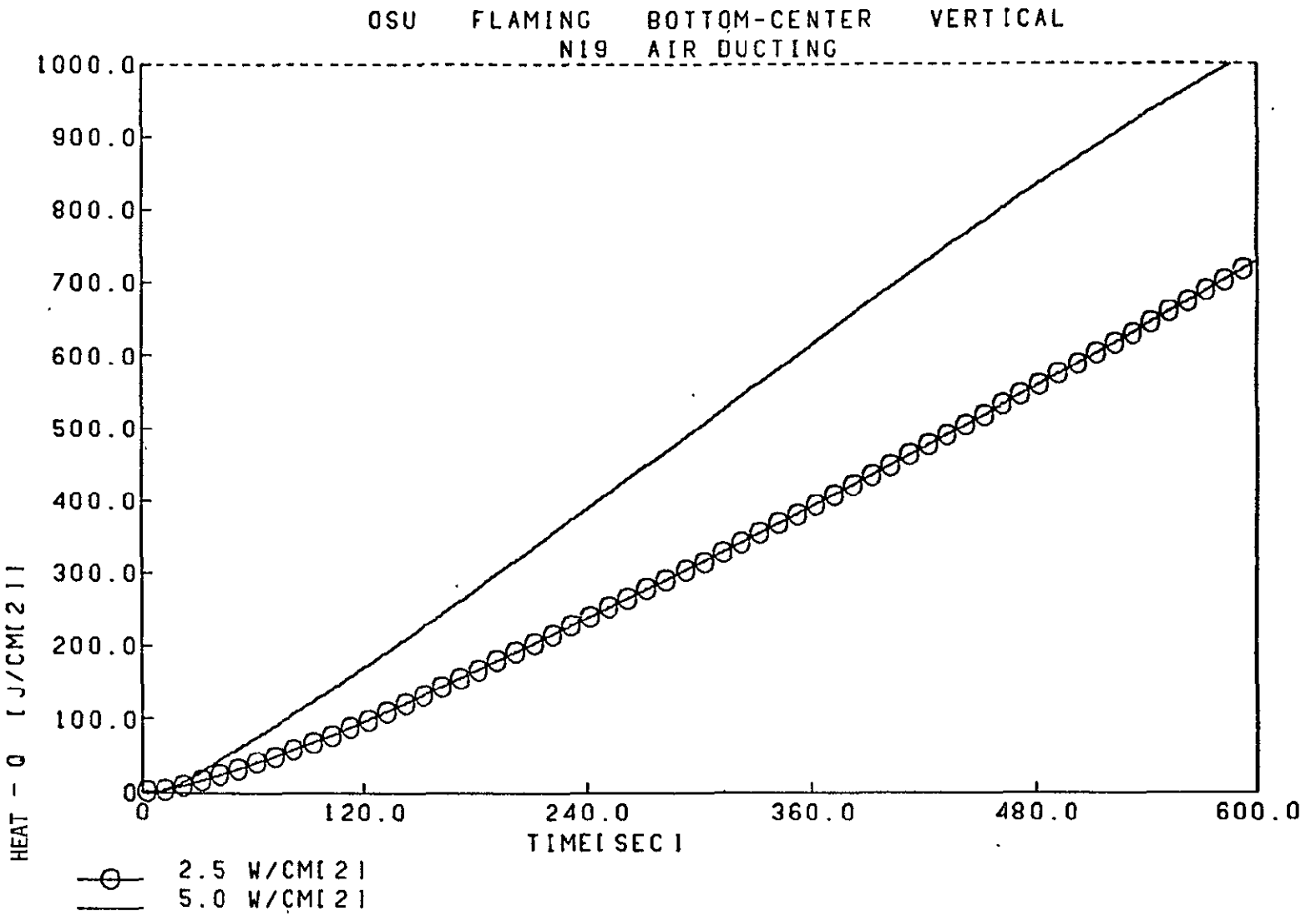

Figure E-8.—Heat Release in the OSU Apparatus in the Vertical Bottom-Center Ignition Mode—N18/N19

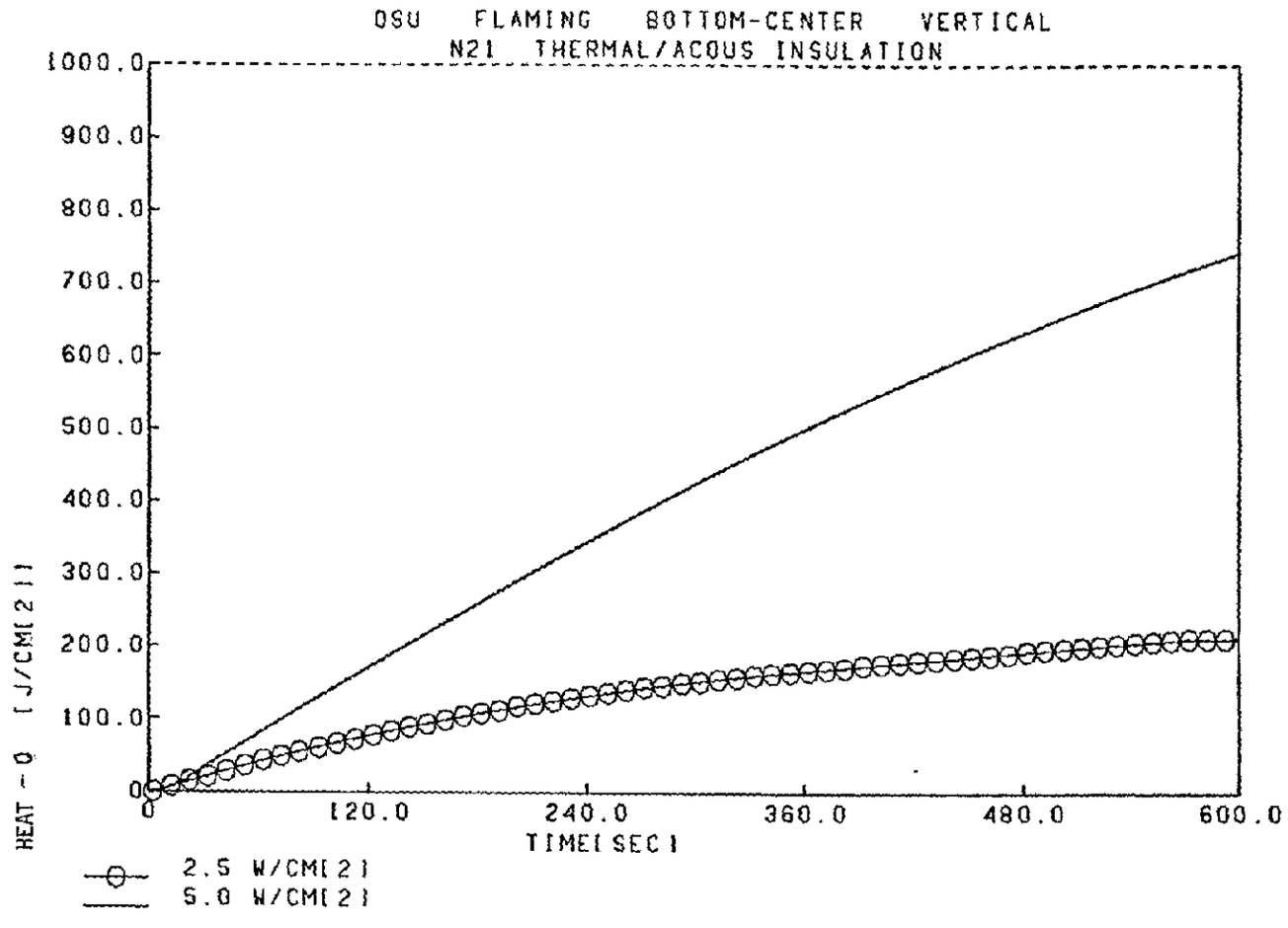

Figure E-9.—Heat Release in the OSU Apparatus in the Vertical Bottom-Center Ignition Mode--N21

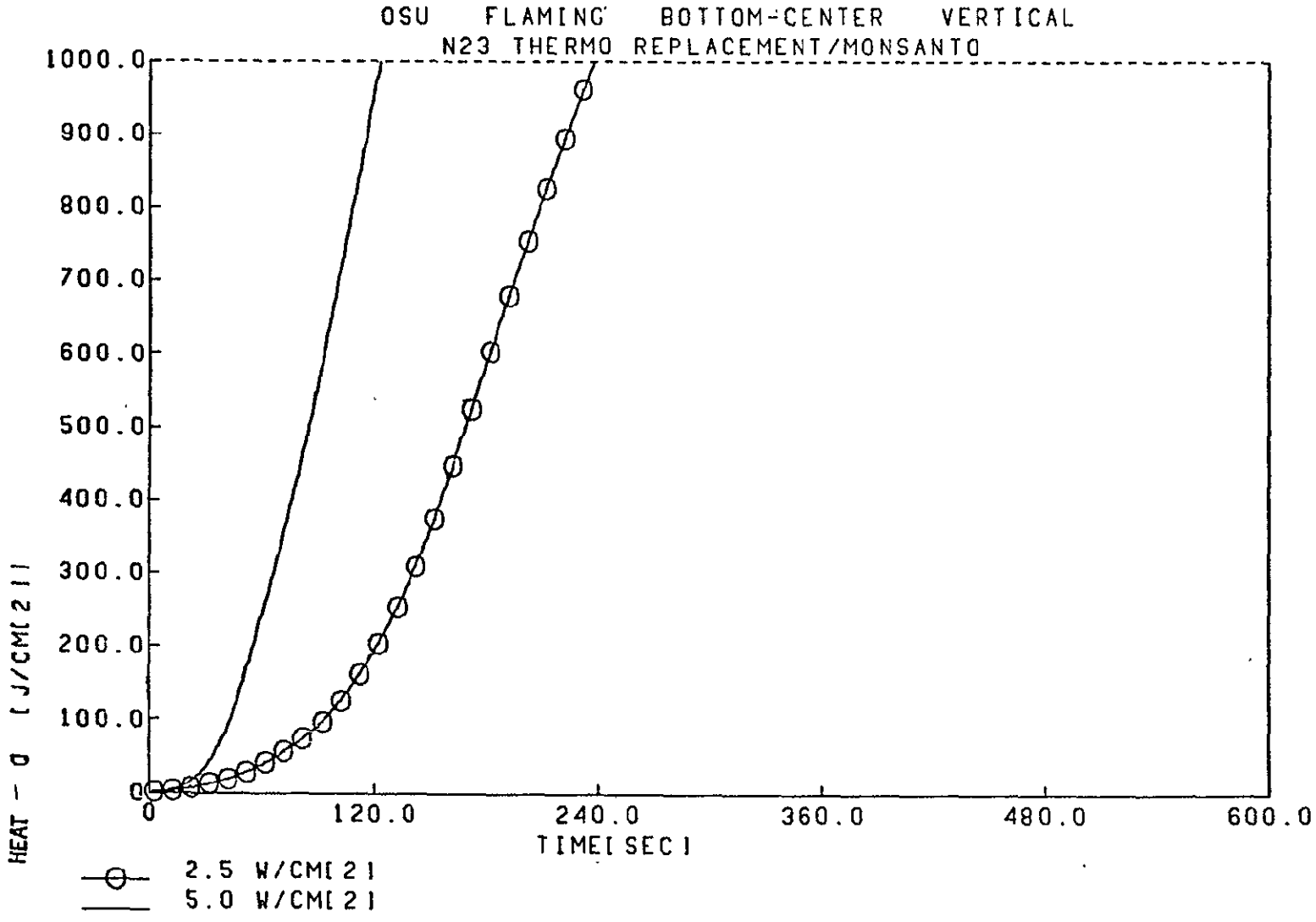

Figure E-10.—Heat Release in the OSU Apparatus in the Vertical Bottom-Center Ignition Mode—N22/N23

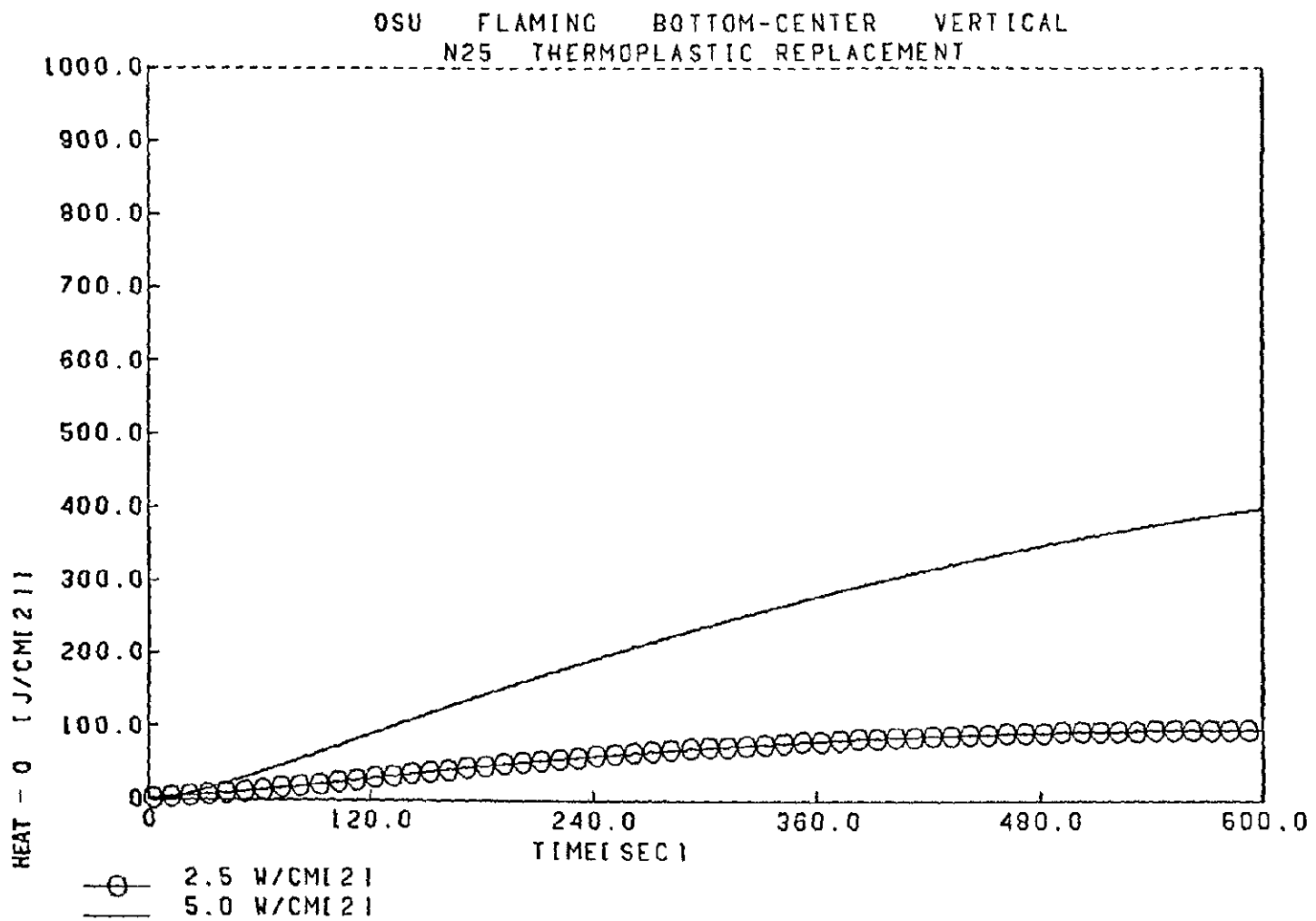

Figure E-11.—Heat Release in the OSU Apparatus in the Vertical Bottom-Center Ignition Mode—N24/N25

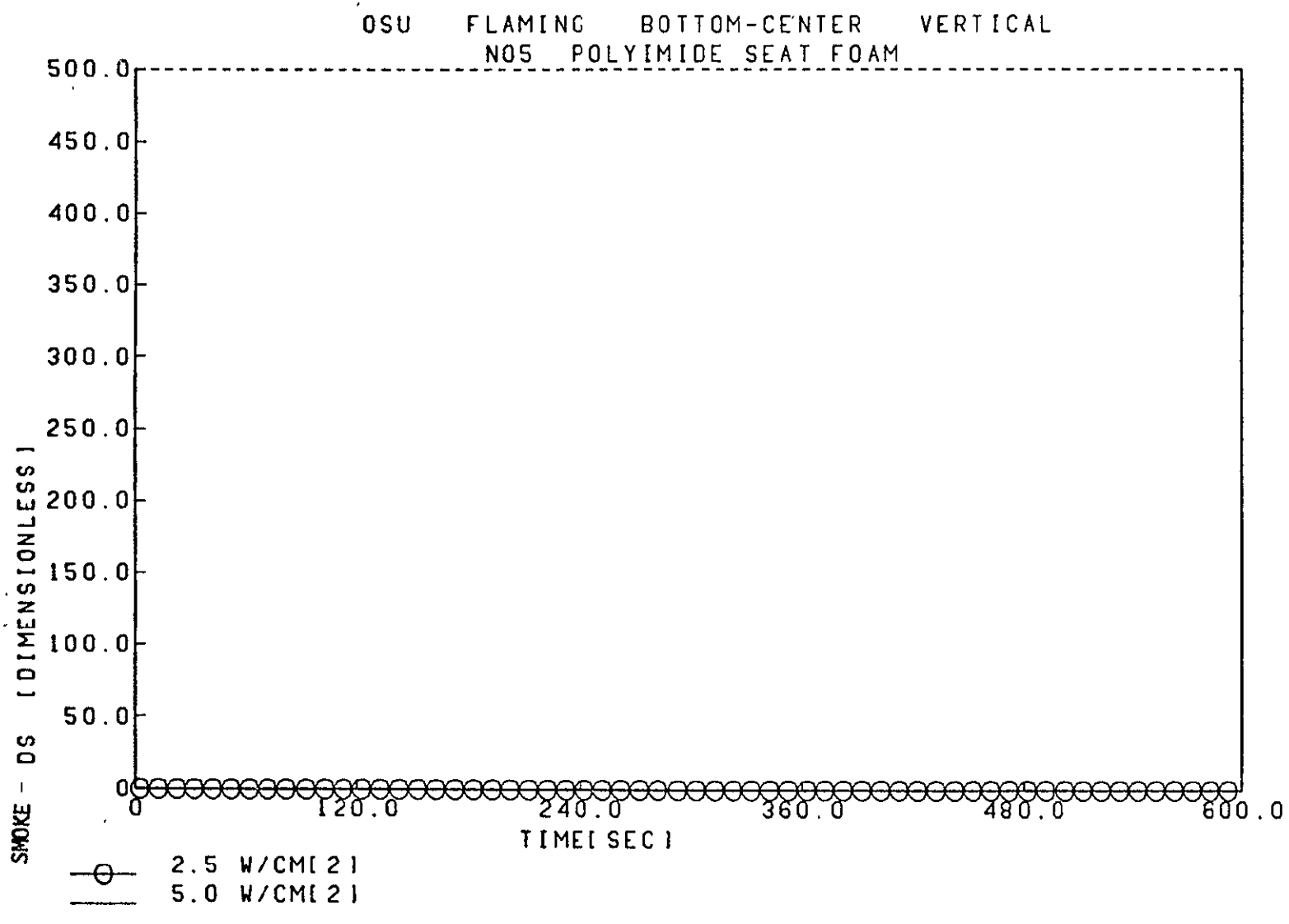

Figure E-12.—Smoke Release in the OSU Apparatus in the Vertical Bottom-Center Ignition Mode—N05

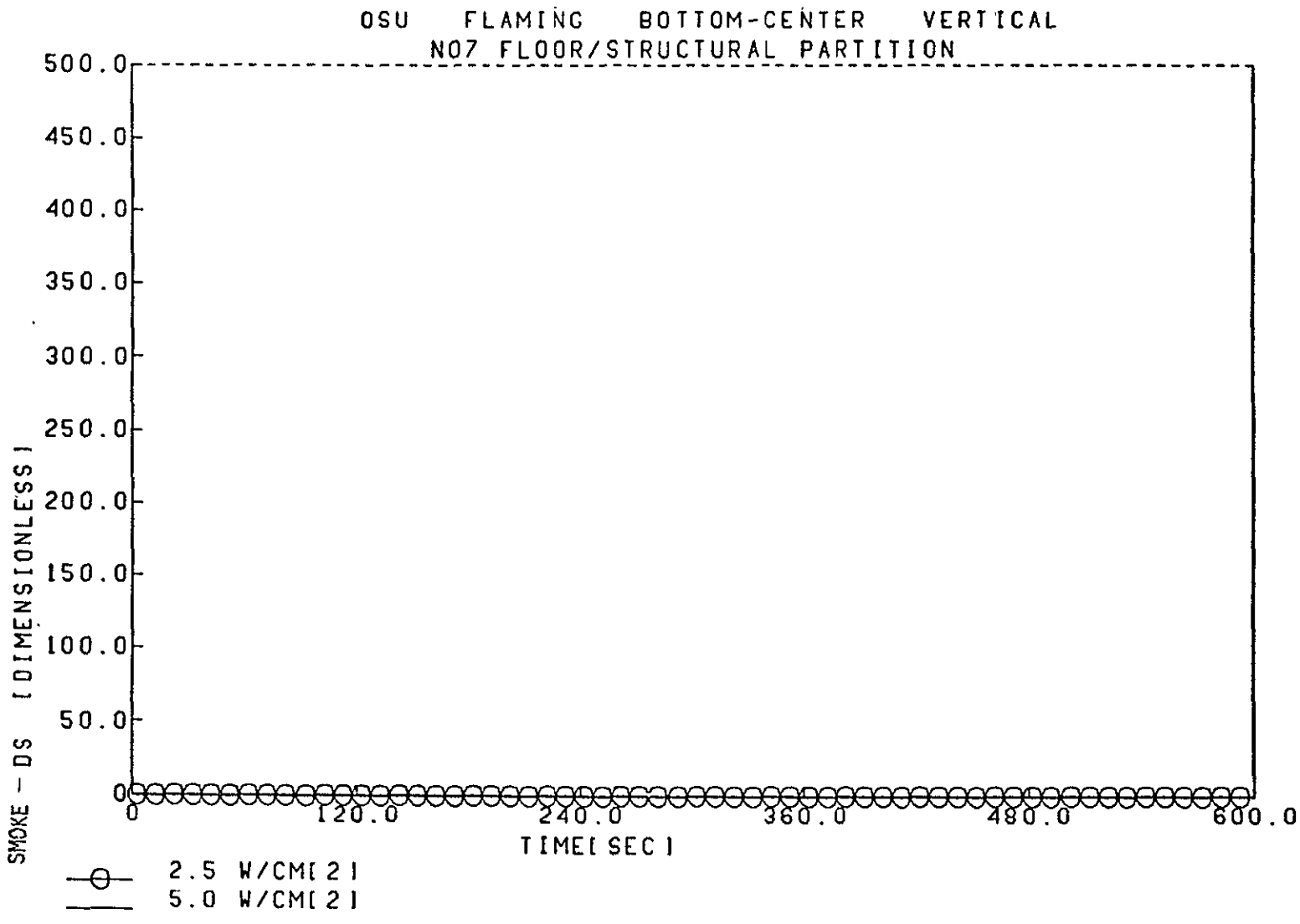

Figure E-13.—Smoke Release in the OSU Apparatus in the Vertical Bottom-Center Ignition Mode—N06/N07

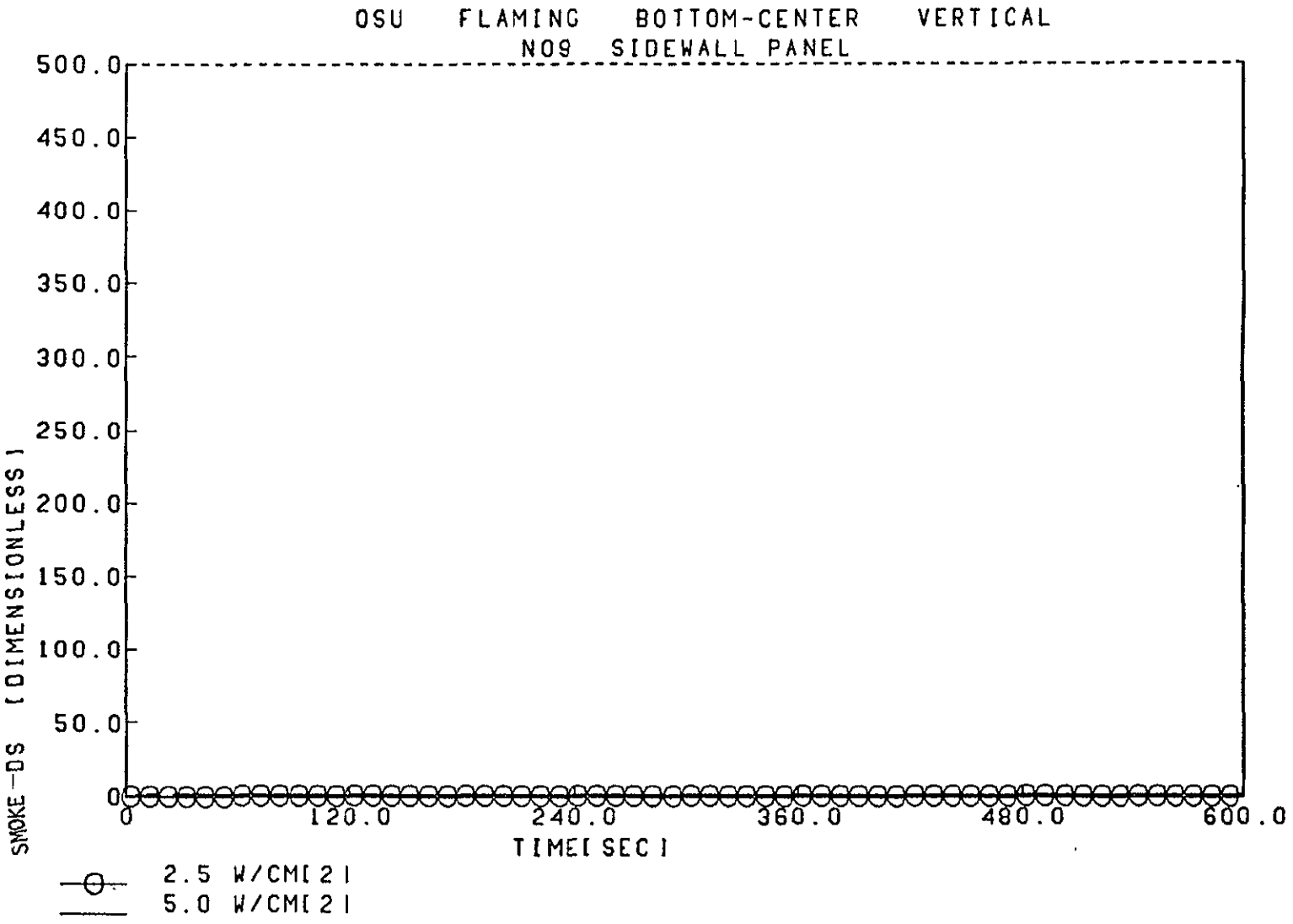

Figure E-14.—Smoke Release in the OSU Apparatus in the Vertical Bottom-Center Ignition Mode—N08/N09

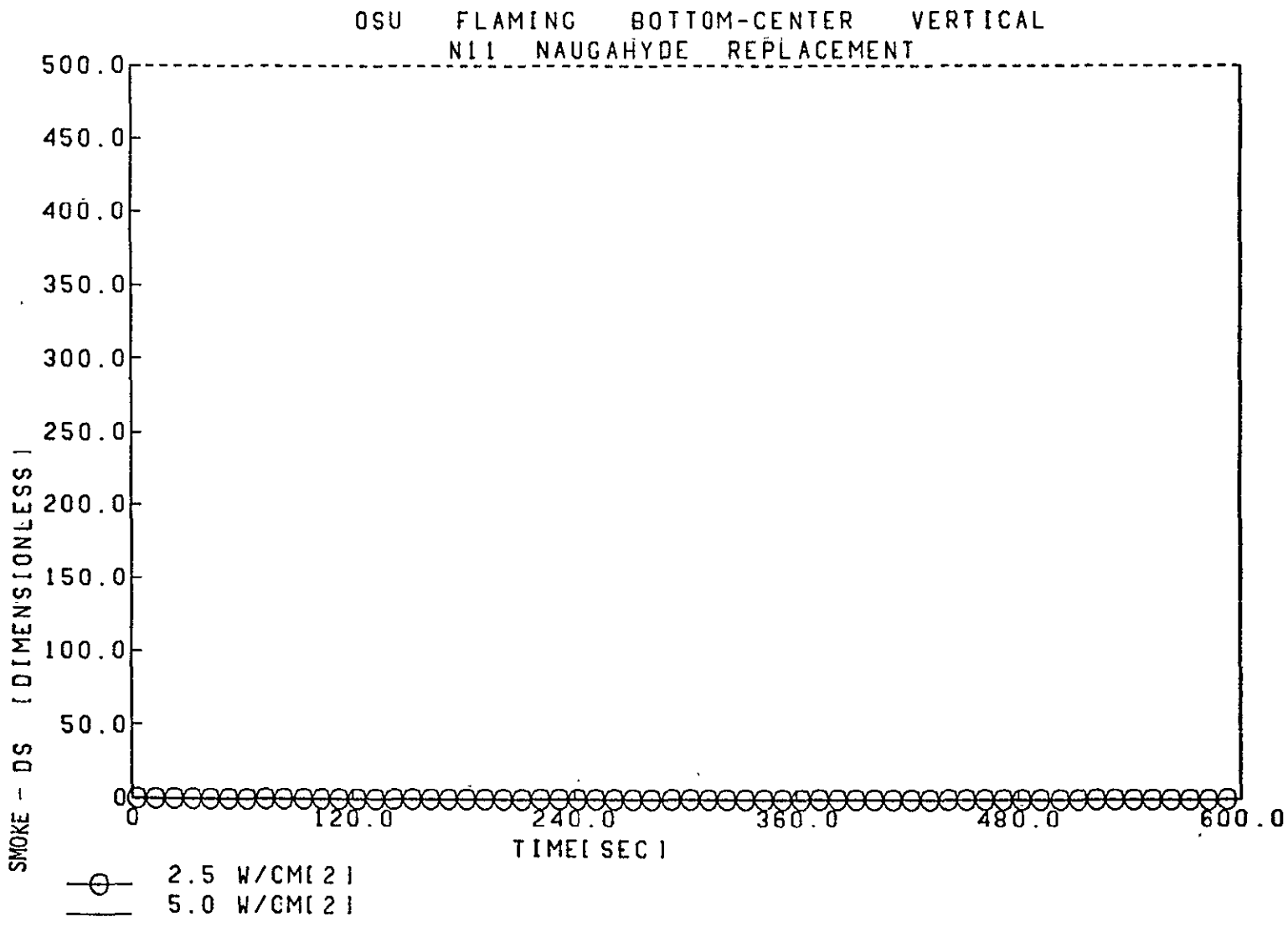

Figure E-15.—Smoke Release in the OSU Apparatus in the Vertical Bottom-Center Ignition Mode—N10/N11

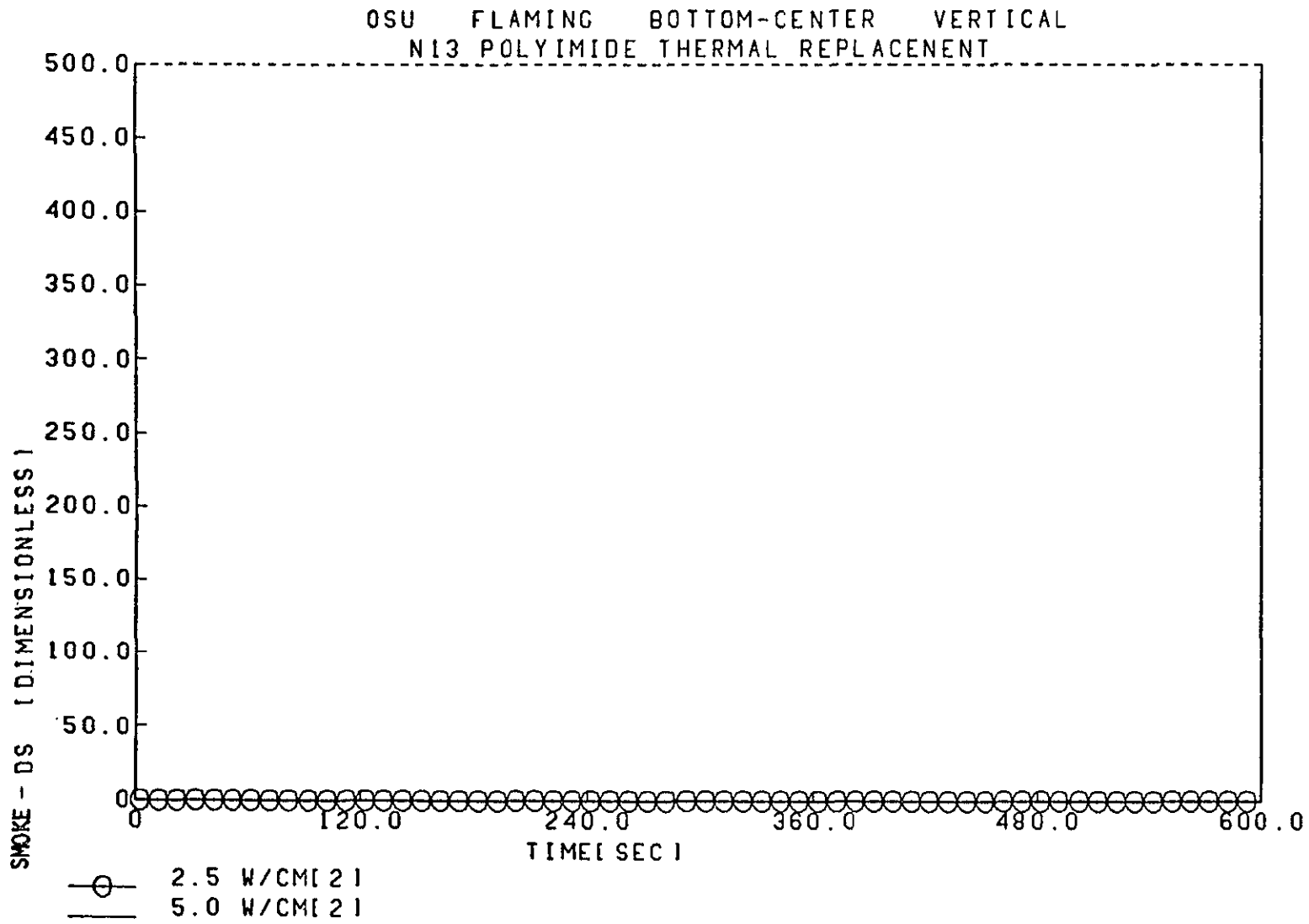

Figure E-16.—Smoke Release in the OSU Apparatus in the Vertical Bottom-Center Ignition Mode—N12/N13

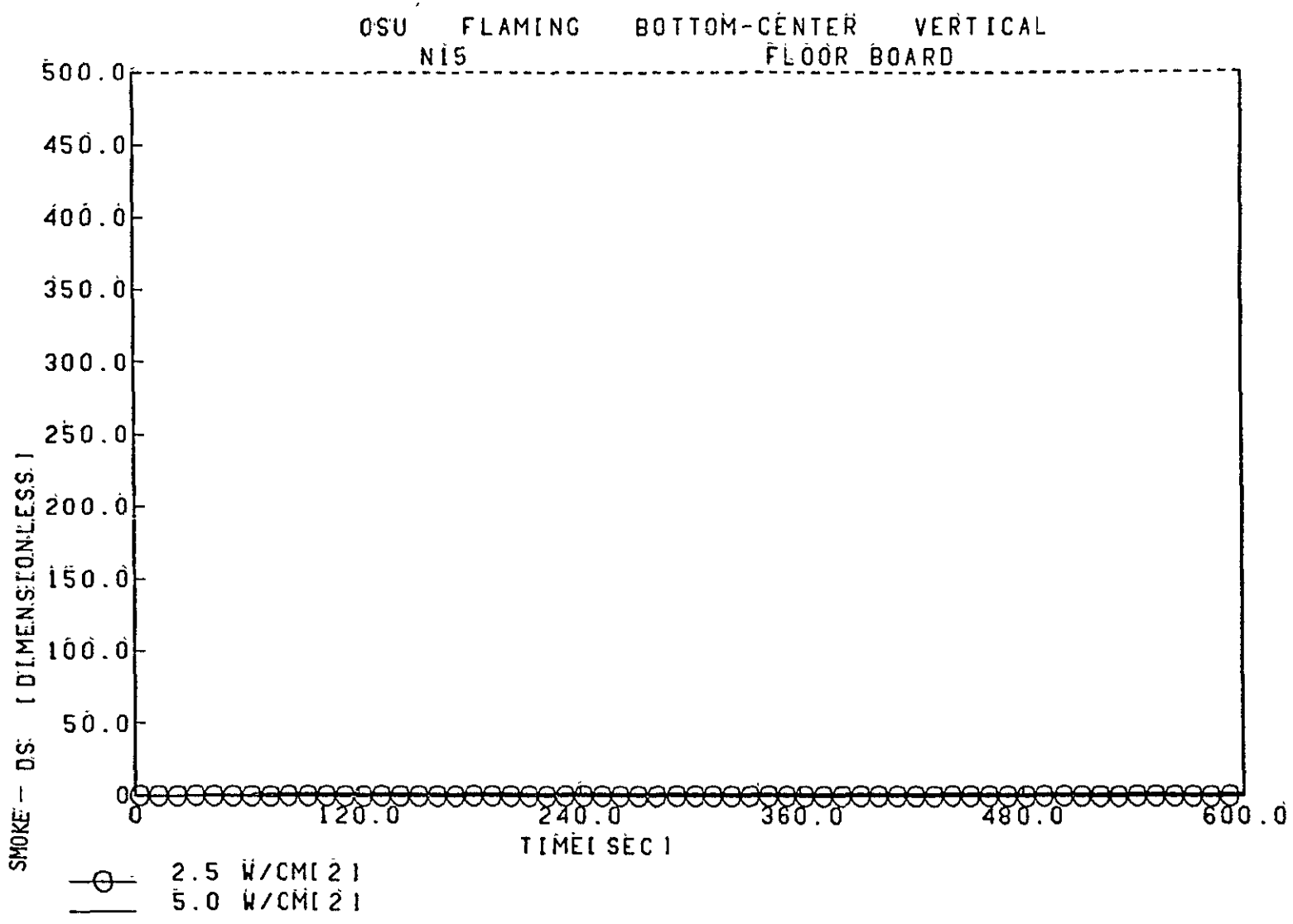

Figure E-17.—Smoke Release in the OSU Apparatus in the Vertical Bottom-Center Ignition Mode—N14/N15

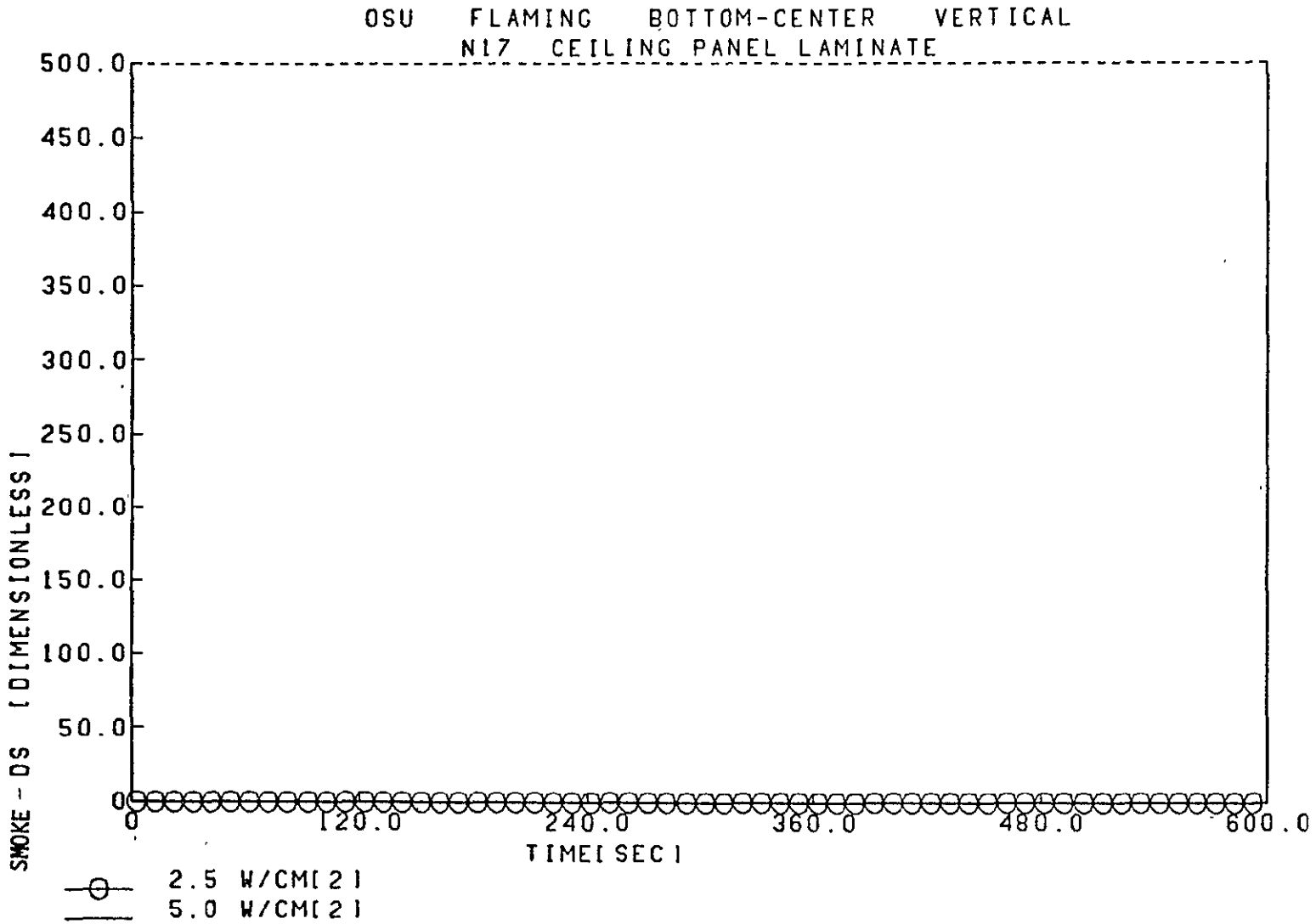

Figure E-18.—Smoke Release in the OSU Apparatus in the Vertical Bottom-Center Ignition Mode—N16/N17

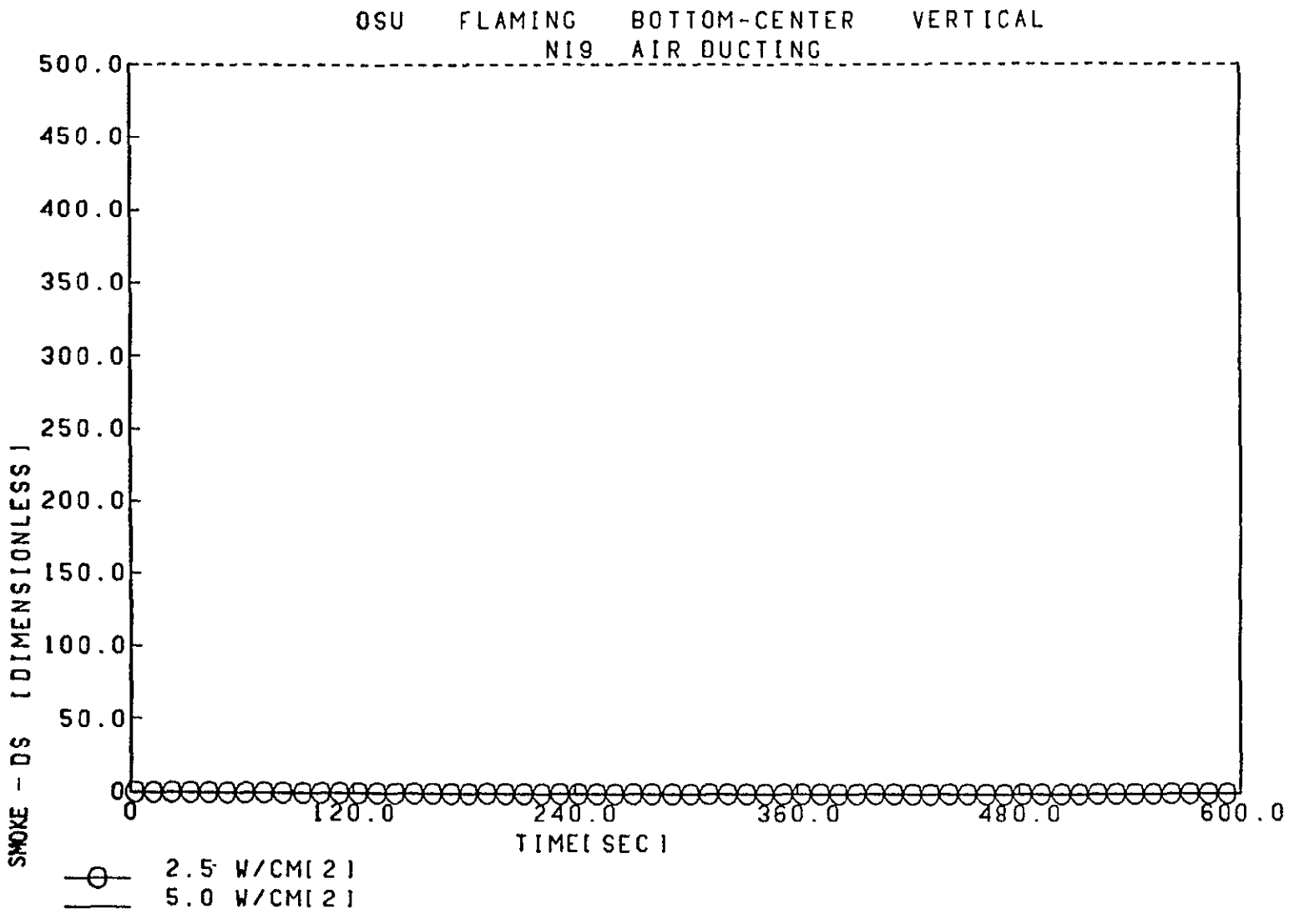

Figure E-19.—Smoke Release in the OSU Apparatus in the Vertical Bottom-Center Ignition Mode—N18/N19

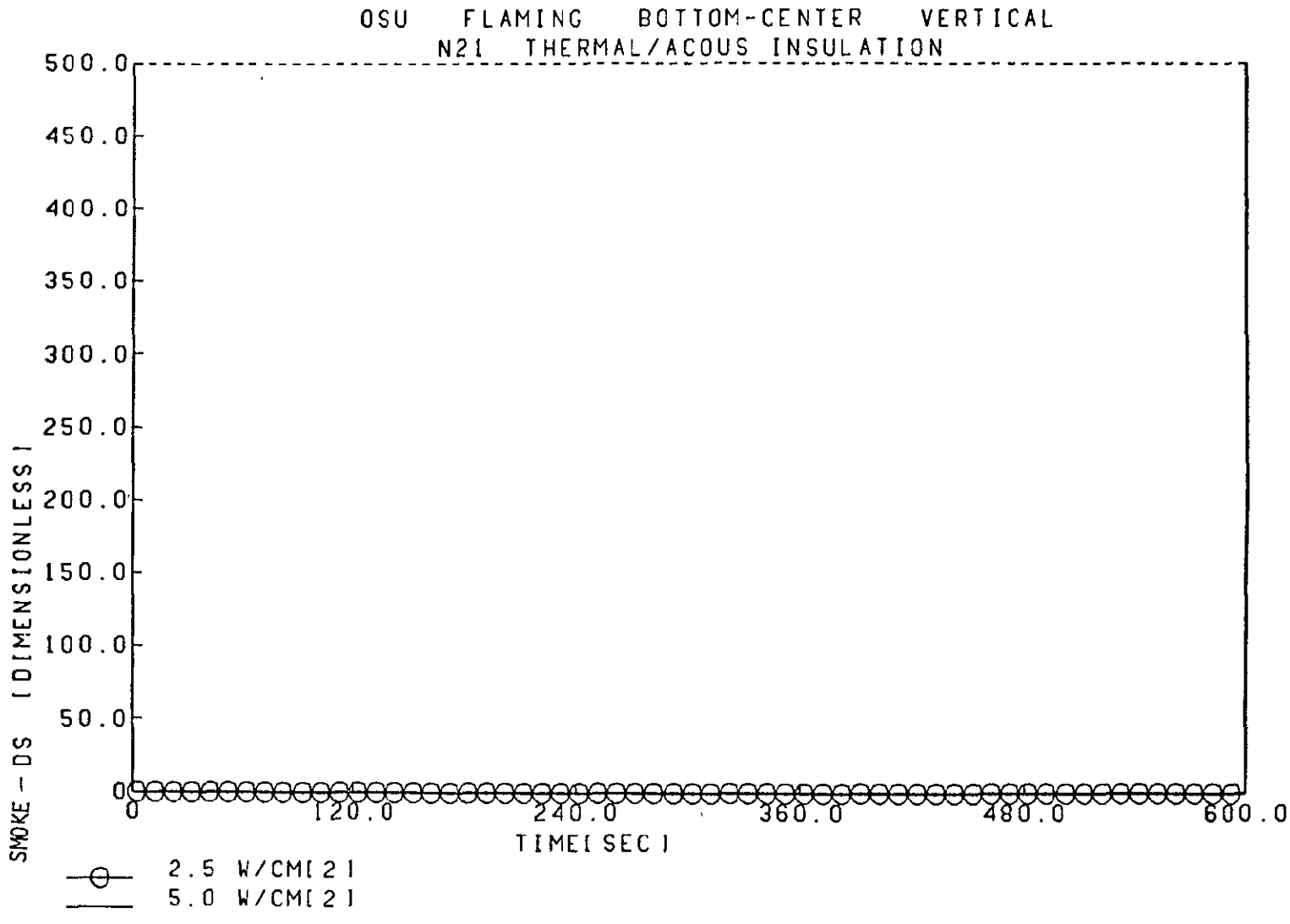

Figure E-20.—Smoke Release in the OSU Apparatus in the Vertical Bottom-Center Ignition Mode—N21

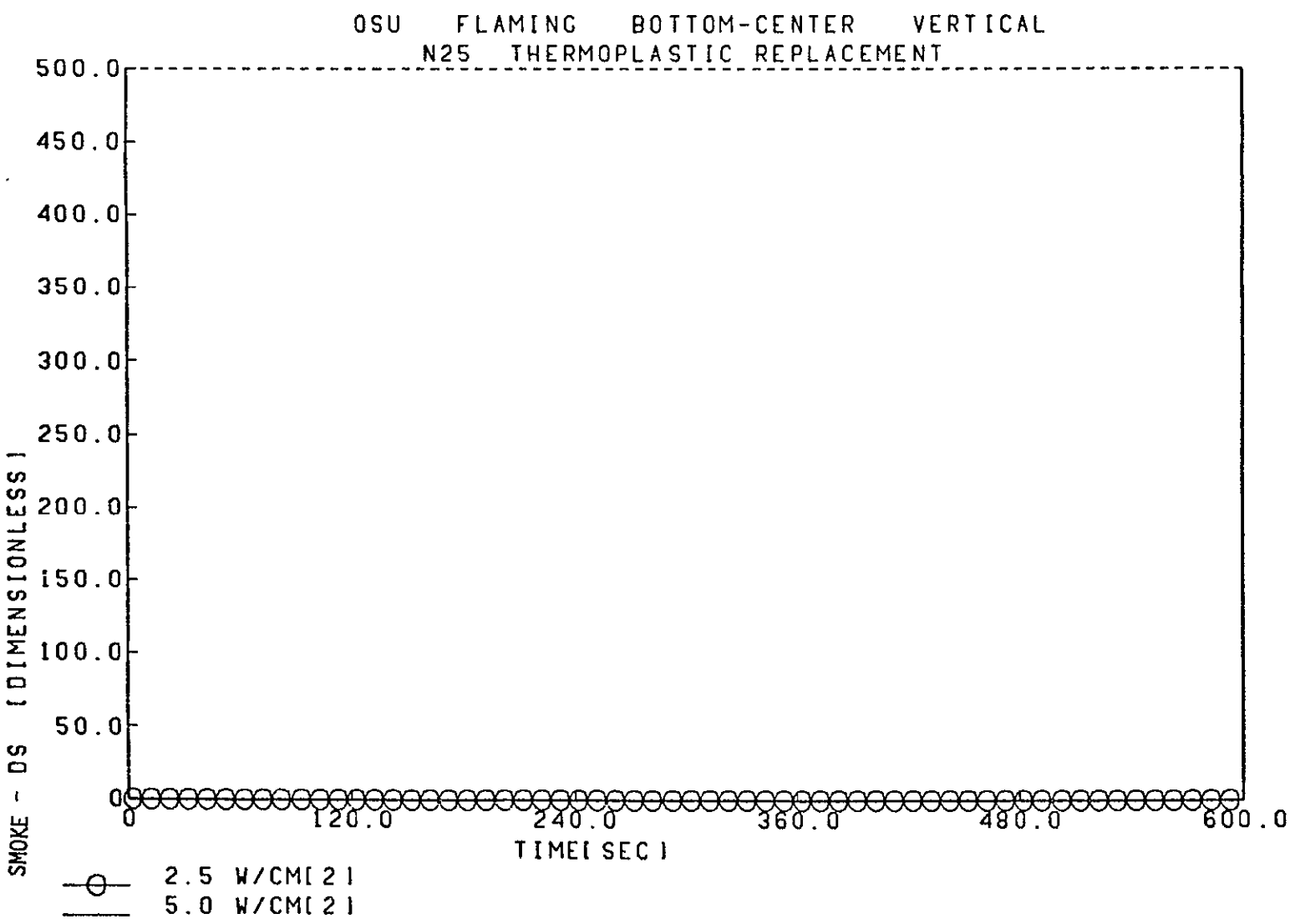

Figure E-22.—Smoke Release in the OSU Apparatus in the Vertical Bottom-Center Ignition Mode—N24/N25

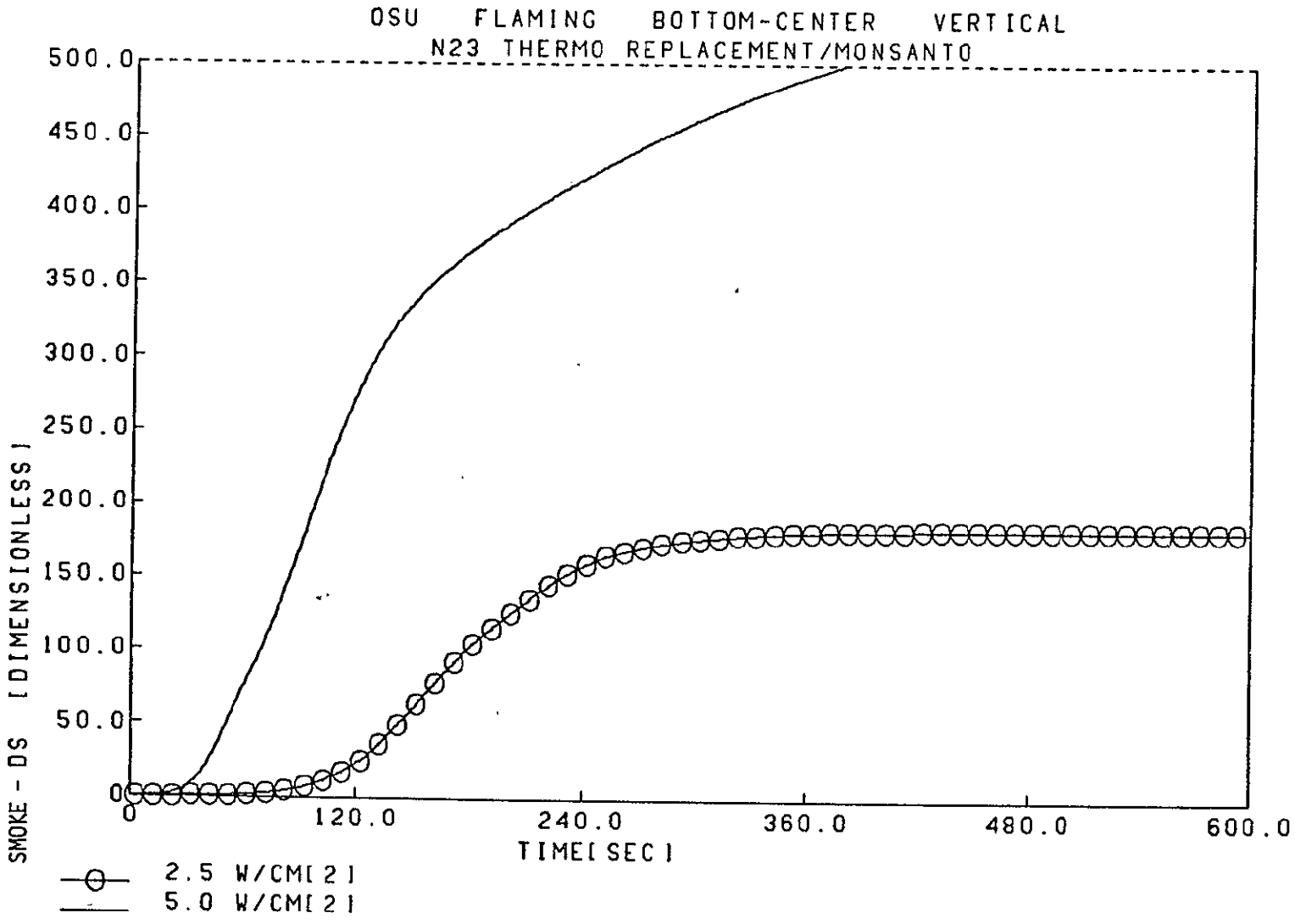

Figure E-21.—Smoke Release in the OSU Apparatus in the Vertical Bottom-Center Ignition Mode—N22/N23

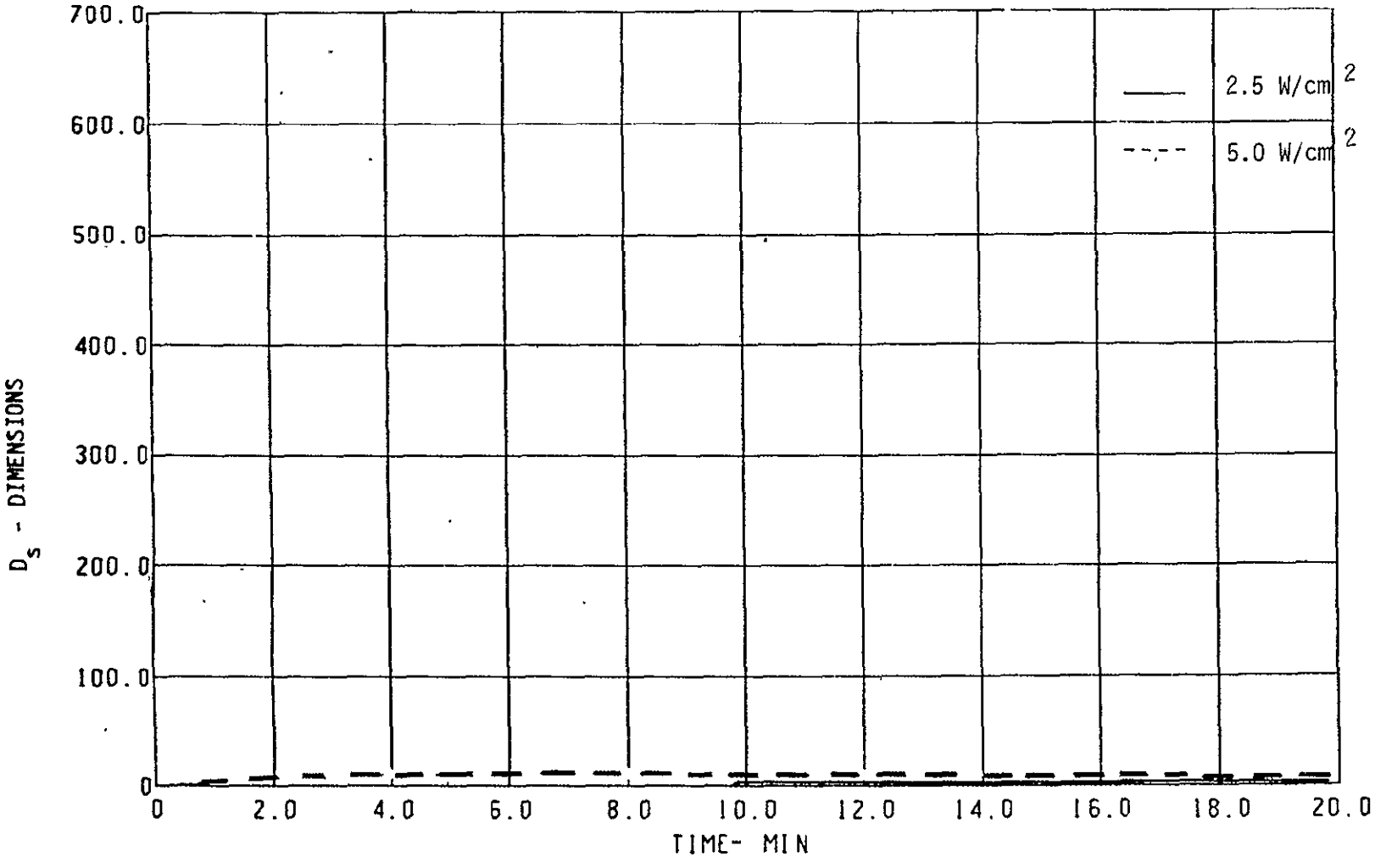

Figure E-23.—Smoke Release in the NBS Chamber in the Flaming Mode—N05

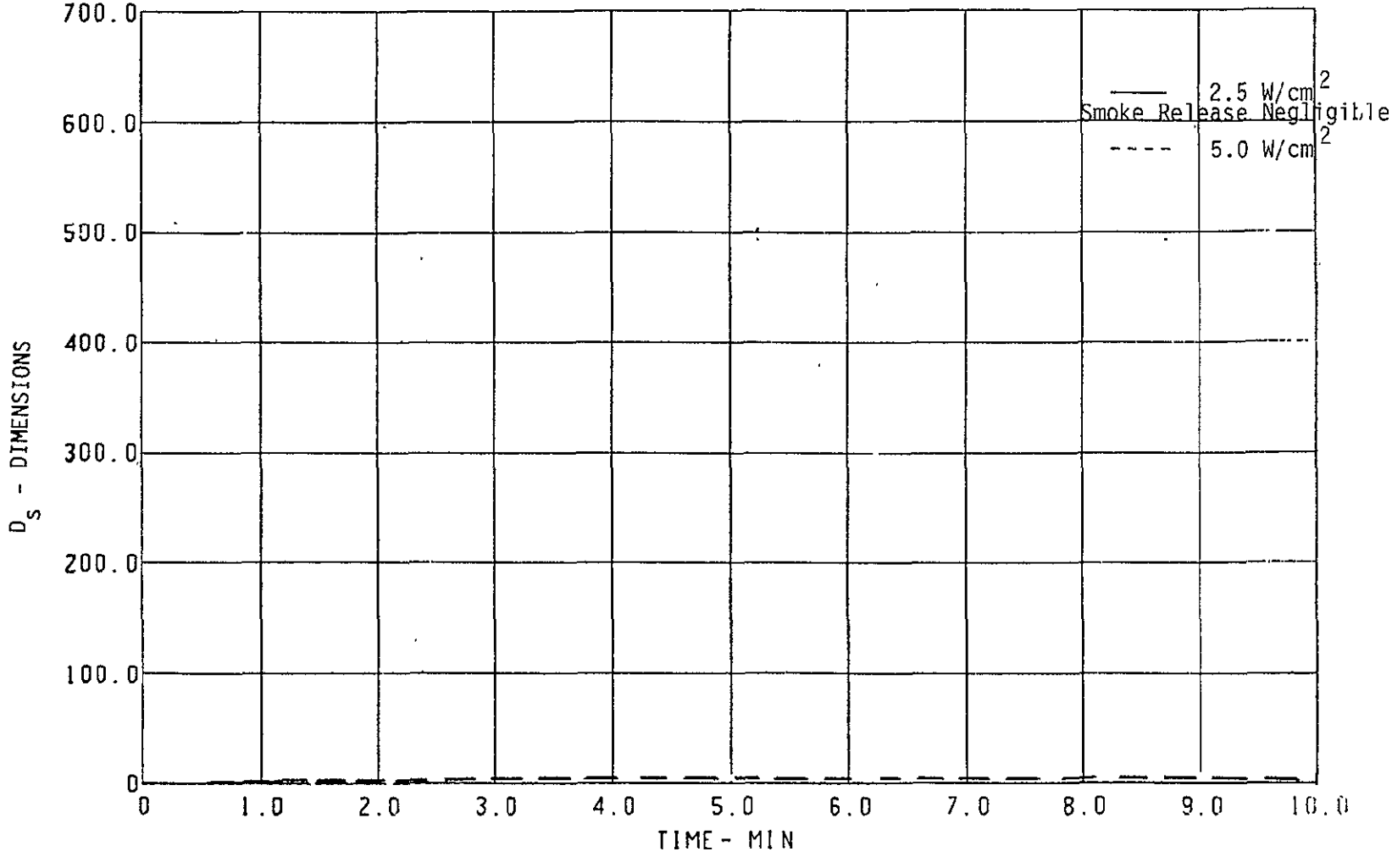

Figure E-24.—Smoke Release in the NBS Chamber in the Flaming Mode--N06/N07

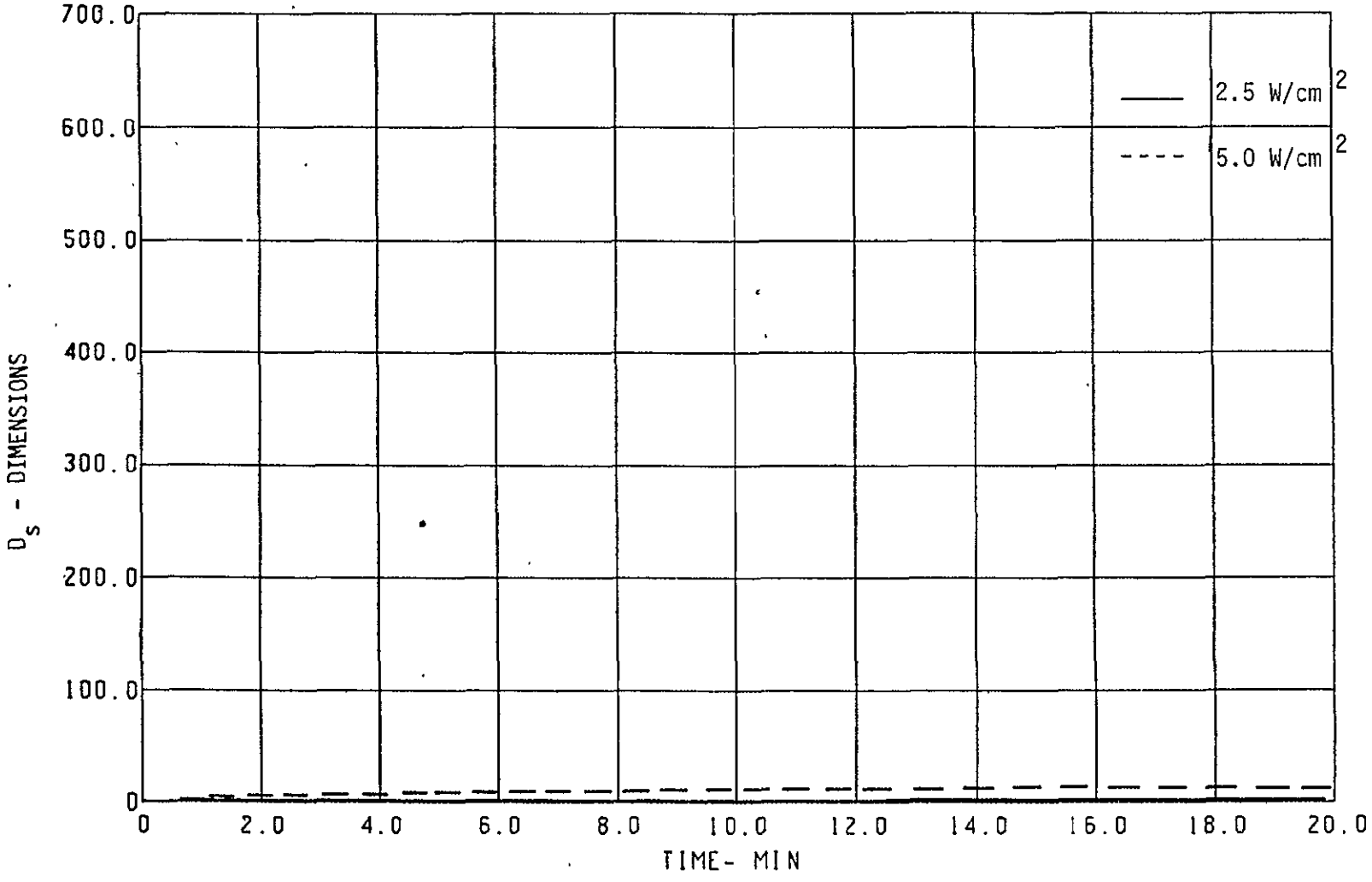

Figure E-25.—Smoke Release in the NBS Chamber in the Flaming Mode—N08/N09

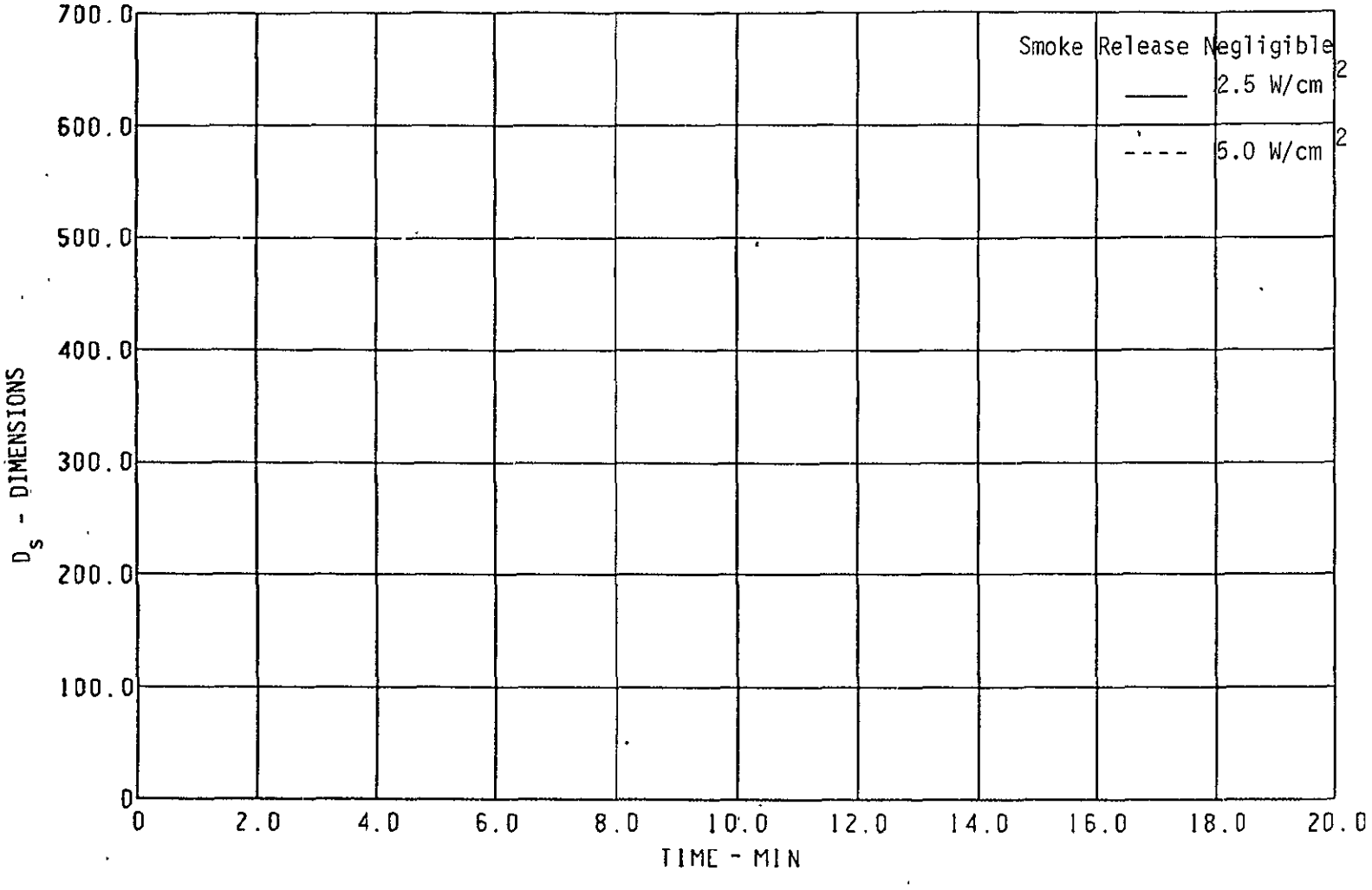

Figure E-26.—Smoke Release in the NBS Chamber in the Flaming Mode—N10/N11

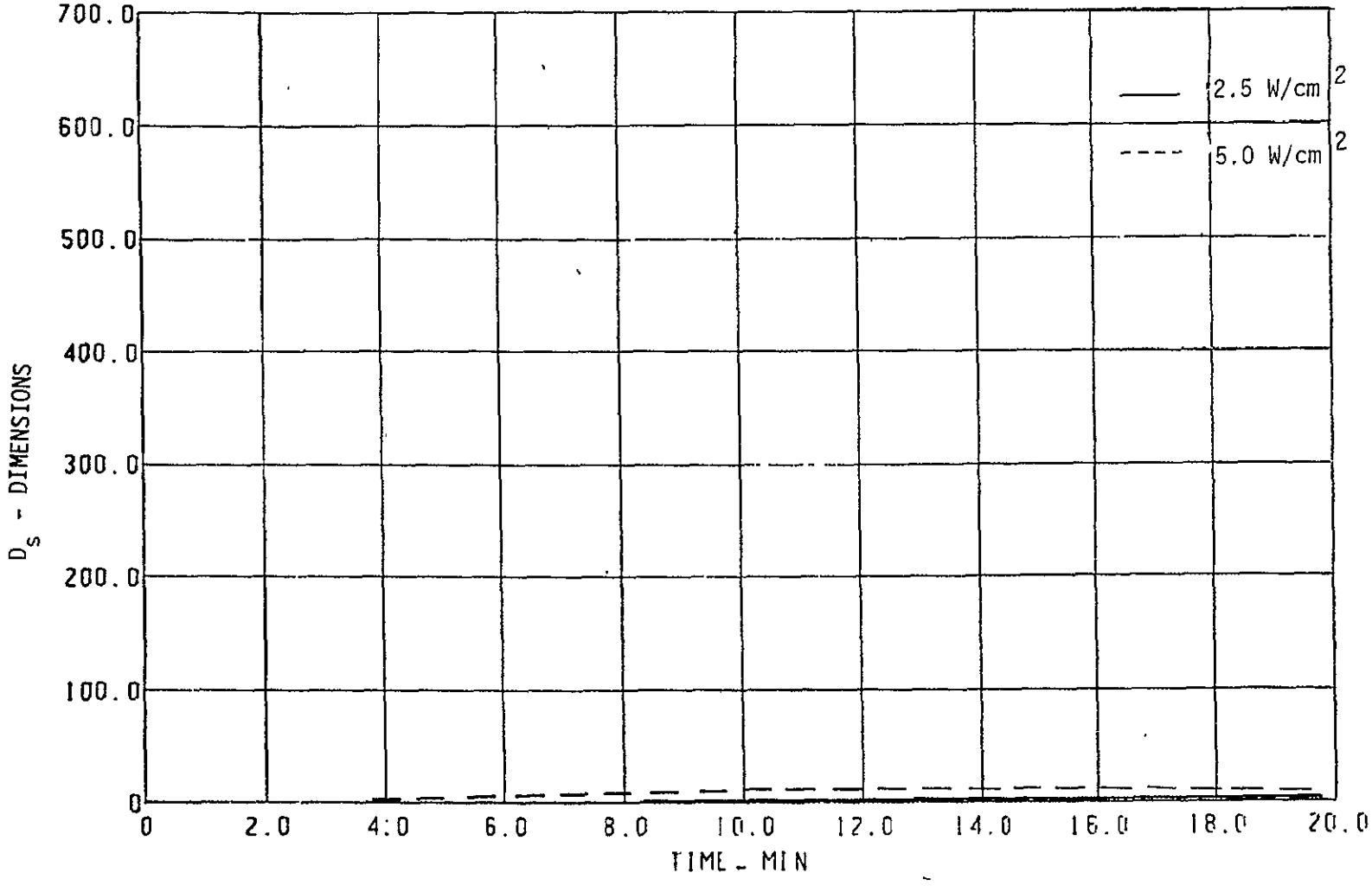

Figure E-27.—Smoke Release in the NBS Chamber in the Flaming Mode—N12/N13

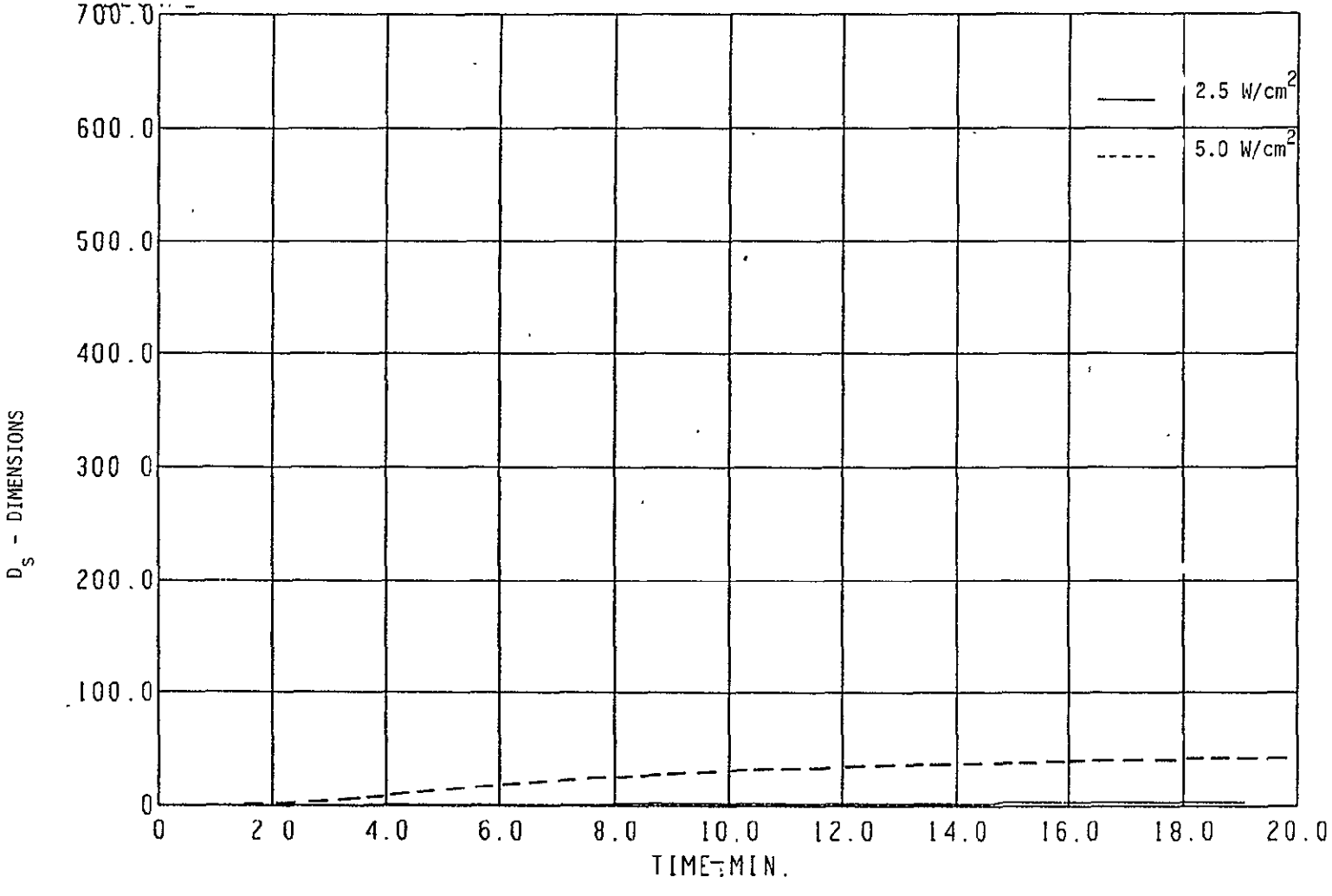

Figure E-28.—Smoke Release in the NBS Chamber in the Flaming Mode—N14/N15

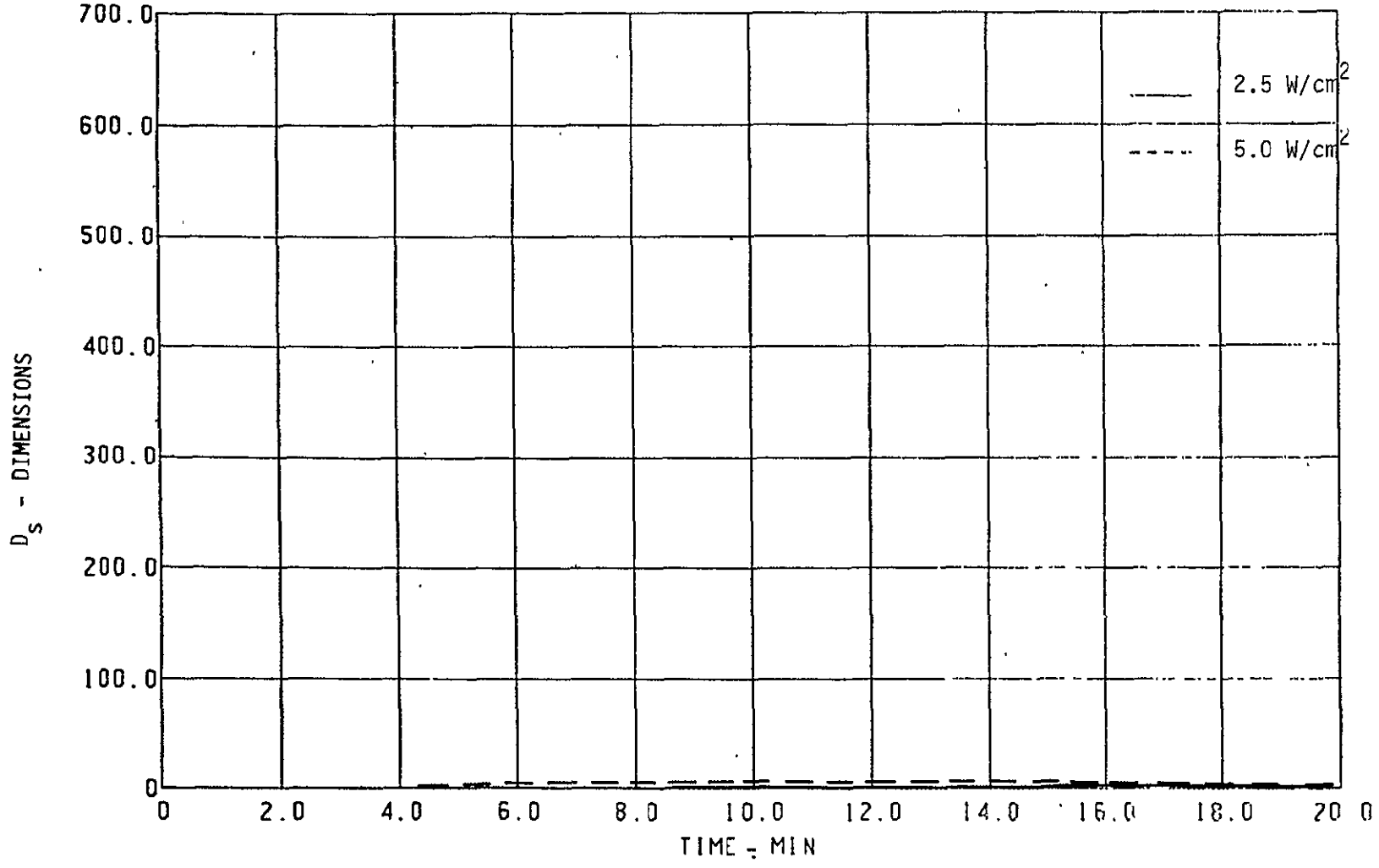

Figure E-29.—Smoke Release in the NBS Chamber in the Flaming Mode—N16/N17

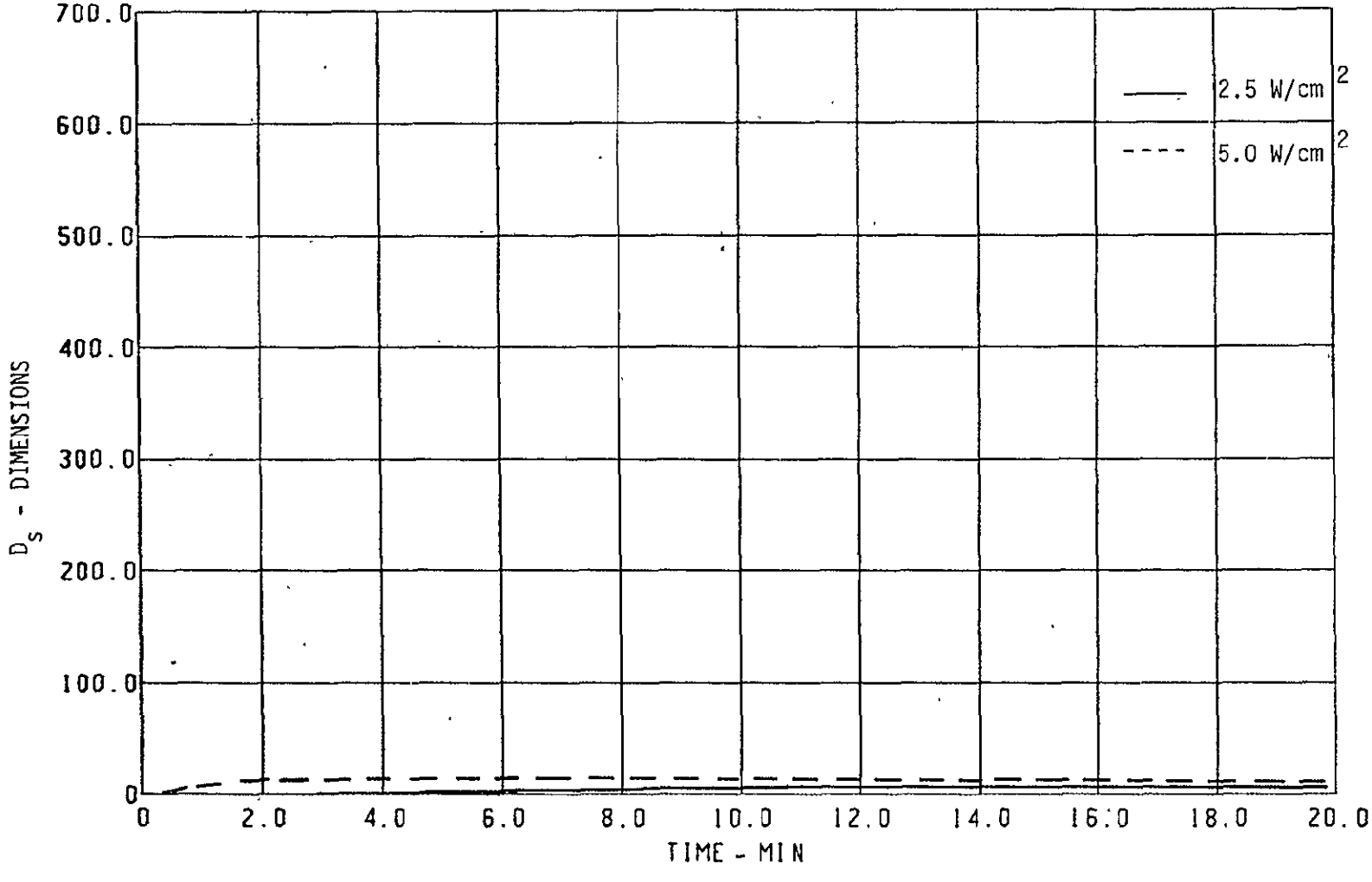

Figure E-30.—Smoke Release in the NBS Chamber in the Flaming Mode—N18/N19

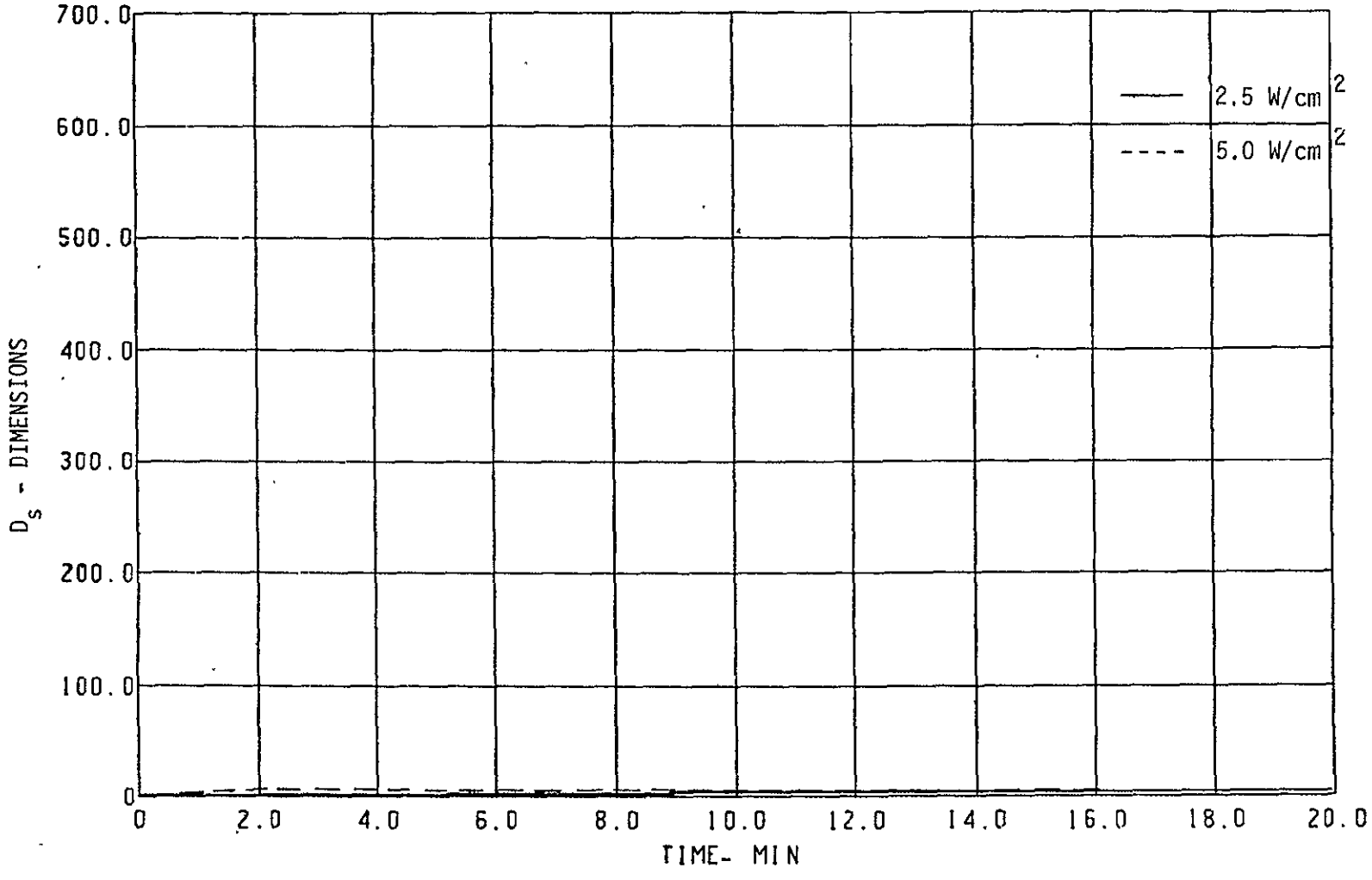

Figure E-31.–Smoke Release in the NBS Chamber in the Flaming Mode–N21

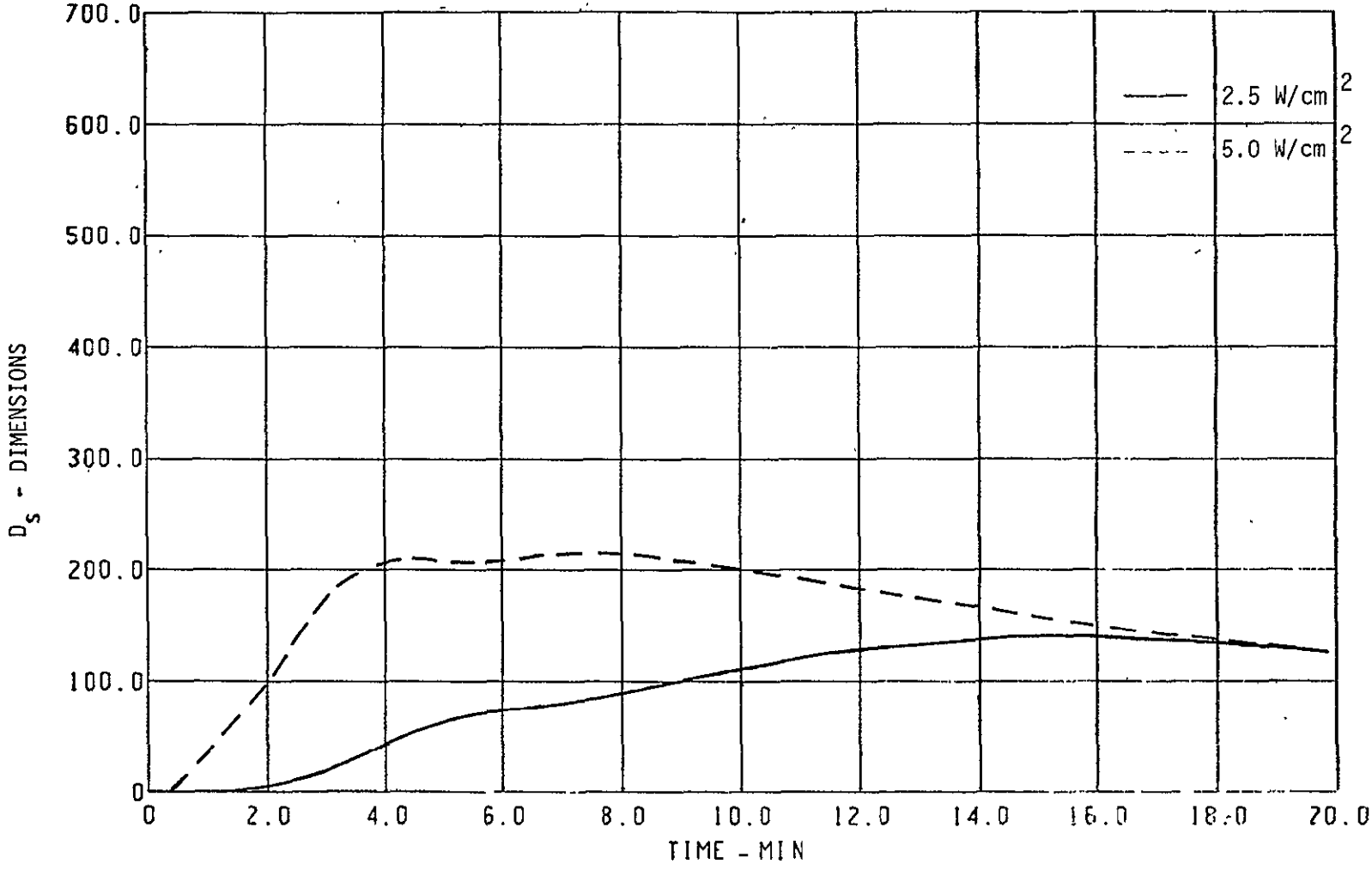

Figure E-32.—Smoke Release in the NBS Chamber in the Flaming Mode—N22/N23

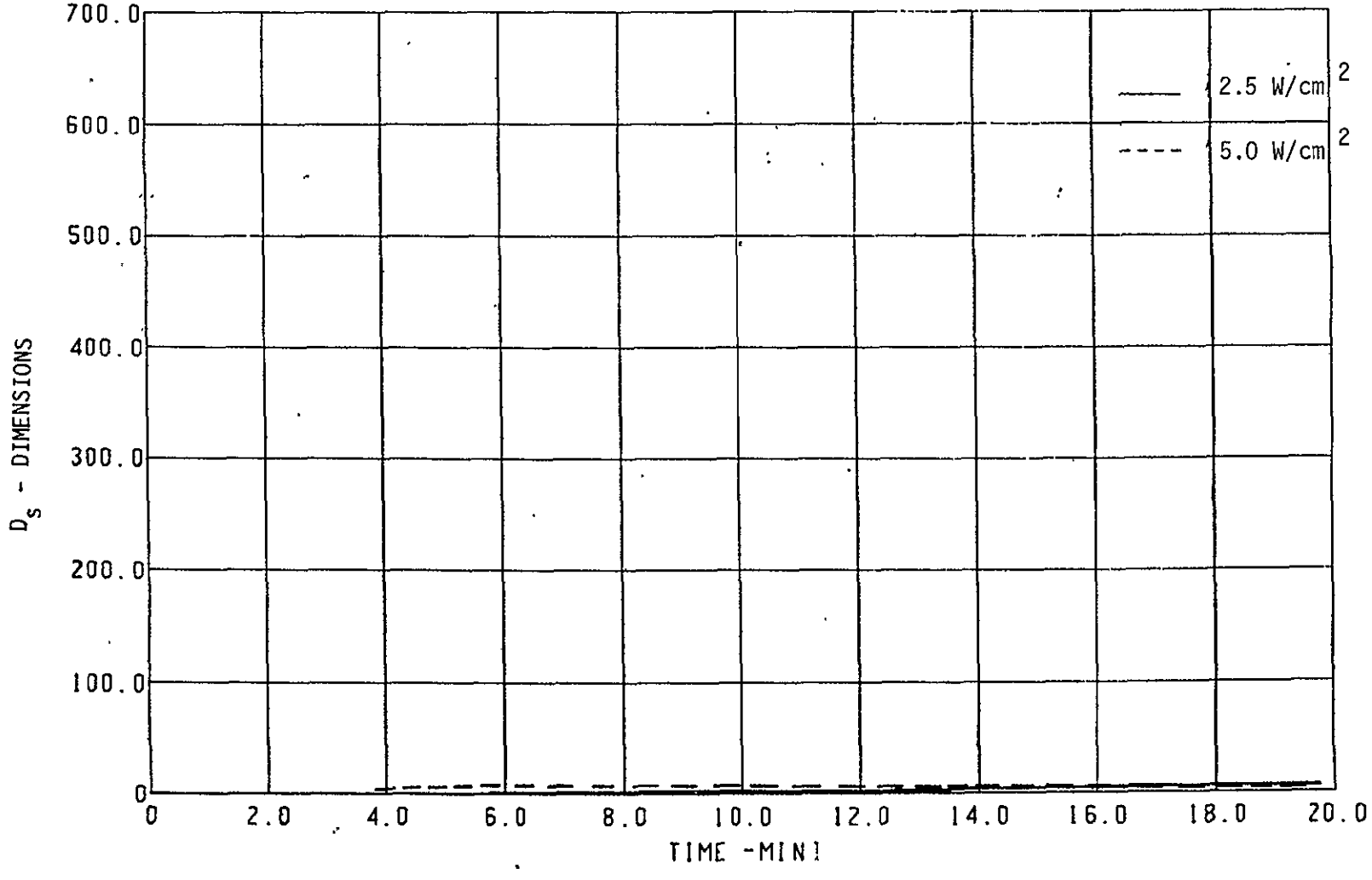

Figure E-33.—Smoke Release in the NBS Chamber in the Flaming Mode—N24/N25

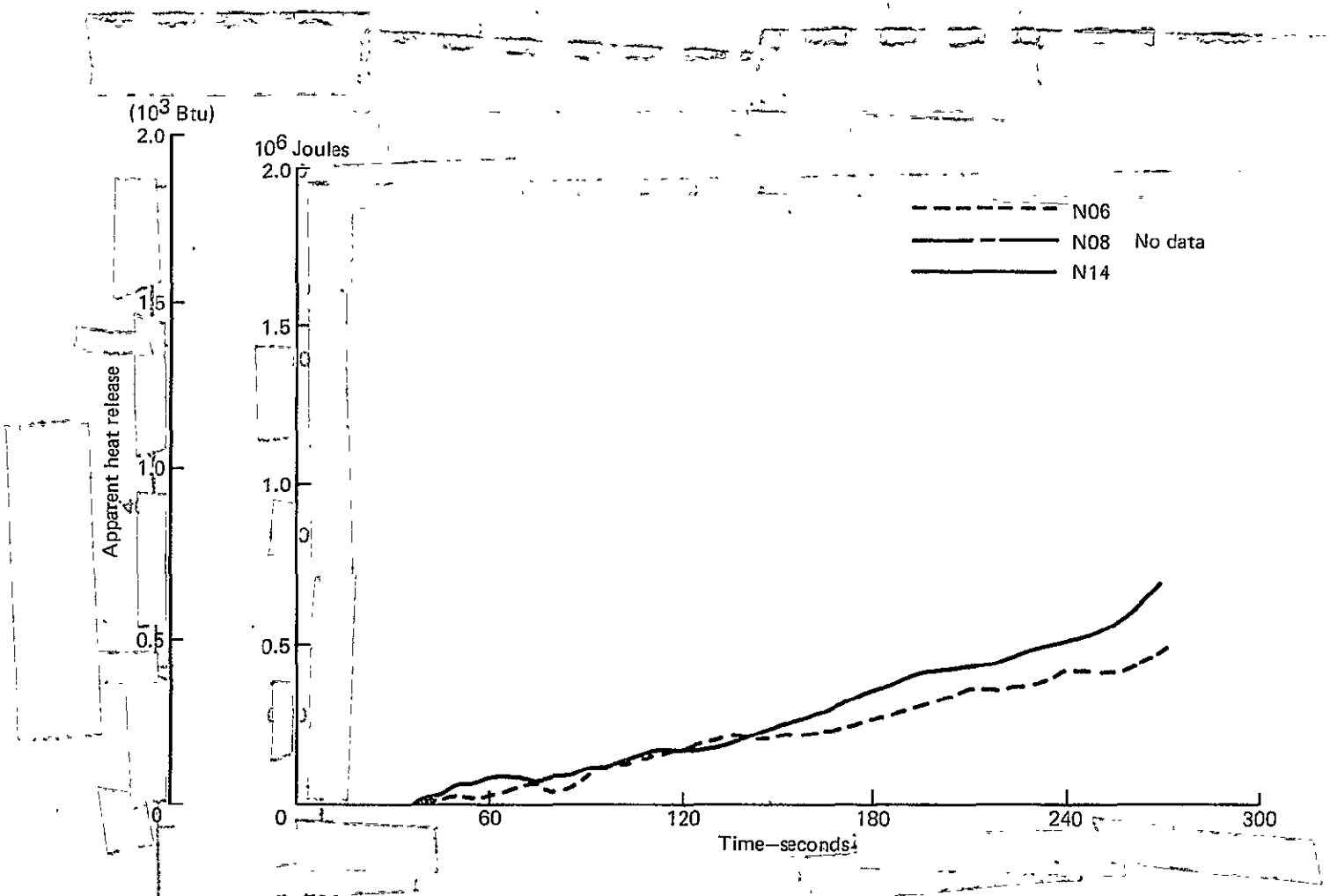

Figure E-34.—Apparent Heat Release from Simulated Design Post-crash-Fire Source Tests—New Materials

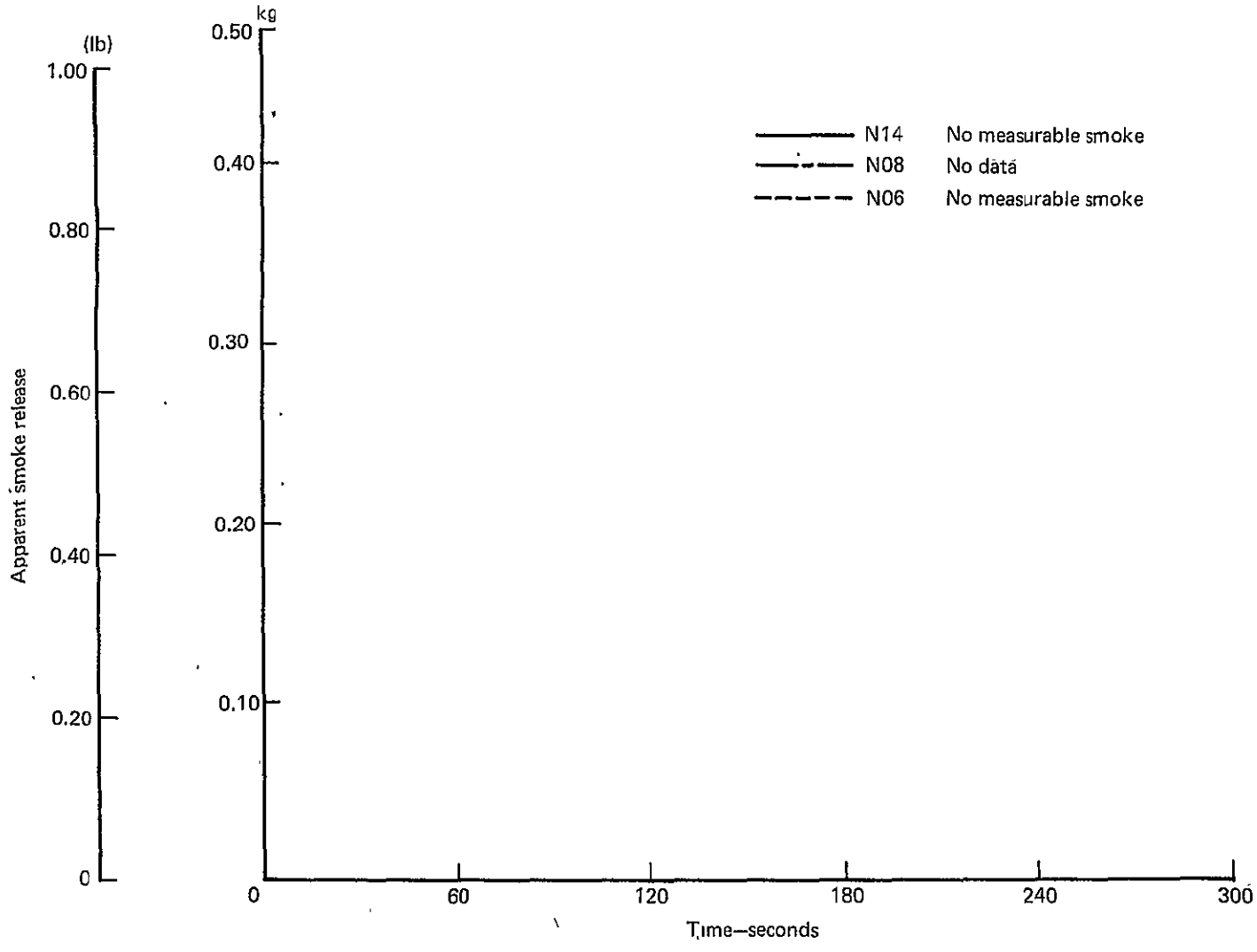

Figure E-35.—Apparent Smoke Release from Simulated Design Post-crash Fire Source Tests—New Materials

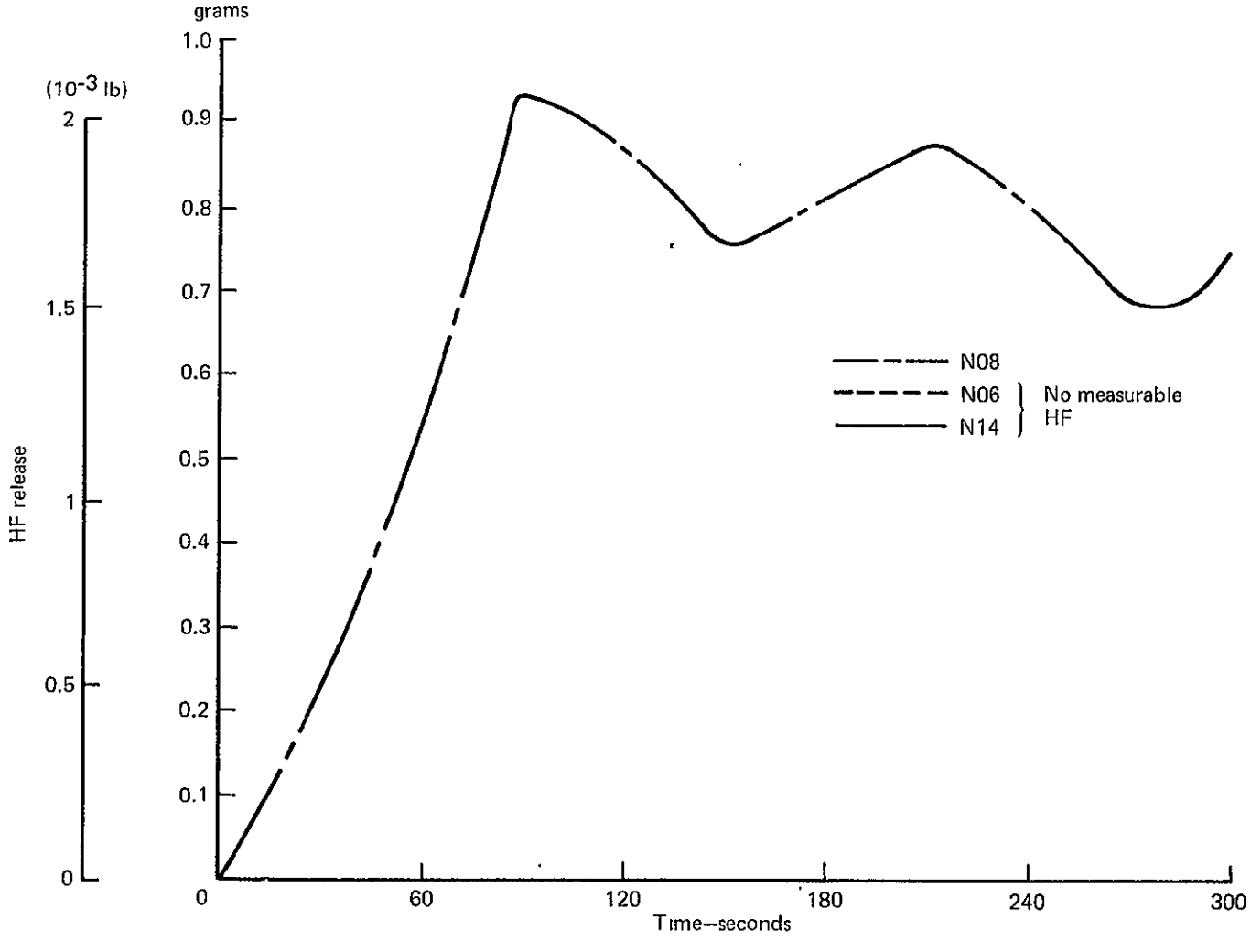

Figure E-36.—Apparent Hydrogen Fluoride (HF) Release from the Simulated Design Post-crash Fire Source Tests—New Materials

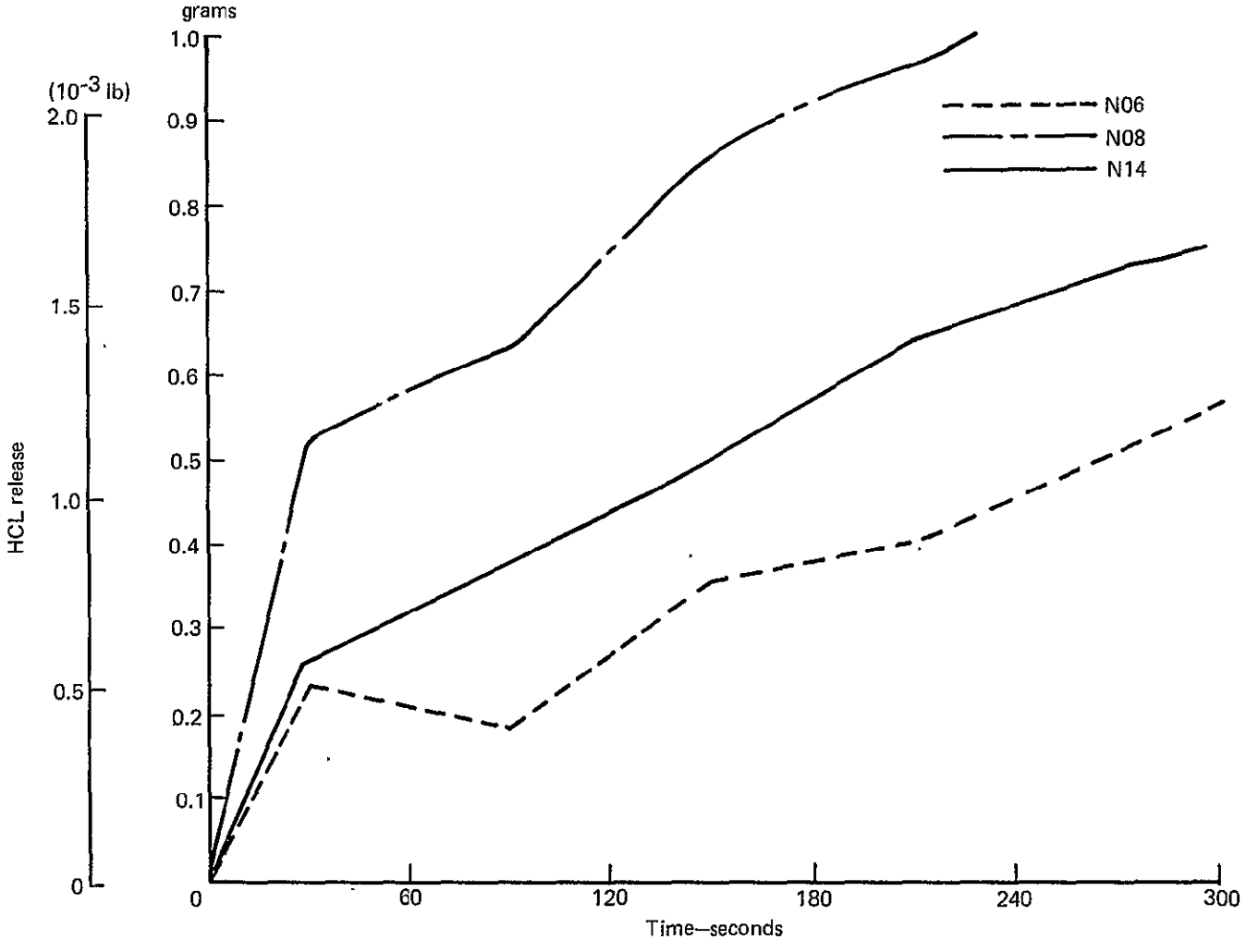

Figure E-37.—Apparent Hydrogen Chloride (HCL) Release from the Simulated Design Post-crash Fire Source Tests—New Materials

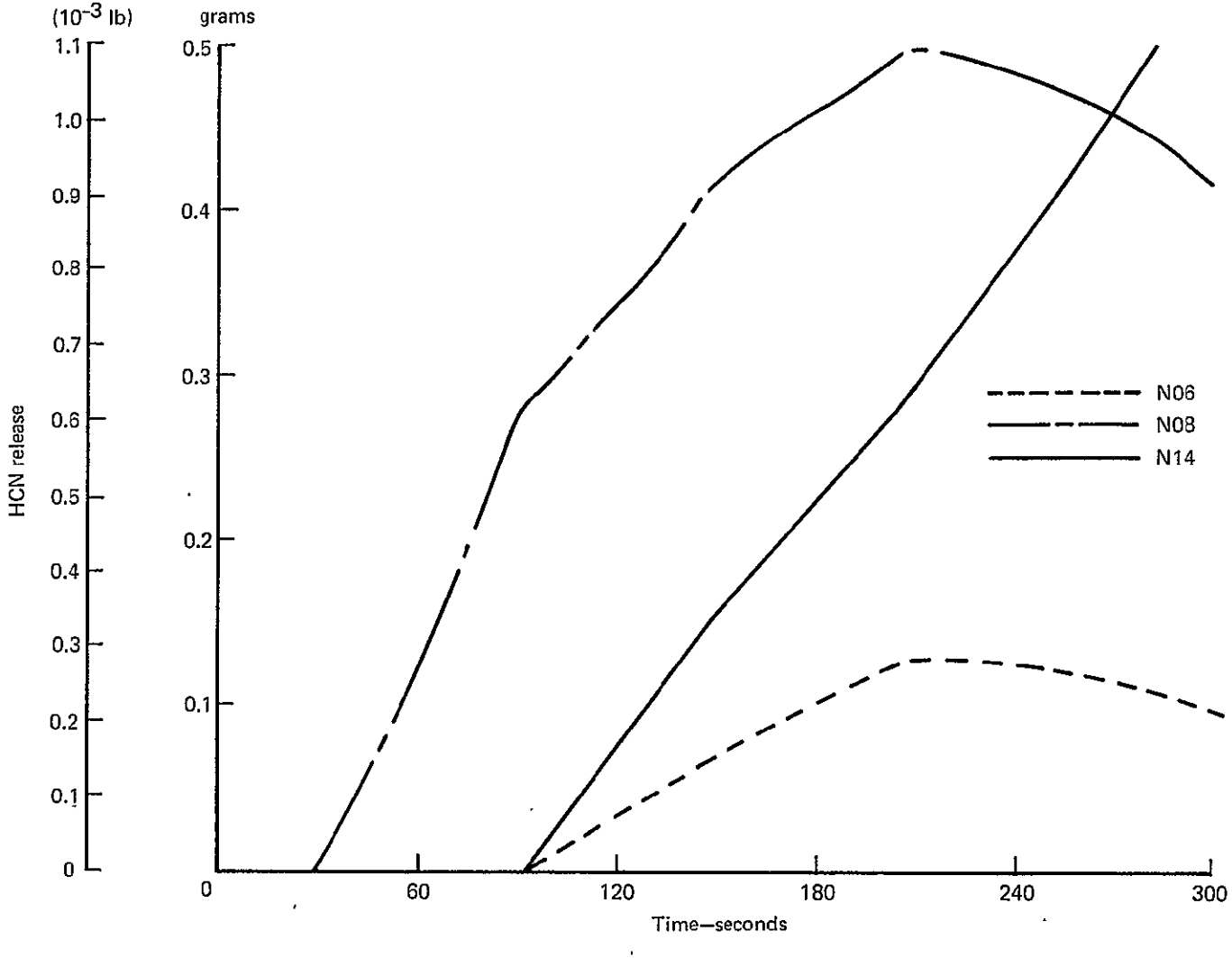

Figure E-38.—Apparent Hydrogen Cyanide (HCN) Release from the Simulated Design Post-crash Fire Source Tests—New Materials

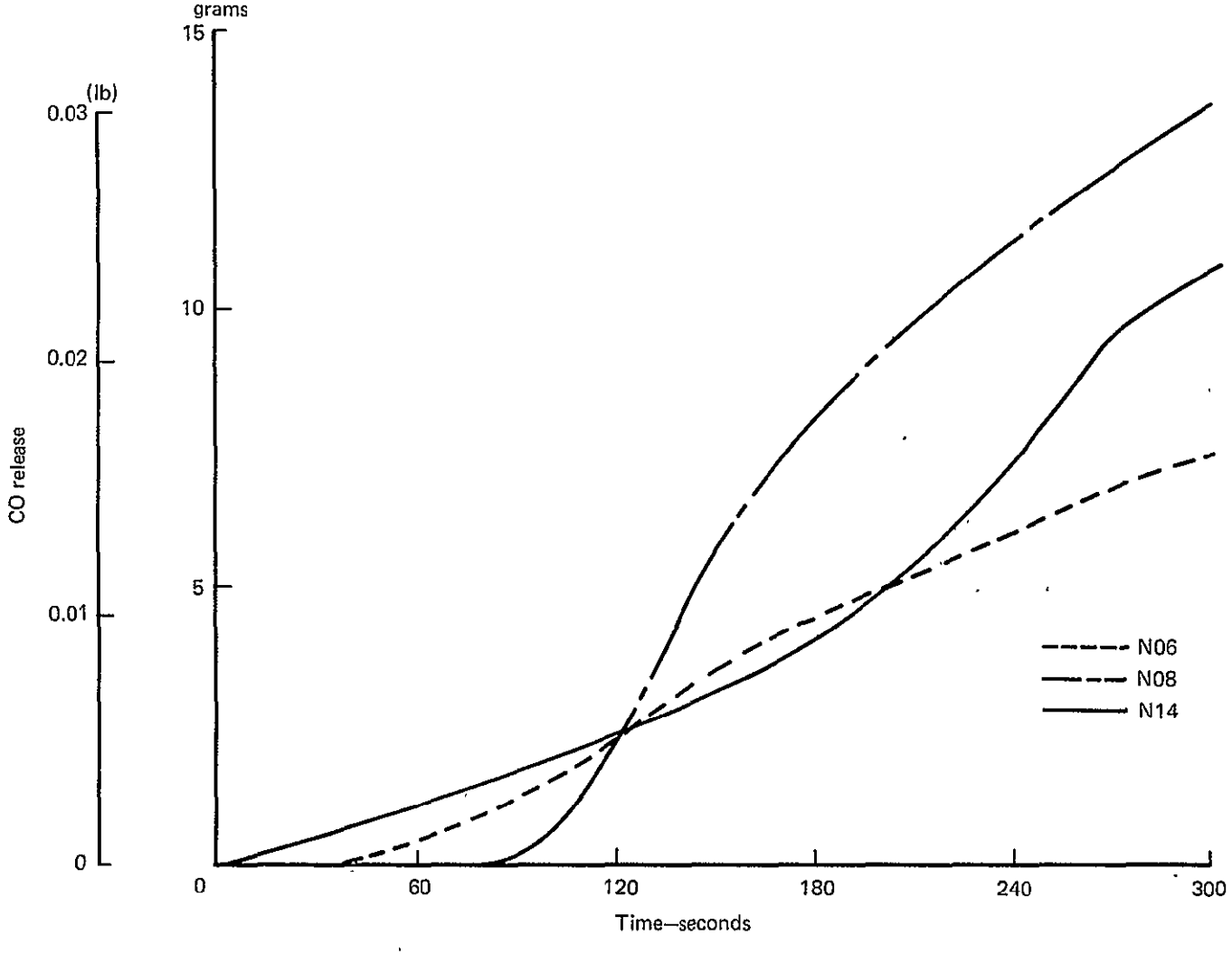

Figure E-39.—Apparent Carbon Monoxide (CO) Release from the Simulated Design Post-crash Fire Source Tests—New Materials

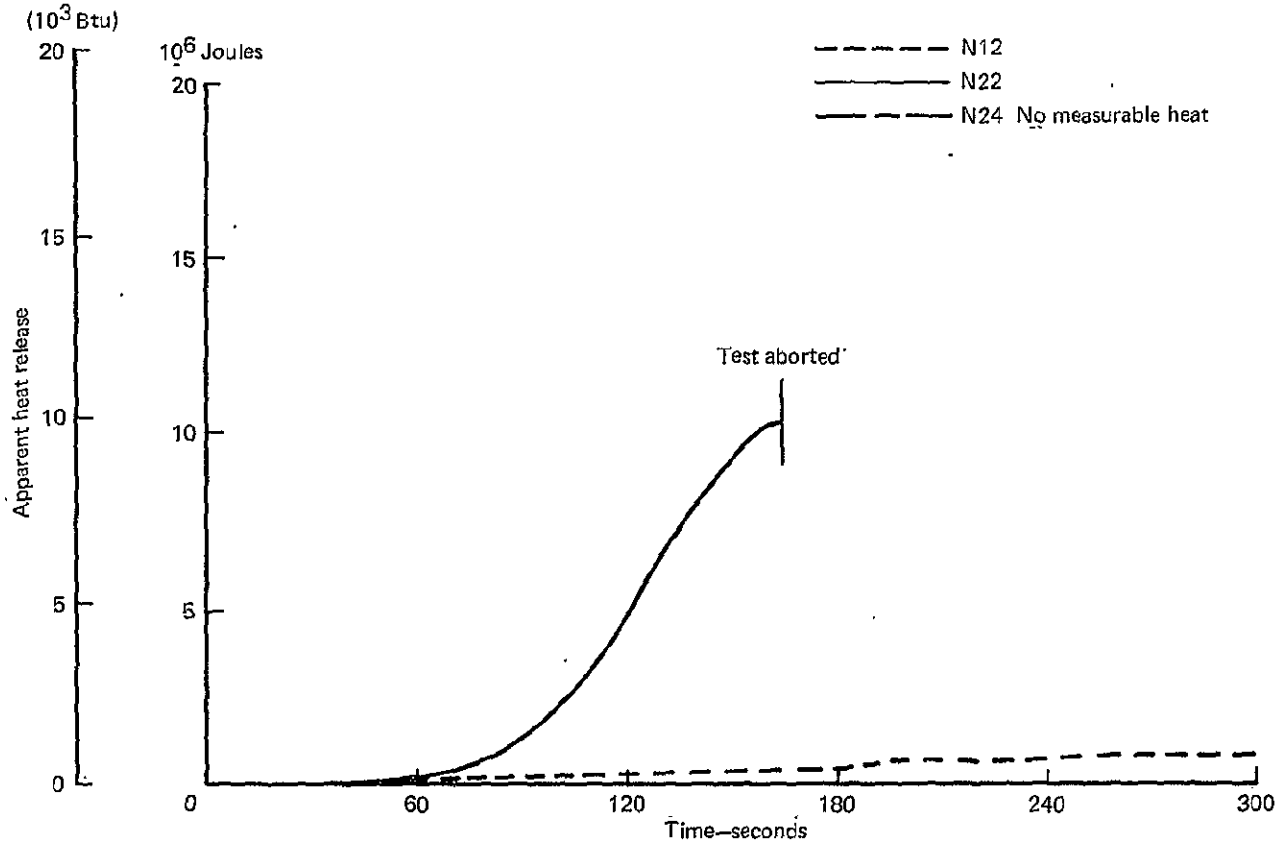

Figure E-40.—Apparent Heat Release from Simulated Design Post-crash Fire Source Tests—New Materials

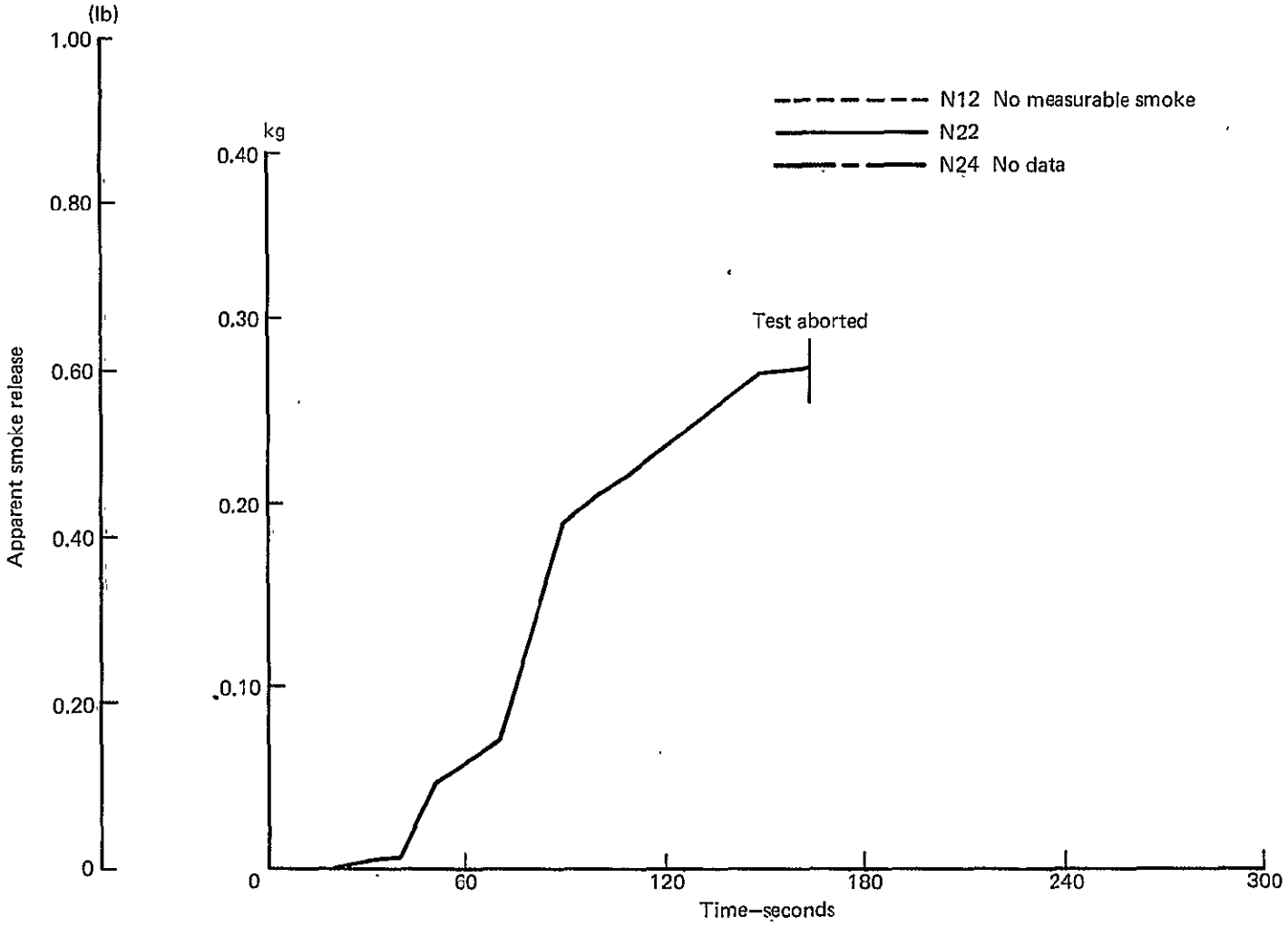

Figure E-41.—Apparent Smoke Release from Simulated Design Post-crash Fire Source Tests—New Materials

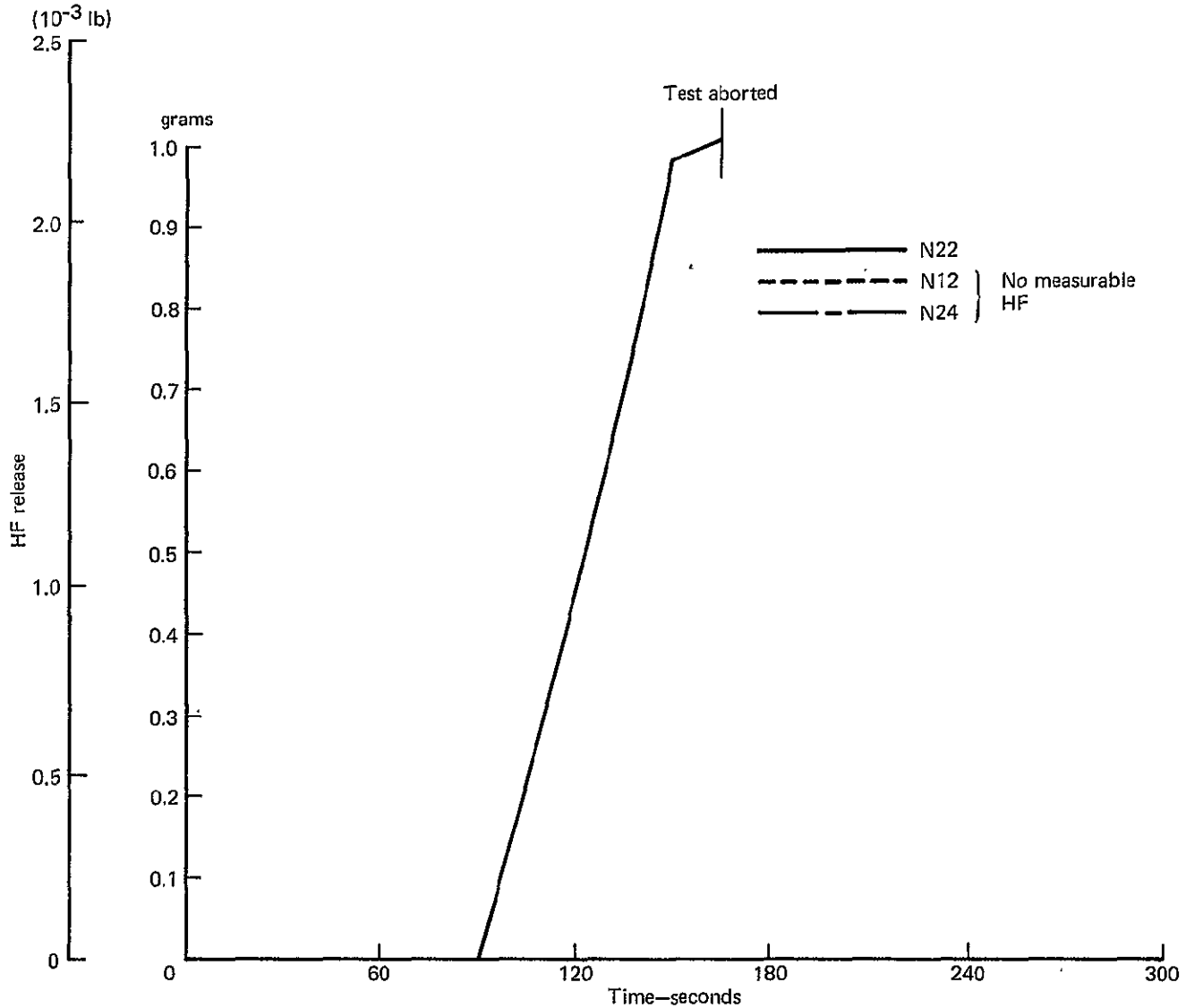

Figure E-42.—Apparent Hydrogen Fluoride (HF) Release from the Simulated Design Post-crash Fire Source Tests—New Materials

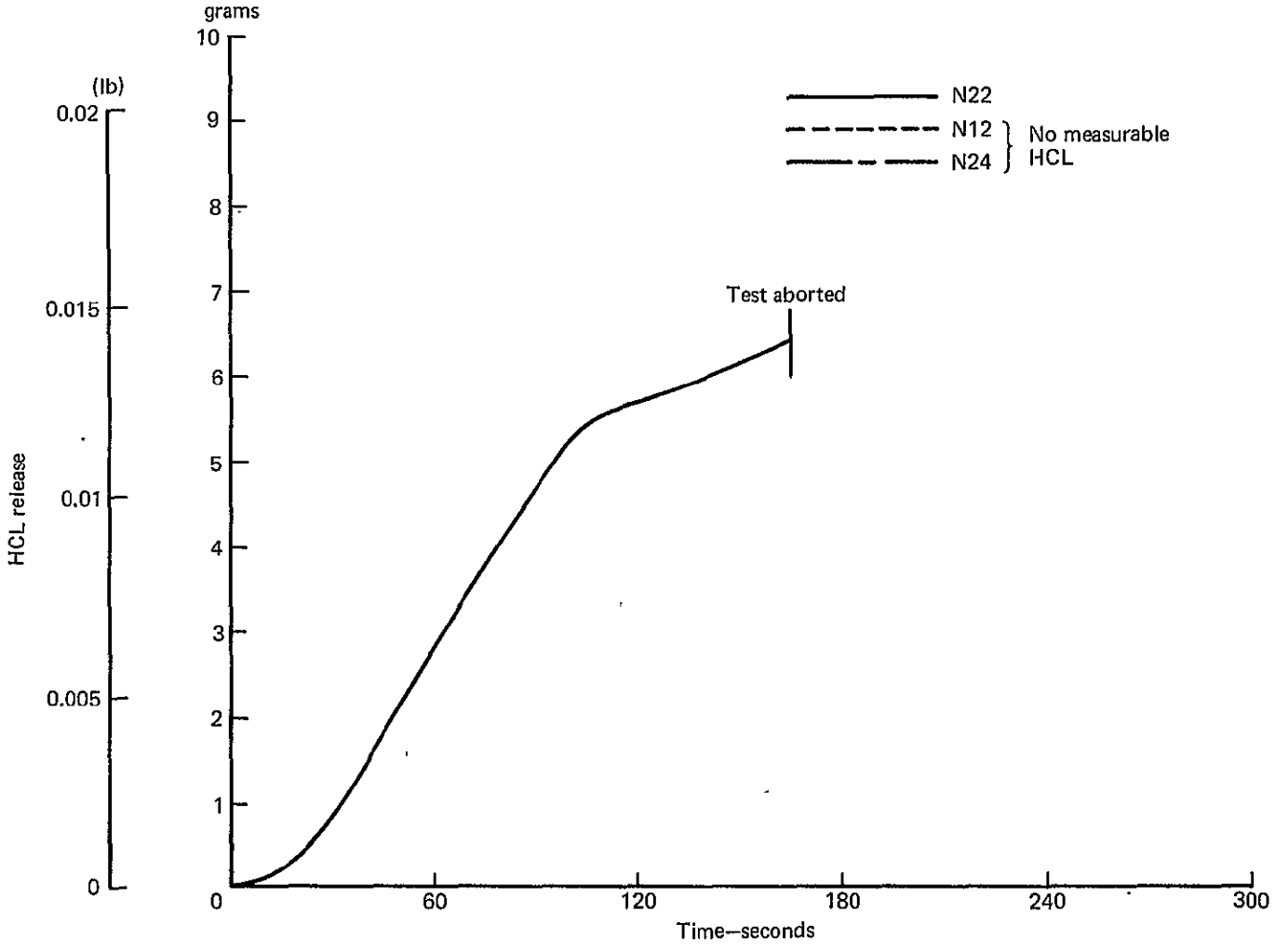

Figure E-43.—Apparent Hydrogen Chloride (HCL) Release from the Simulated Design Post-crash Fire Source Tests—New Materials

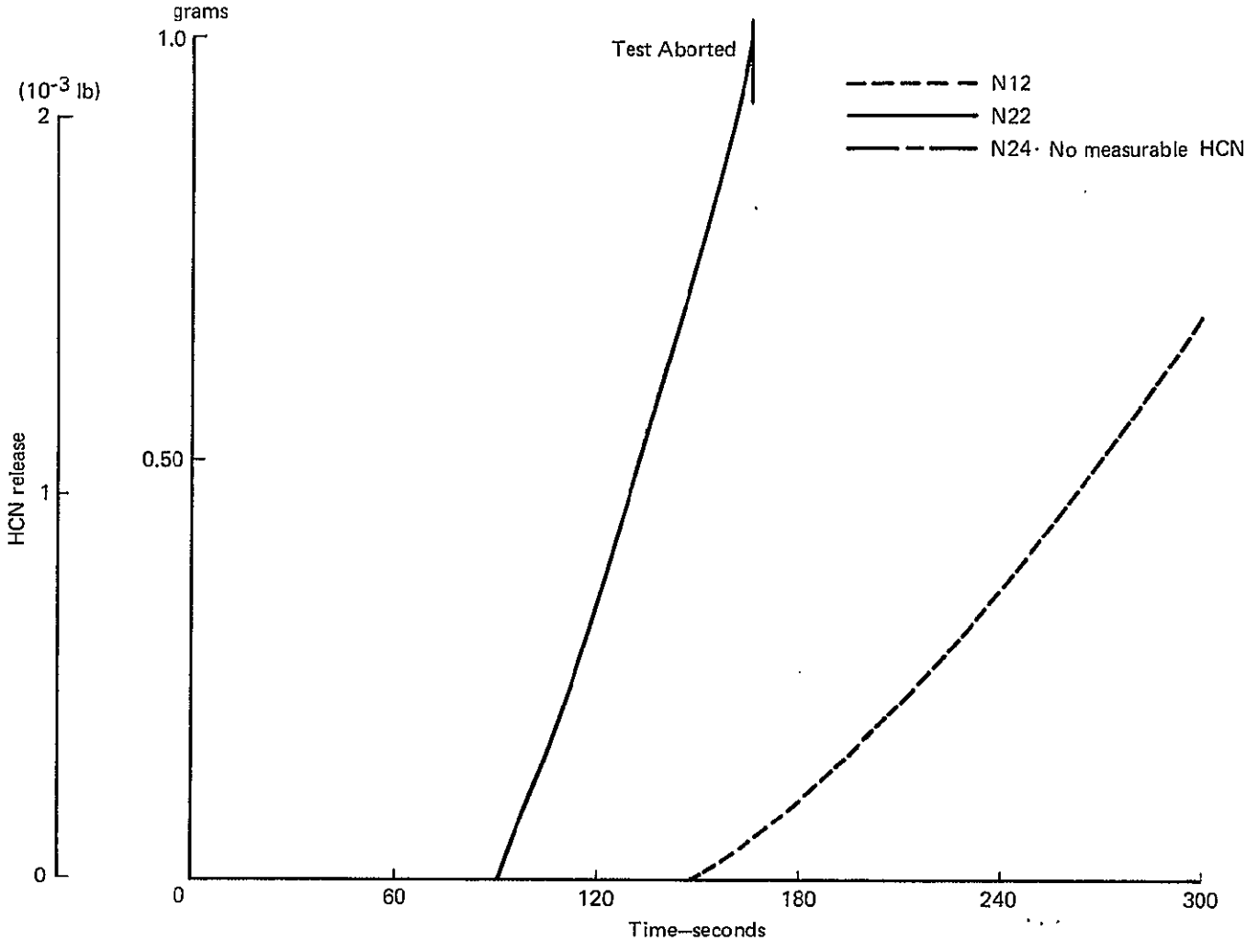

Figure E-44.— Apparent Hydrogen Cyanide (HCN) Release from the Simulated Design Post-crash Fire Source Tests—New Materials

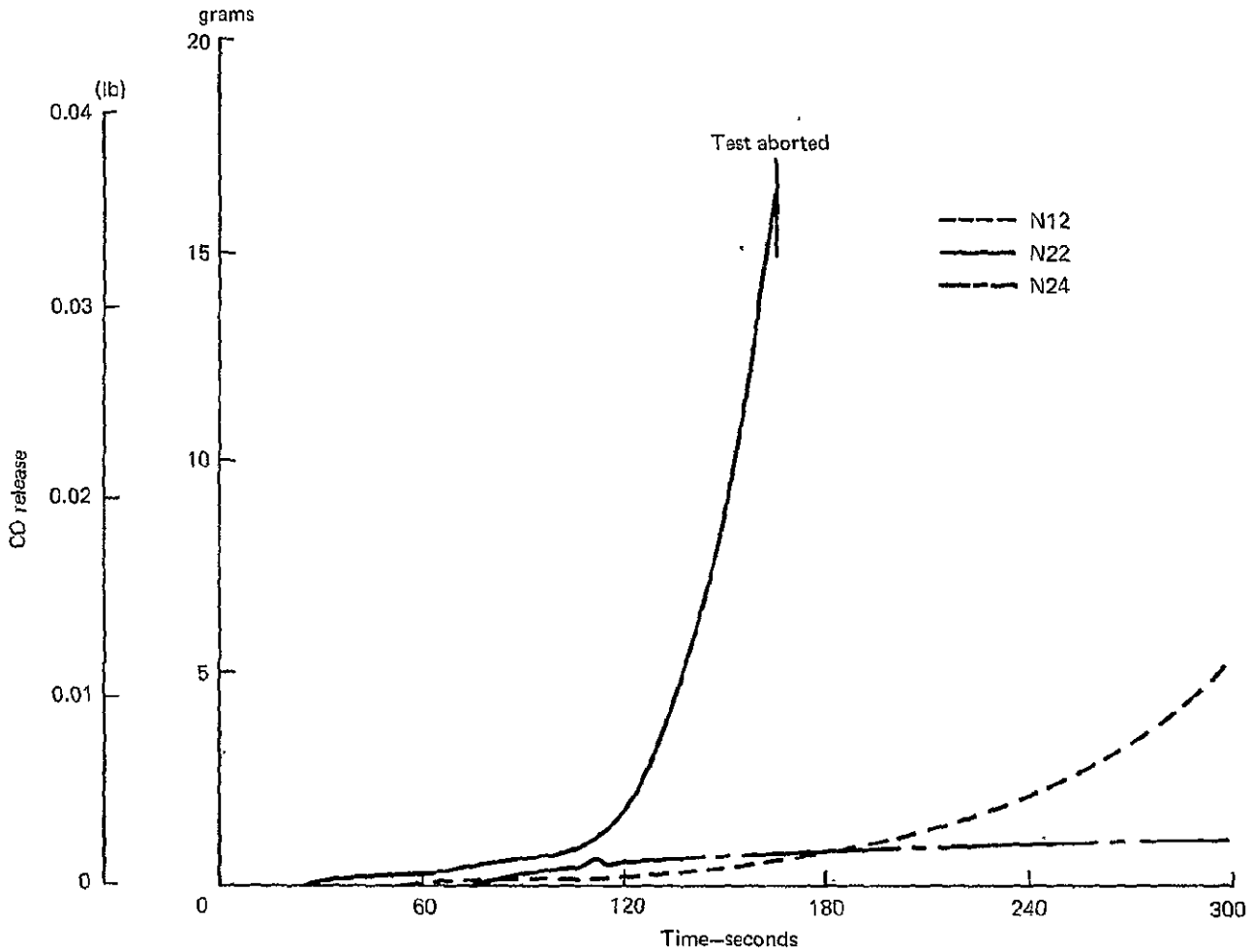

Figure E-45.—Apparent Carbon Monoxide (CO) Release from the Simulated Design Post-crash Fire Source Tests—New Materials

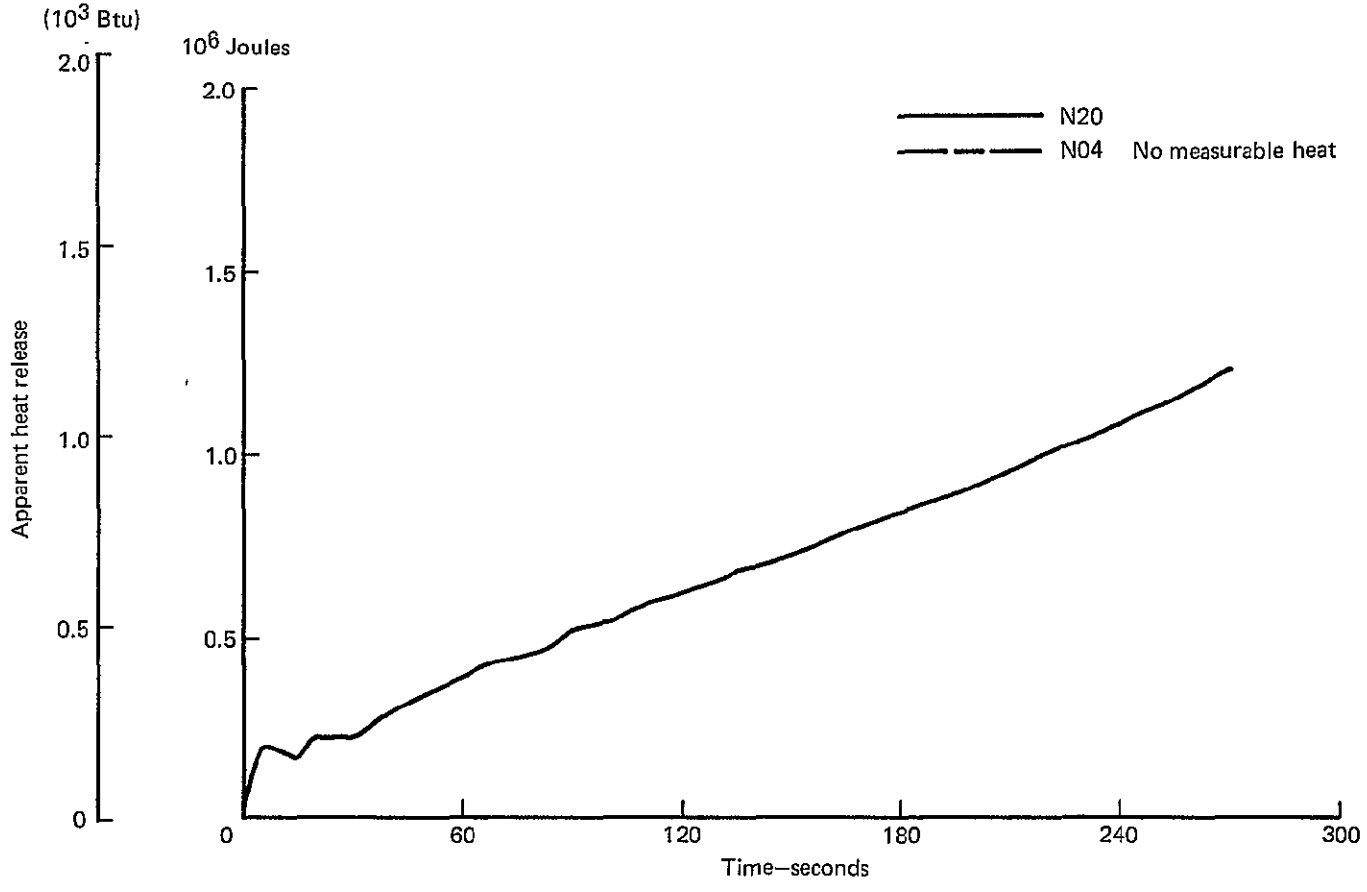

Figure E-46.—Apparent Heat Release from Simulated Design Post-crash Fire Source Tests—New Materials

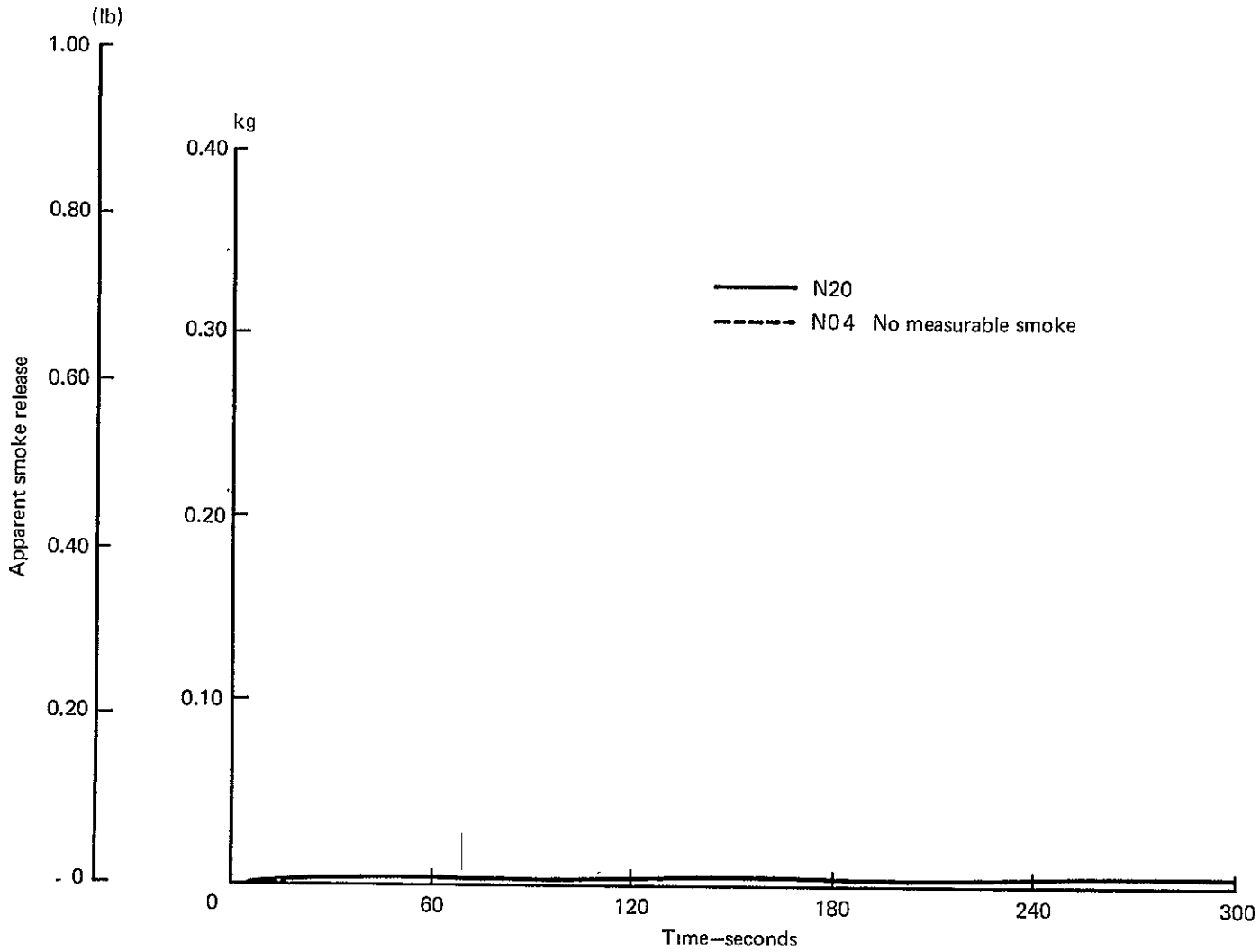

Figure E-47.—Apparent Smoke Release from Simulated Design Post-crash Fire Source Tests—New Materials

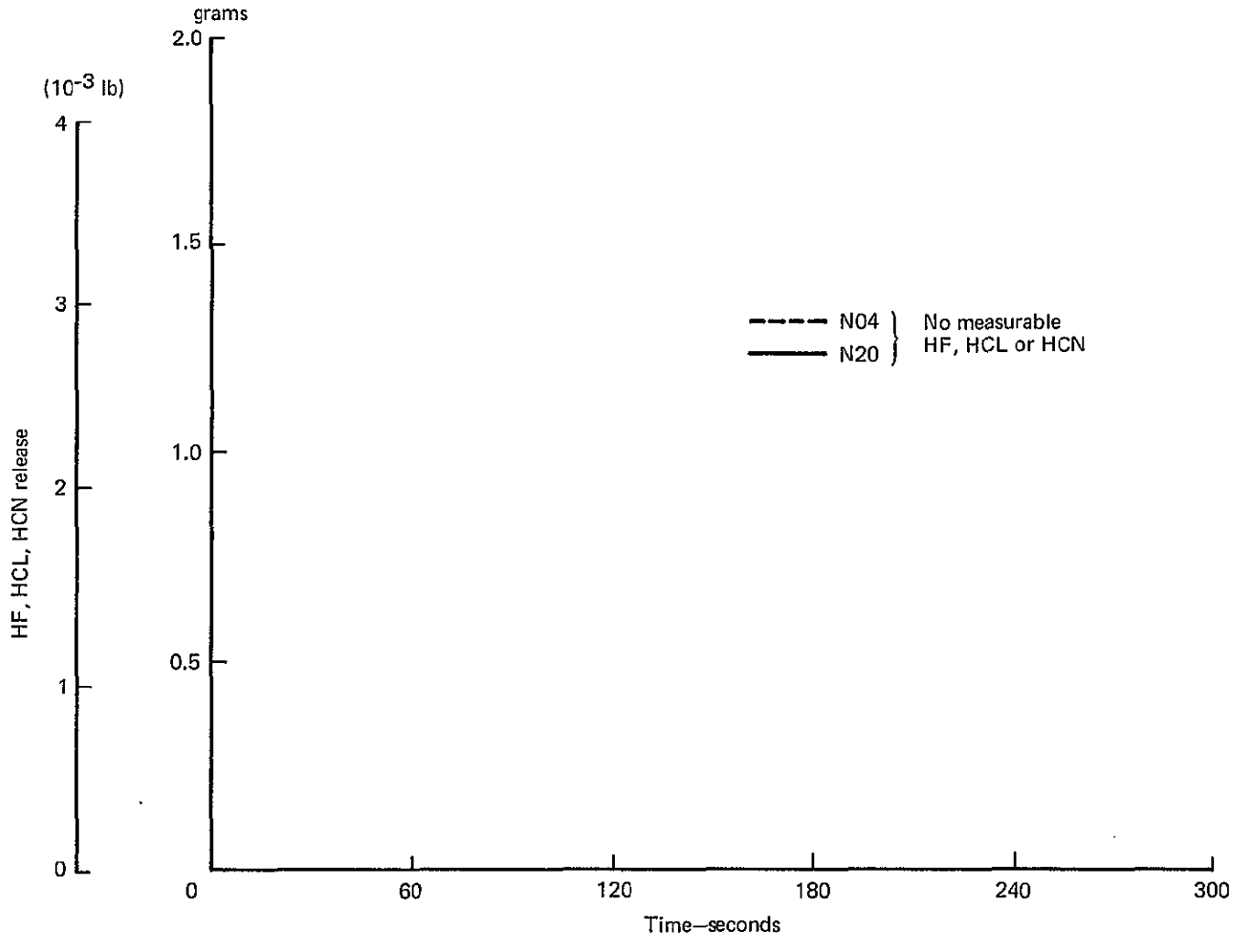

Figure E-48.—Apparent Hydrogen Fluoride (HF), Hydrogen Chloride (HCL), and Hydrogen Cyanide (HCN) Release from the Simulated Design Post-crash Fire Source Tests—New Materials

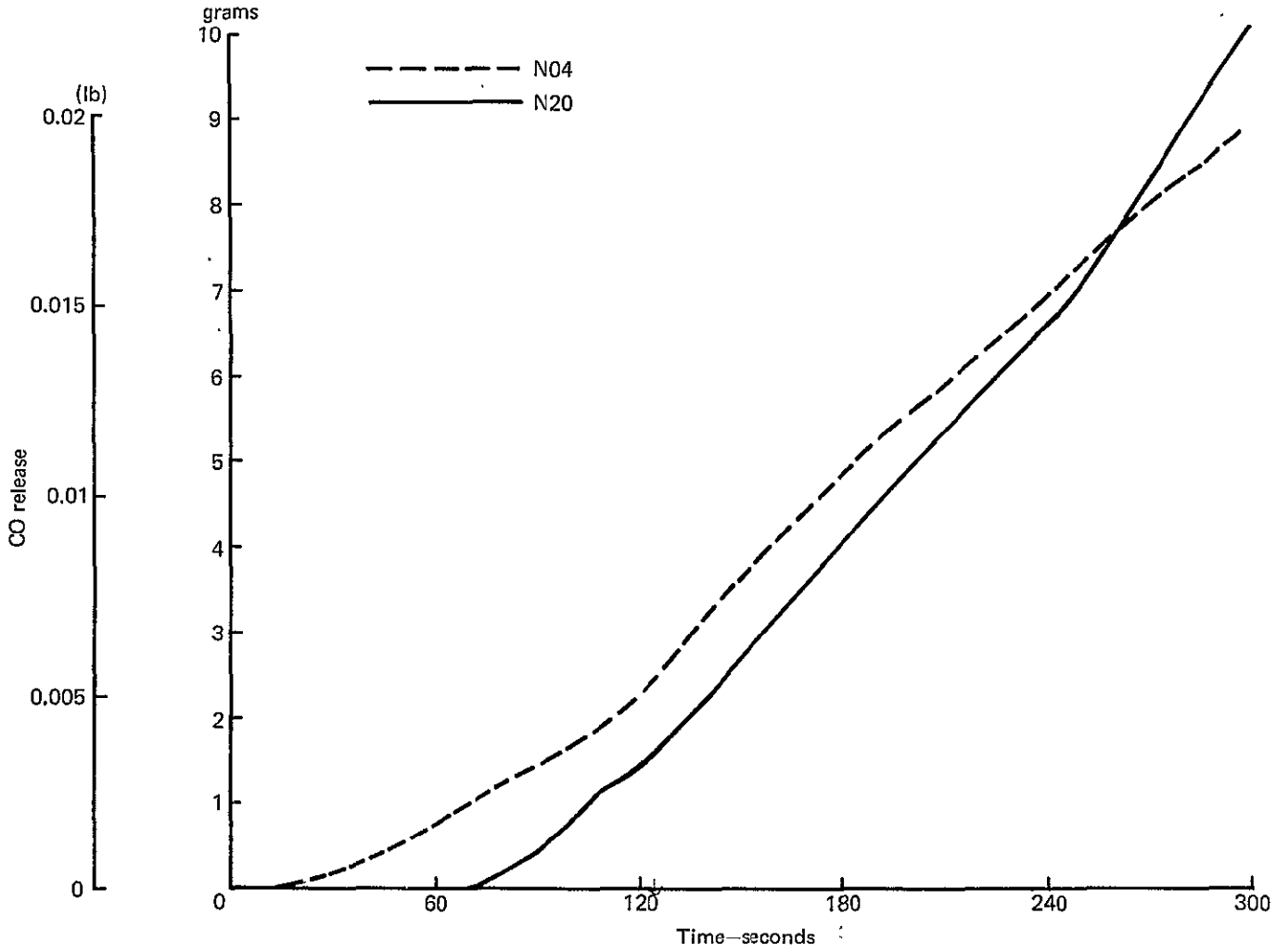

Figure E-49.—Apparent Carbon Monoxide (CO) Release from the Simulated Design Post-crash Fire Source Tests—New Materials

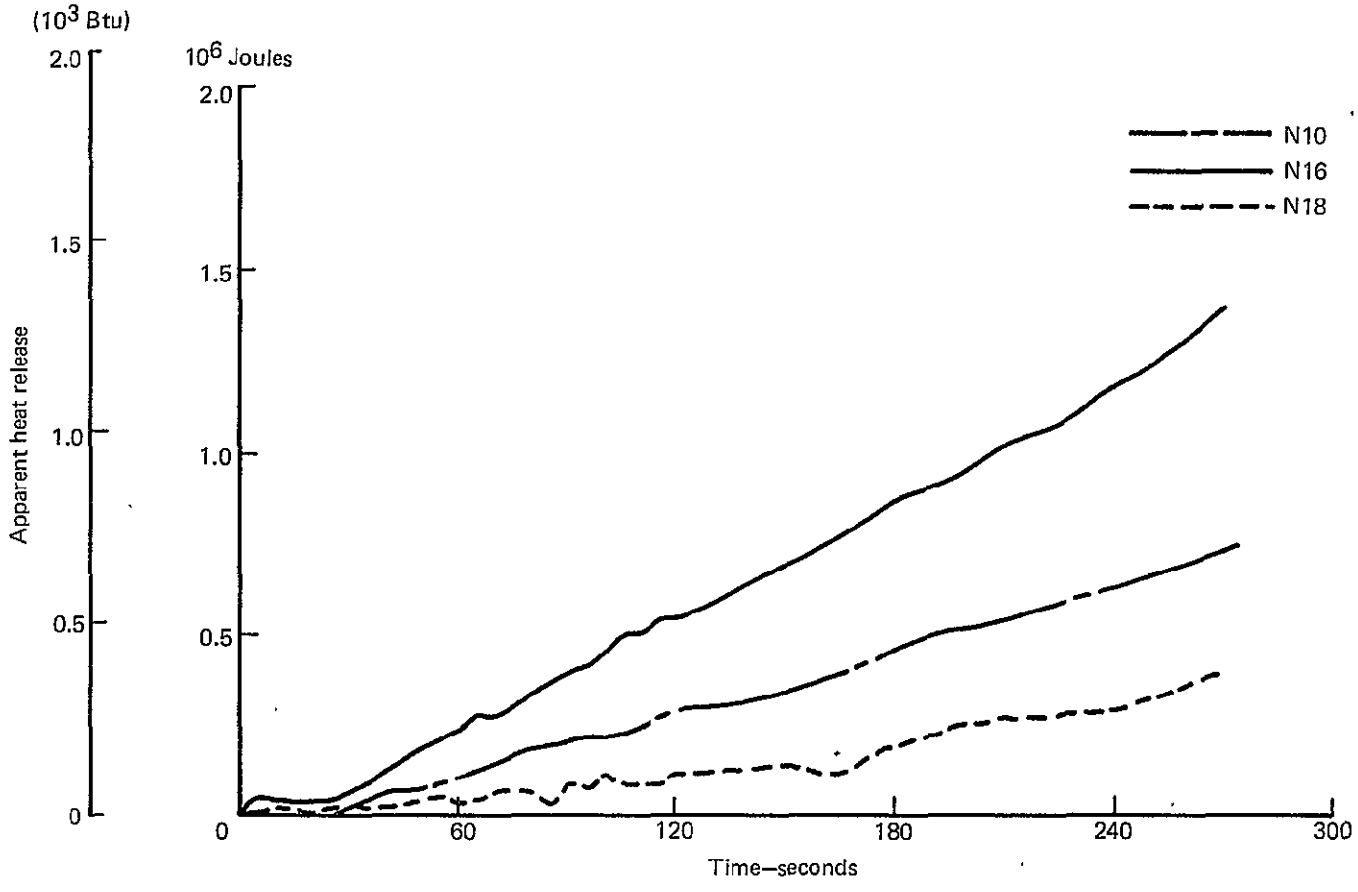

Figure E-50.—Apparent Heat Release from Simulated Design Post-crash Fire Source Tests—New Materials

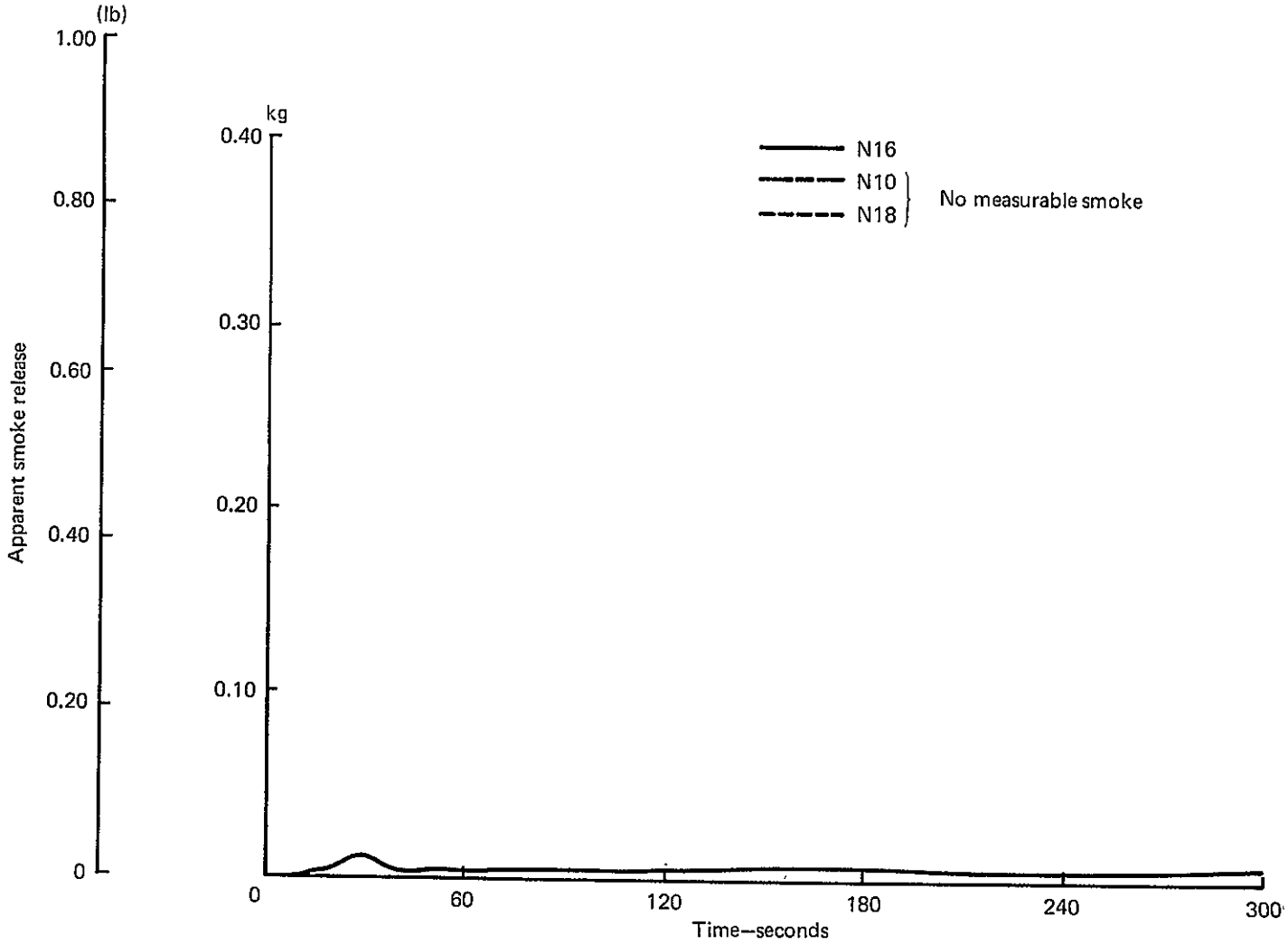

Figure E-51.—Apparent Smoke Release from Simulated Design Post-crash Fire Source Tests—New Materials

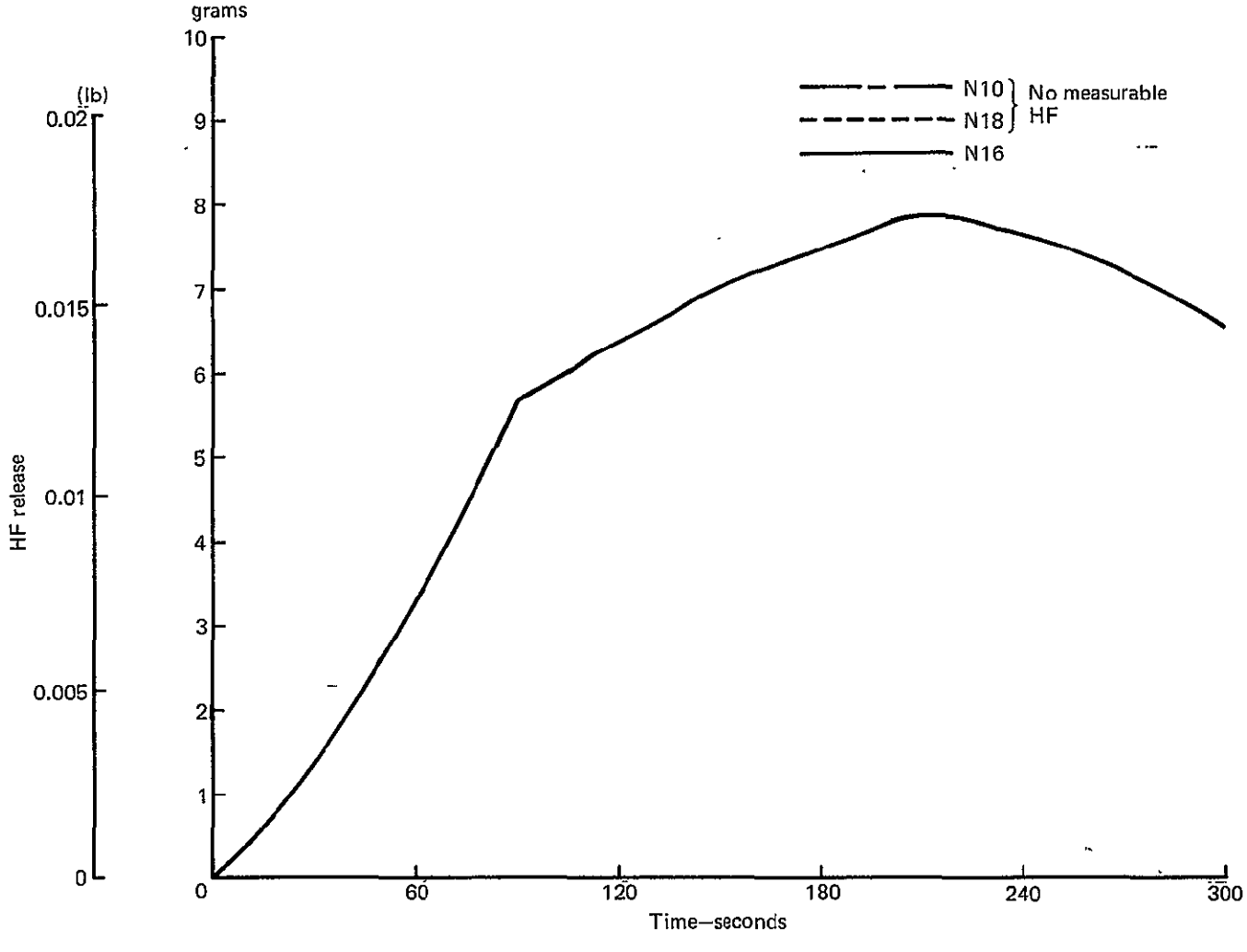

Figure E-52.—Apparent Hydrogen Fluoride (HF) Release from the Simulated Design Post-crash Fire Source Tests—New Materials

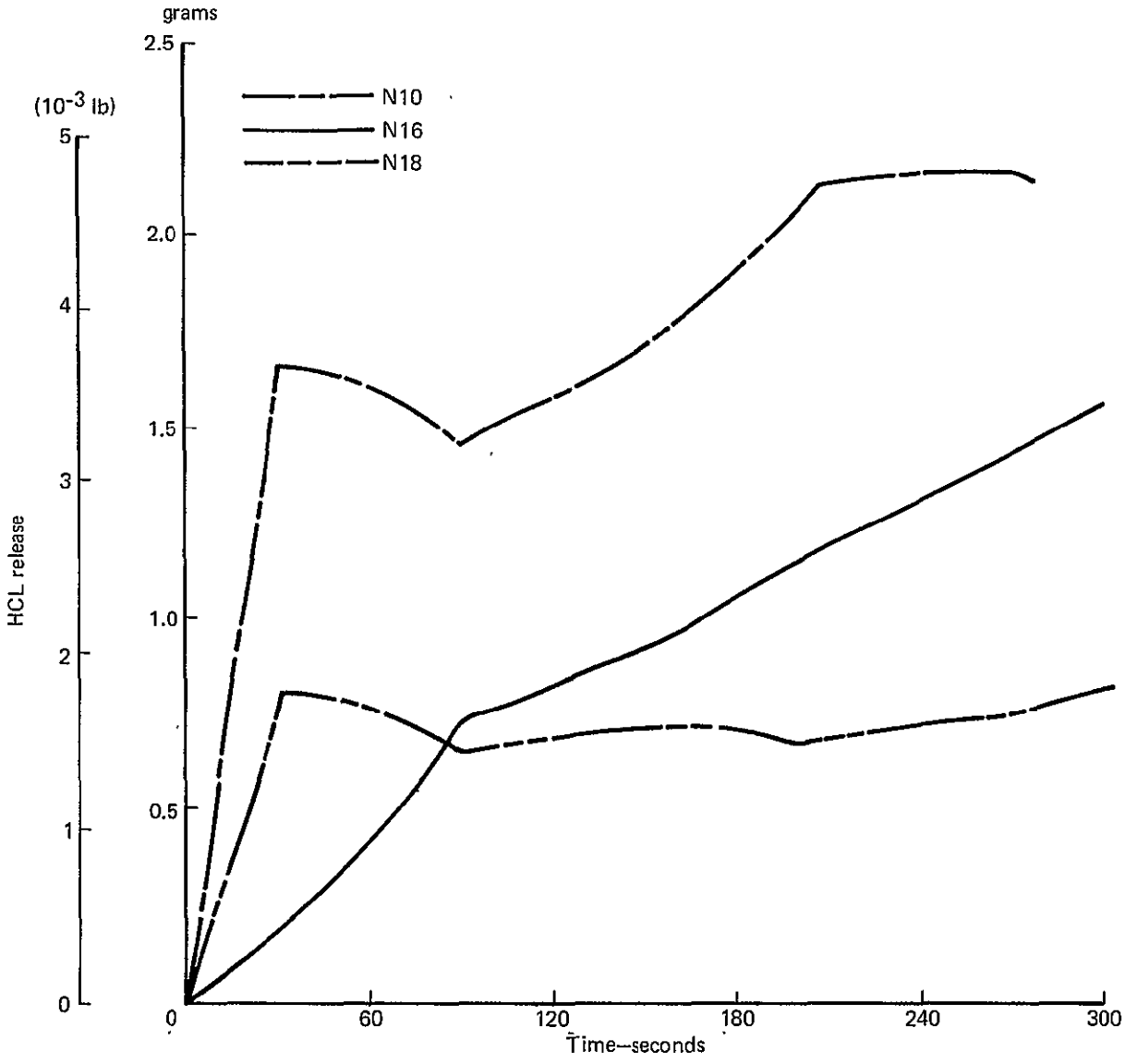

Figure E-53.— Apparent Hydrogen Chloride (HCL) Release from the Simulated Design Post-crash Fire Source Tests—New Materials

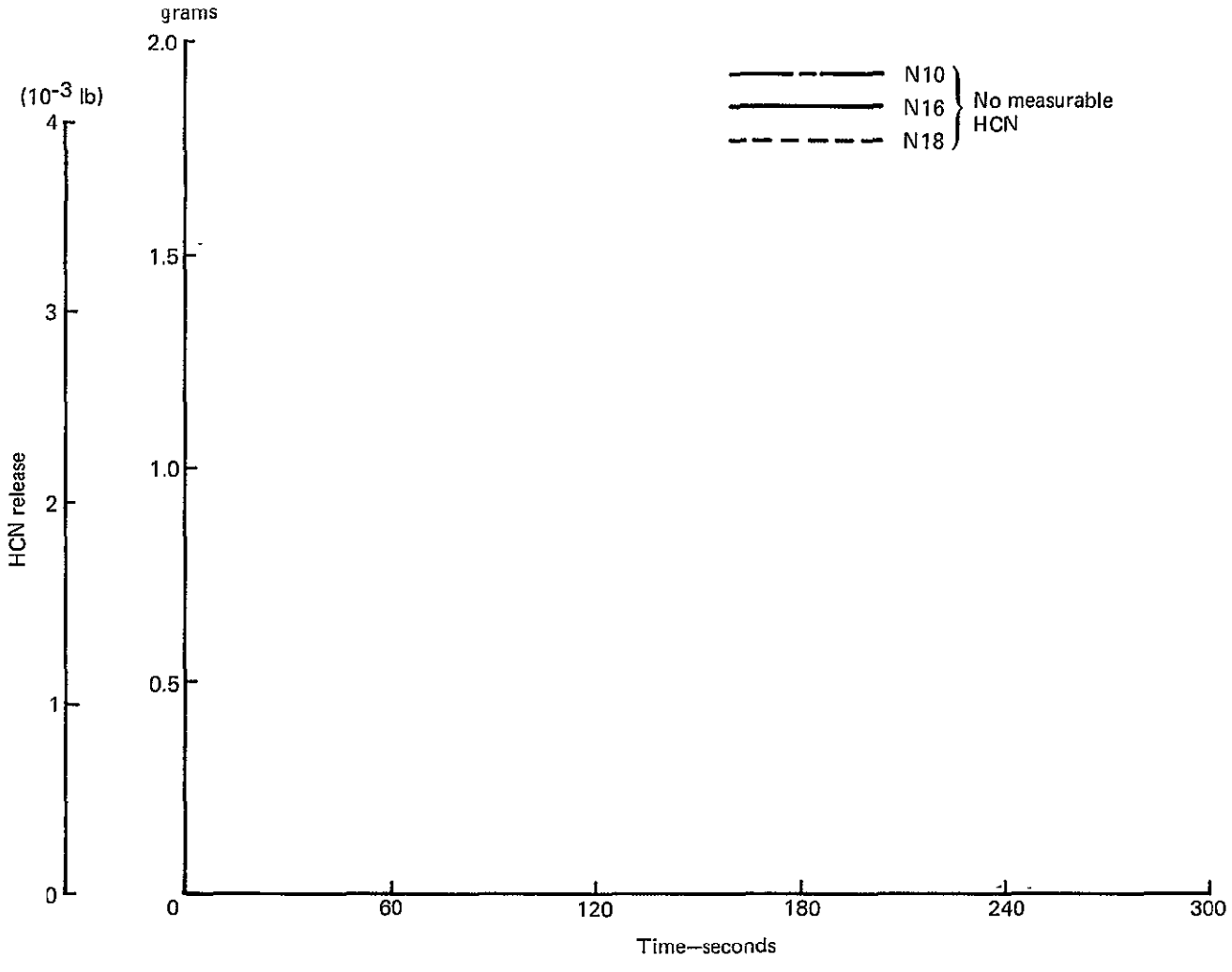

Figure E-54.—Apparent Hydrogen Cyanide (HCN) Release from the Simulated Design Post-crash Fire Source Tests—New Materials

Figure E-55.—Apparent Carbon Monoxide (CO) Release from the Simulated Design Post-crash Fire Source Tests—New Materials

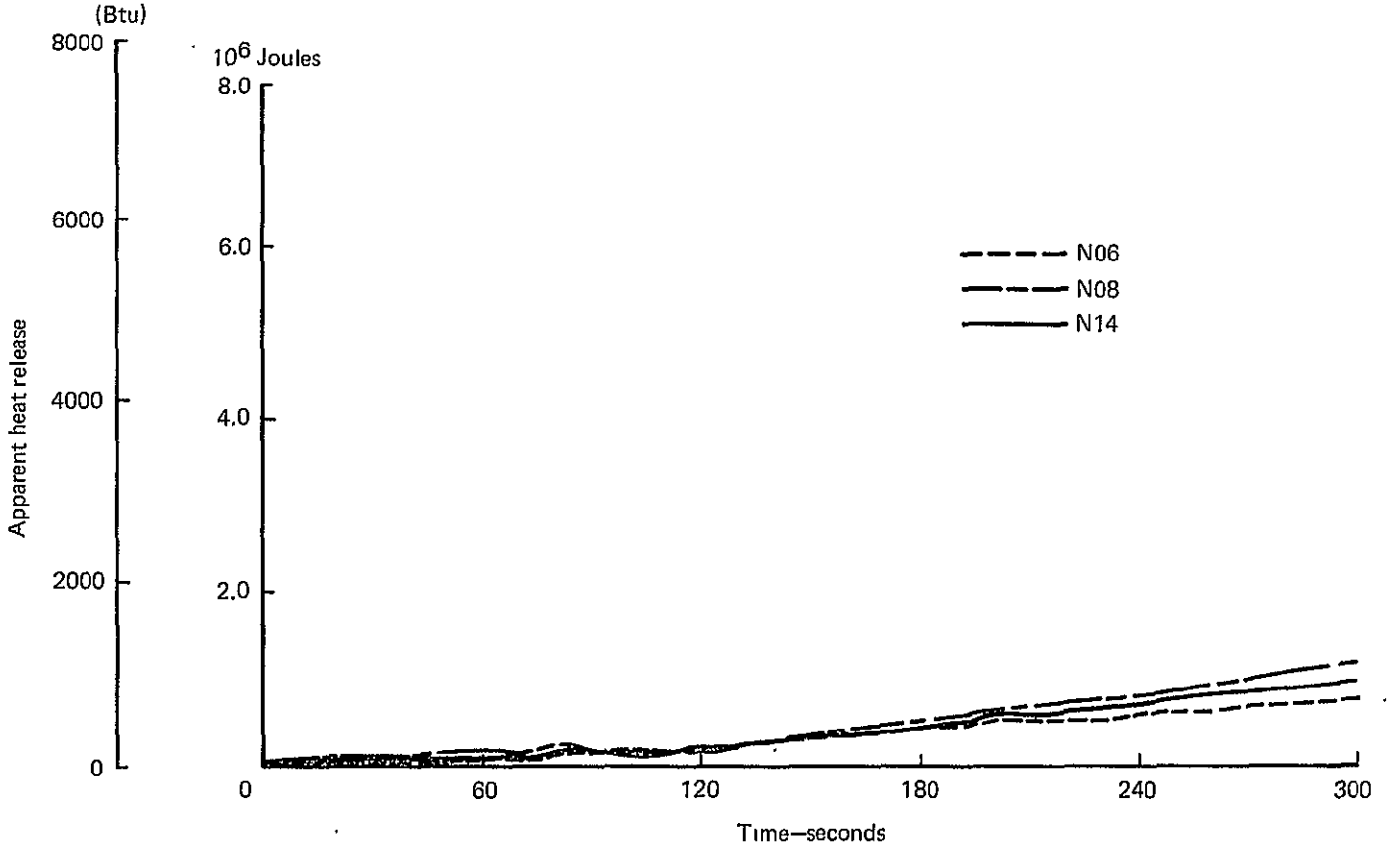

Figure E-56.— Apparent Heat Release from Simulated Design In-flight Fire Source Tests—New Materials

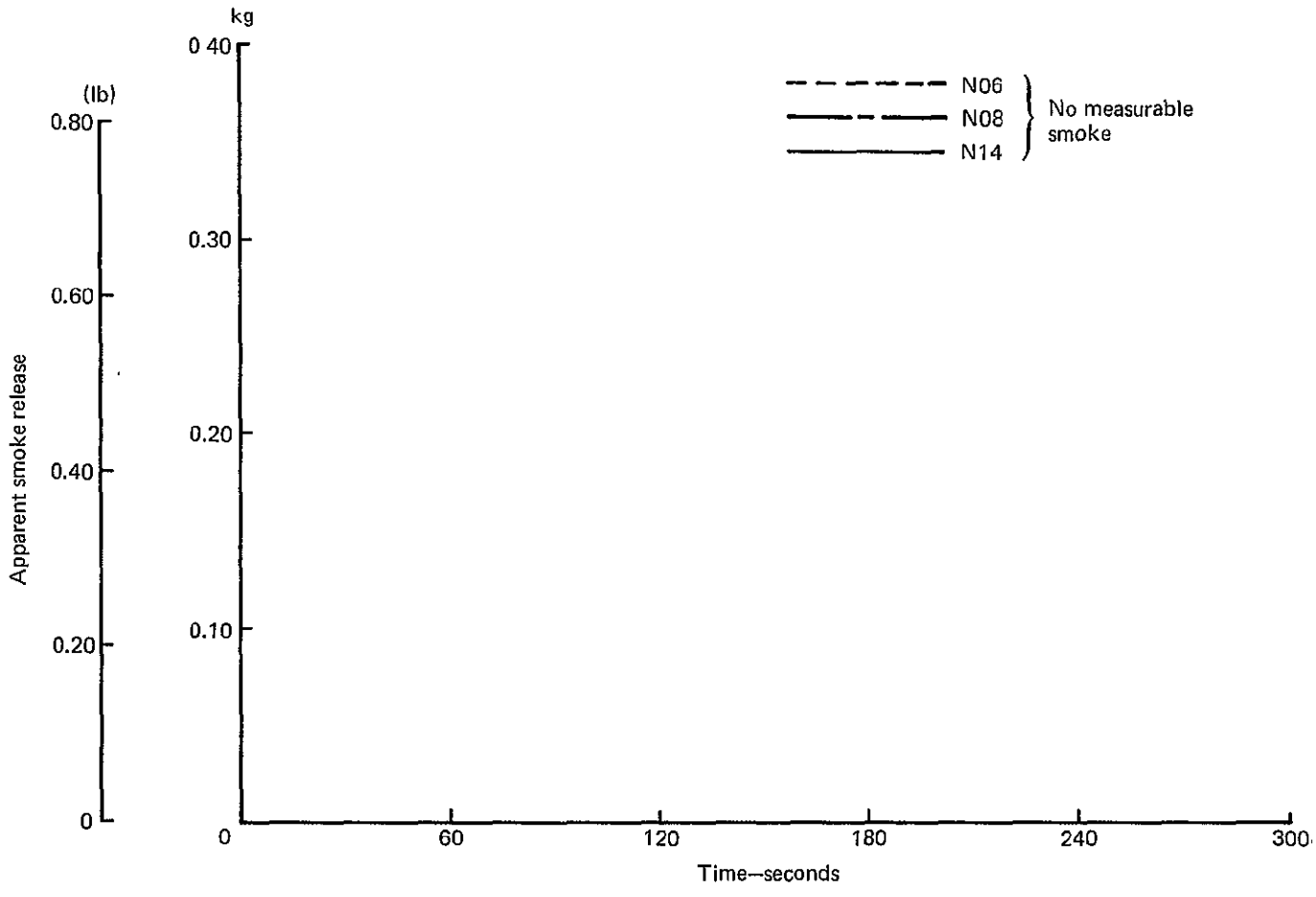

Figure E-57.—Apparent Smoke Release from Simulated Design In-flight Fire Source Tests—New Materials

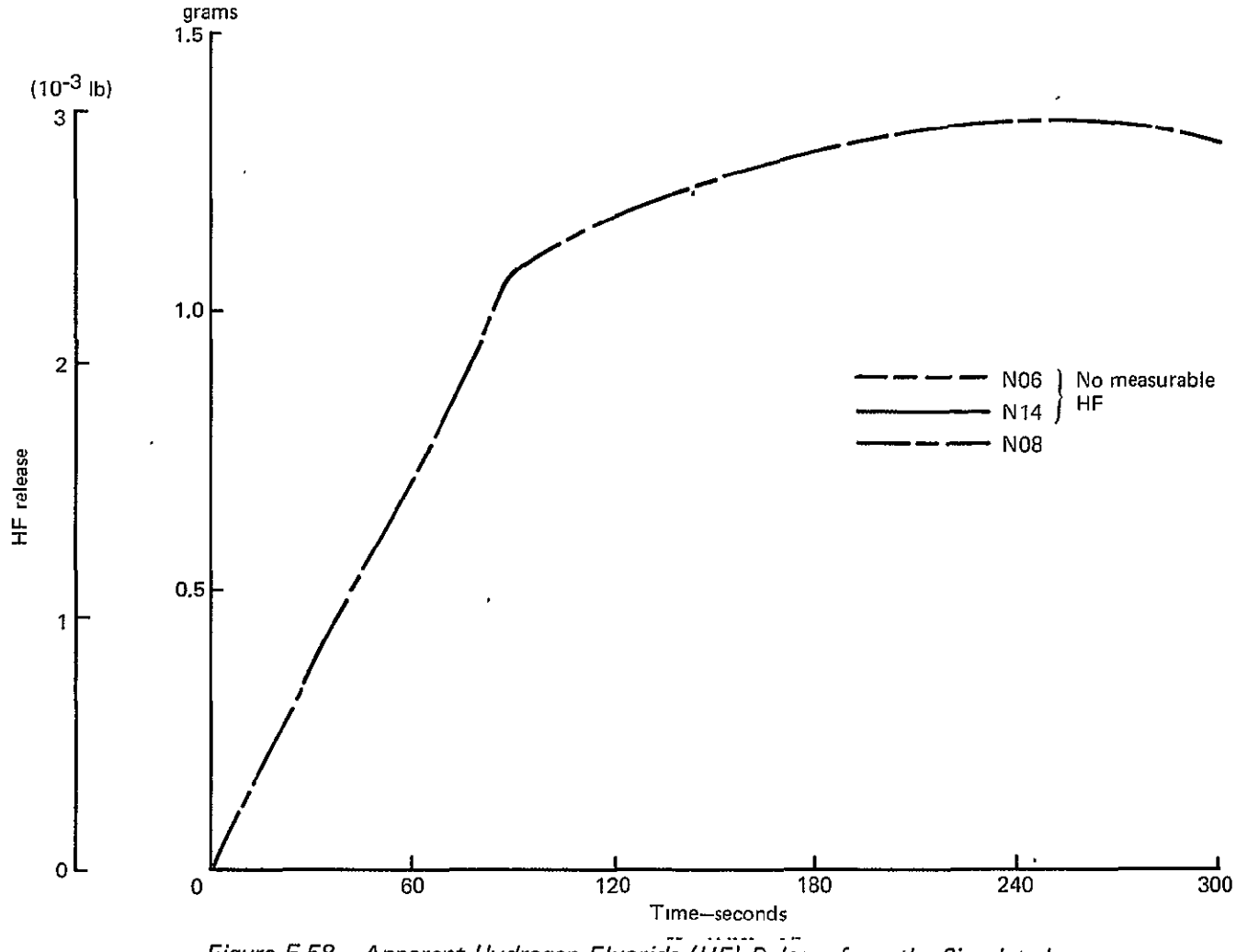

Figure E-58.—Apparent Hydrogen Fluoride (HF) Release from the Simulated Design In-flight Fire Source Tests—New Materials

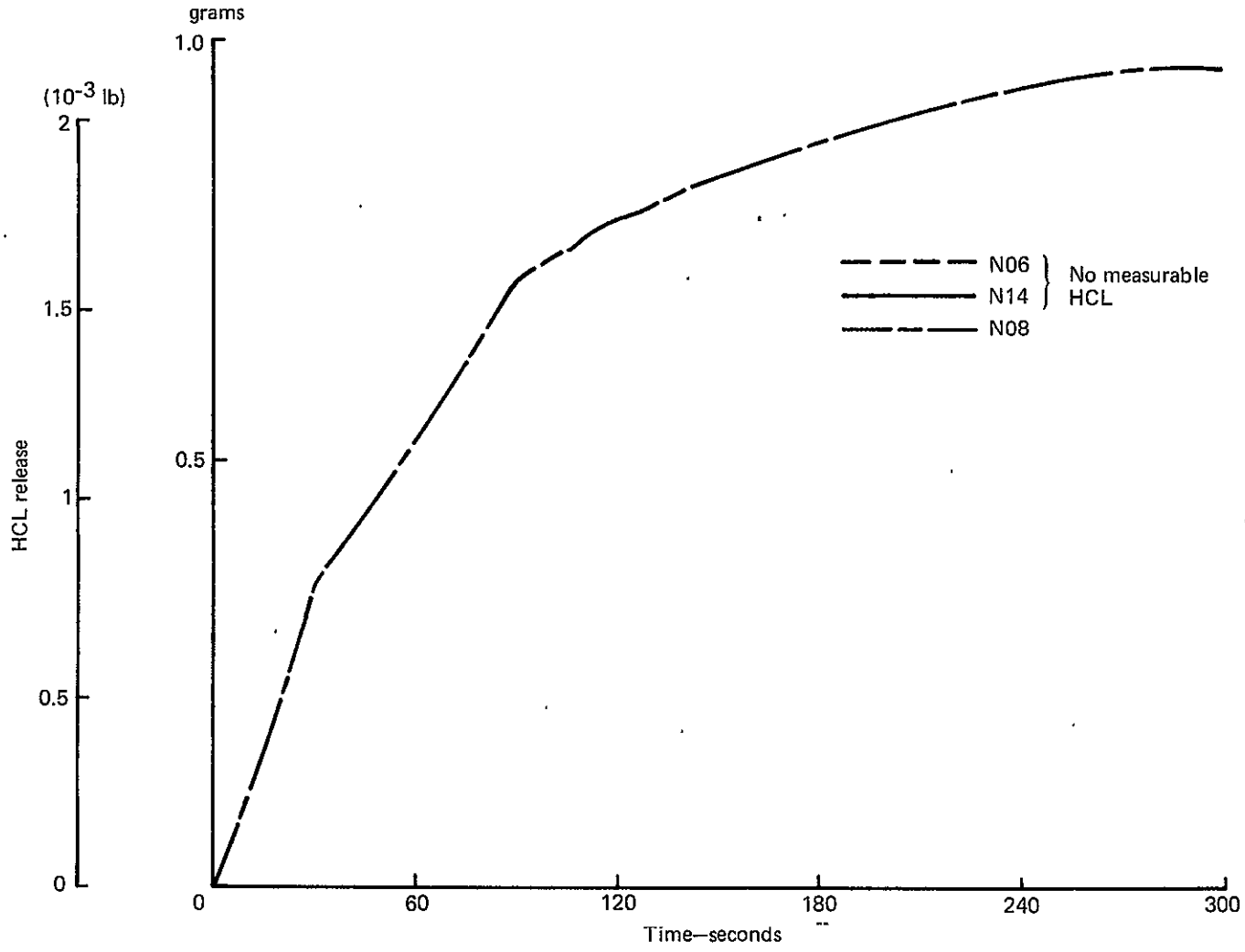

Figure E-59.—Apparent Hydrogen Chloride (HCL) Release from the Simulated Design In-flight Fire Source Tests—New Materials

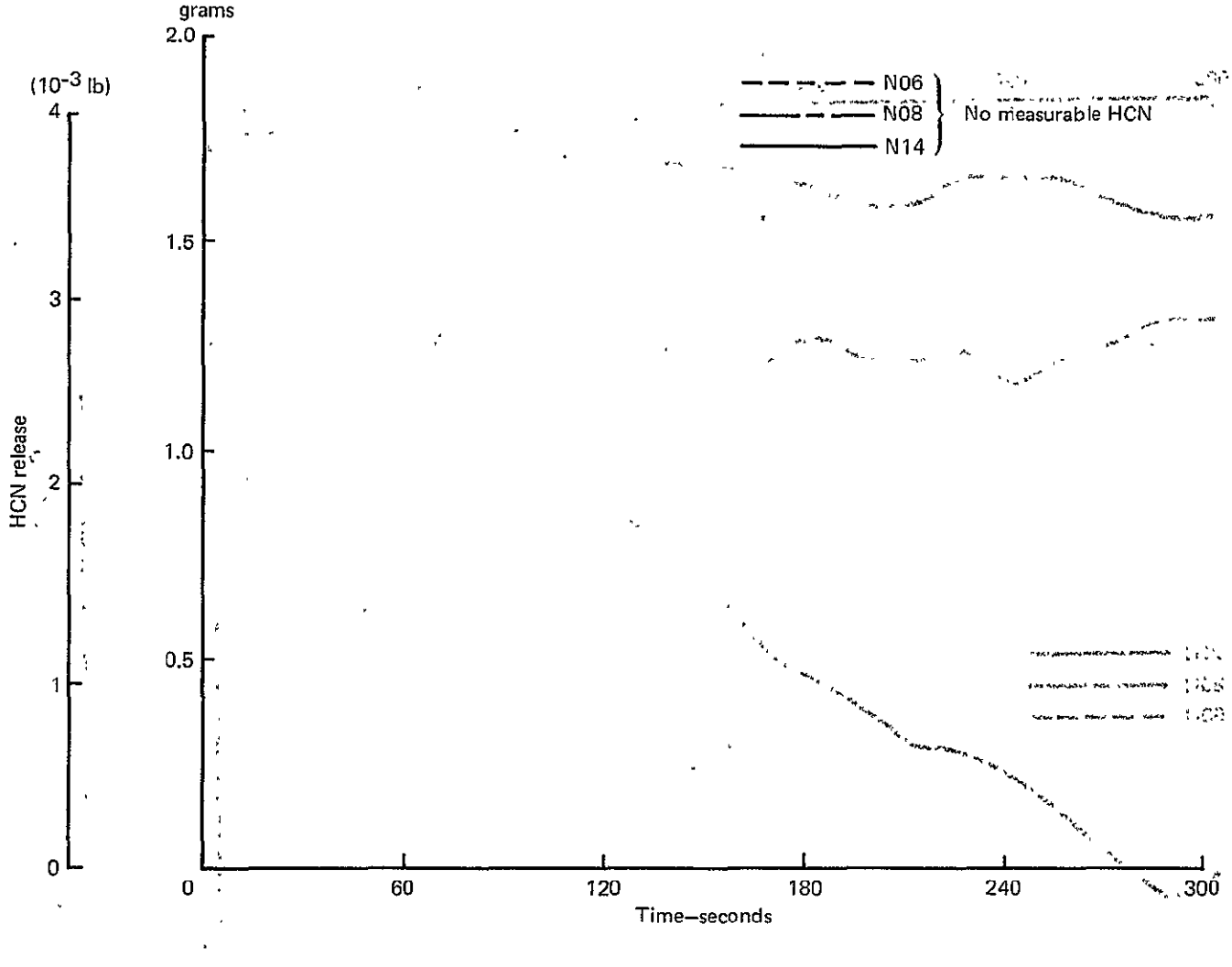

Figure E-60.—Apparent Hydrogen Cyanide (HCN) Release from the Simulated Design In-flight Fire Source Tests—New Materials

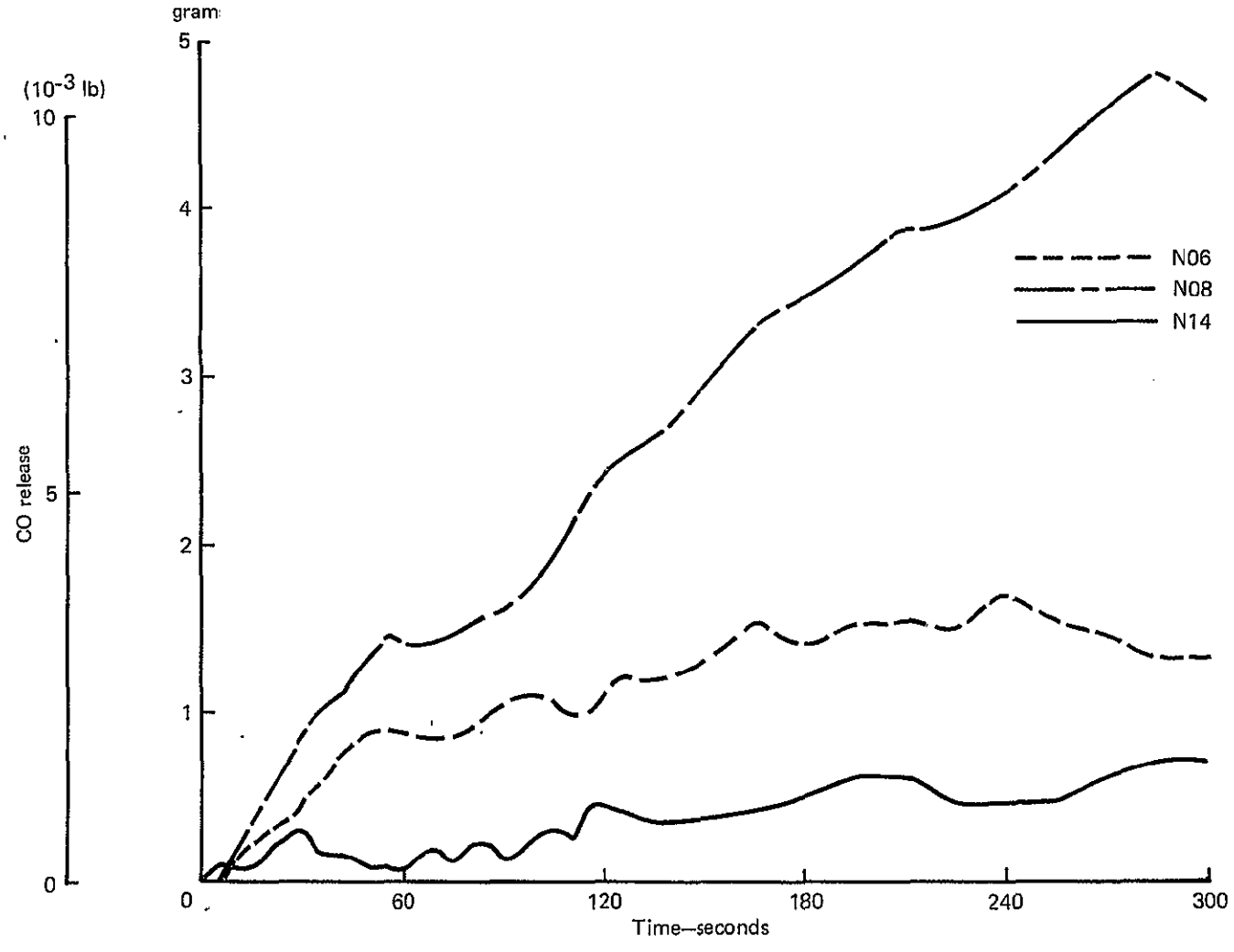

Figure E-61.—Apparent Carbon Monoxide (CO) Release from the Simulated Design In-flight Fire Source Tests—New Materials

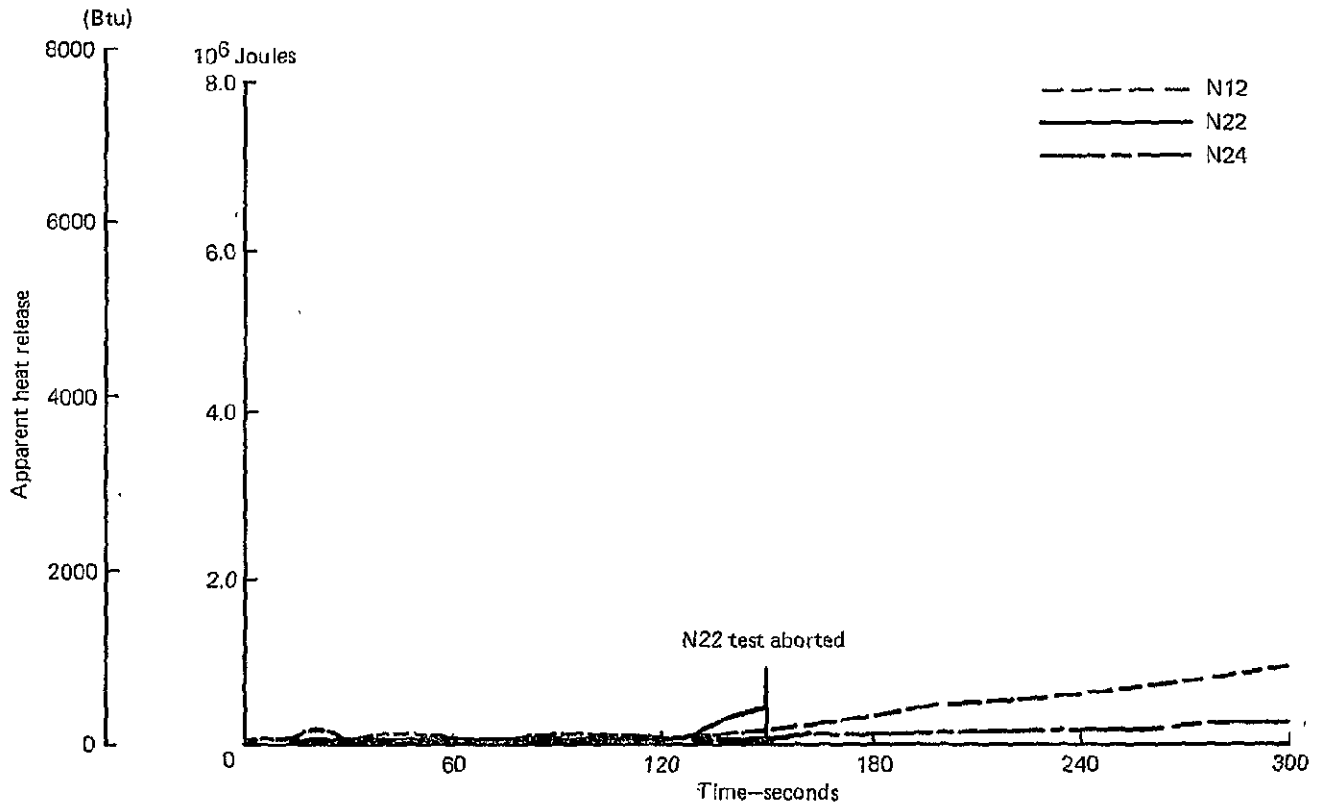

Figure E-62.—Apparent Heat Release from Simulated Design In-flight Fire Source Tests—New Materials

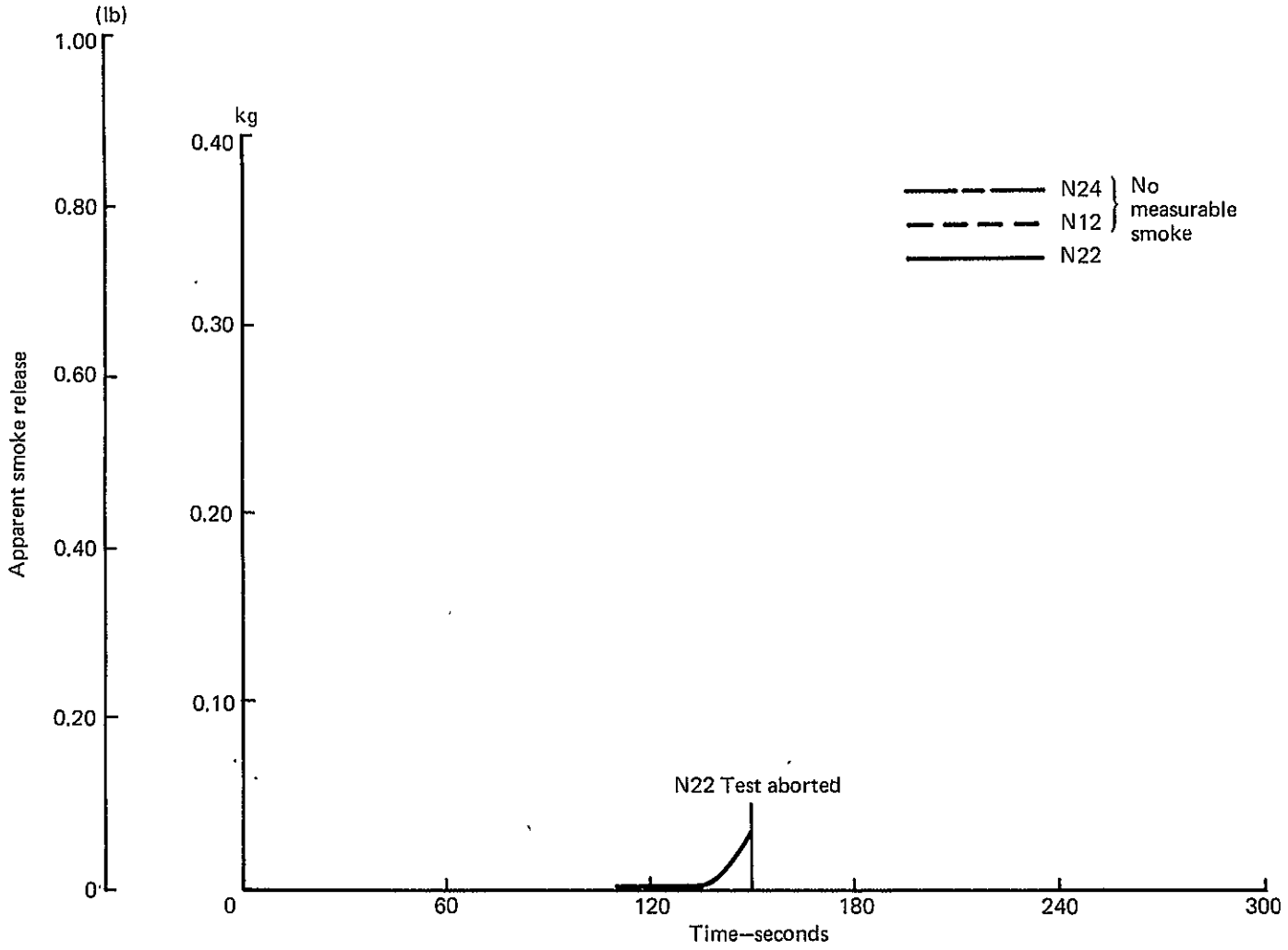

Figure E-63.—Apparent Smoke Release from Simulated Design In-flight Fire Source Tests—New Materials

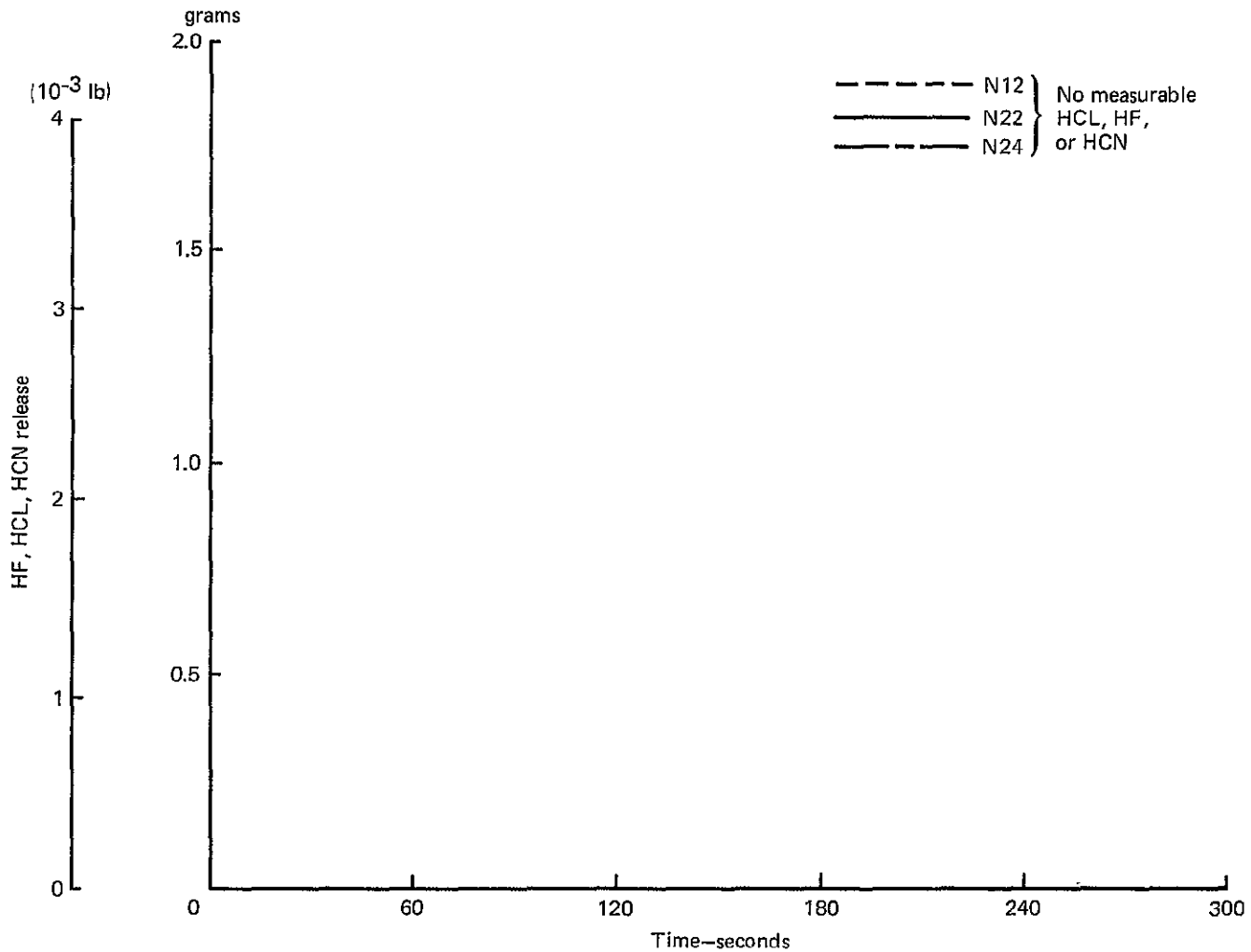

Figure E-64.—Apparent Hydrogen Fluoride (HF), Hydrogen Chloride (HCL) and Hydrogen Cyanide (HCN) Release from the Simulated Design In-flight Fire Source Tests—New Materials

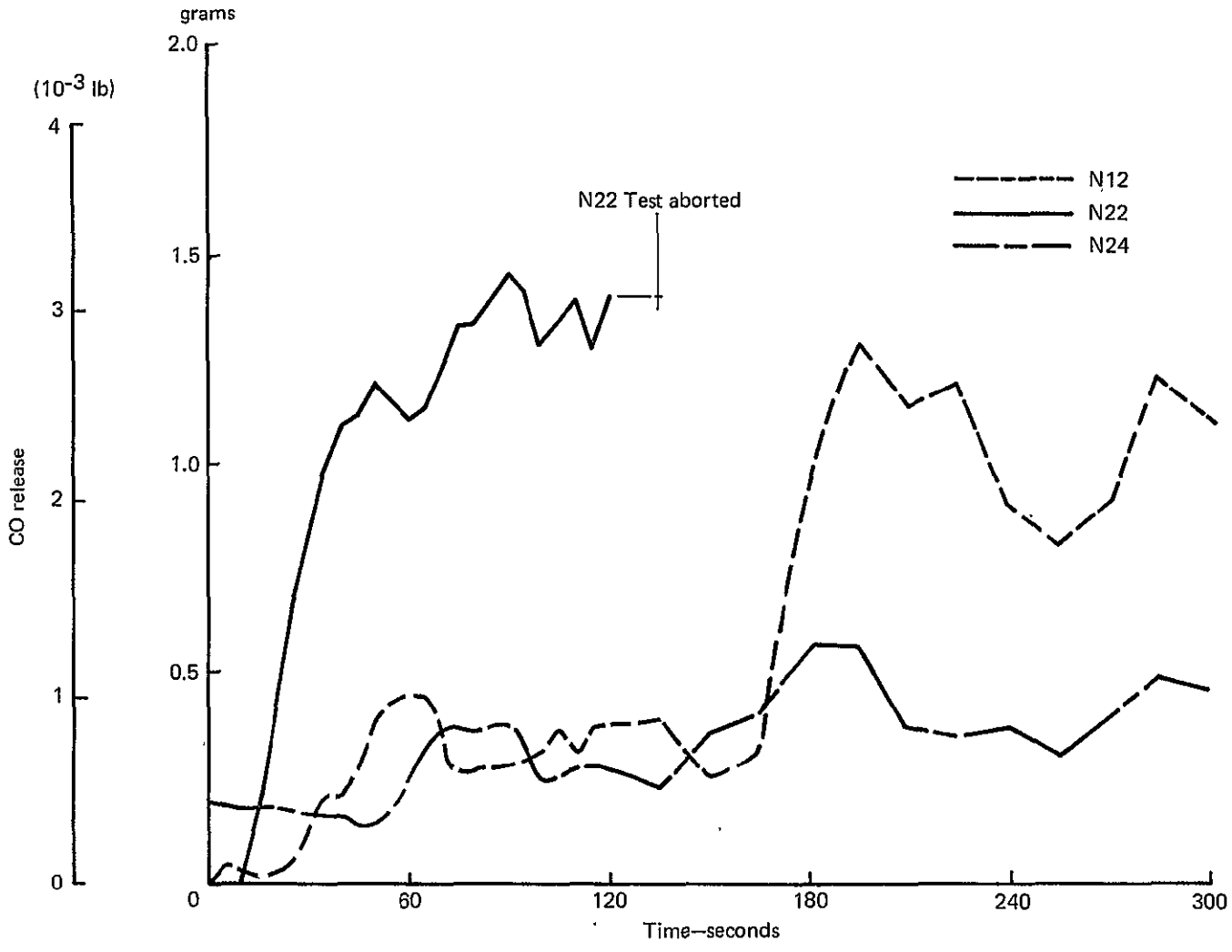

Figure E-65.—Apparent Carbon Monoxide (CO) Release from the Simulated Design In-flight Fire Source Tests—New Materials

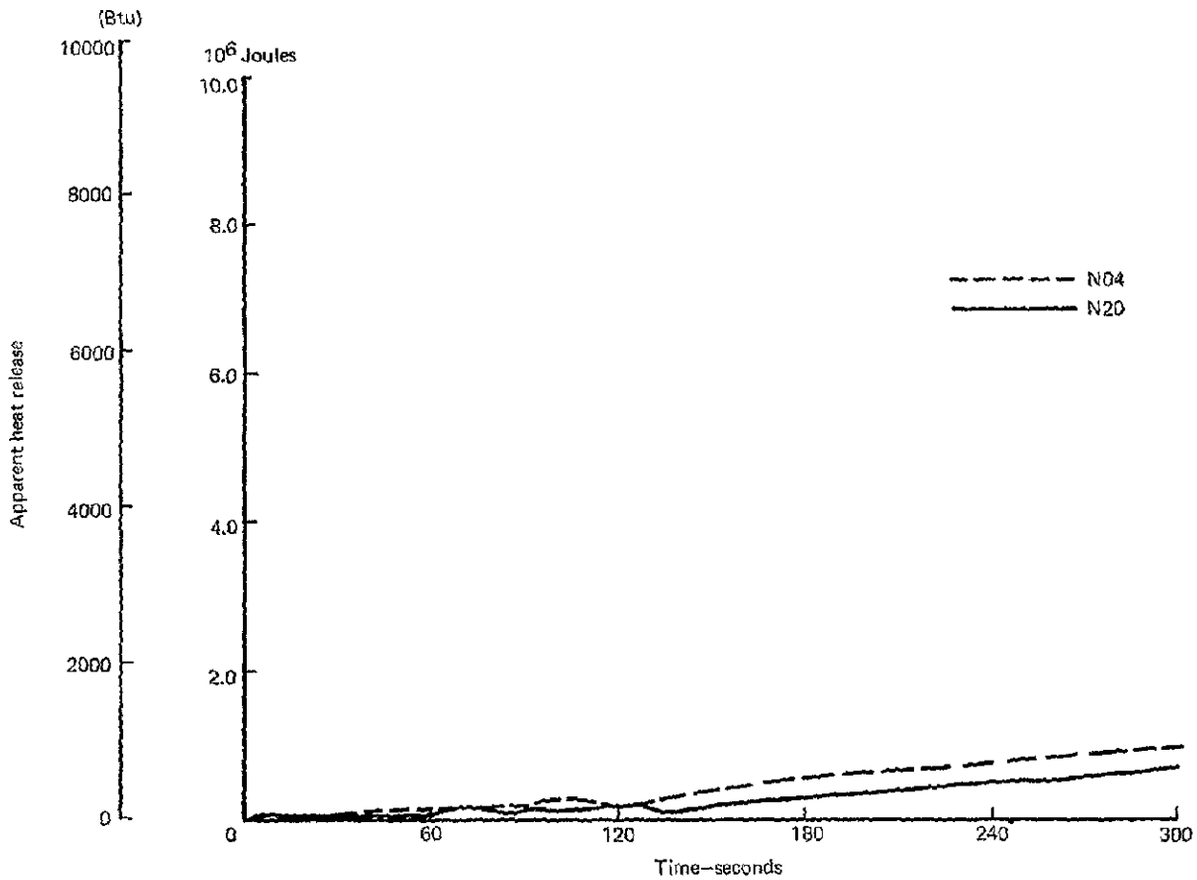

Figure E-66.—Apparent Heat Release from Simulated Design In-flight Fire Source Tests—New Materials

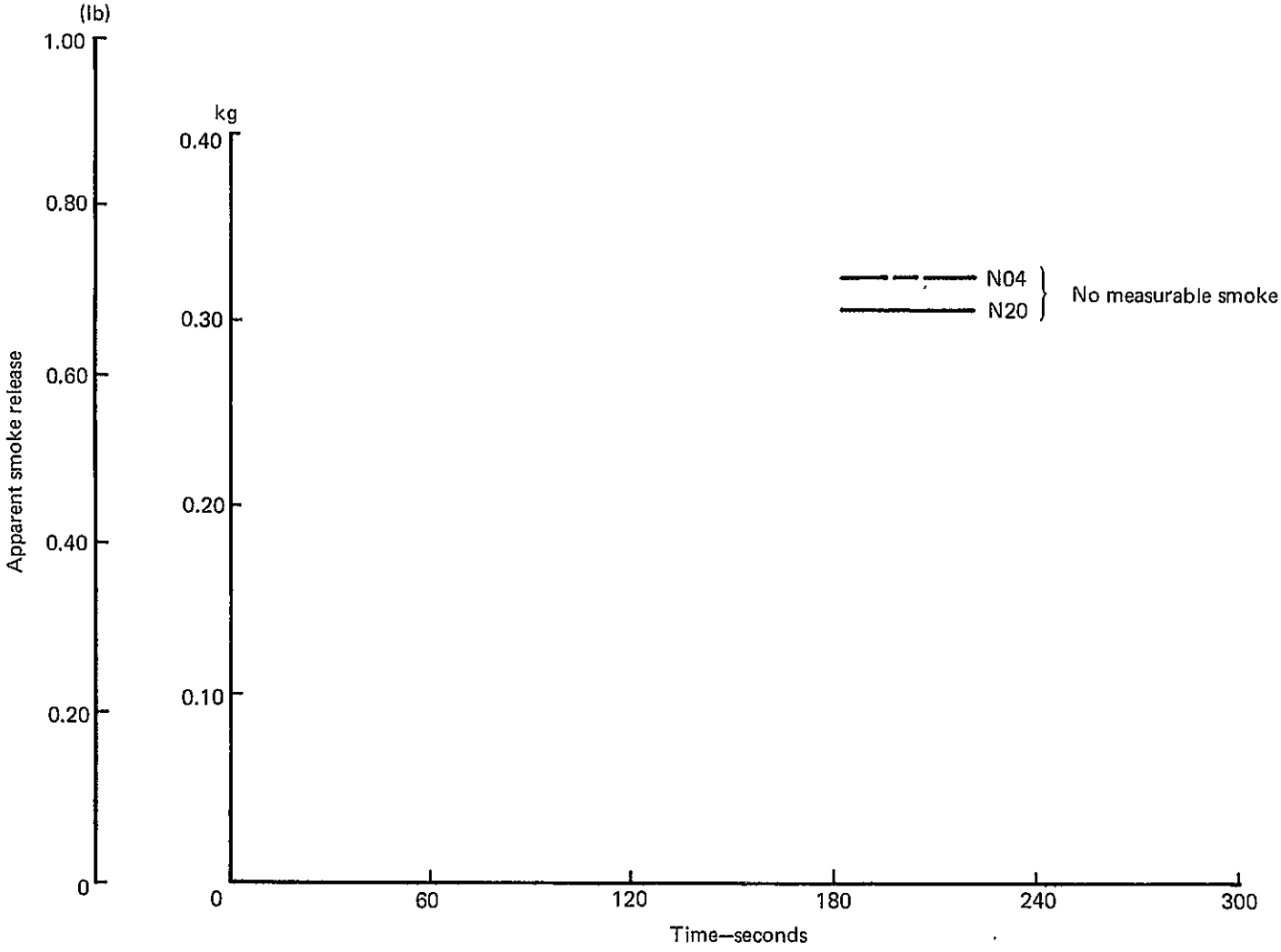

Figure E-67.—Apparent Smoke Release from Simulated Design In-flight Fire Source Tests—New Materials

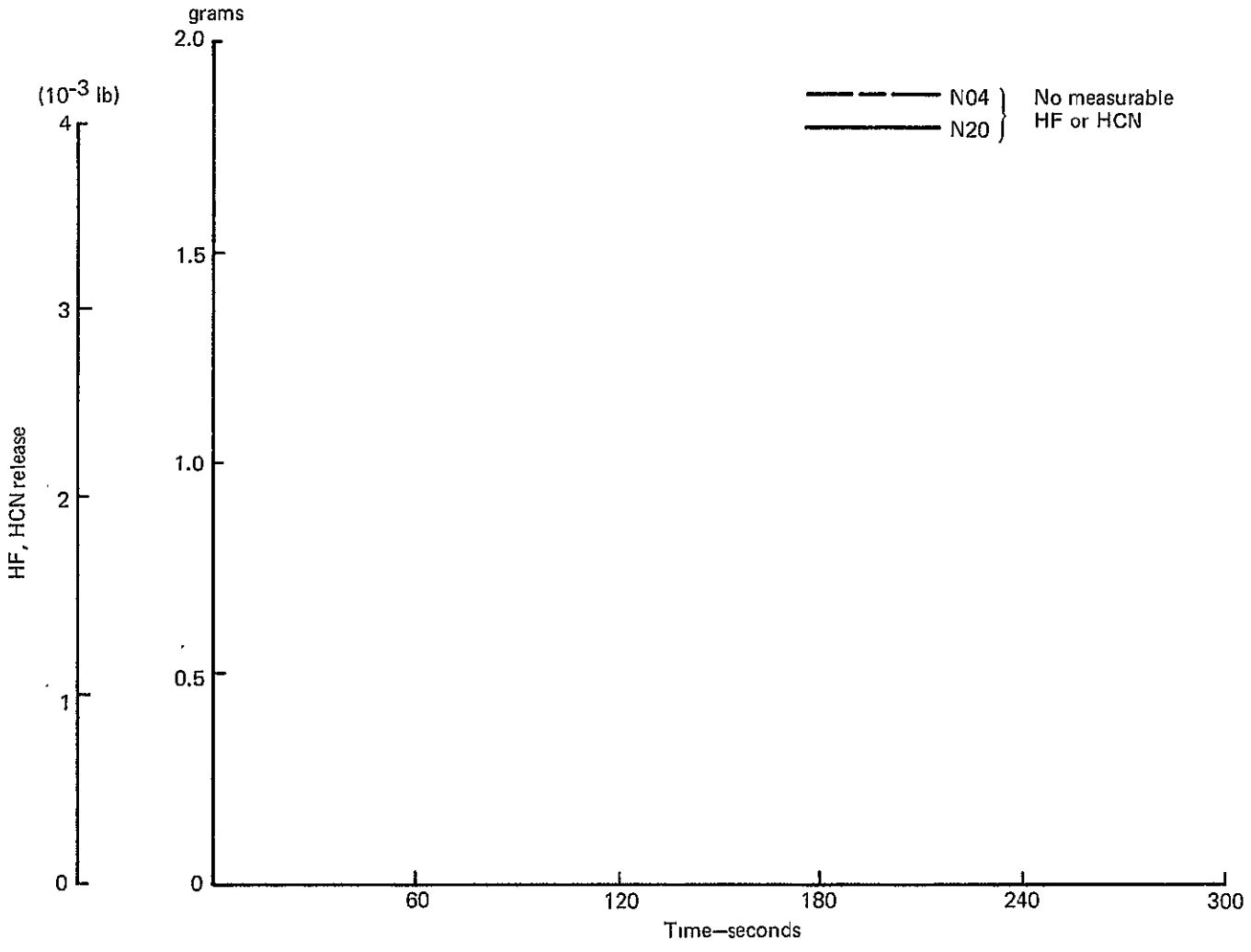

Figure E-68.—Apparent Hydrogen Fluoride (HF) and Hydrogen Cyanide (HCN) Release from the Simulated Design In-flight Fire Source Tests—New Materials

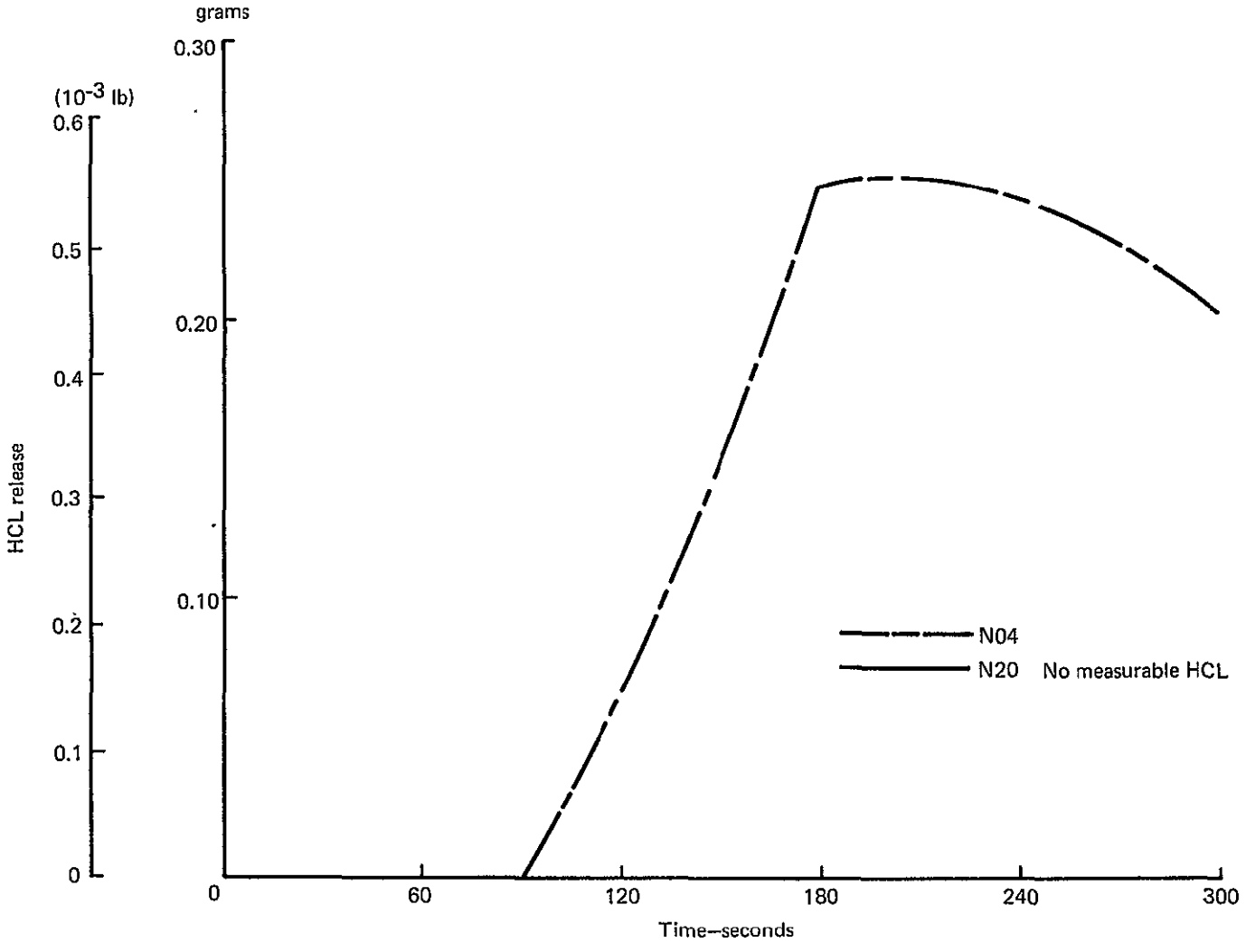

Figure E-69.—Apparent Hydrogen Chloride (HCL) Release from the Simulated Design In-flight Fire Source Tests—New Materials

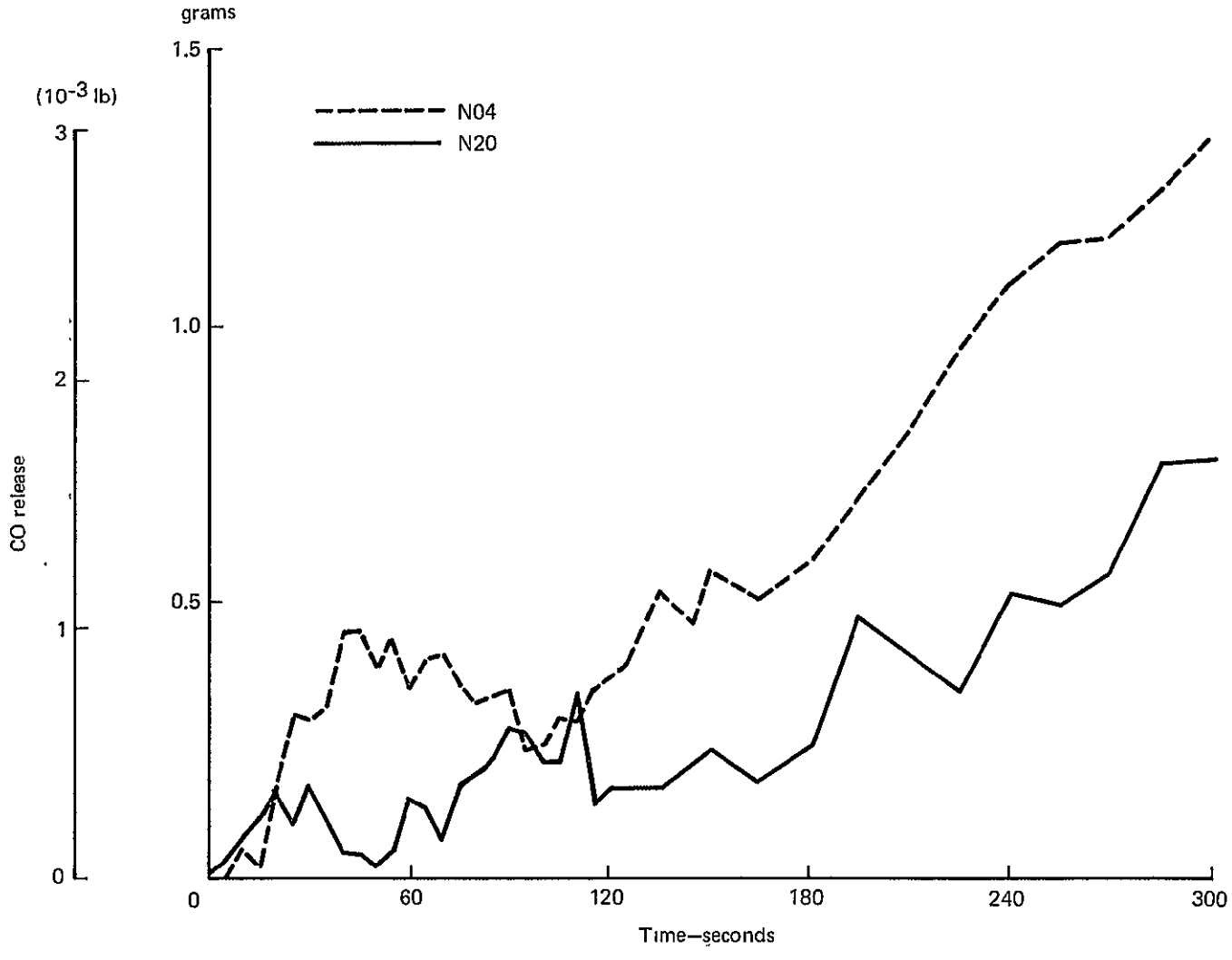

Figure E-70.— Apparent Carbon Monoxide (CO) Release from the Simulated Design In-flight Fire Source Tests—New Materials

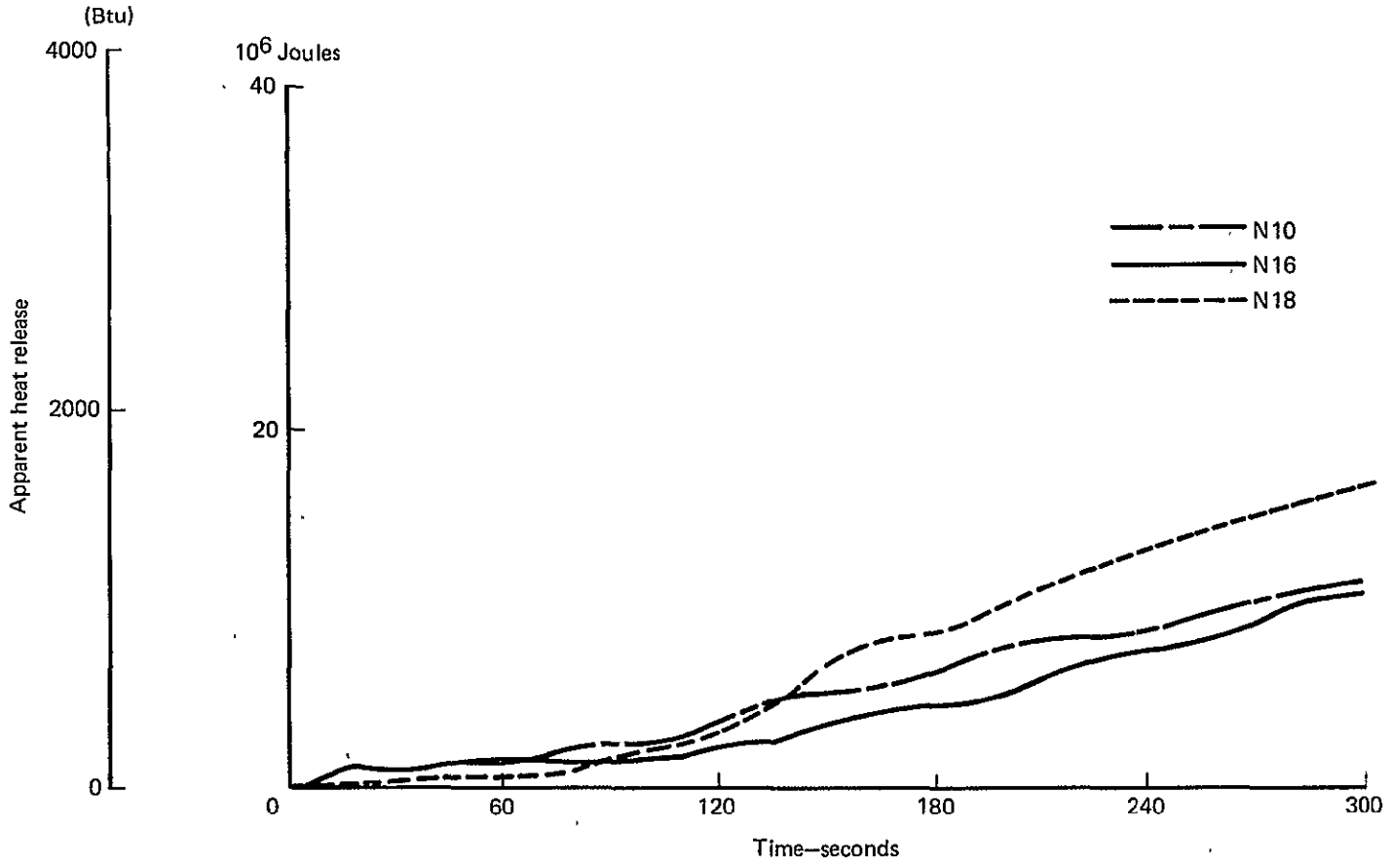

Figure E-71.—Apparent Heat Release from Simulated Design In-flight Fire Source Tests—New Materials

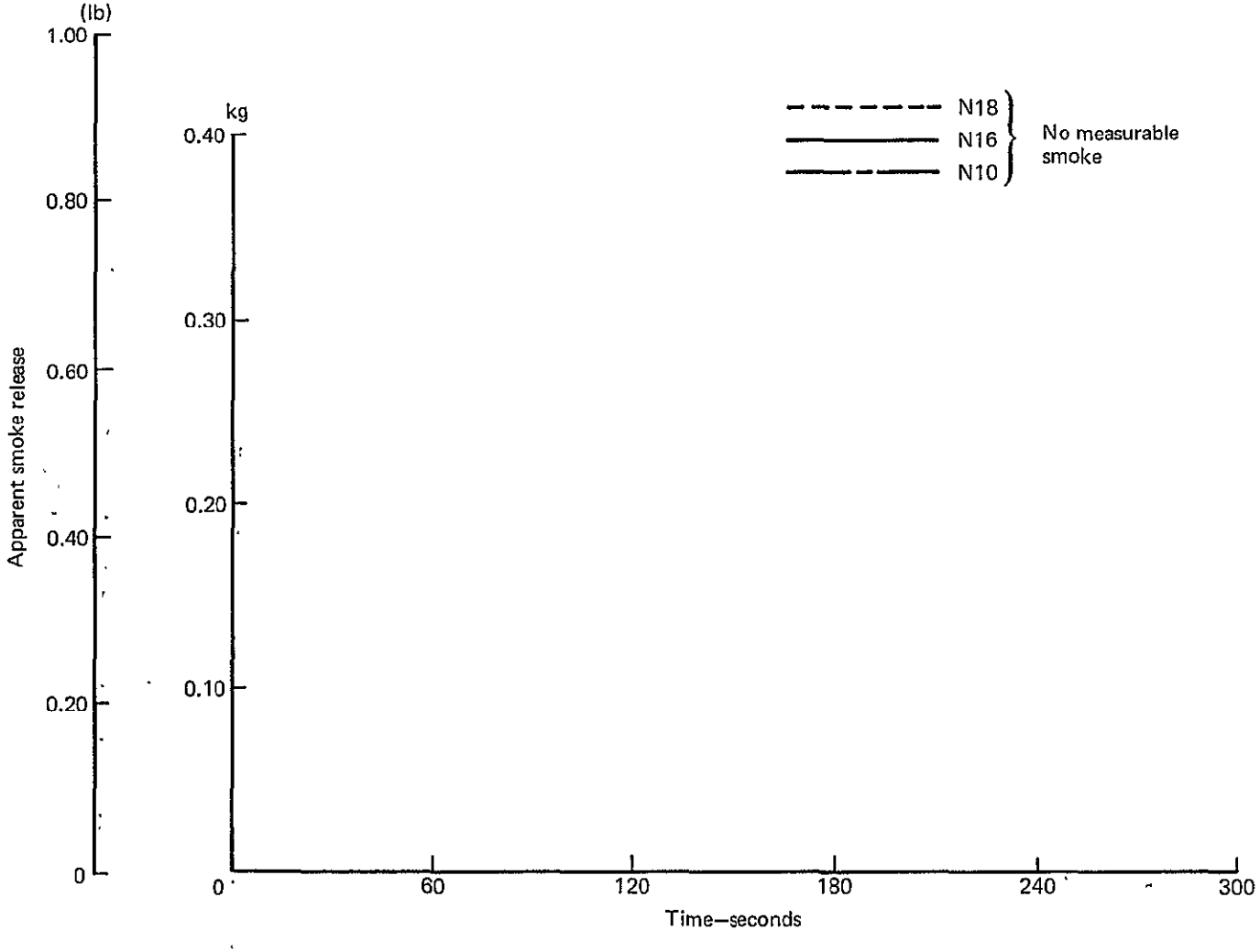

Figure E-72.—Apparent Smoke Release from Simulated Design In-flight Fire Source Tests—New Materials

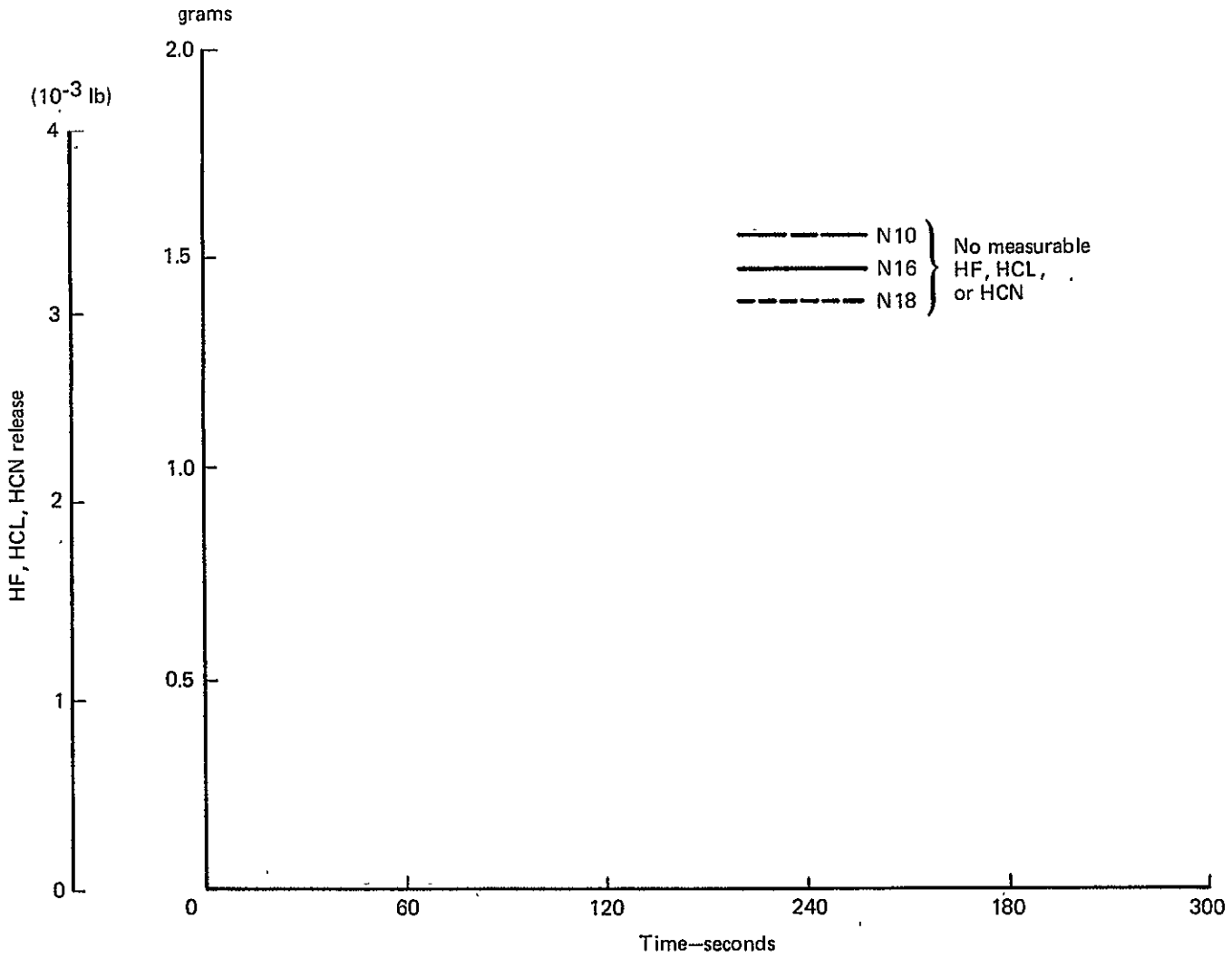

Figure E-73.— Apparent Hydrogen Fluoride (HF), Hydrogen Chloride (HCL) and Hydrogen Cyanide (HCN) Release from the Simulated Design In-flight Fire Source Tests—New Materials

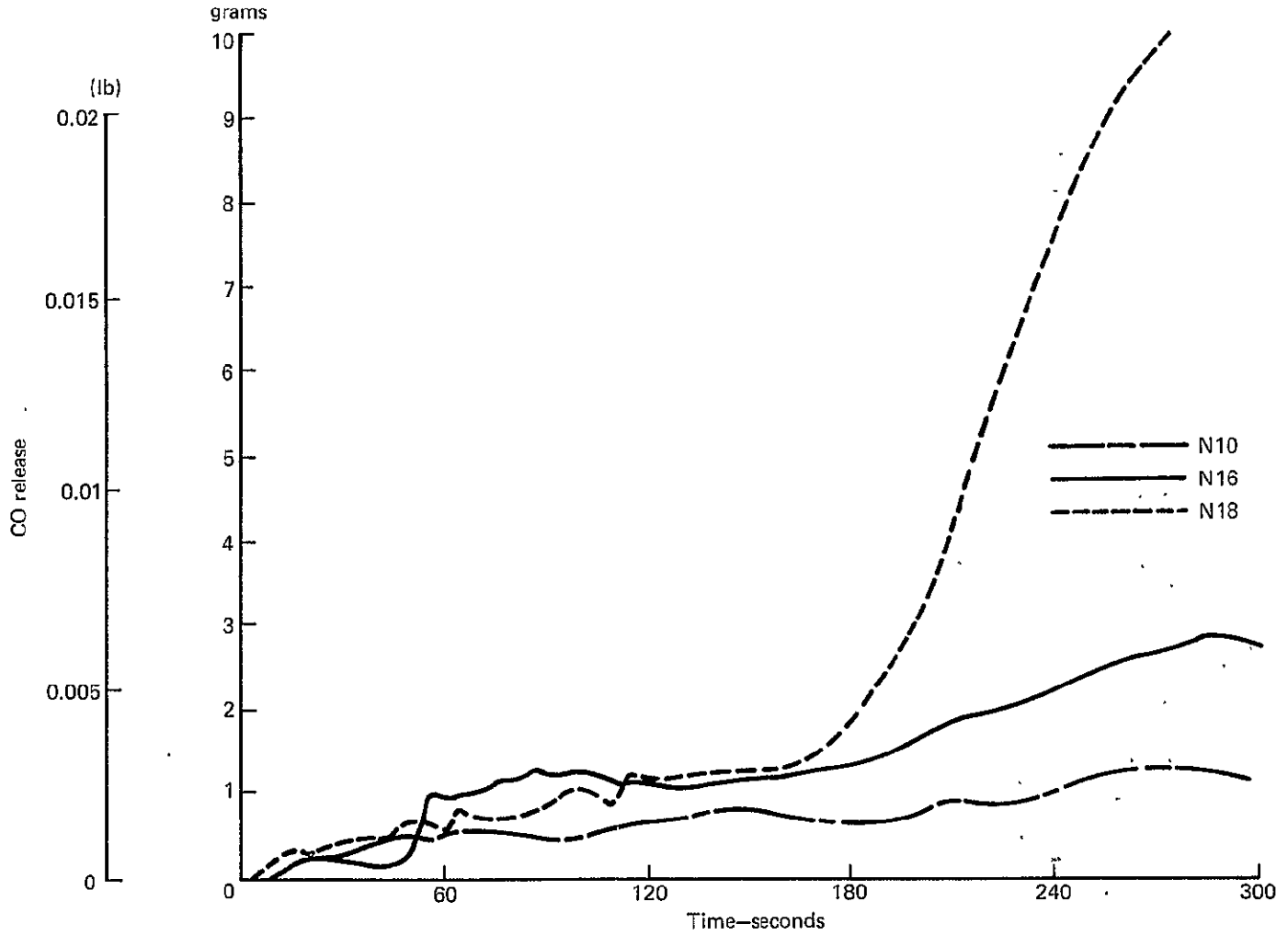

Figure E-74.—Apparent Carbon Monoxide (CO) Release from the Simulated Design In-flight Fire Source—New Materials

REFERENCES

1. Buetner, K., Effects of Extreme Heat on Man, *Journal of the American Medical Association,* Vol. 144, October 28, 1950, pp. 732-738.

2. Kimmerle, Dr. George, Aspects and Methodology for the Evaluation of Toxicological Parameters during Fire Exposure, *Journal of Fire and Flammability/Combustion Toxicology,* Vol. 1, February, 1974, pp. 4-51.

3. Allen, S. P., Nemeth, S. R., Peterson, J. M., and Tustin, E. A., *Airplane Interior Materials Fire Test Methodology,* Boeing Document D6-46952, October 1978.

4. Aerospace Industries of America, Inc., *Document AIA-CDP-3, Lighting and Exit Awareness,* July 1968.

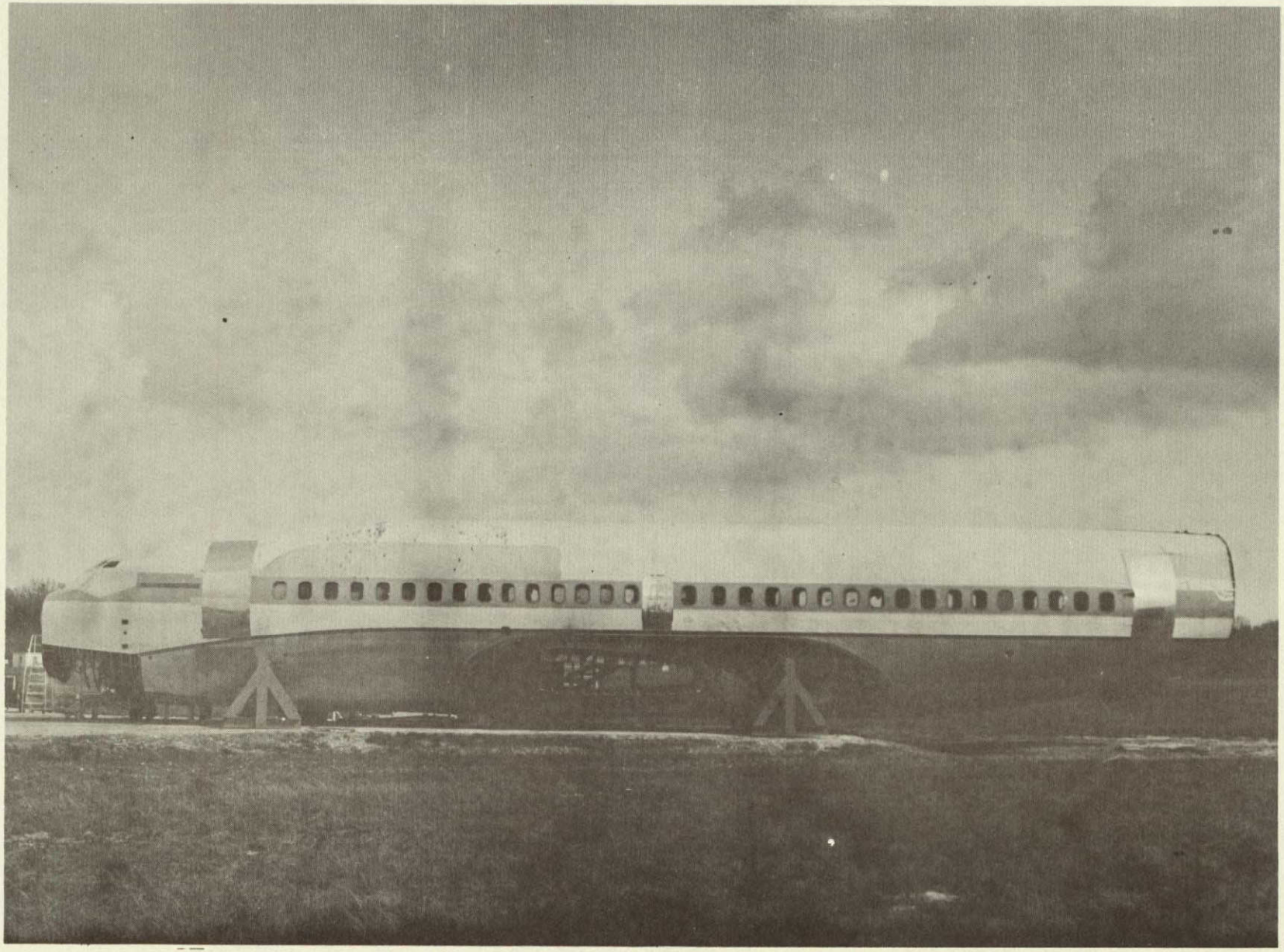

Figure 1.—NASA-JSC 737 Fire Test Fuselage

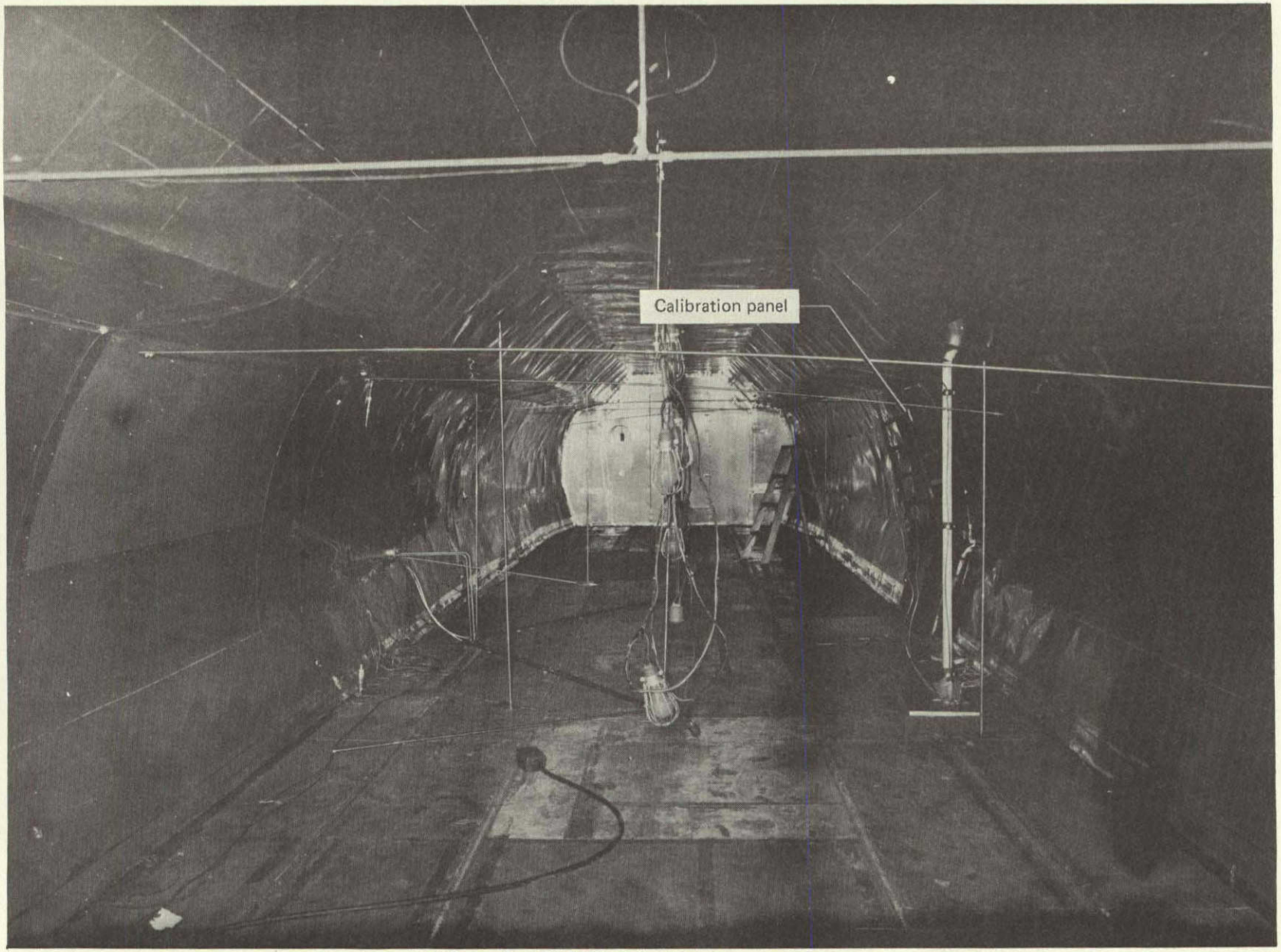

Figure 2.—737 Fire Test Fuselage Interior

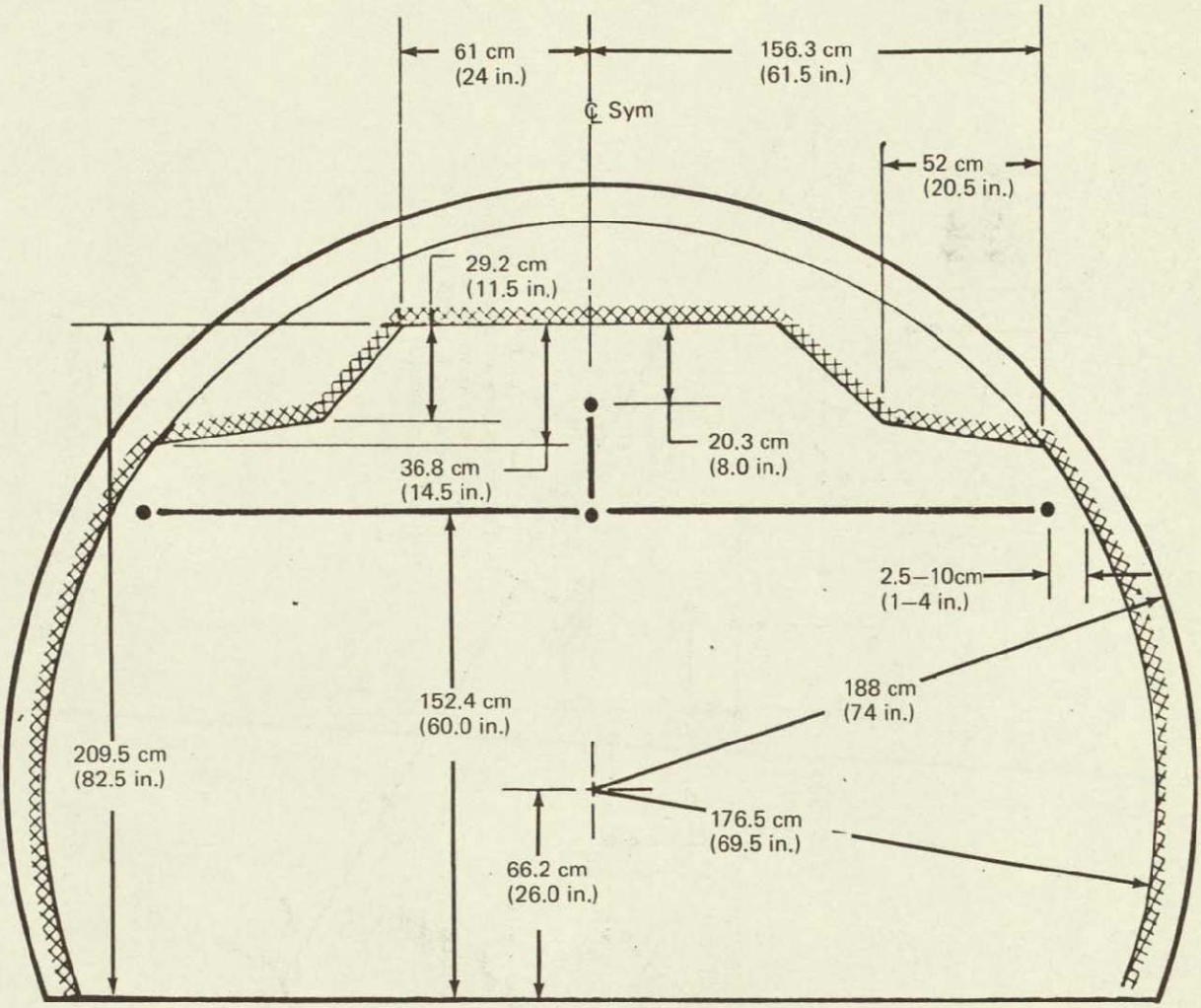

Figure 3.—Cabin Thermocouple Locations—Cabin Cross Section

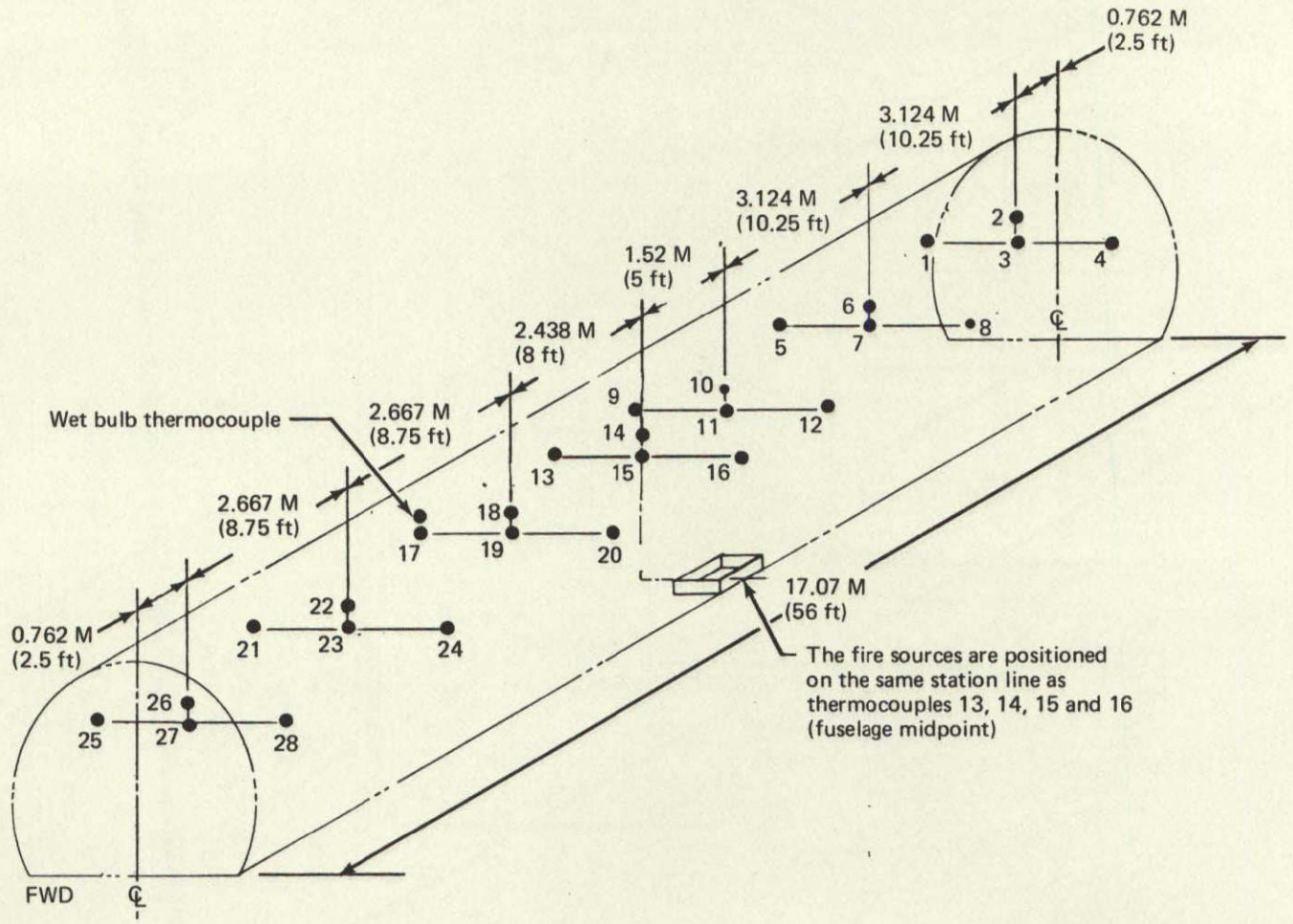

● Thermocouple

Figure 4.—17.07 M (56 Ft) Cabin Thermocouple Locations

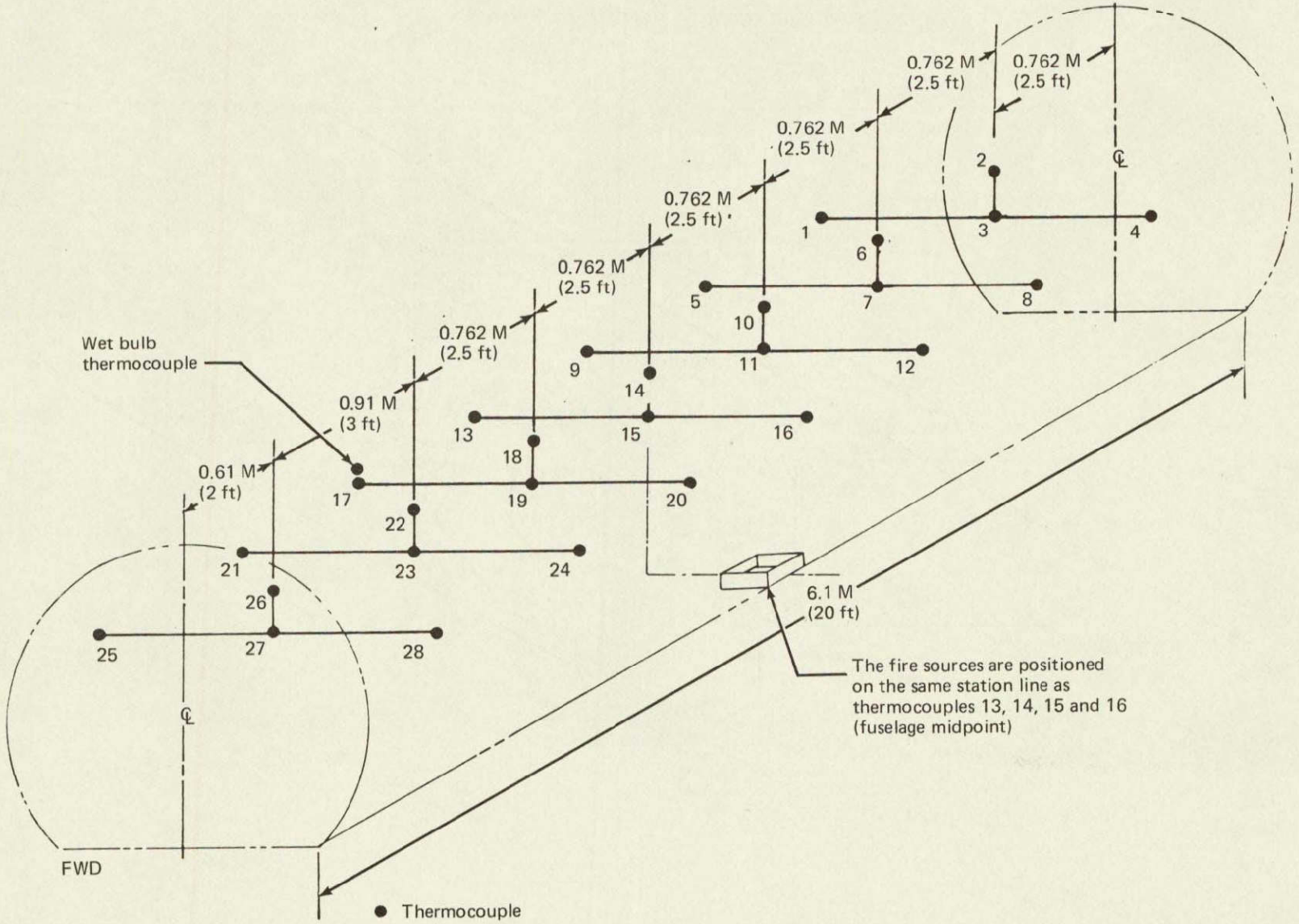

Figure 5.–6.1 M (20 Ft) Cabin Thermocouple Locations

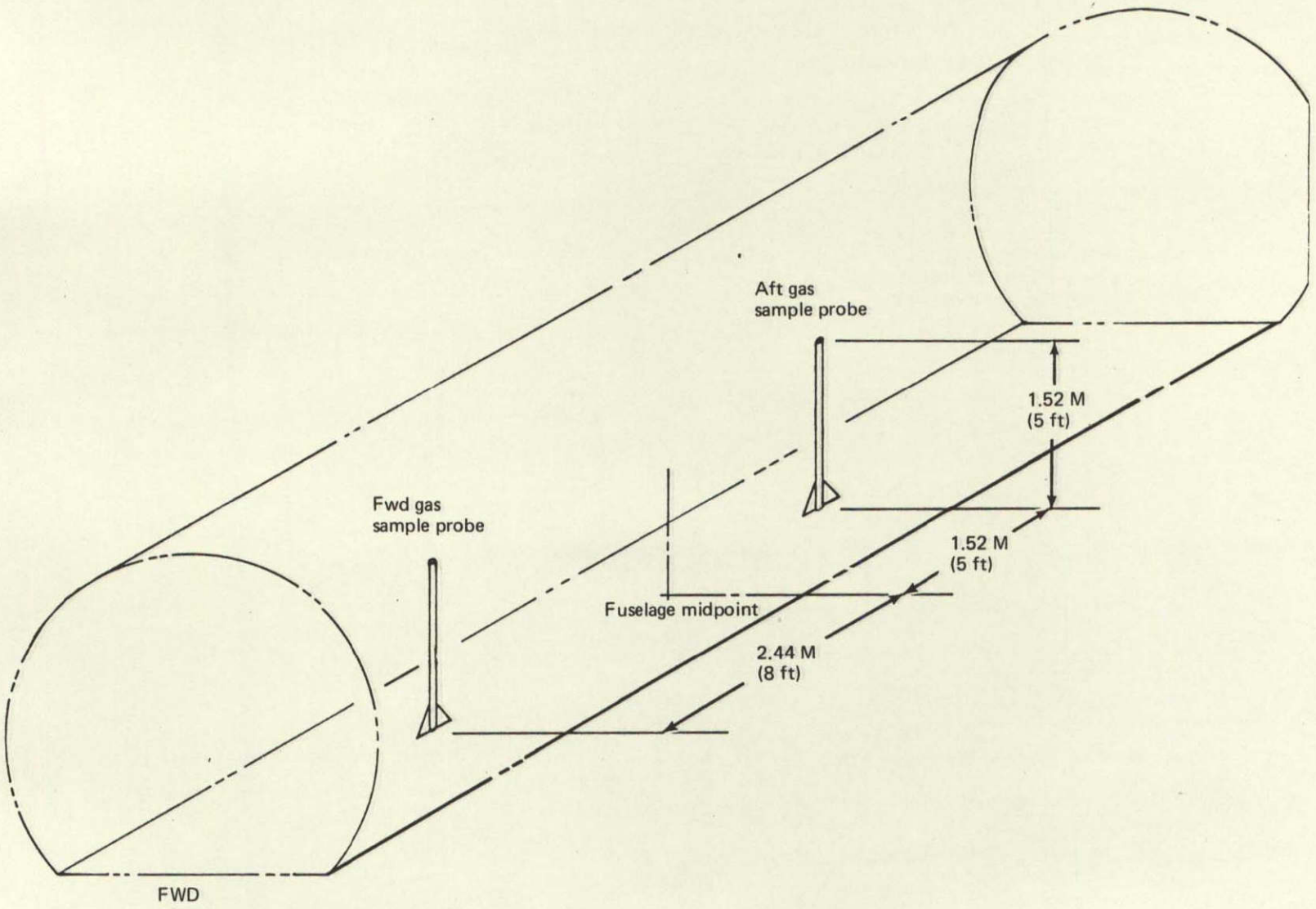

Figure 6.—Gas Sampling Probe Locations

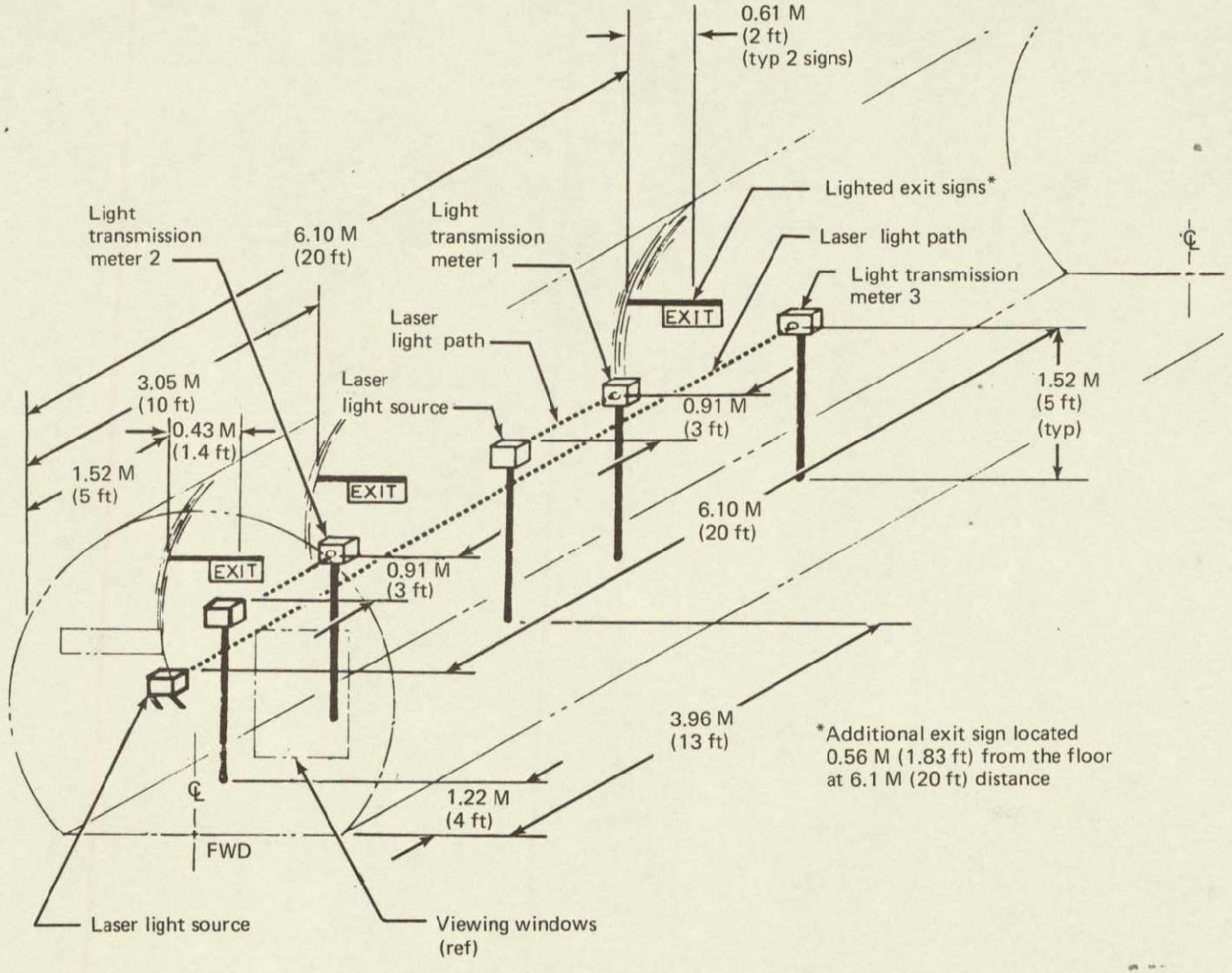

Figure 7.—Light Transmission—Exit Sign Setup

Figure 8.—Calibration Panel for Sidewall Heat and Temperature Exposure

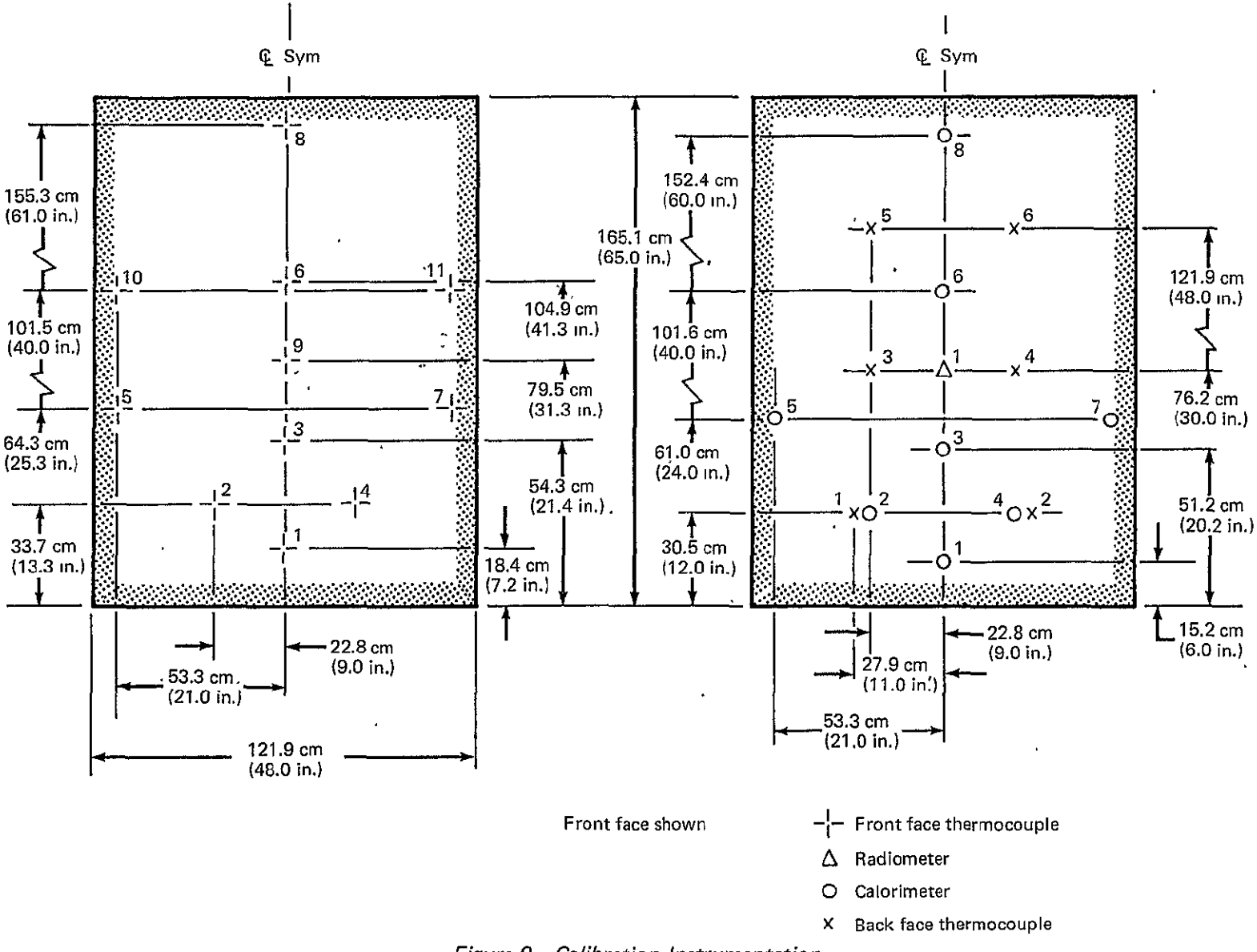

Figure 9.—Calibration Instrumentation

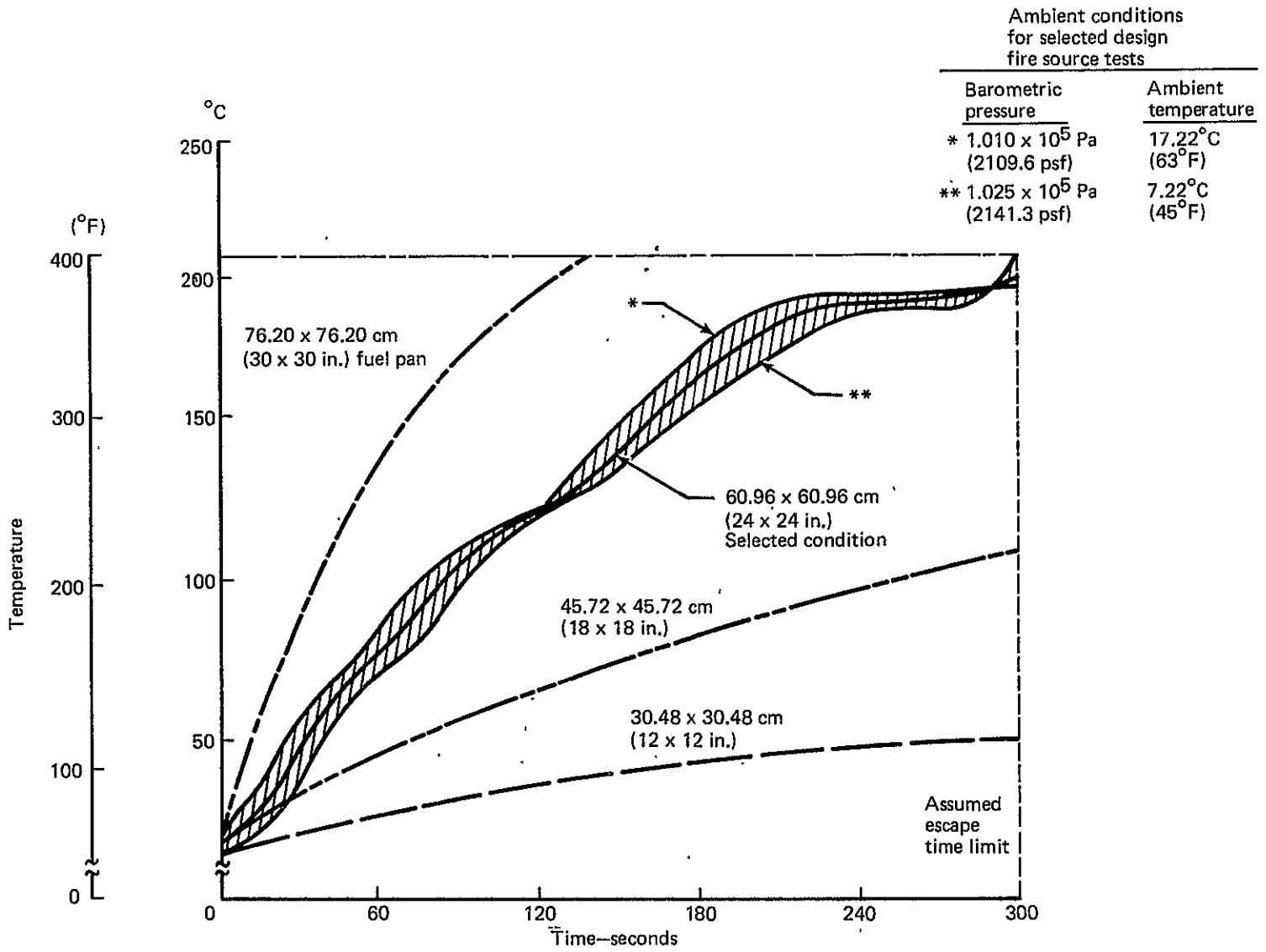

Figure 10.— Average Cabin Centerline Air Temperature at Head Level Post-crash Fire Source Tests in 17.07 M (56 Ft) Section

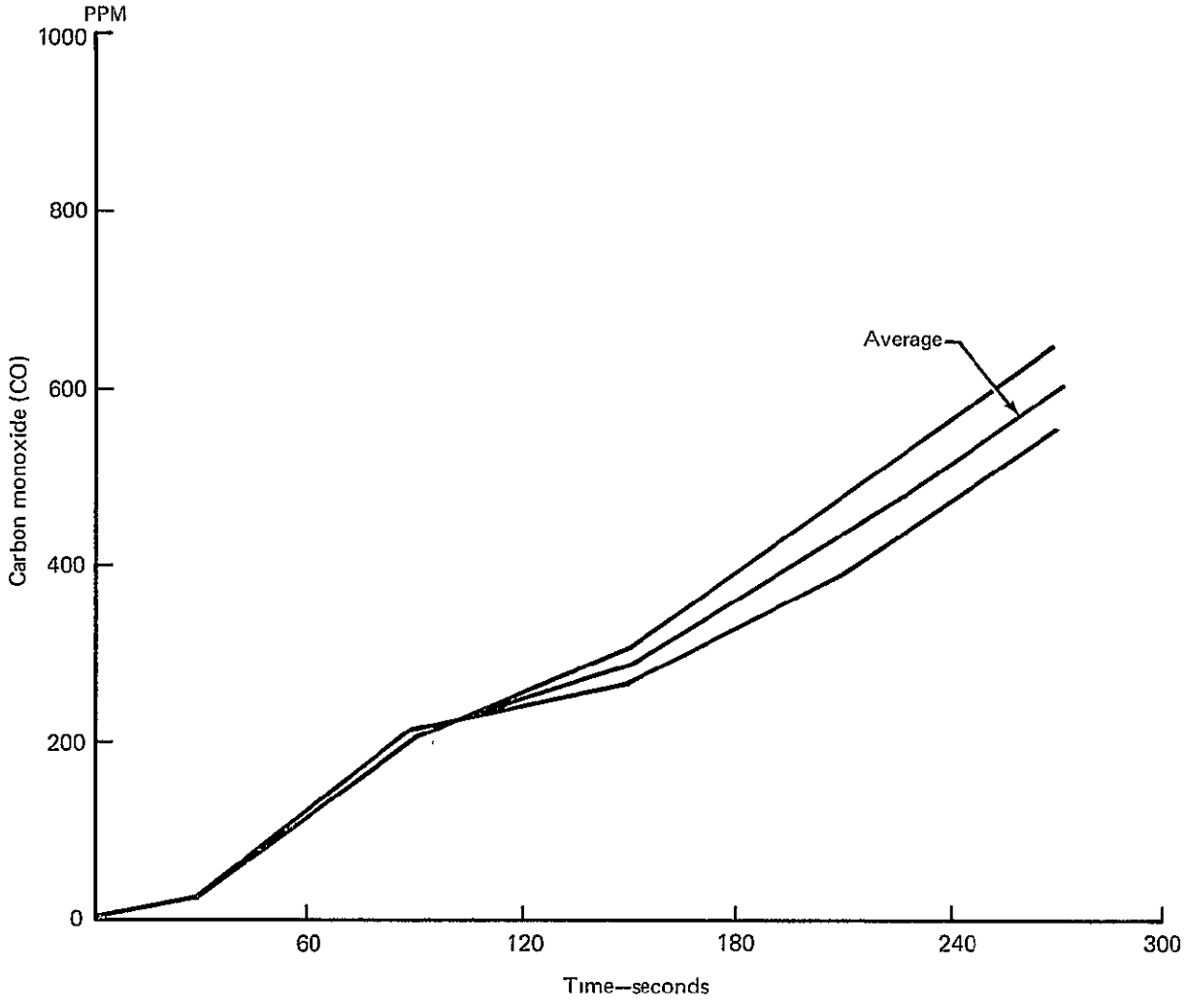

Figure 11.— Design Post-crash Fire Sources Carbon Monoxide (CO) Concentration in 17.07 M (56 Ft) Cabin Length at the 1.52 M (5 Ft) Head Level

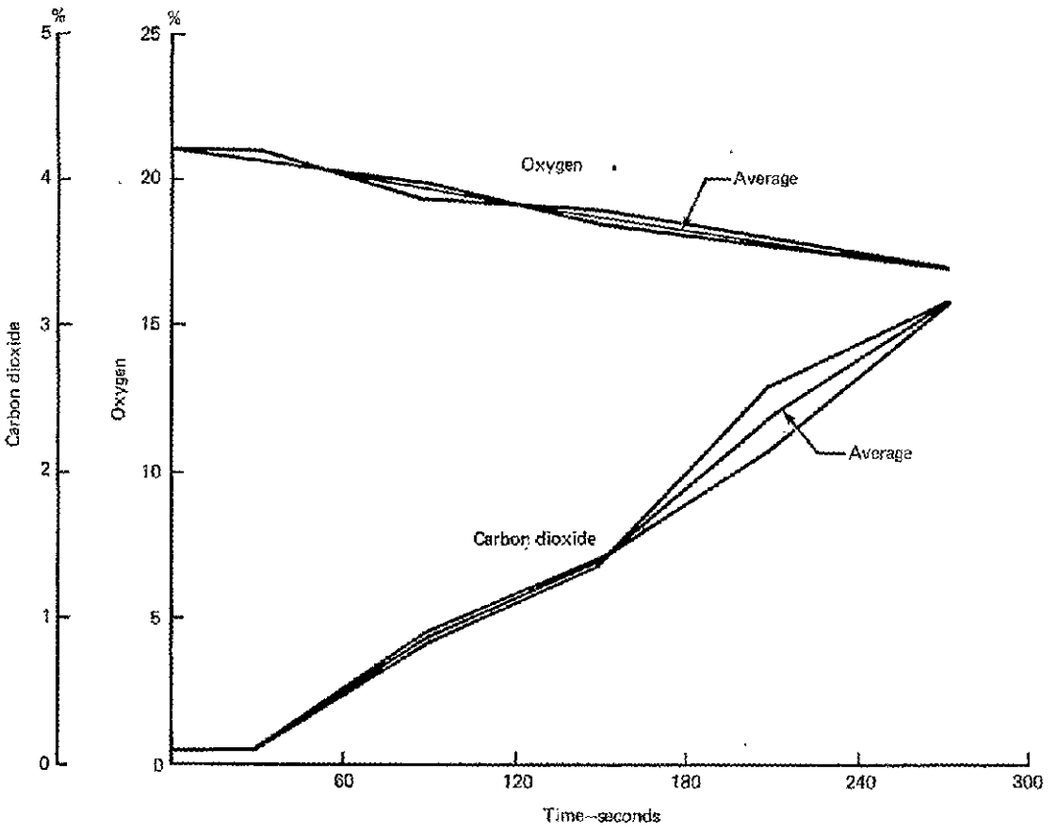

Figure 12.— Design Post-crash Fire Sources Carbon Dioxide (CO_2), Oxygen (O_2) Concentrations in 17.07 M (56 Ft) Cabin Length at the 1.52 M (5 Ft) Head Level

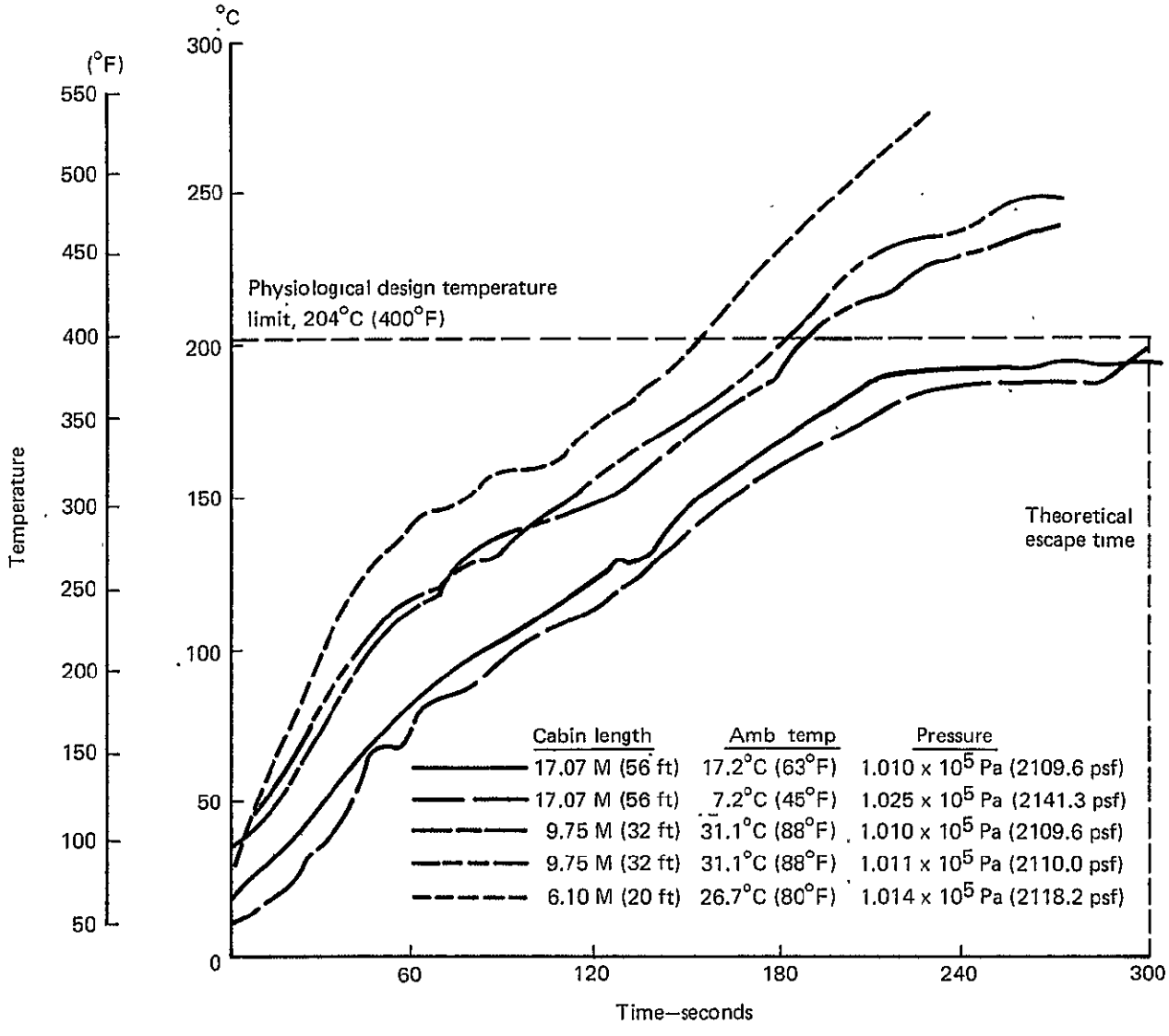

Figure 13.— Design Post-crash Fire Source Average Centerline Cabin Temperature at the 1.52 M (5 Ft) Head Level for Various Cabin Lengths

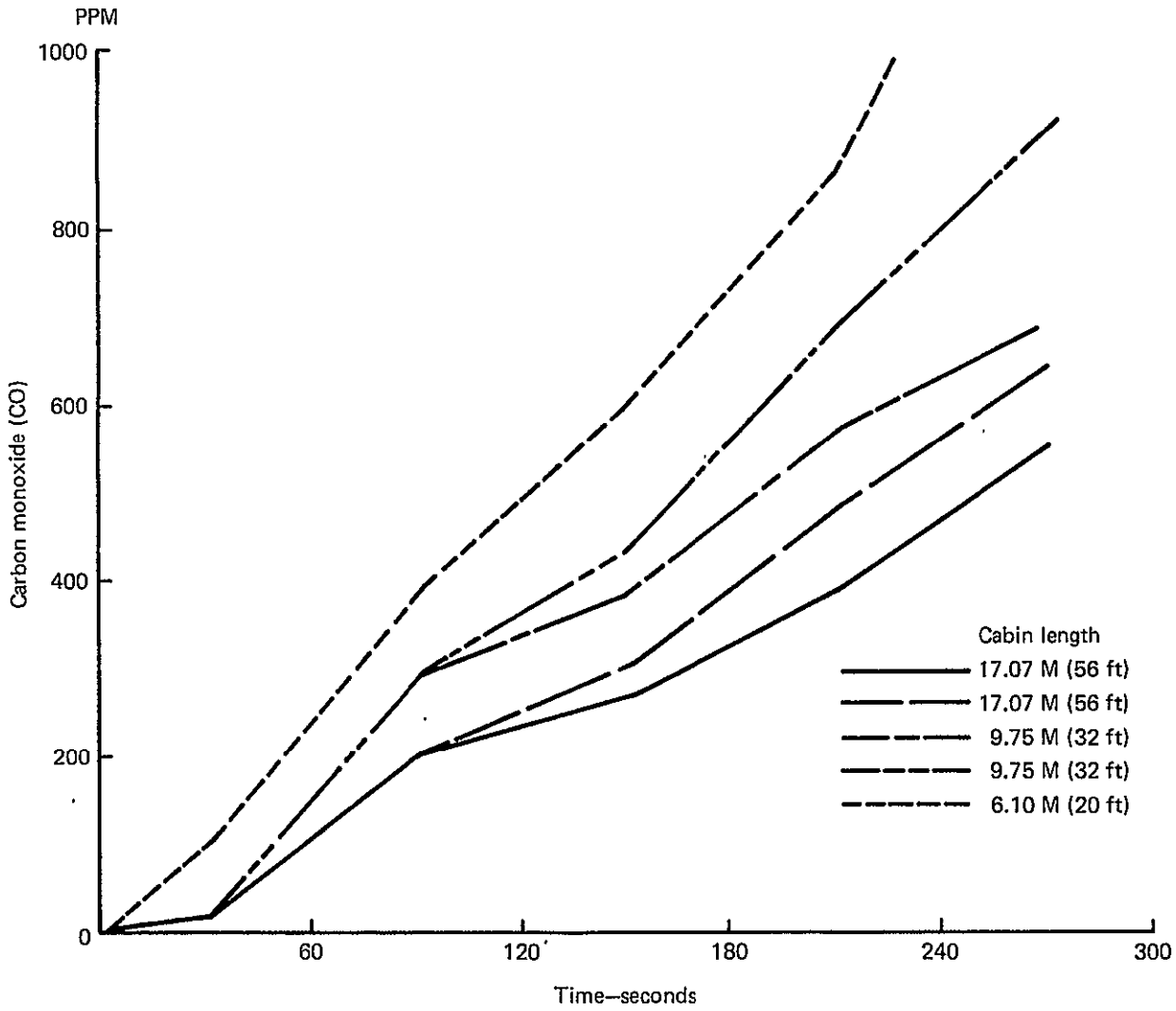

Figure 14.— Design Post-crash Fire Source Carbon Monoxide (CO) Concentrations in Various Cabin Lengths at the 1.52 M (5 Ft) Head Level

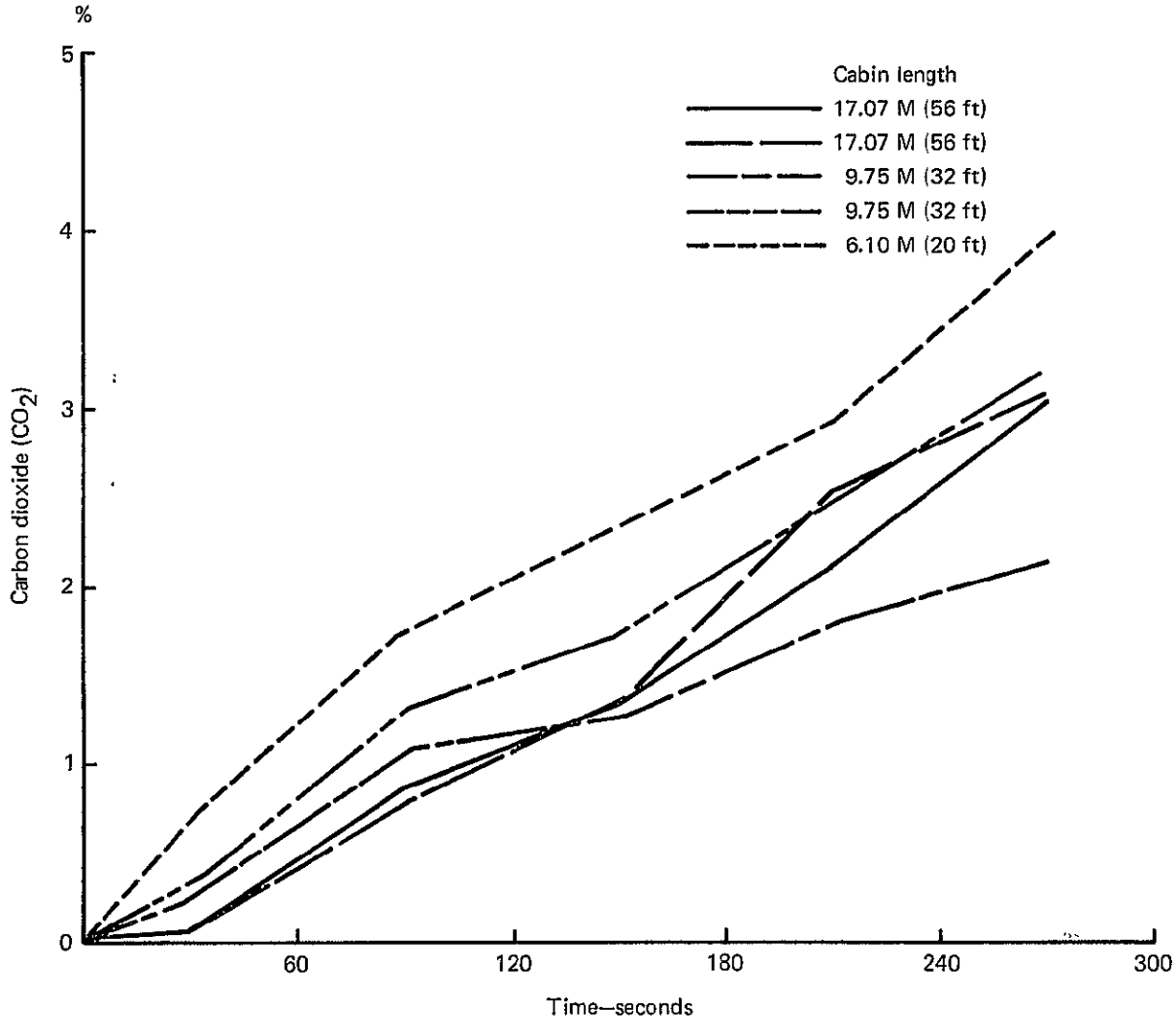

Figure 15.— Design Post-crash Fire Source Carbon Dioxide (CO_2) Concentrations in Various Cabin Lengths at the 1.52 M (5 Ft) Head Level

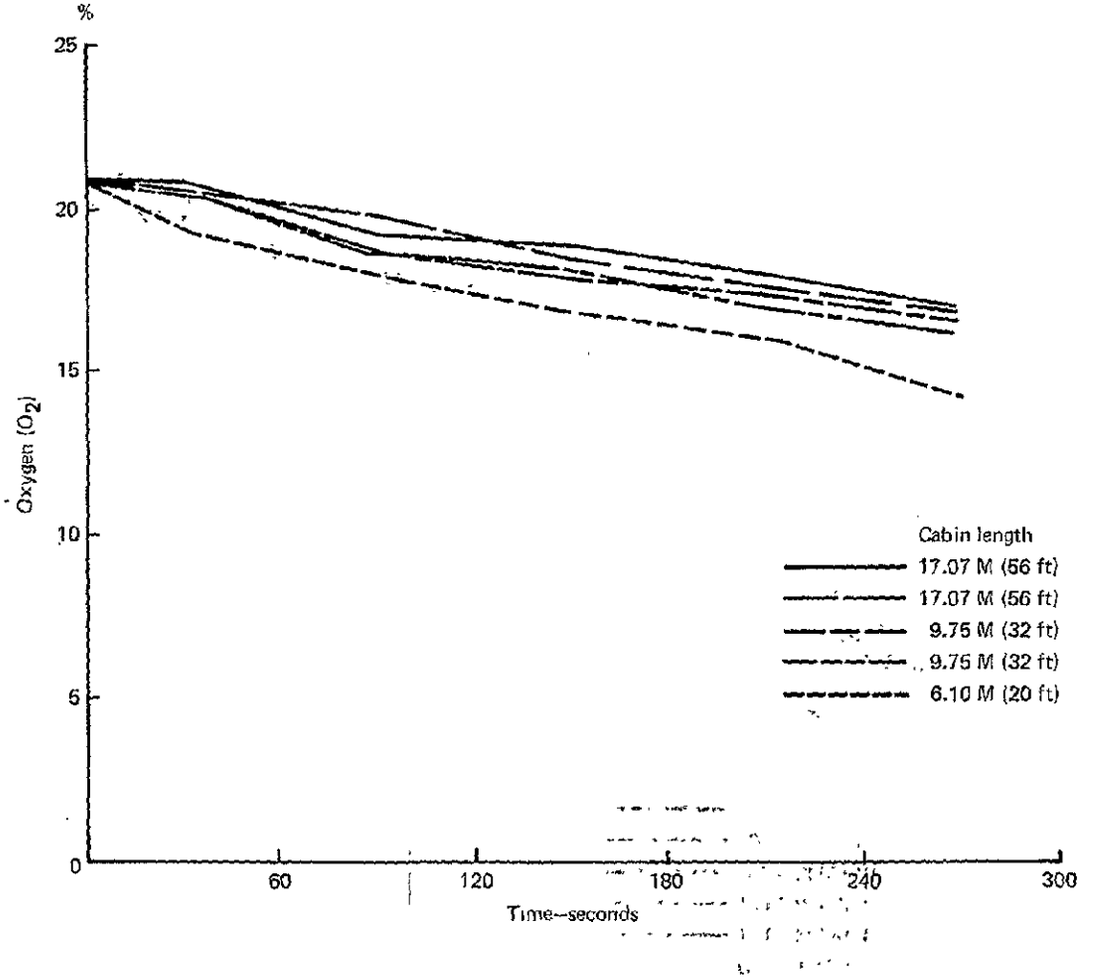

Figure 16.— Design Post-crash Fire Source Oxygen (O_2) Concentrations in Various Cabin Lengths

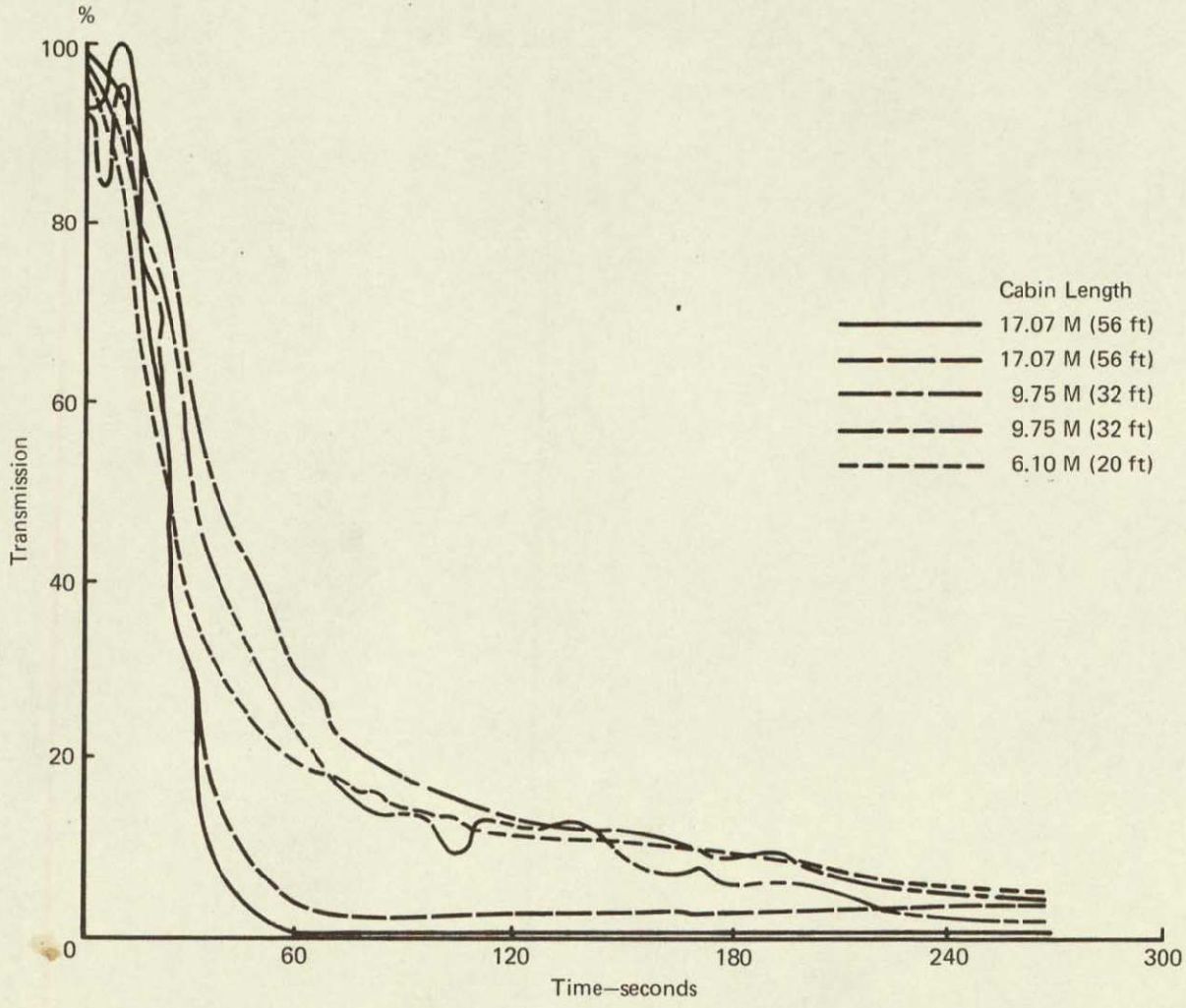

Figure 17.— Design Post-crash Fire Source Light Transmission Over 0.92 M (3 Ft) in Various Cabin Lengths at the 1.52 M (5 Ft) Head Level

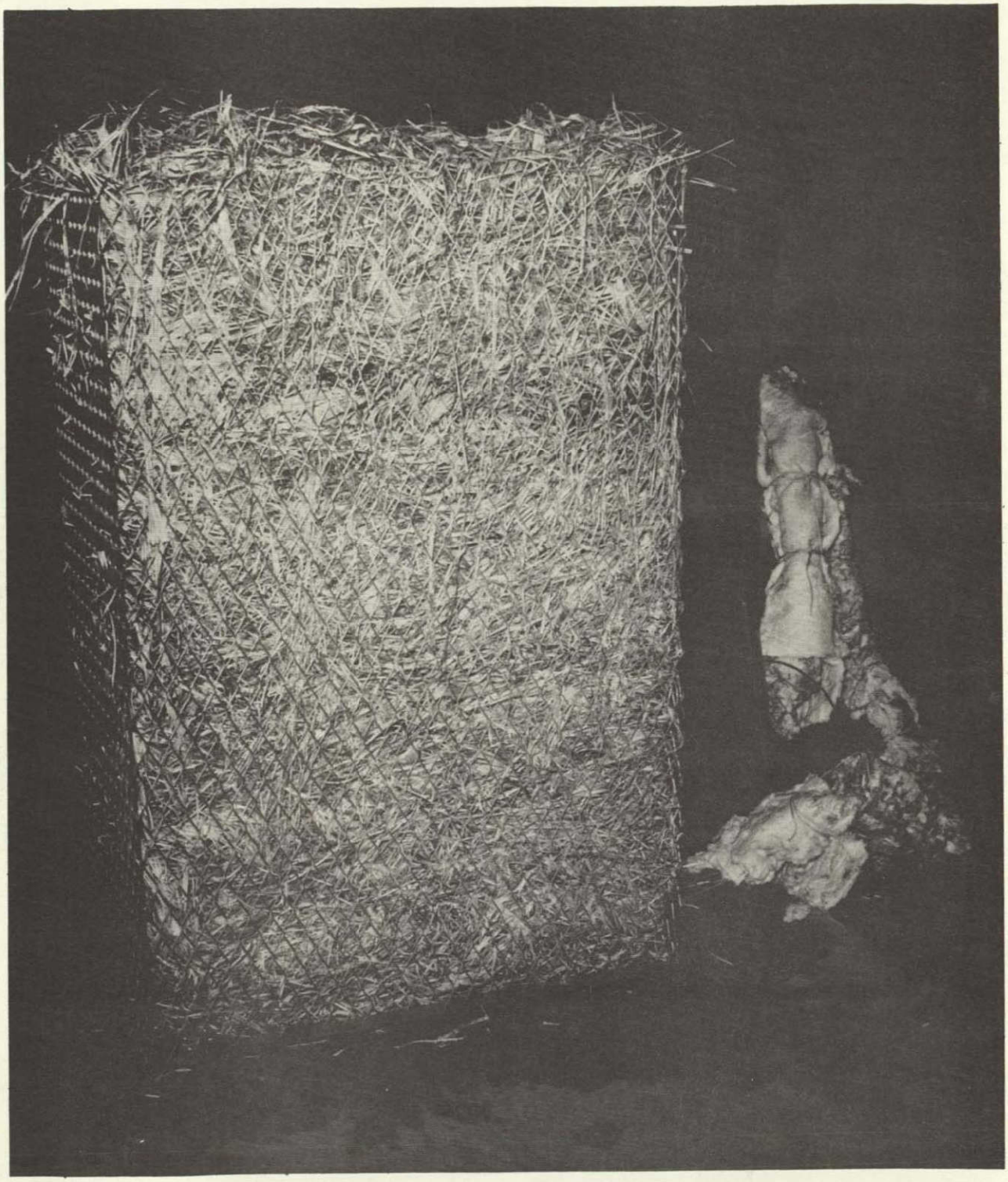

Figure 18.—Shredded Newspaper Fire Source

C-3

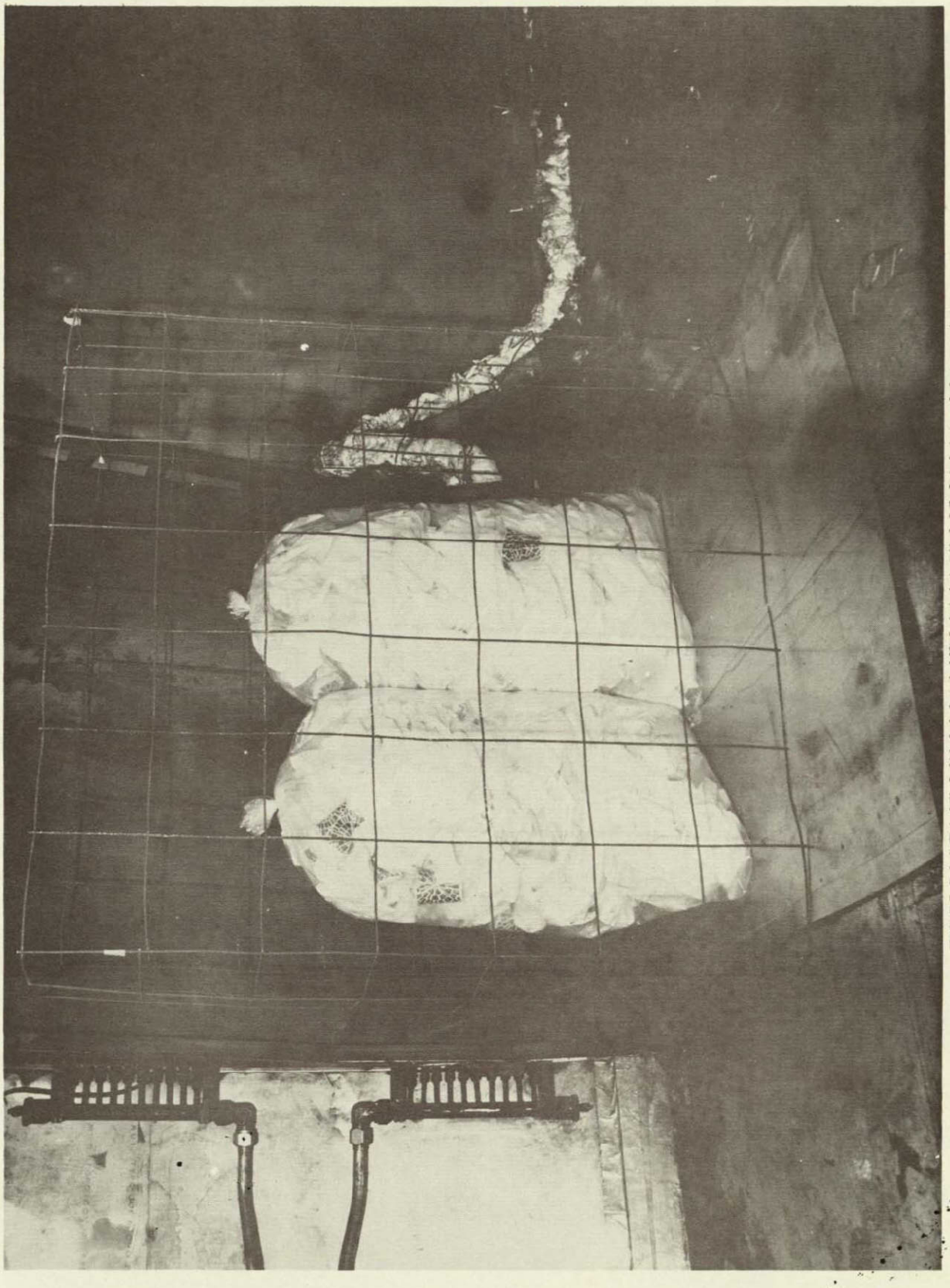

Figure 19.—Cabin and Lavatory Trash—Design In-flight Fire Source

Figure 20.—Simulated Under Seat Baggage Fire Source

Figure 21.—Airline Pillows Fire Source

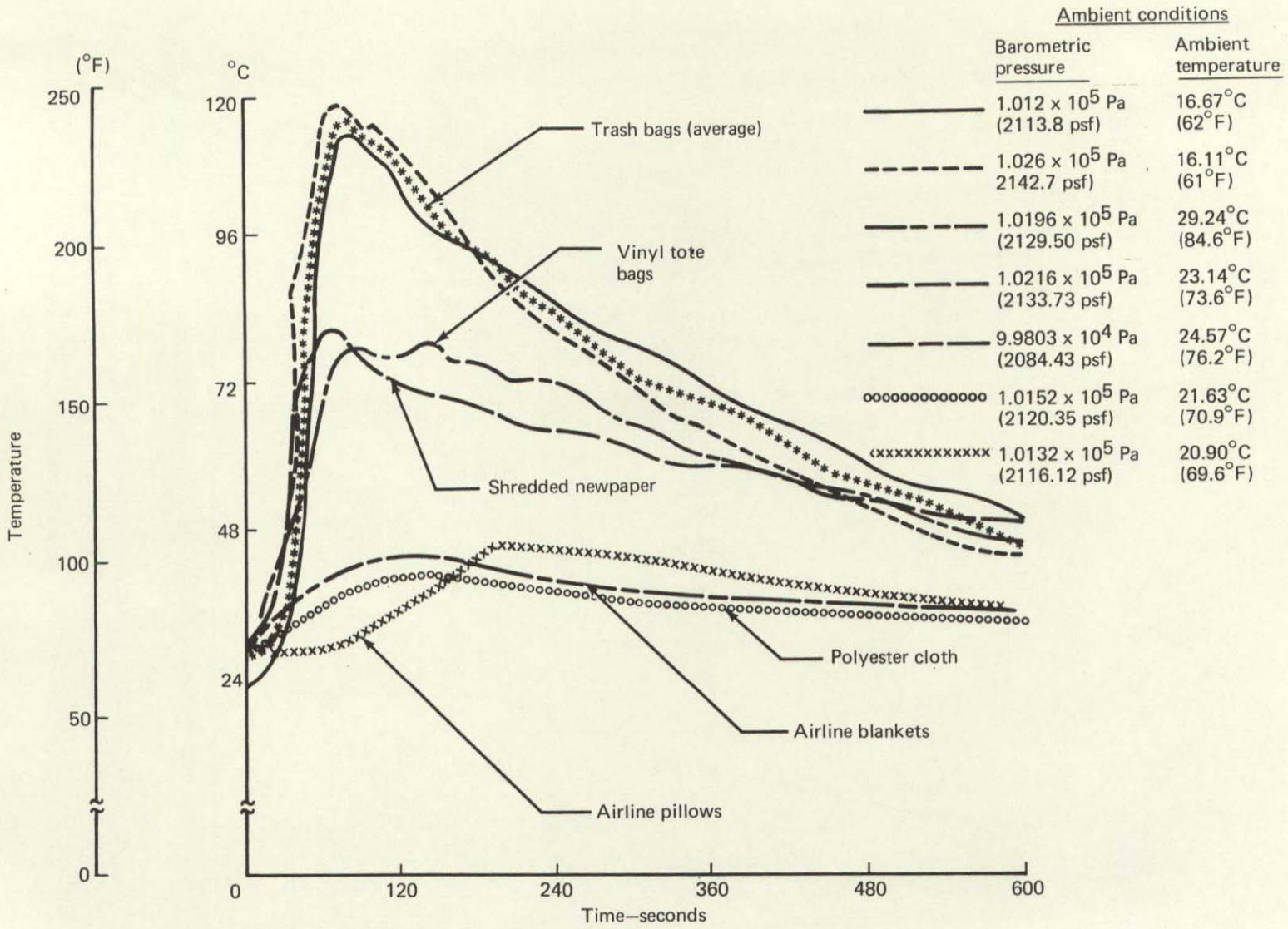

Figure 22.— Average Cabin Centerline Air Temperature at Head Level— In-flight Fire Source Tests in 17.07 M (56 Ft) Section

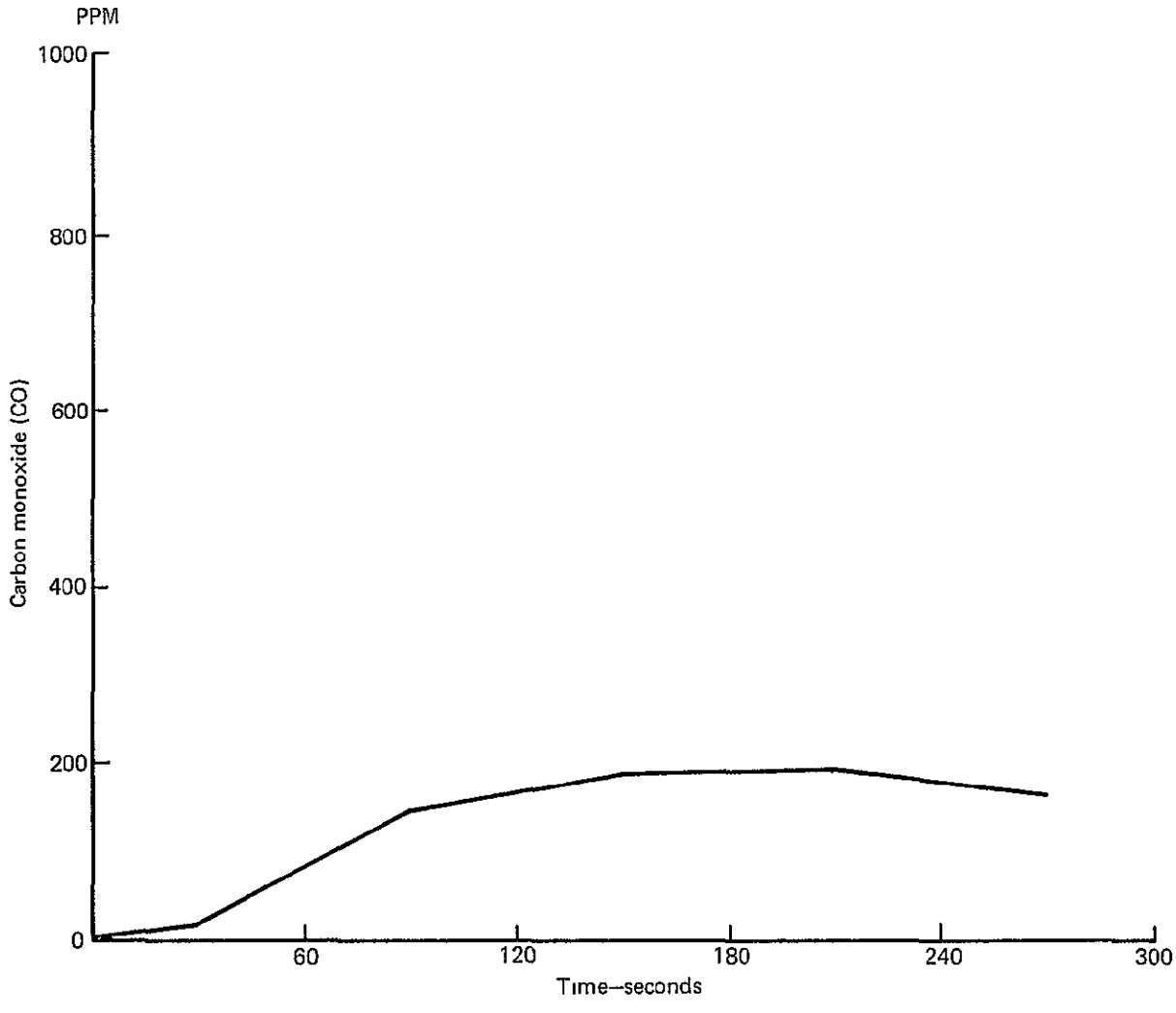

Figure 23.— Design In-flight Fire Source Carbon Monoxide (CO) Concentration in 17.07 M (56 Ft) Cabin Length at the 1.52 M (5 Ft) Head Level

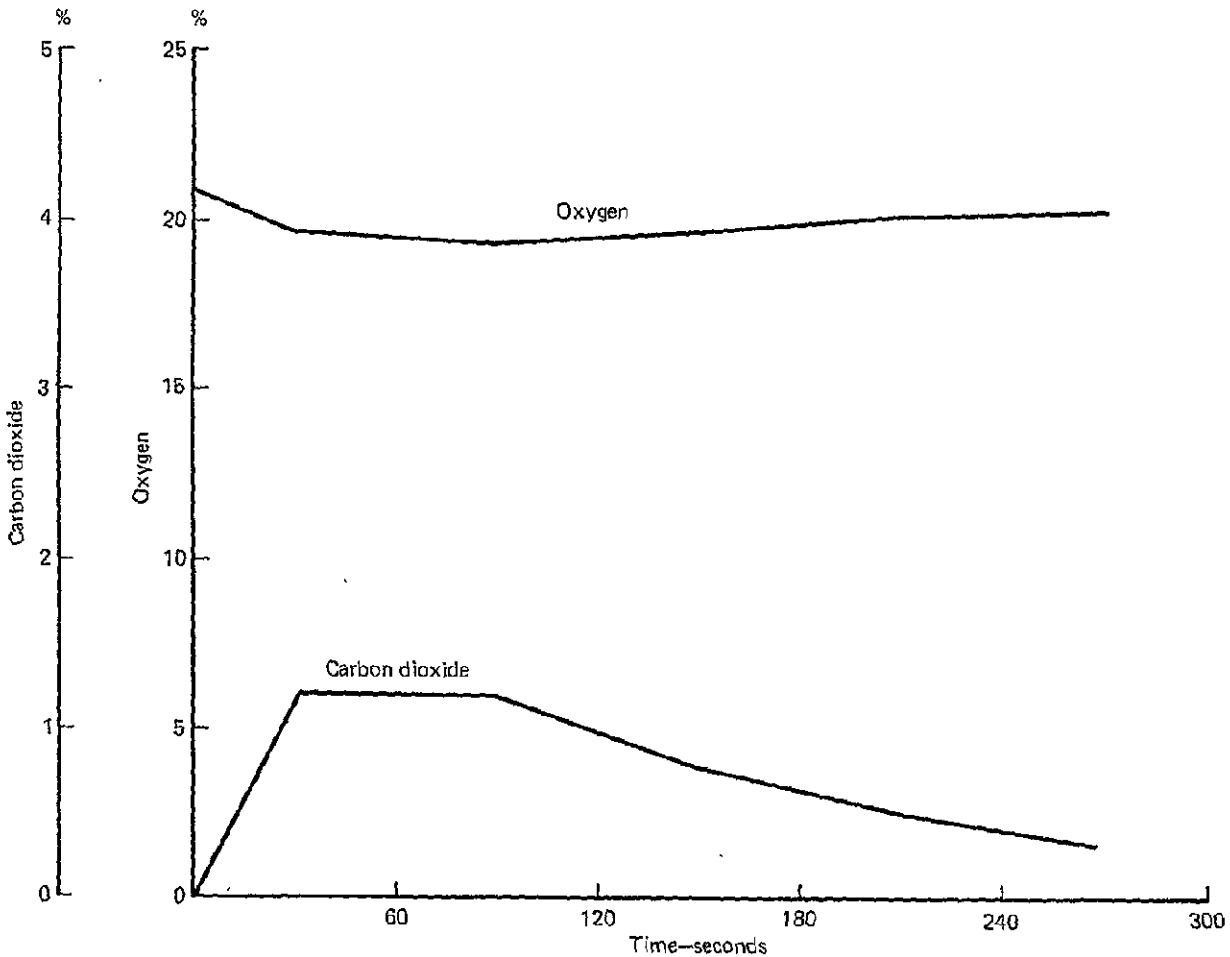

Figure 24.— Design In-flight Fire Source Carbon Dioxide (CO_2), Oxygen (O_2) Concentration in 17.07 M (56 Ft) Cabin Length at the 1.52 M (5 Ft) Head Level

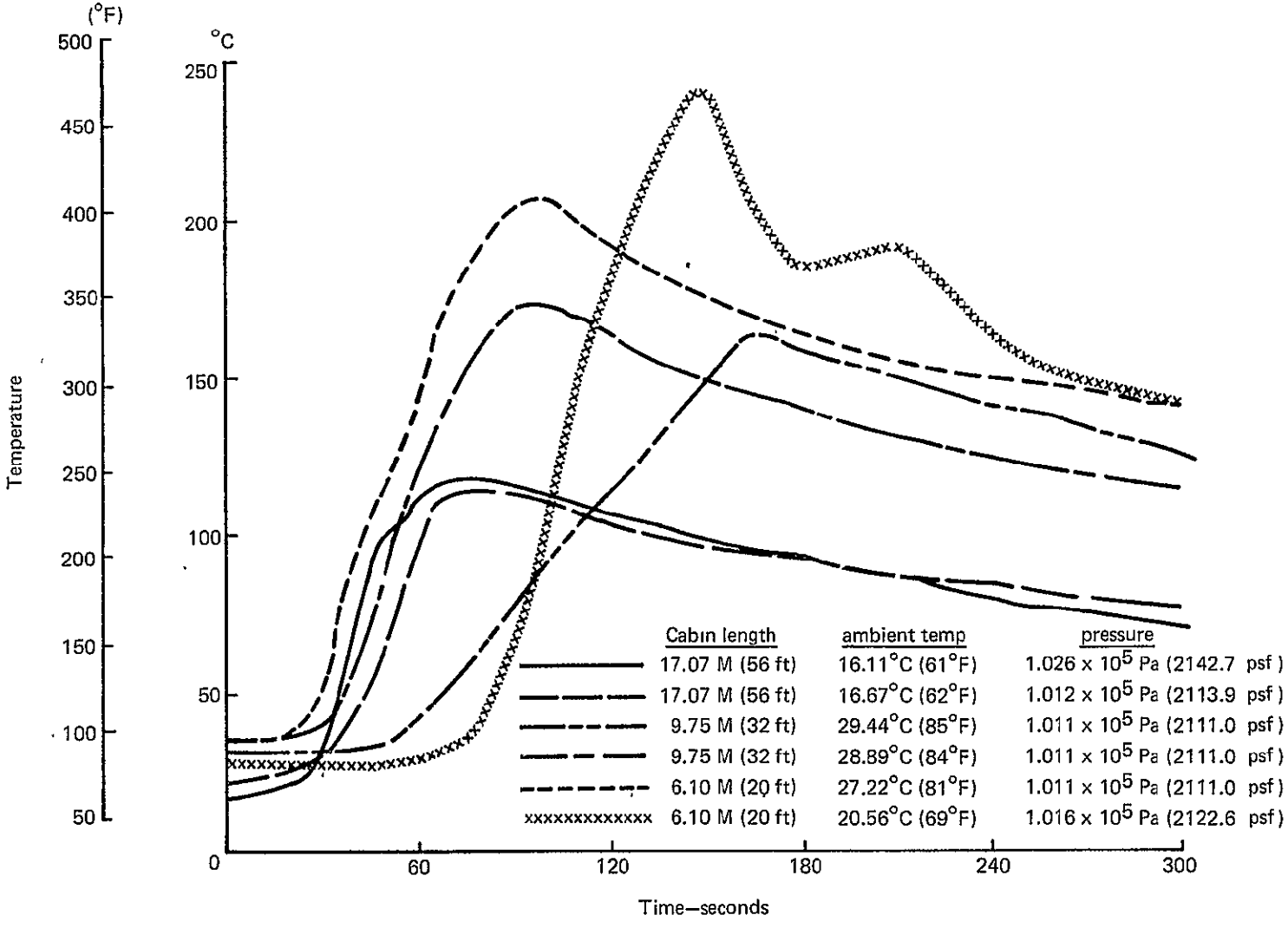

Figure 25.— Design In-flight Fire Source Average Centerline Cabin Temperature at the 1.52 M (5 Ft) Head Level for Various Cabin Lengths

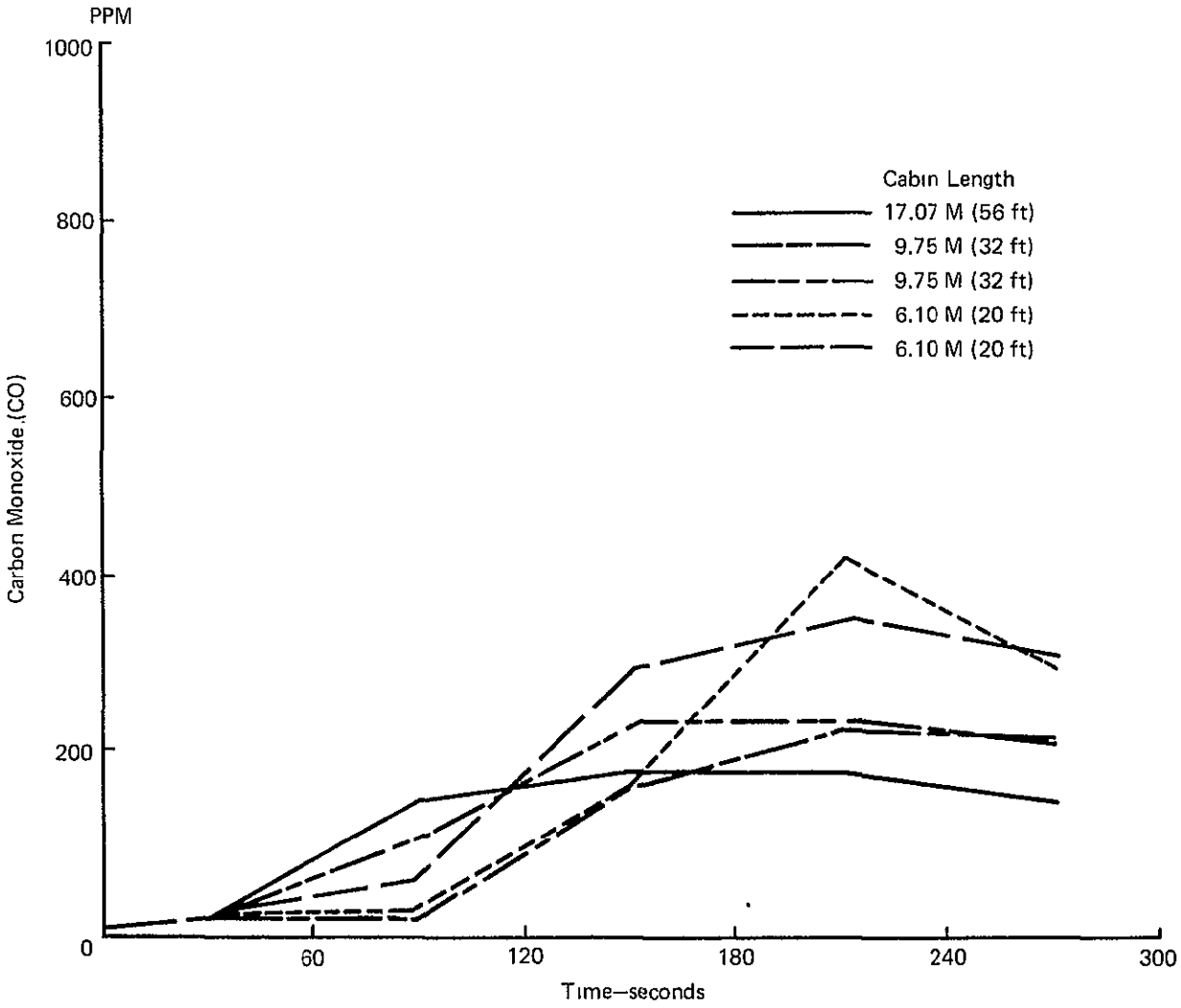

Figure 26.— Design In-flight Fire Source Carbon Monoxide (CO) Concentrations in Various Cabin Lengths at the 1.52 M (5 Ft) Head Level

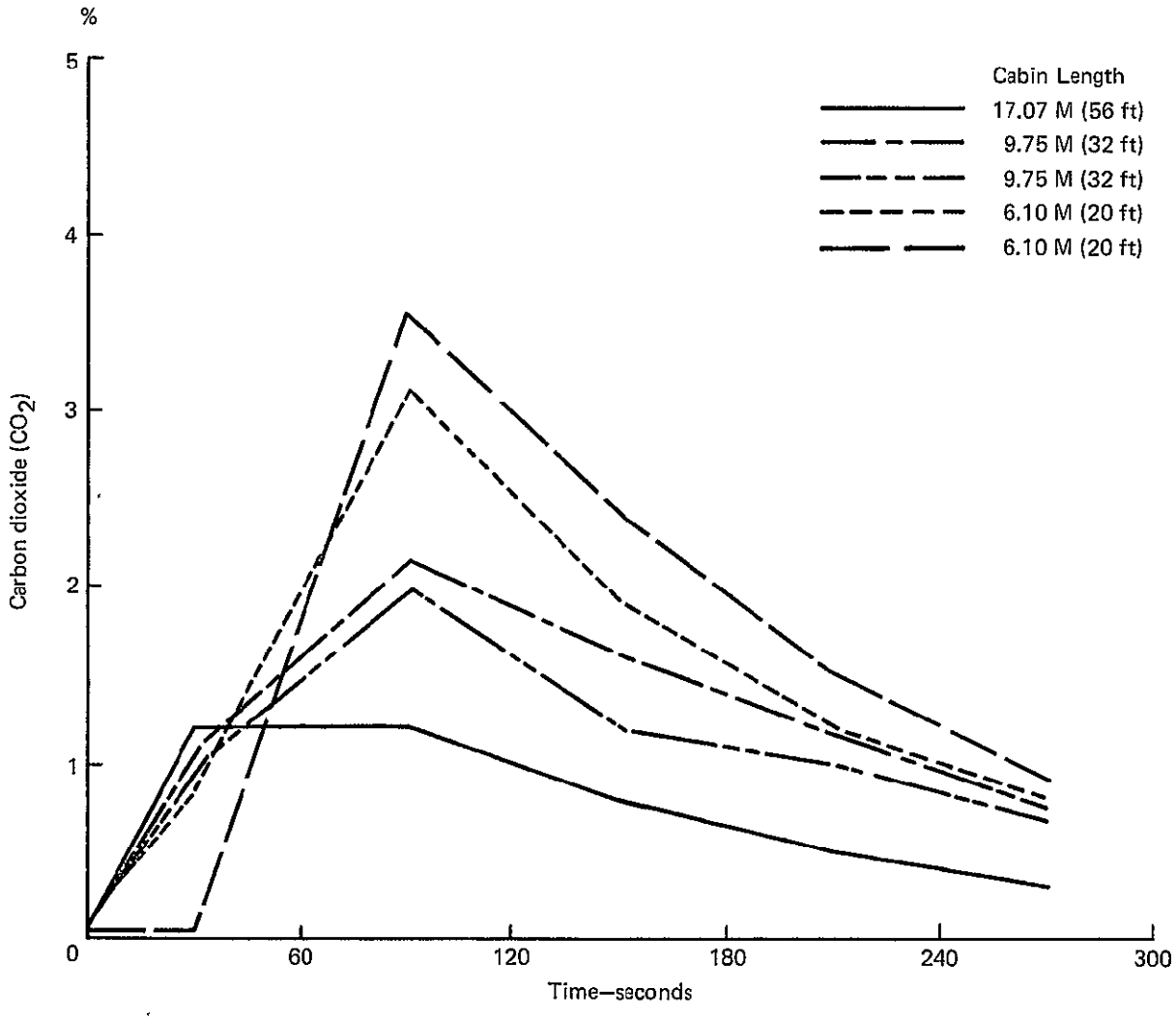

Figure 27.— Design In-flight Fire Source Carbon Dioxide (CO_2) Concentrations in Various Cabin Lengths at the 1.52 M (5 Ft) Head Level

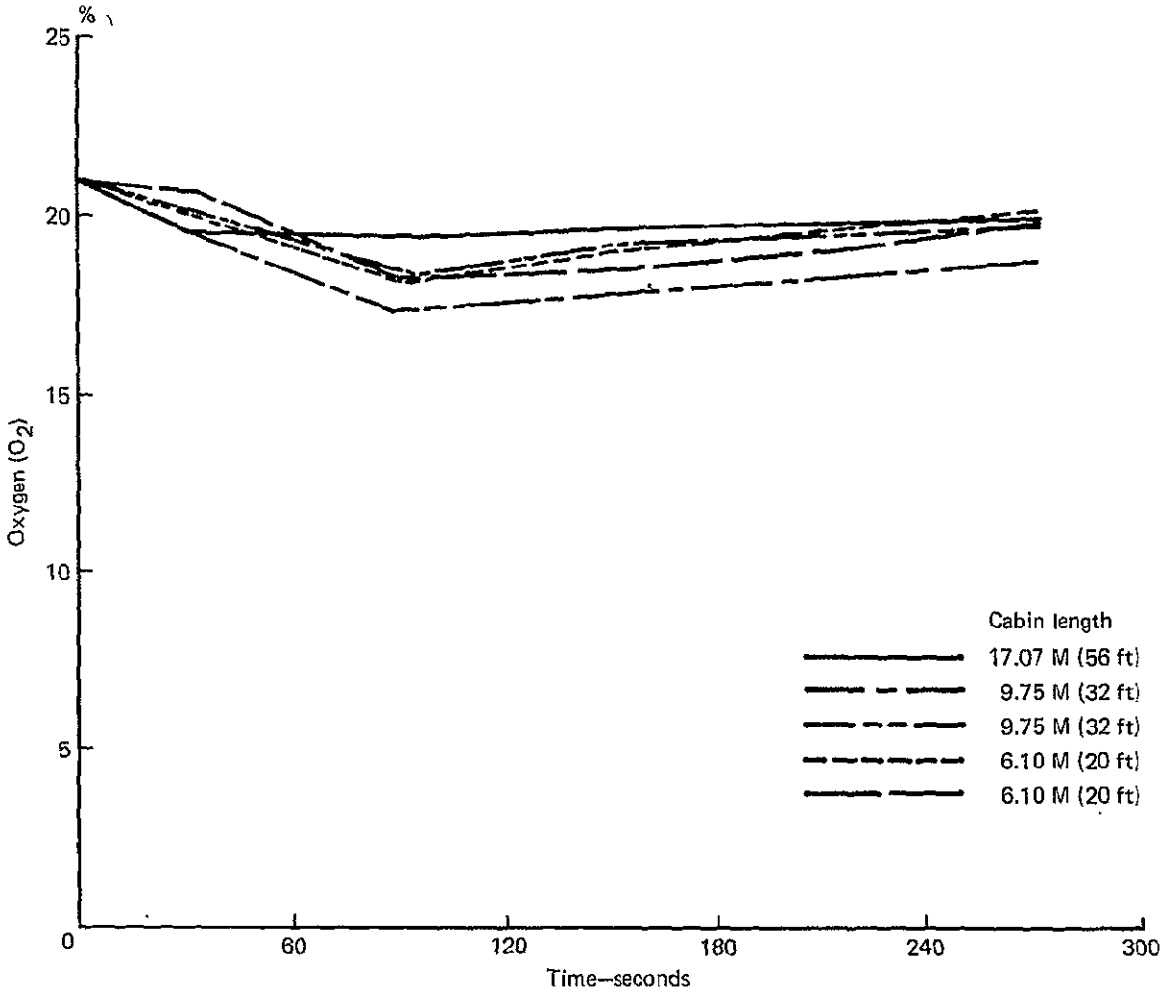

Figure 28.—Design In-flight Fire Source Oxygen (O_2) Concentrations in Various Cabin Lengths at the 1.52 M (5 ft) Head Level

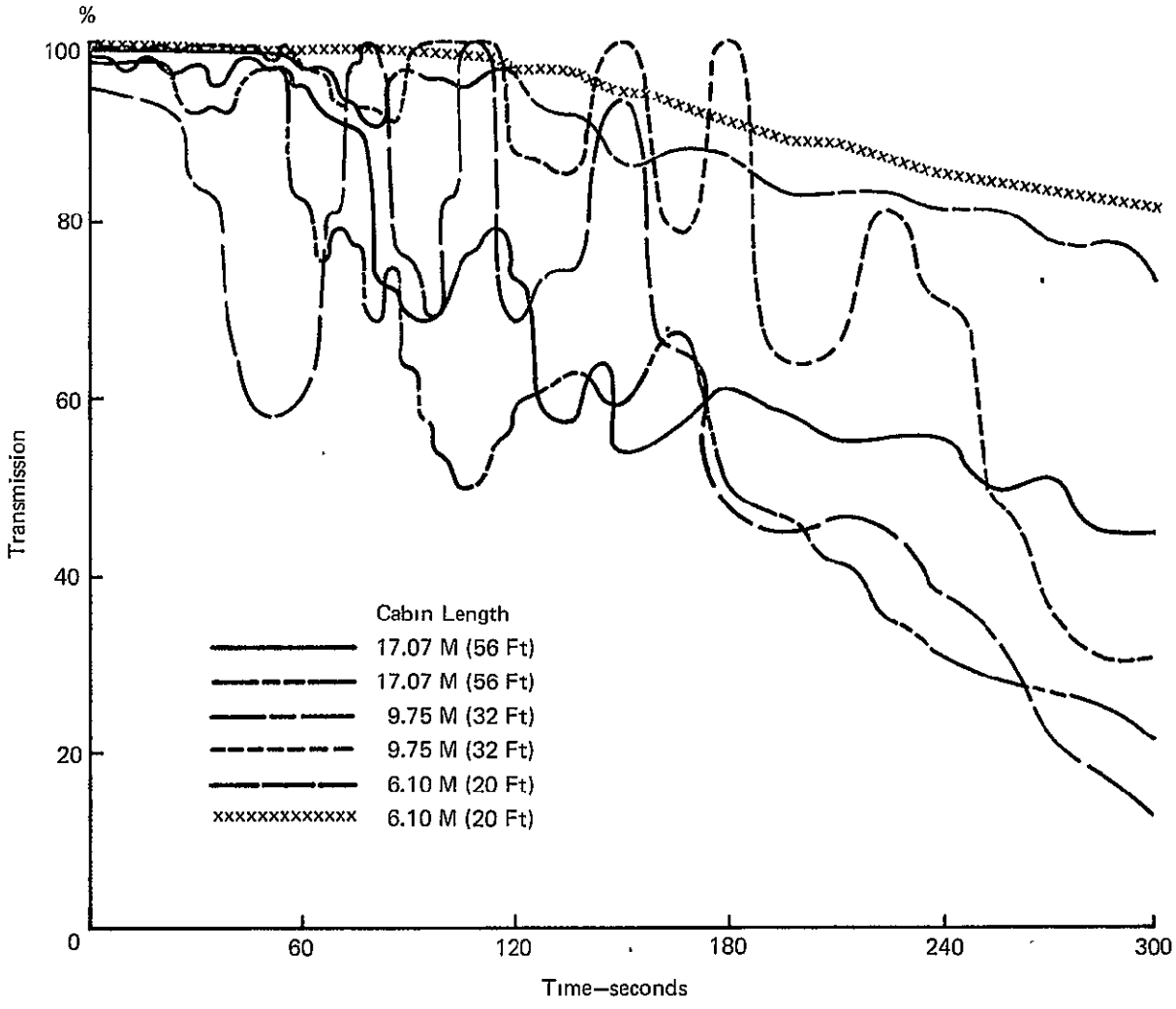

Figure 29.—Design In-flight Fire Source—Light Transmission over a 0.92 M (3 Ft) Path at the 1.52 M (5 Ft) Head Level

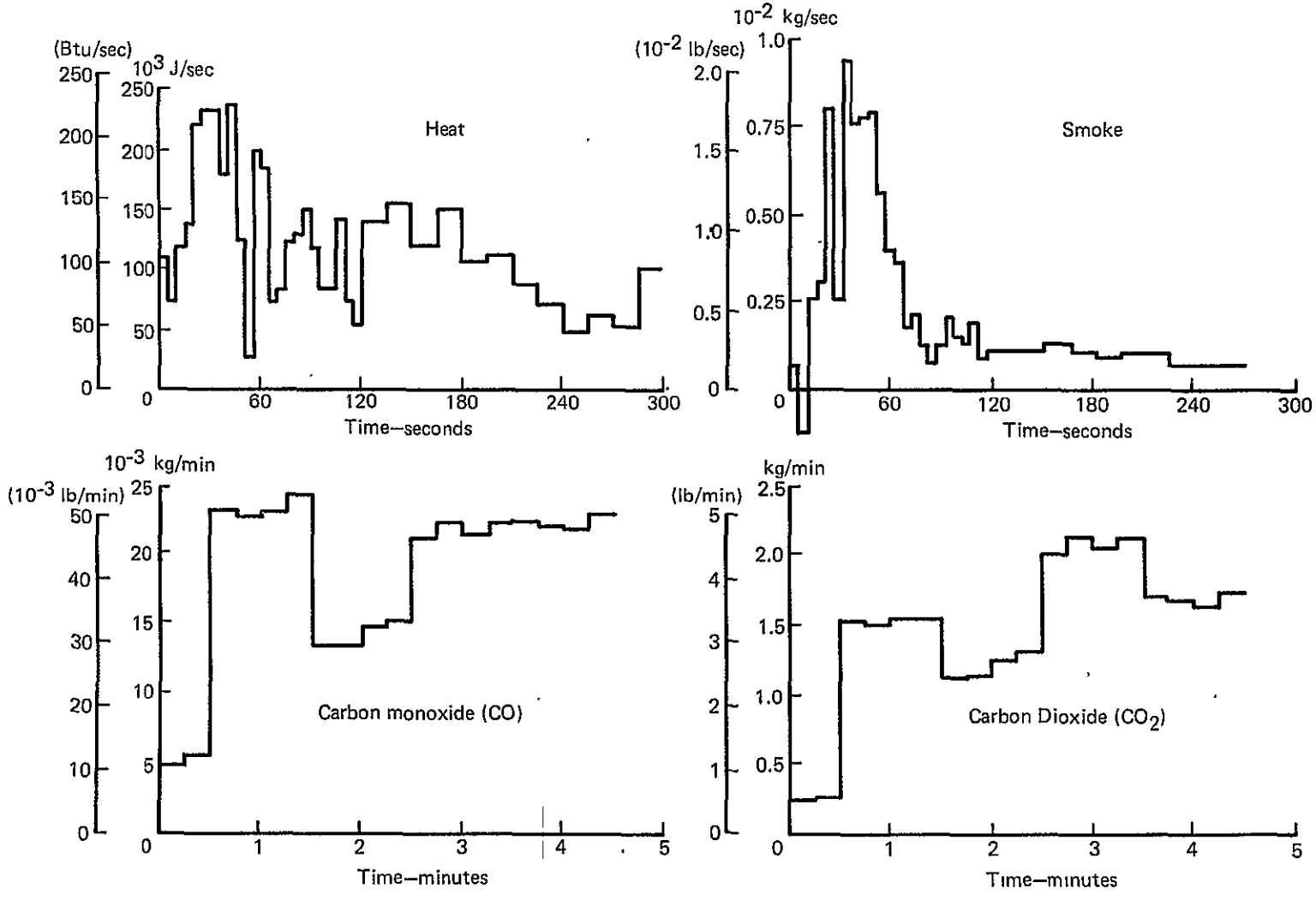

Figure 30.—Design Post-crash Fire Source Apparent Release Rates

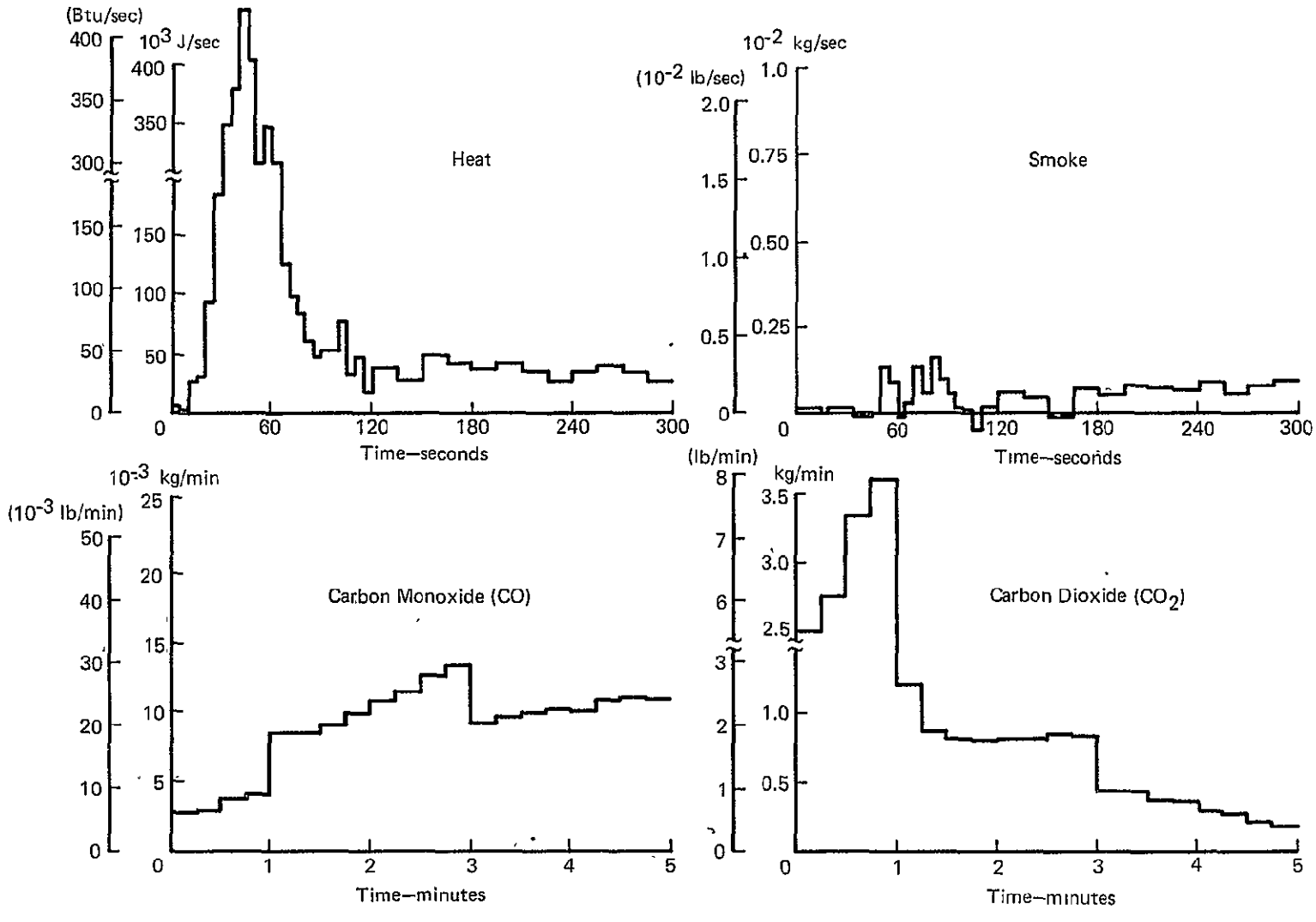

Figure 31.—Design In-flight Fire Source Apparent Release Rates

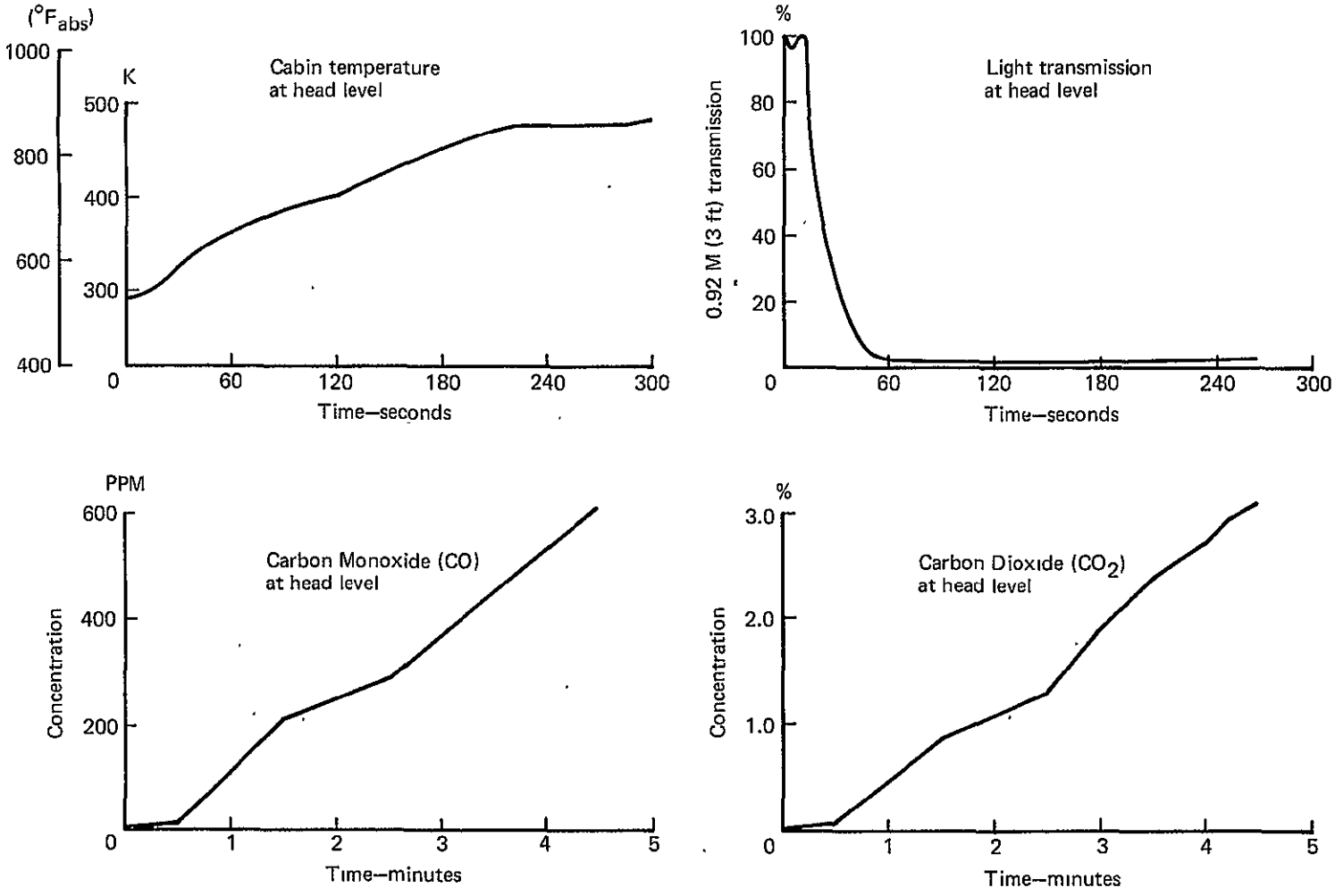

Standard conditions: ambient pressure—1.01×10^5 Pa (2110.29 psf); ambient temperature 294 K (530°F_{abs})

Figure 32.—Design Post-crash Fire Source—Standardized Conditions

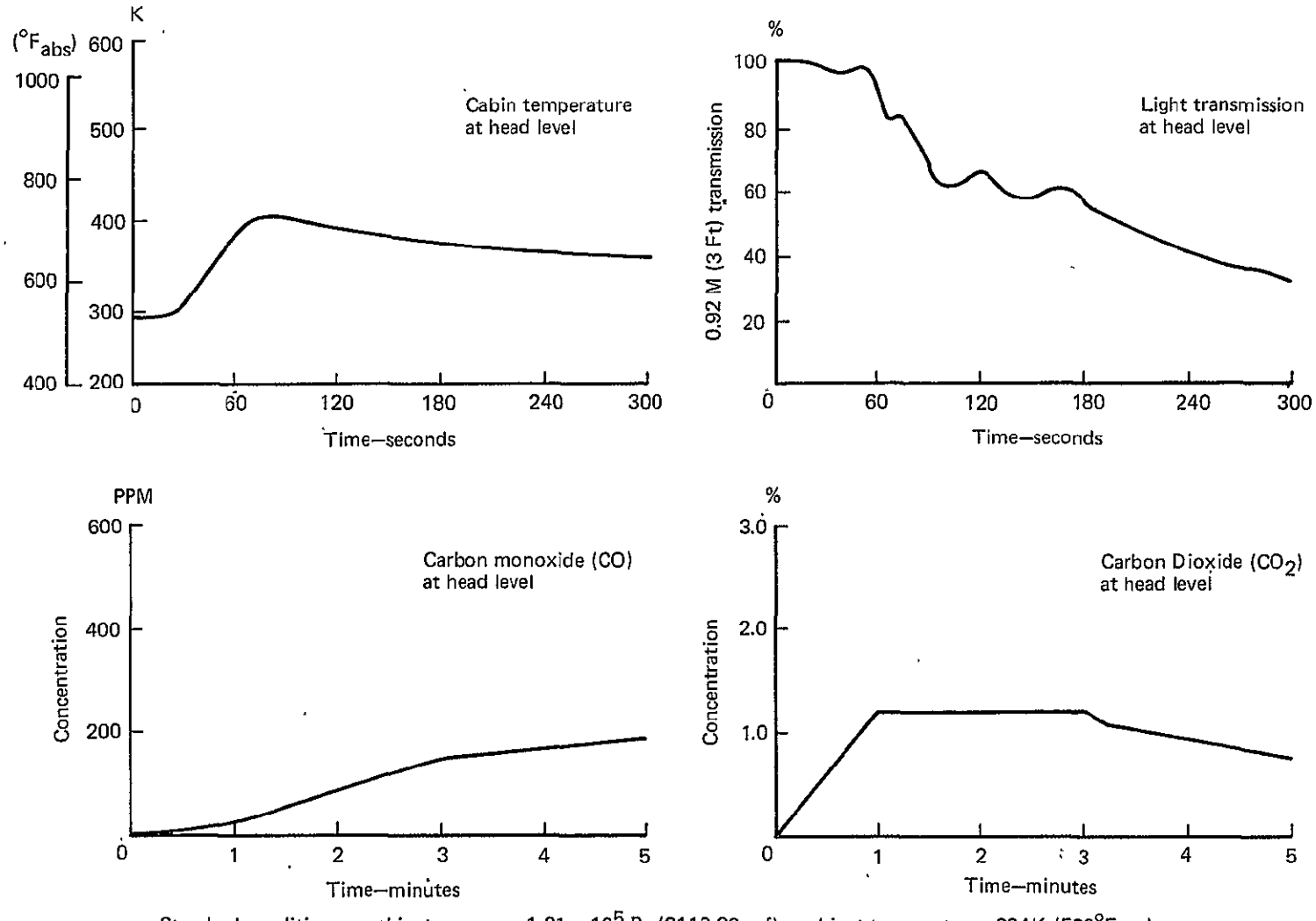

Standard conditions: ambient pressure—1.01 x 10^5 Pa (2110.29 psf); ambient temperature—294K (530°F_{abs})

Figure 33.—Design In-flight Fire Source—Standardized Conditions

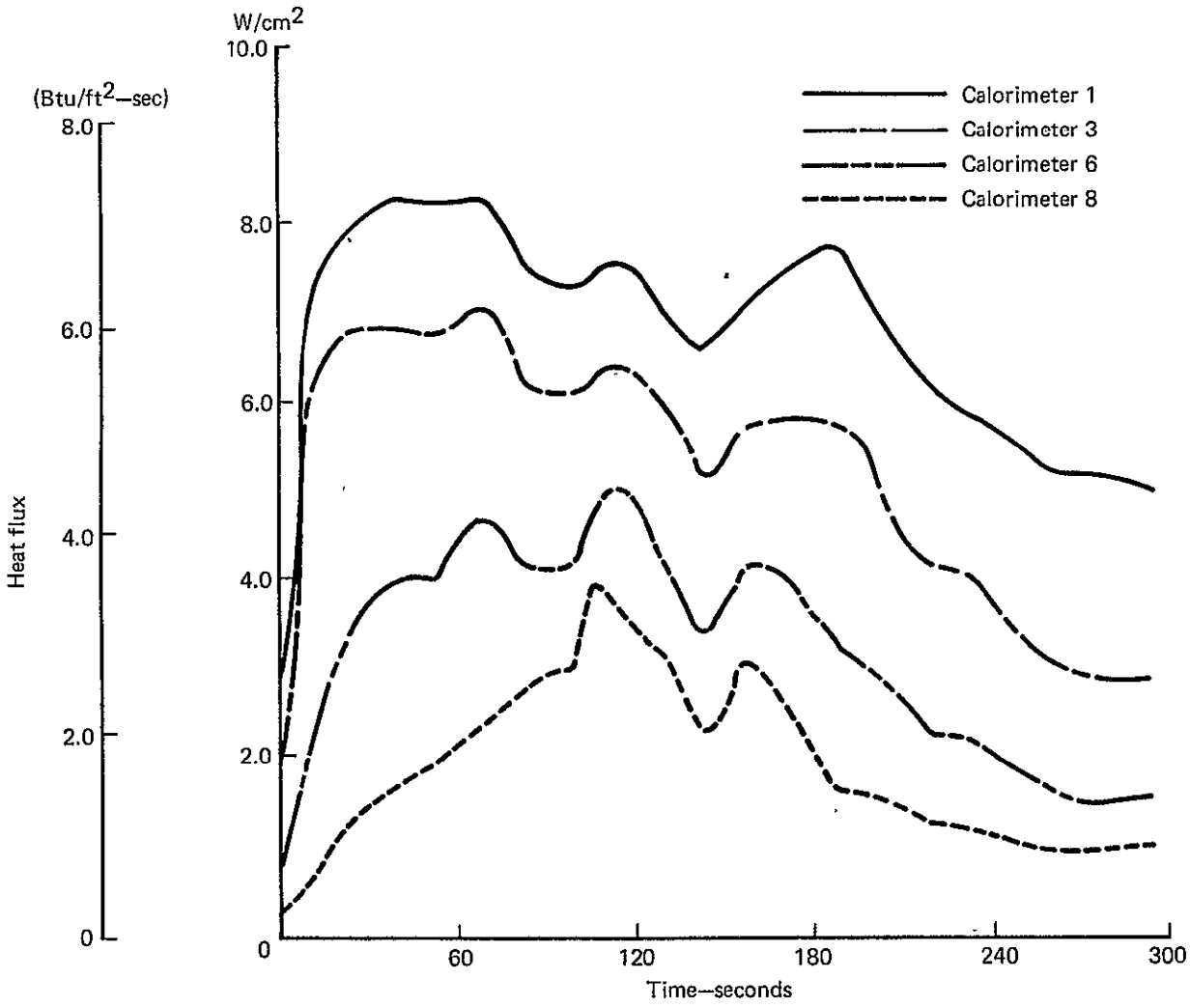

Figure 34.—Design Post-crash Fire Source Average Calorimeter Data (Calorimeters 1,3, 6 and 8)

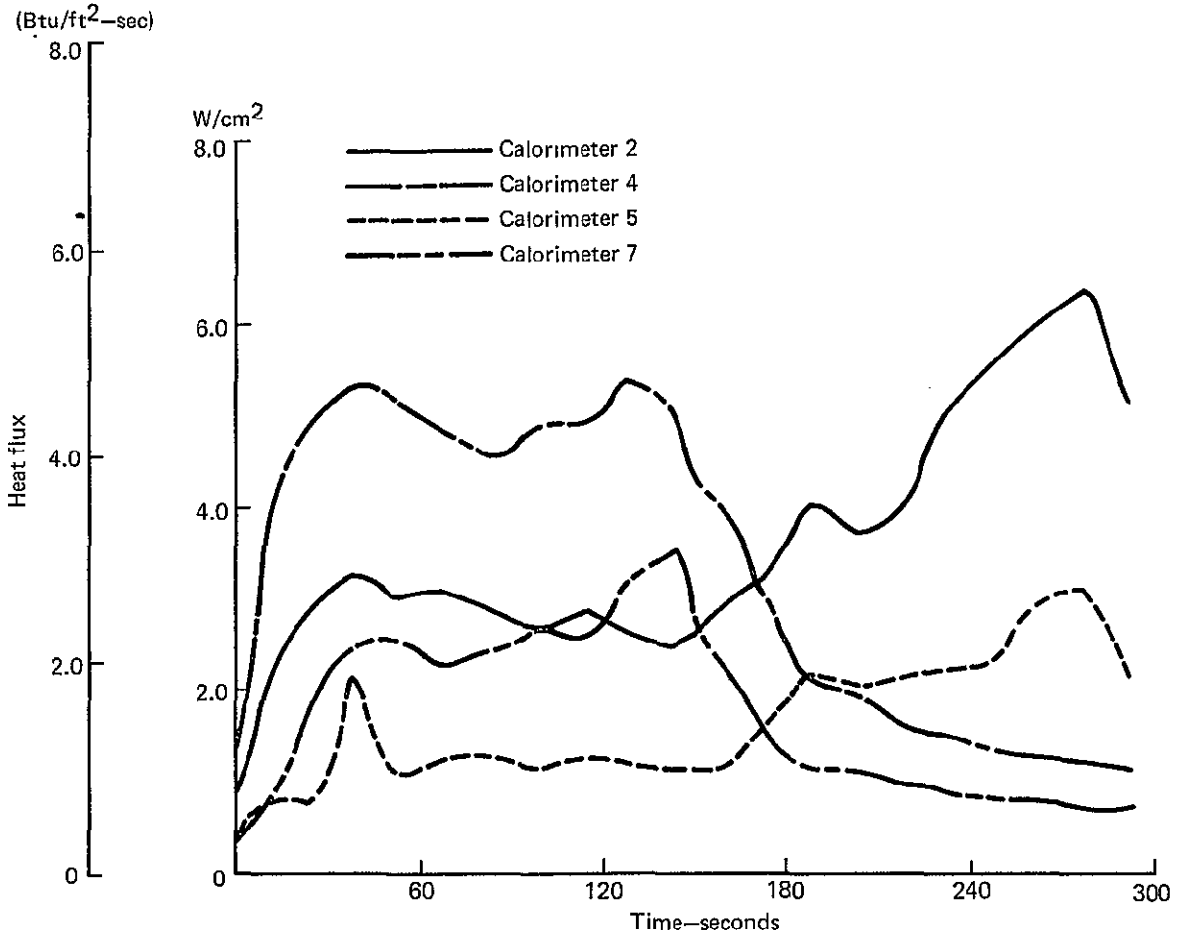

Figure 35.—Design Post-crash Fire Source Average Calorimeter Data (Calorimeters 2, 4, 5 and 7)

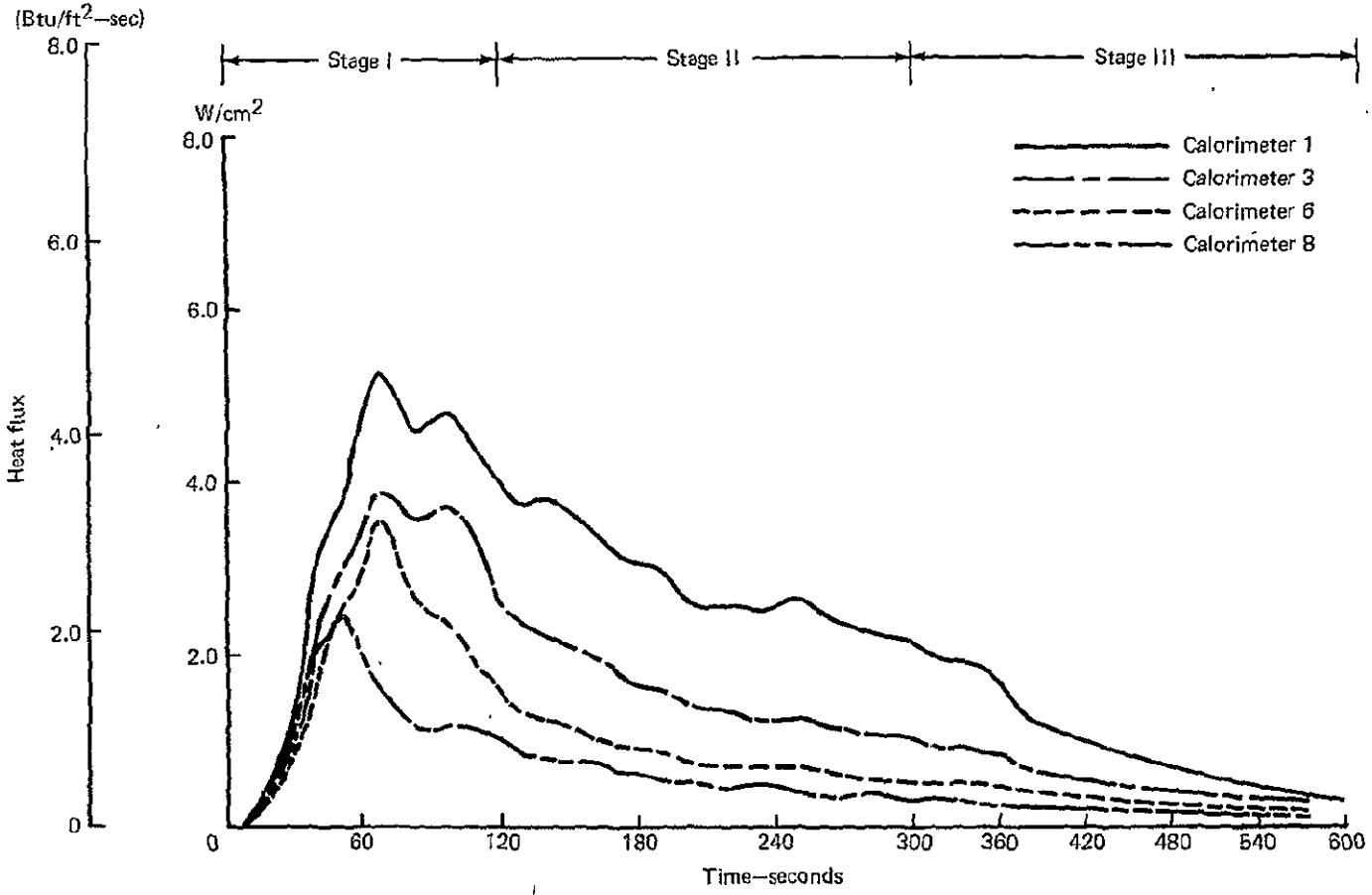

Figure 36.—Design In-flight Fire Source Average Calorimeter Data (Calorimeters 1, 3, 6 and 8)

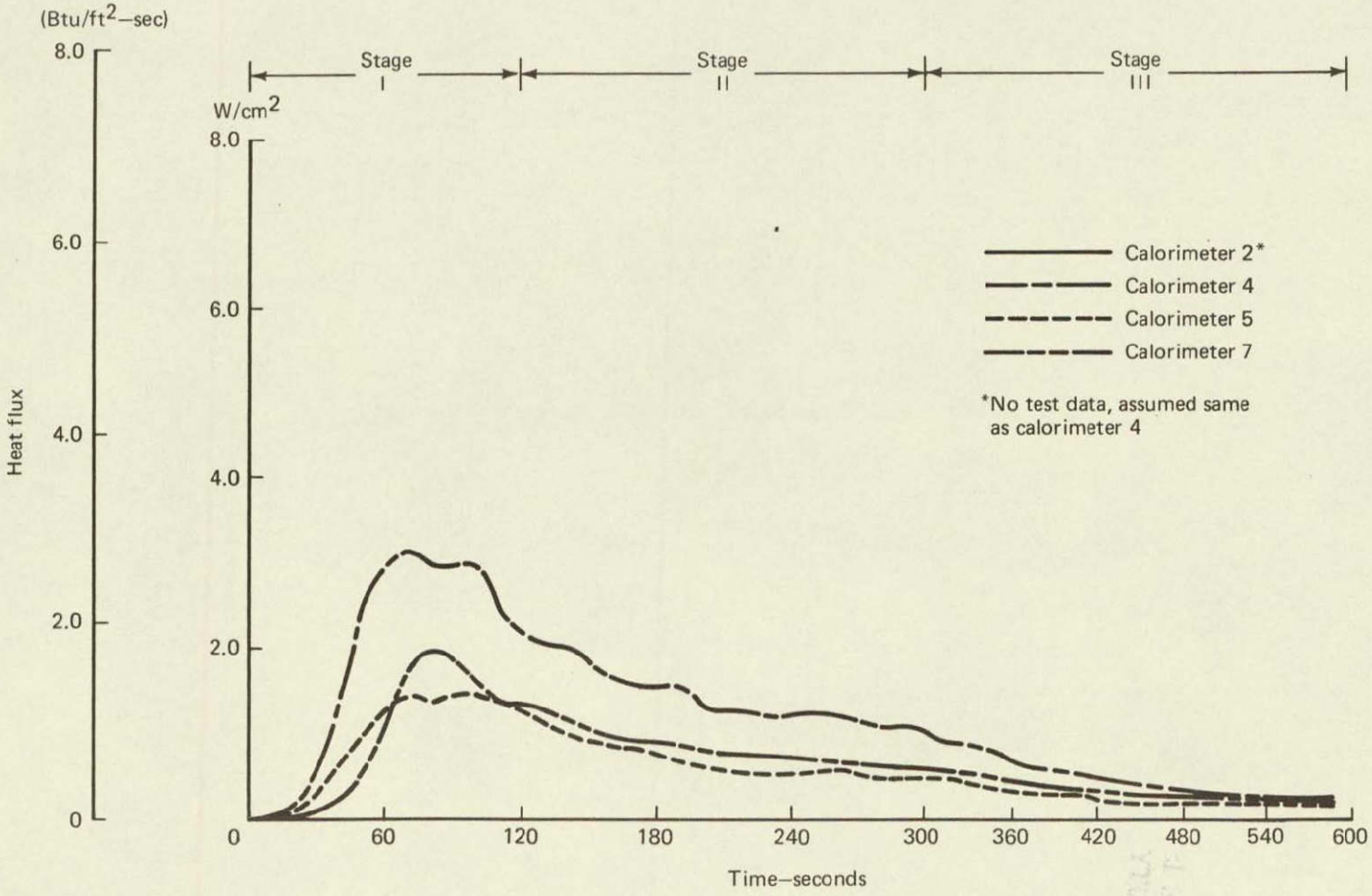

Figure 37.– Design Inflight Fire Source Average Calorimeter Data (Calorimeters 2, 4, 5 and 7)

Figure 38.—Boeing 707 Fire Test Section

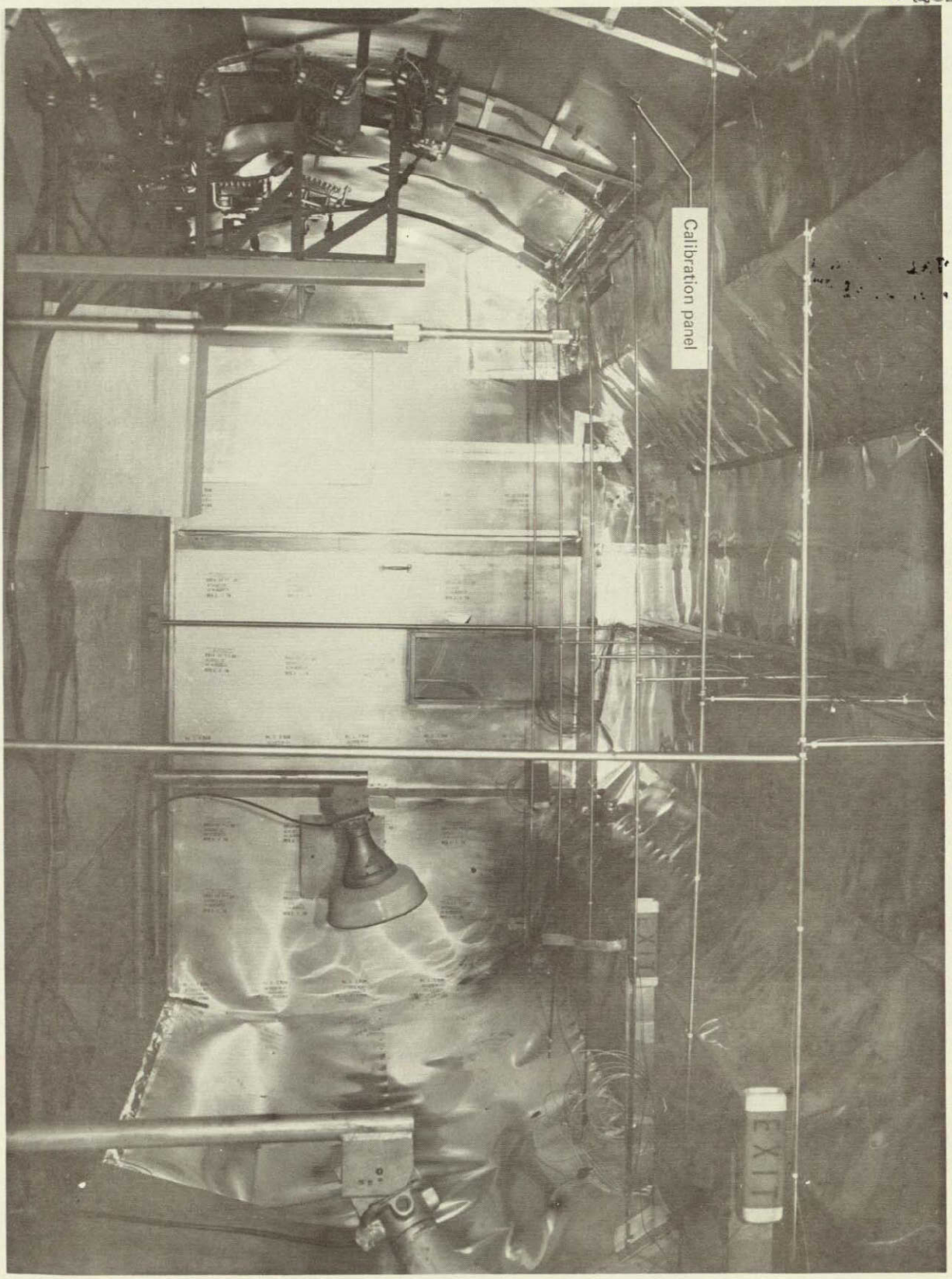

Figure 39.—707 Fire Test Section Interior

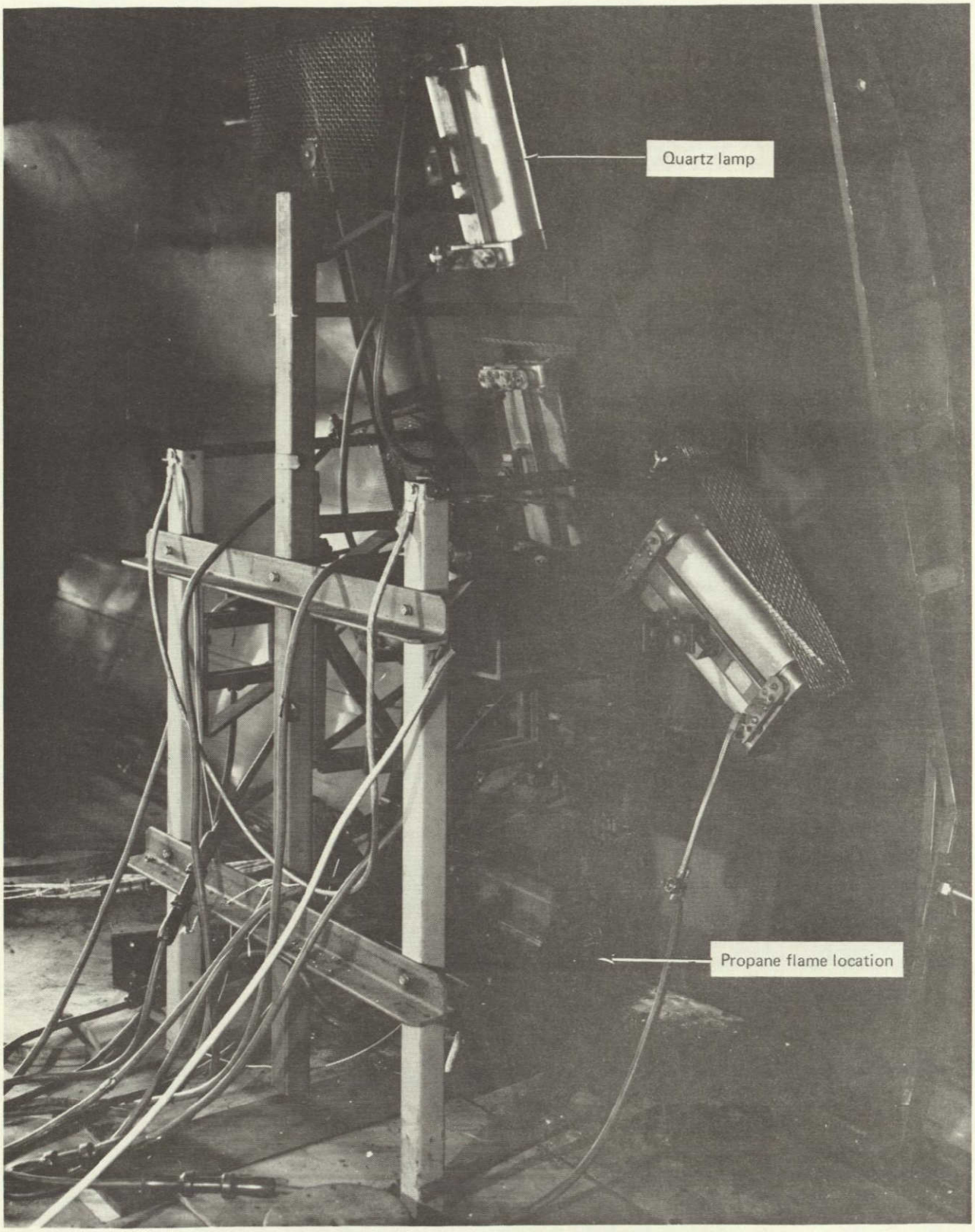

Figure 40.—Design Fire Simulating Apparatus in 707 Fire Test Section

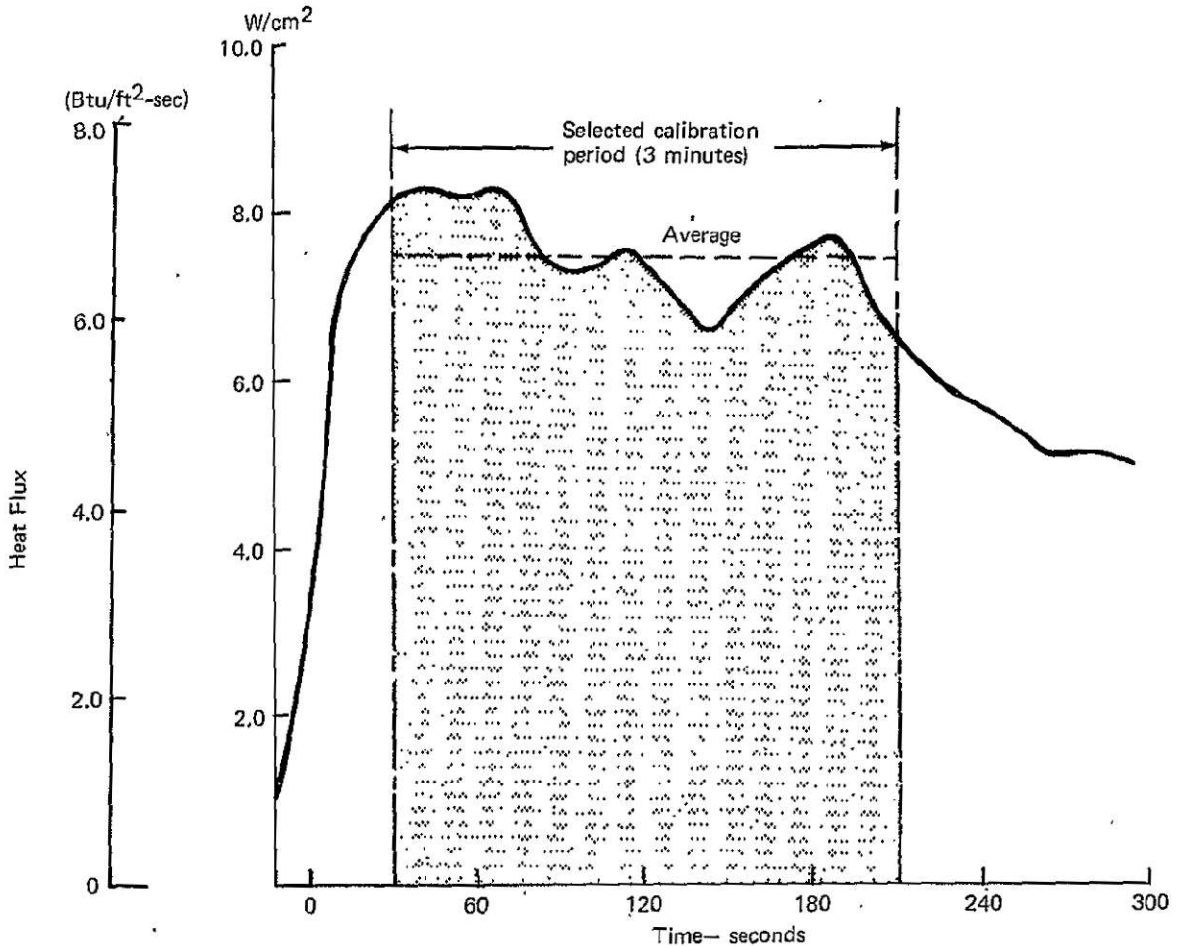

Figure 41.—Heat Flux at Calorimeter 1 for Design Post-Crash Fire

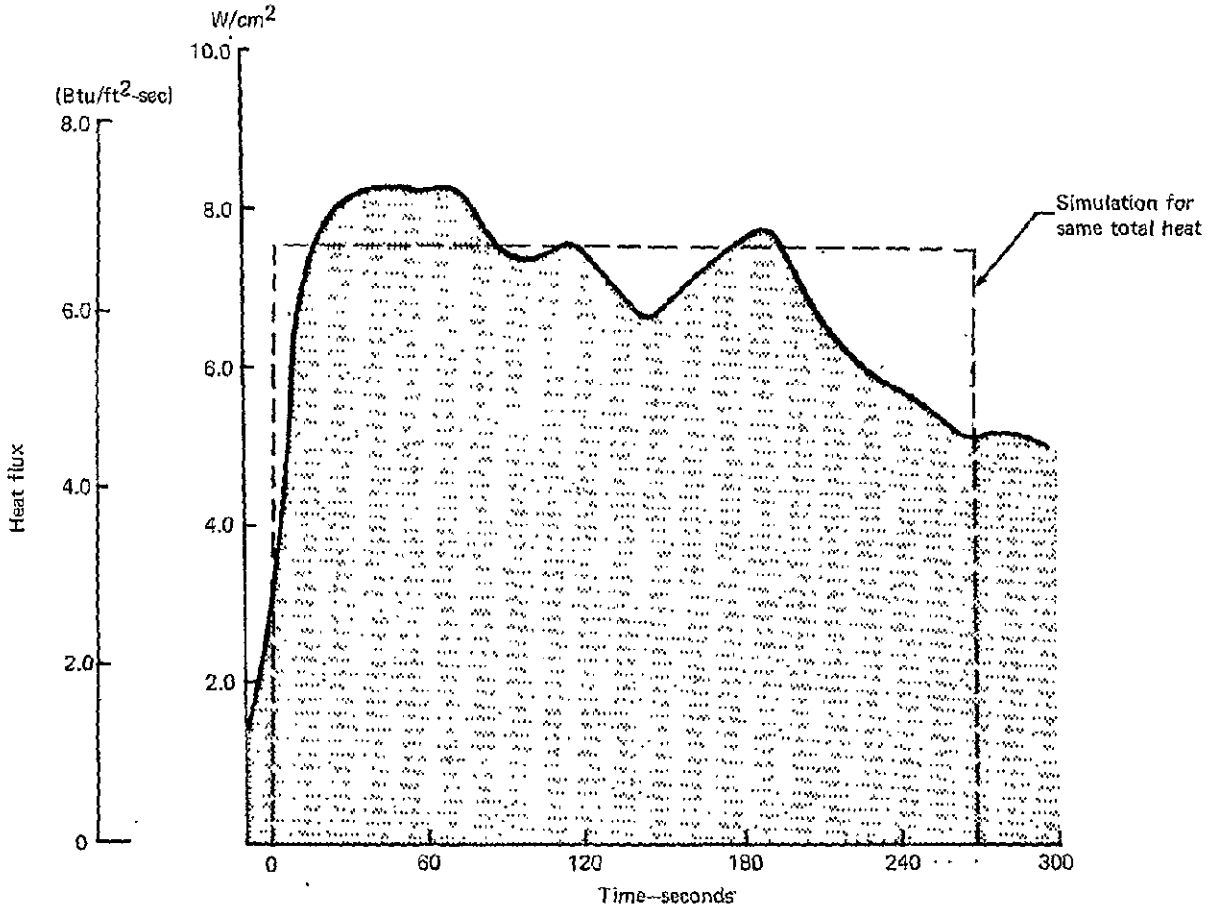

Figure 42.—Total Heat at Calorimeter 1 for Design Post-Crash Fire Source

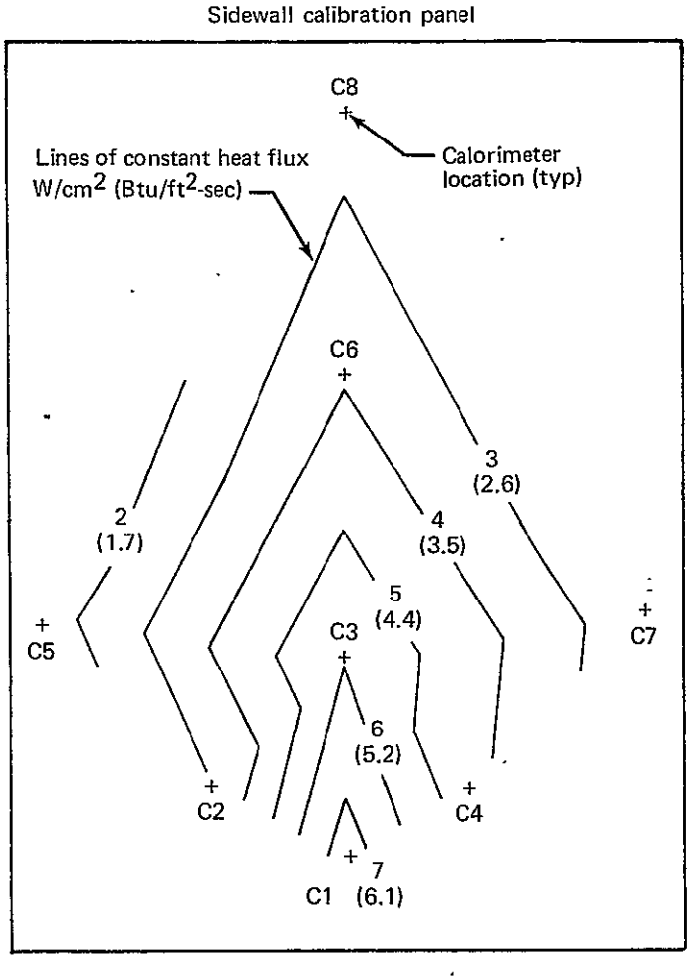

Figure 43.—Design Post-Crash Fire Source Heat Flux Distribution

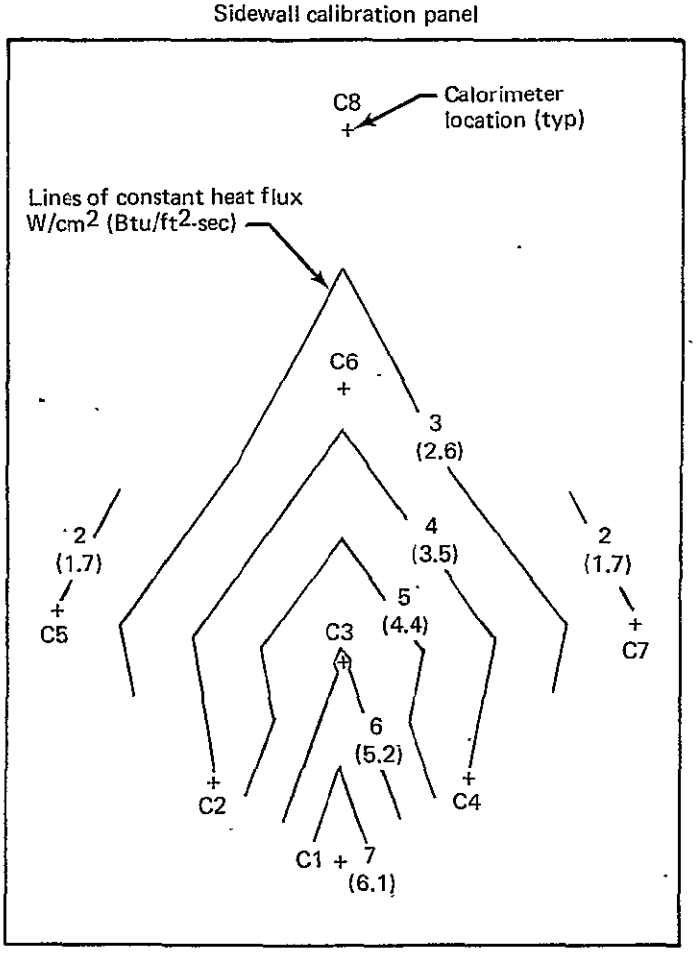

Figure 44.—Simulated Design Post-Crash Fire Source Heat Flux Distribution

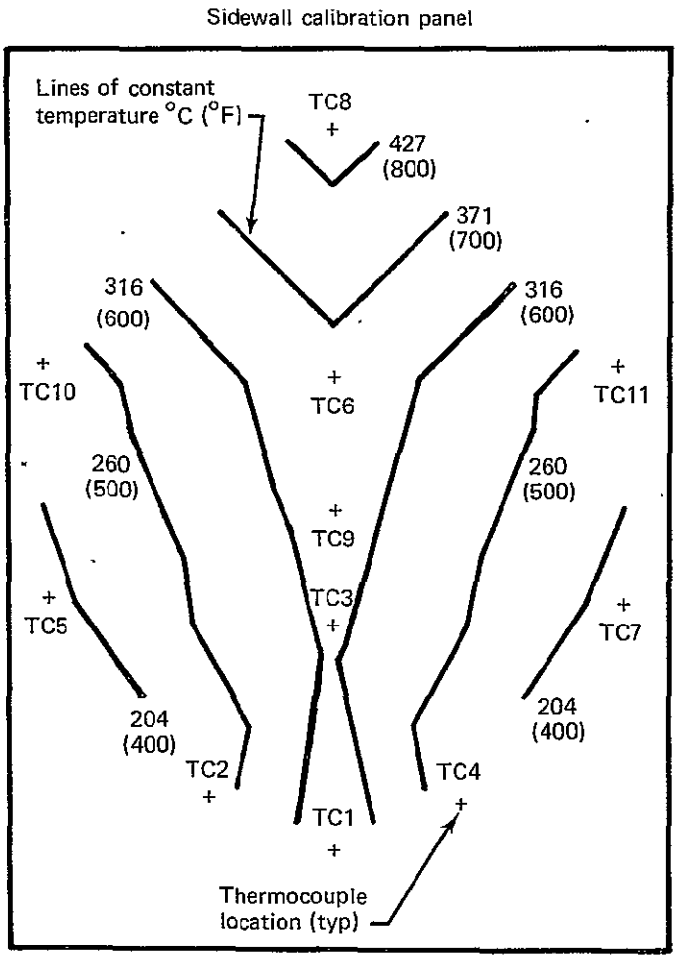

Figure 45.—Design Post-Crash Fire Source Temperature Distribution

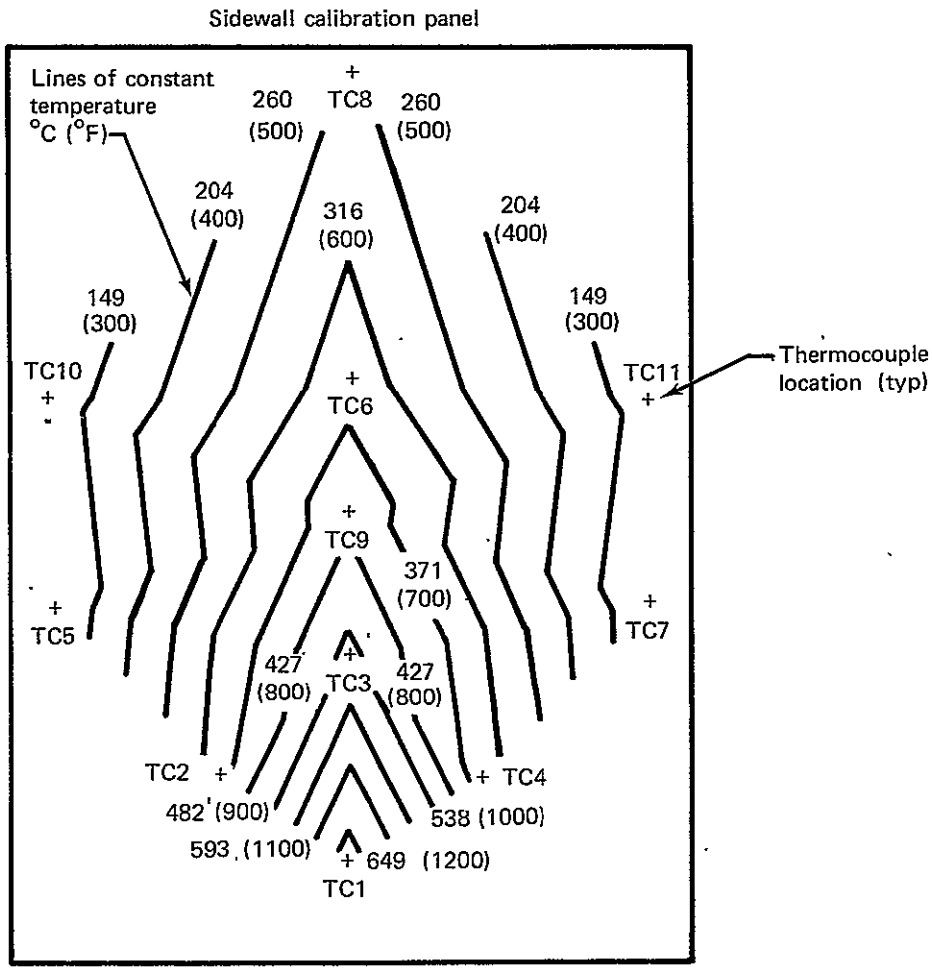

Figure 46.—Simulated Design Post-Crash Fire Source Temperature Distribution

Material sample number	Fire damage % loss of wt		Calculated total toxicant released—grams (10^{-2} lb)					
	NASA fuel fire	Boeing simulated fire	HF		HCL		HCN	
			NASA	Boeing	NASA	Boeing	NASA	Boeing
N00	~100	~100	—	0 (0)	12.25 (2.7)	42.54 (9.378)	1.81 (0.40)	5.91 (1.303)
N02	~100	~100	0.91 (0.20)	0 (0)	35.20 (7.76)	428.6 (94.5)①	—	Not tested for
402	27–32	12–13	—	13.05 (2.877)	12.38 (2.73)	19.89 (4.384)	1.93 (0.426)	0.85 (0.187)
416	9–13②	5–10	1.81 (0.40)	7.16 (1.579)③	5.34 (1.177)	90.15 (19.875)③	—	Not tested for

① Large value due to HCN-ion interference

② Does not include aluminum wt loss

③ Average of two tests

Figure 47.—Comparison of Fuel Pan and Simulated Fire Results

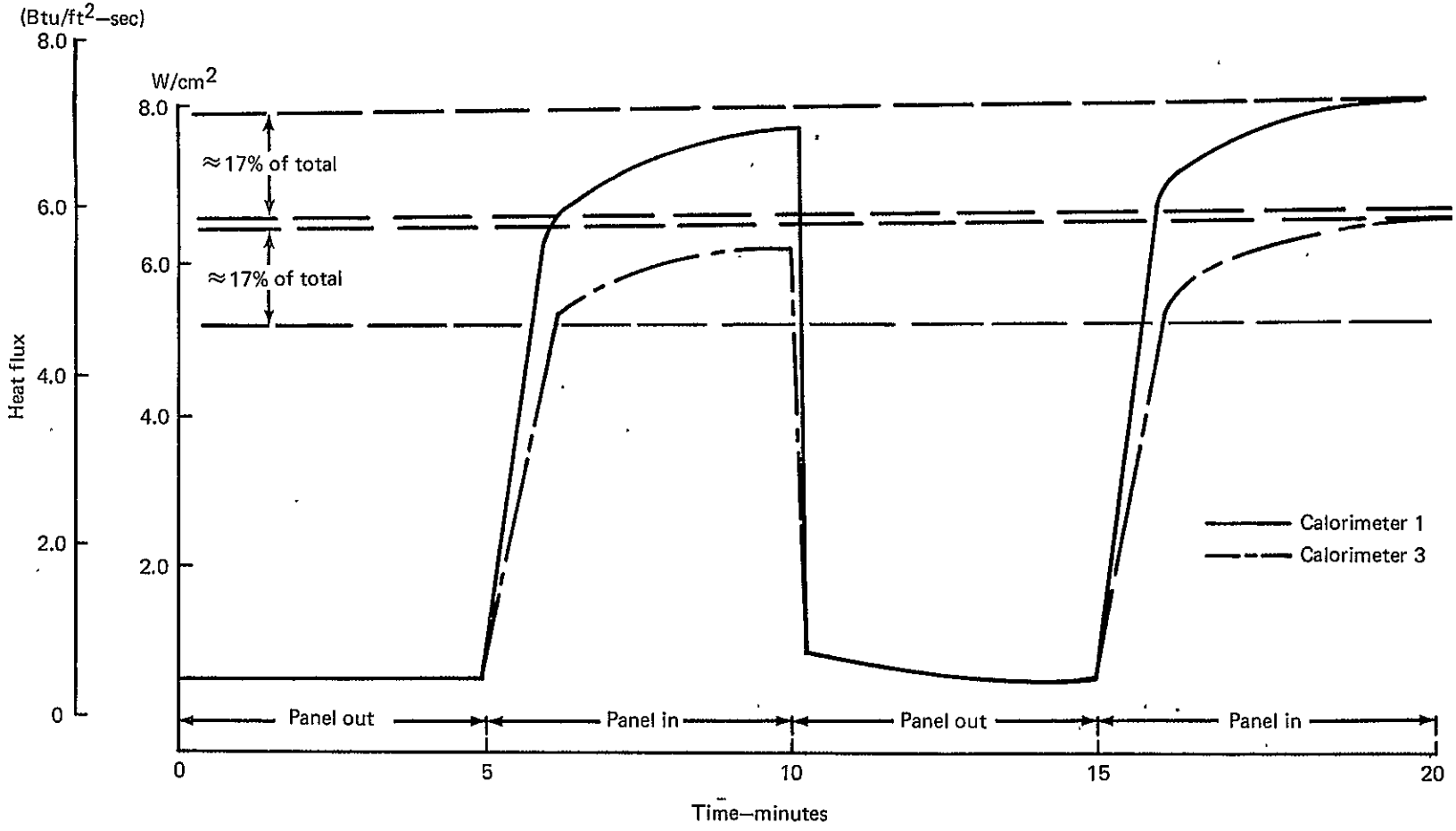

Figure 48.— Increased Heating from Reradiation

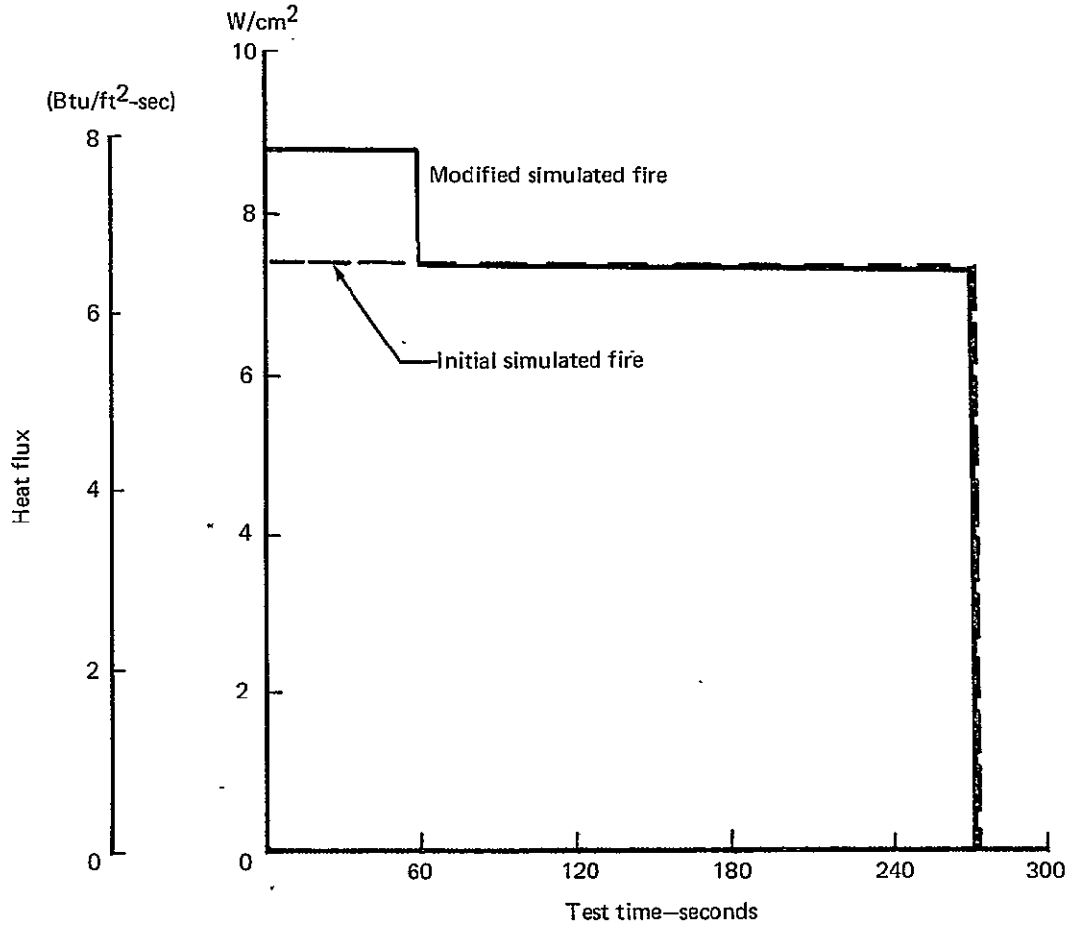

Figure 49.—Adjustment of Simulated Fire for Maximum Heat Flux, Calorimeter 1

Material sample number	Fire damage % loss of wt		Calculated total toxicant released—grams (lb x 10^{-2})					
	NASA fuel fire	Boeing simulated fire	HF		HCL		HCN	
			NASA	Boeing	NASA	Boeing	NASA	Boeing
N00 Modified Boeing fire simulation	~100	~100	–	0 (0)	12.25 (2.7)	1.03 (0.227)	1.81 (0.40)	2.93 (0.646)
N02 Modified Boeing fire simulation	~100	~100	0.91 (0.20)	0 (0)	35.20 (7.76)	1.71 (0.376)	–	0.549 (0.121)
402 Modified Boeing fire simulation	9-13①	8-14	–	18.78 (4.13)	12.38 (2.73)	63.07 (13.90)	1.93 (0.426)	0.41 (0.09)
416 Modified Boeing fire simulation	27-32	18-19	1.81 (0.40)	5.94 (1.31)	5.34 (1.177)	45.99 (10.14)	–	0 (0)

① Does not include aluminum wt loss

Figure 50.—Comparison of Fuel Pan and Modified Simulated Fire Results

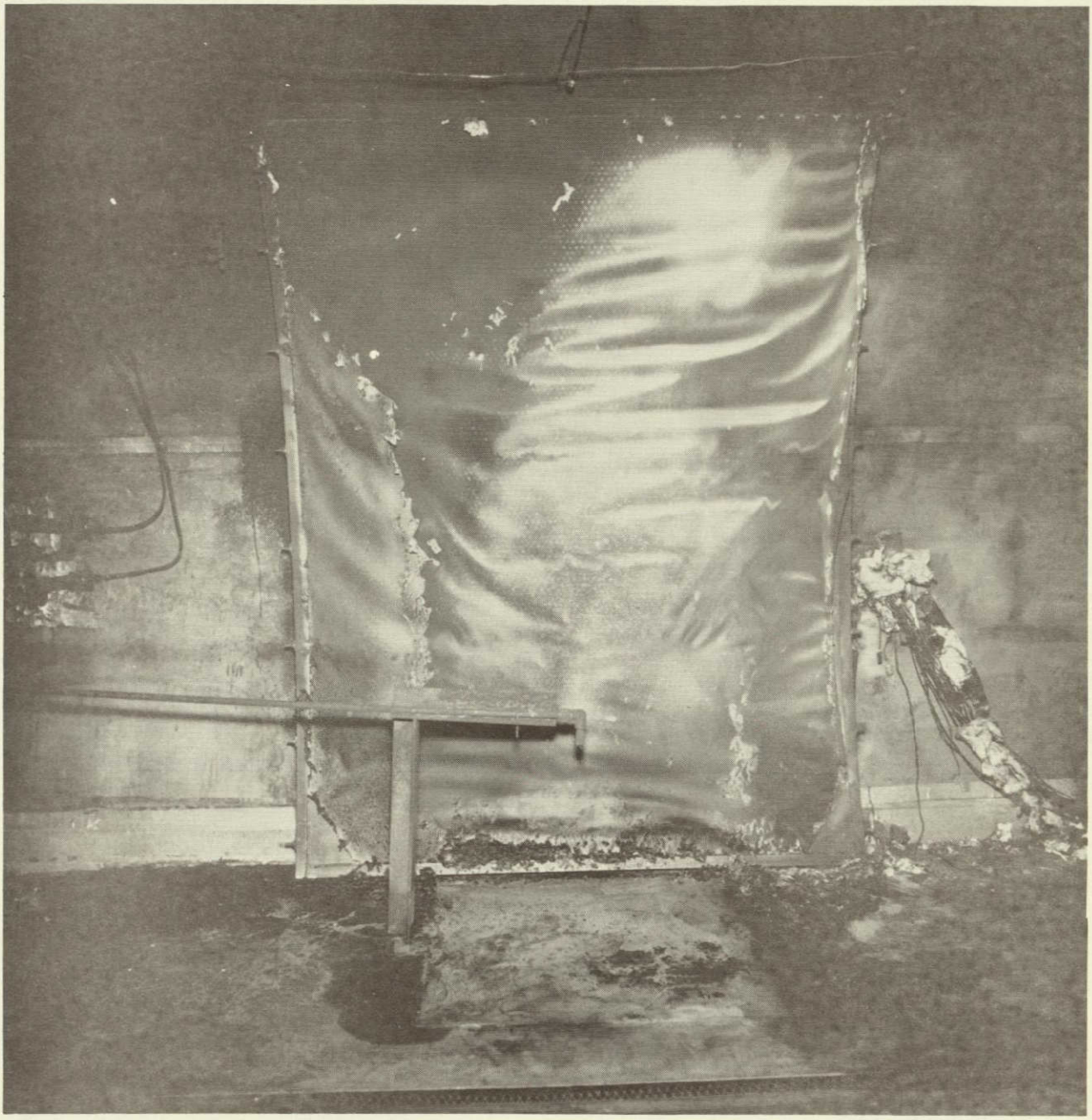

Figure 51.—Material 402 After Design Post-crash Fire Source Test

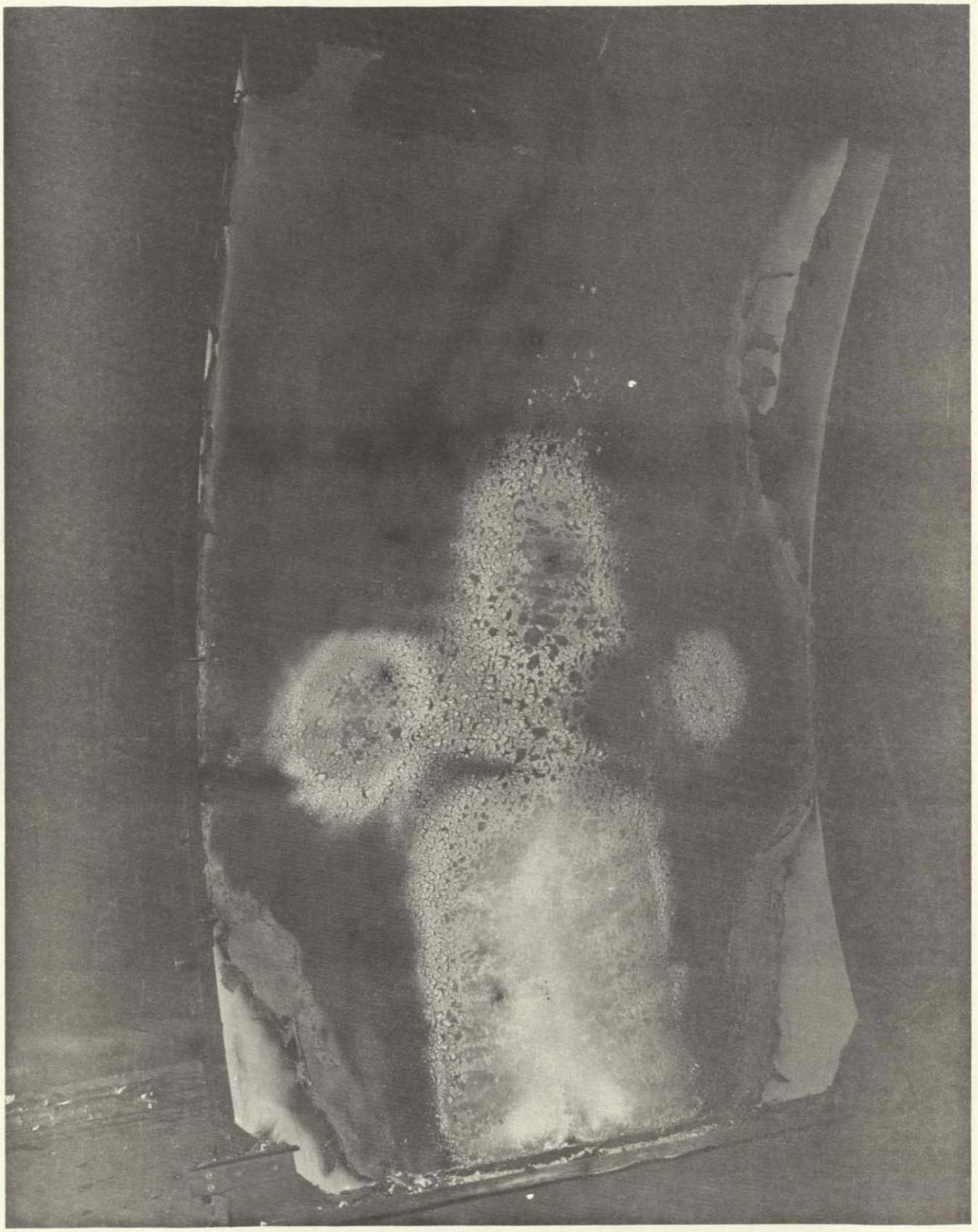

Figure 52.—Material 402 After Simulated Post-crash Fire Source Test

*Figure 53.—Material **416 After Design** Post-crash Fire Source Test*

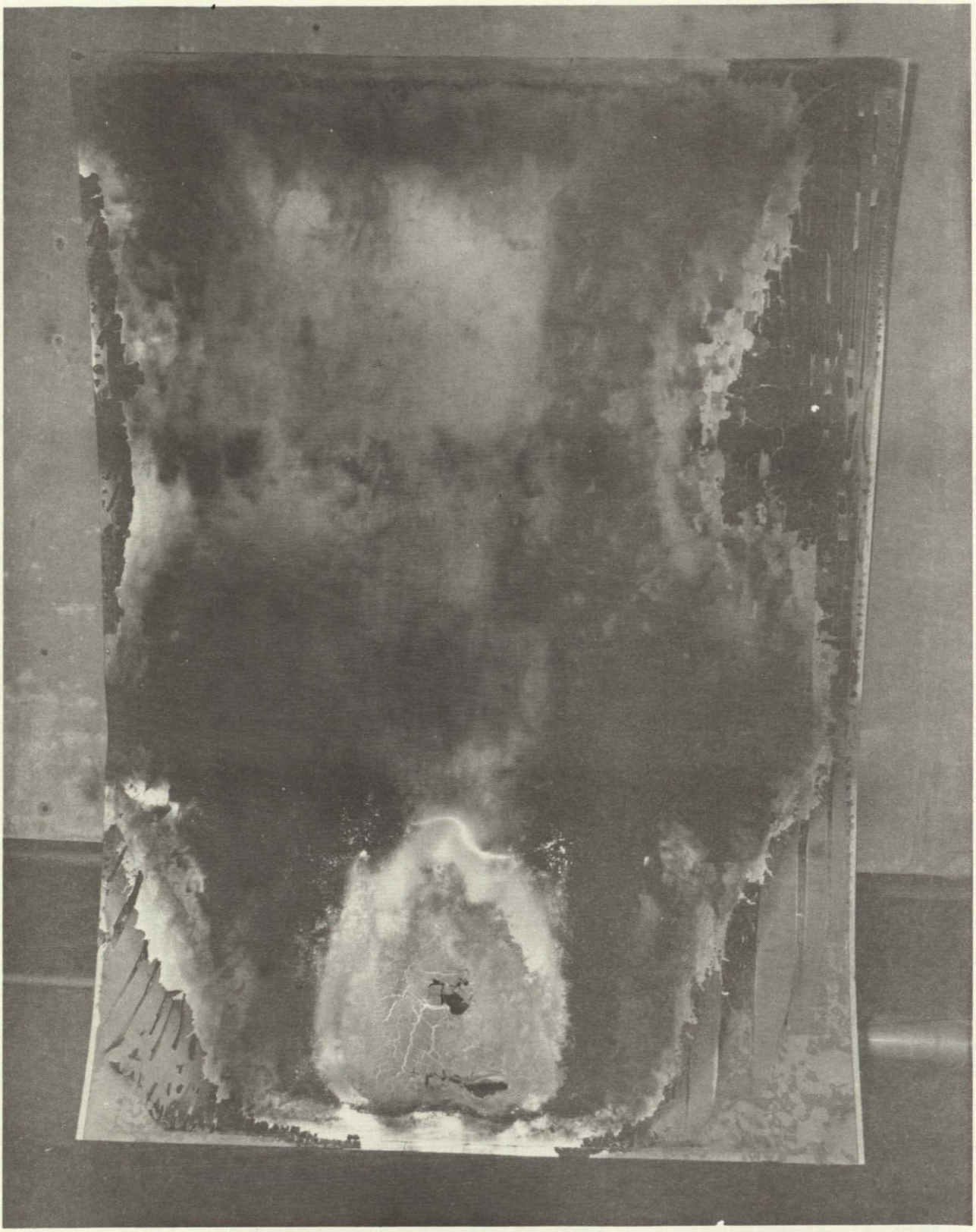

Figure 54.—Material 416 After Simulated Design Post-crash Fire Source Test

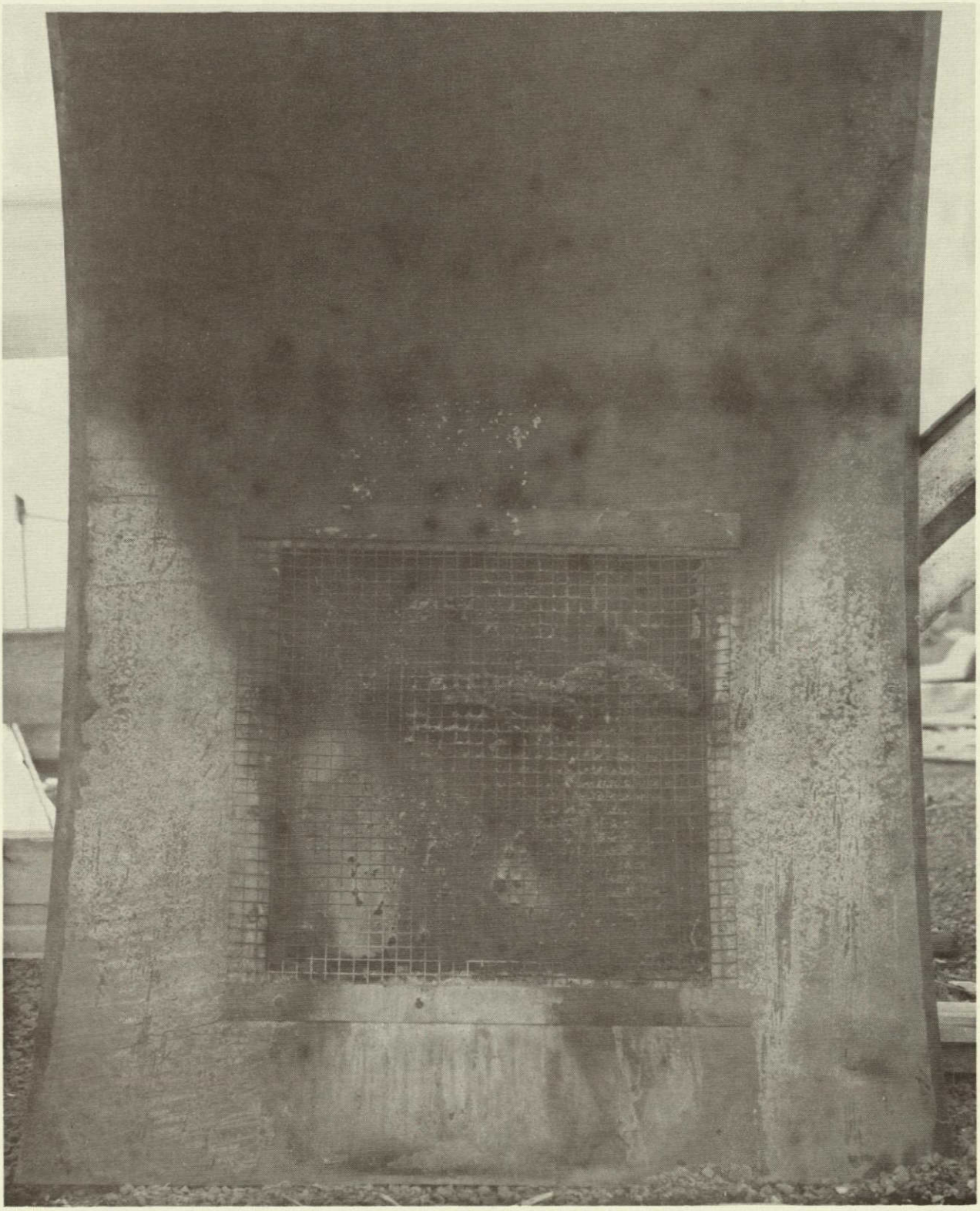

Figure 55.—Material N00 After Simulated Design Post-crash Fire Source Test

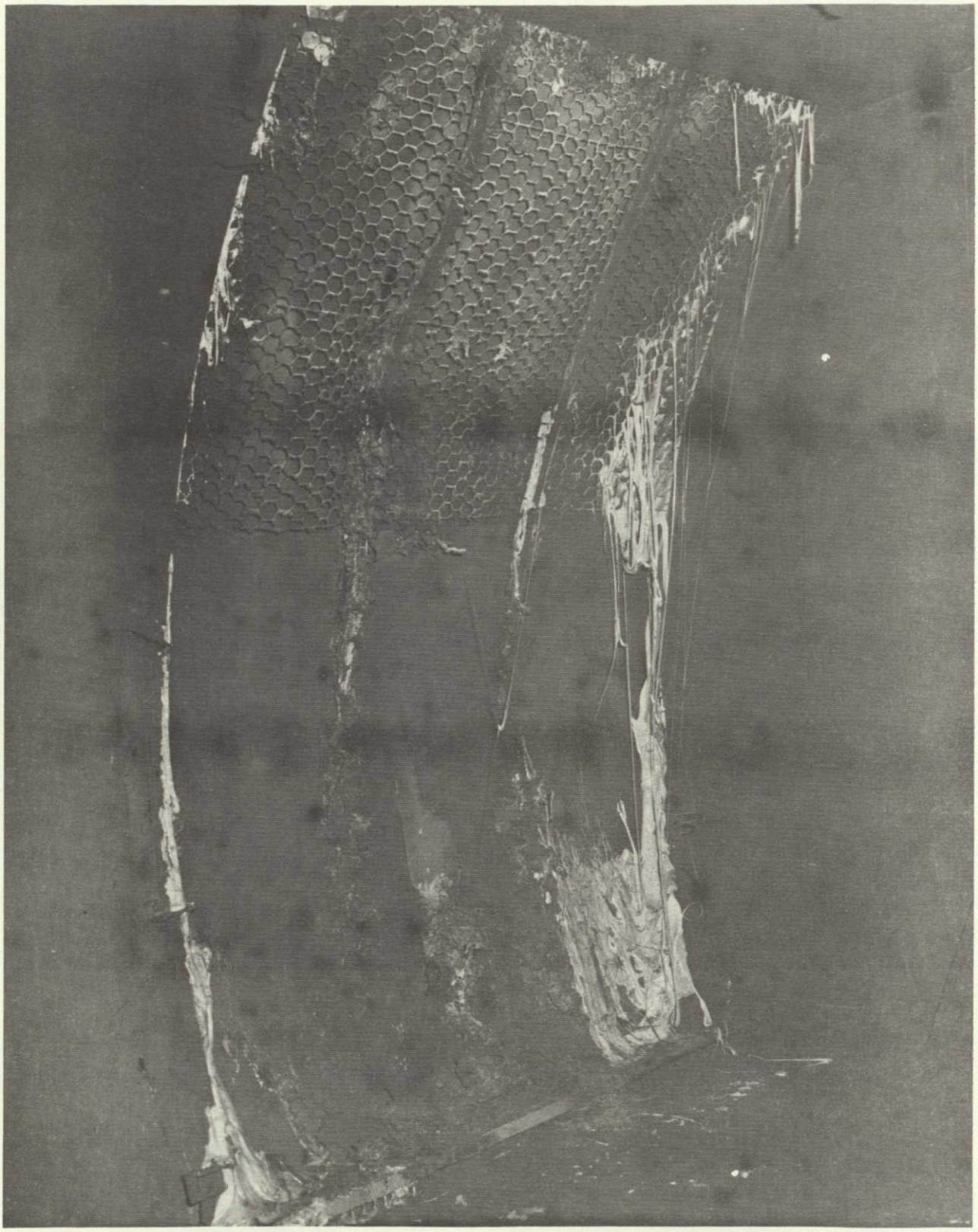

Figure 56.—Material 412 After Simulated Design Post-crash Fire Source Test

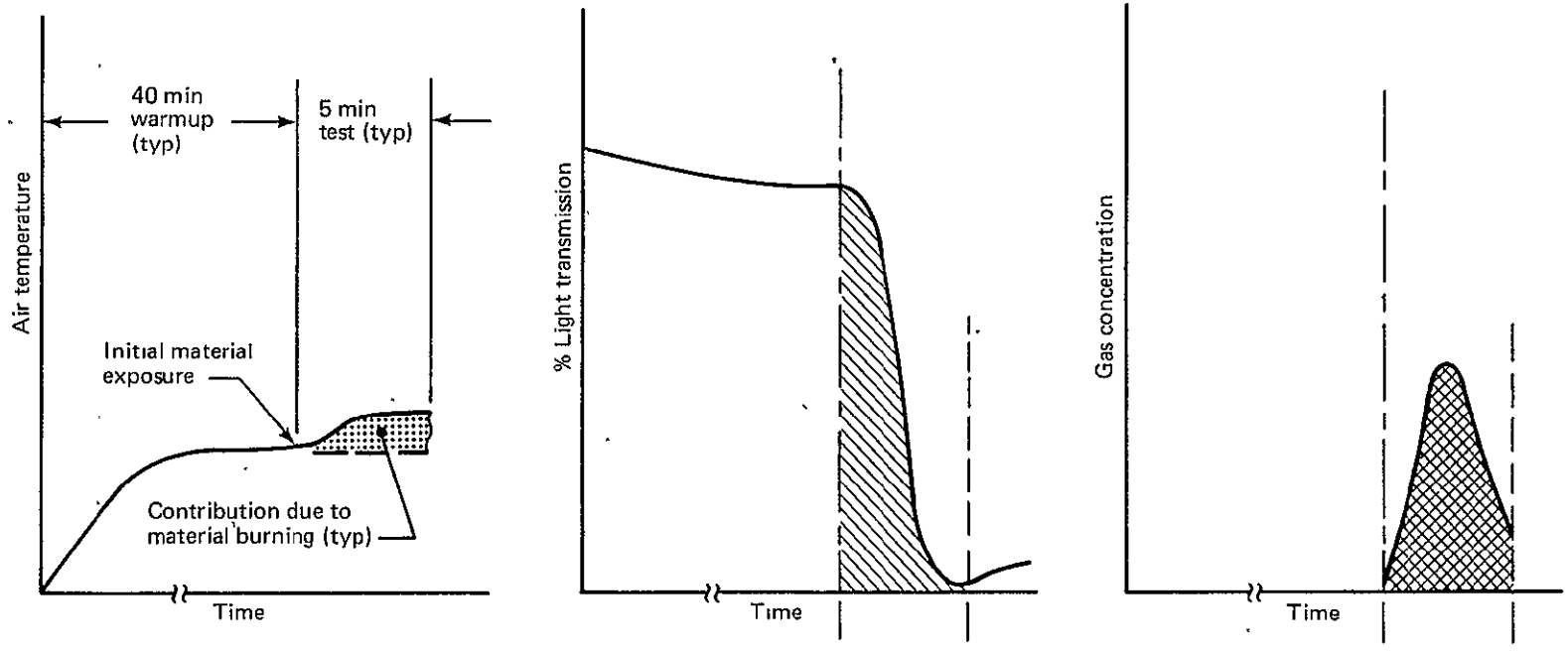

Figure 57.— Typical Cabin Environment Data from Simulated Design Fires

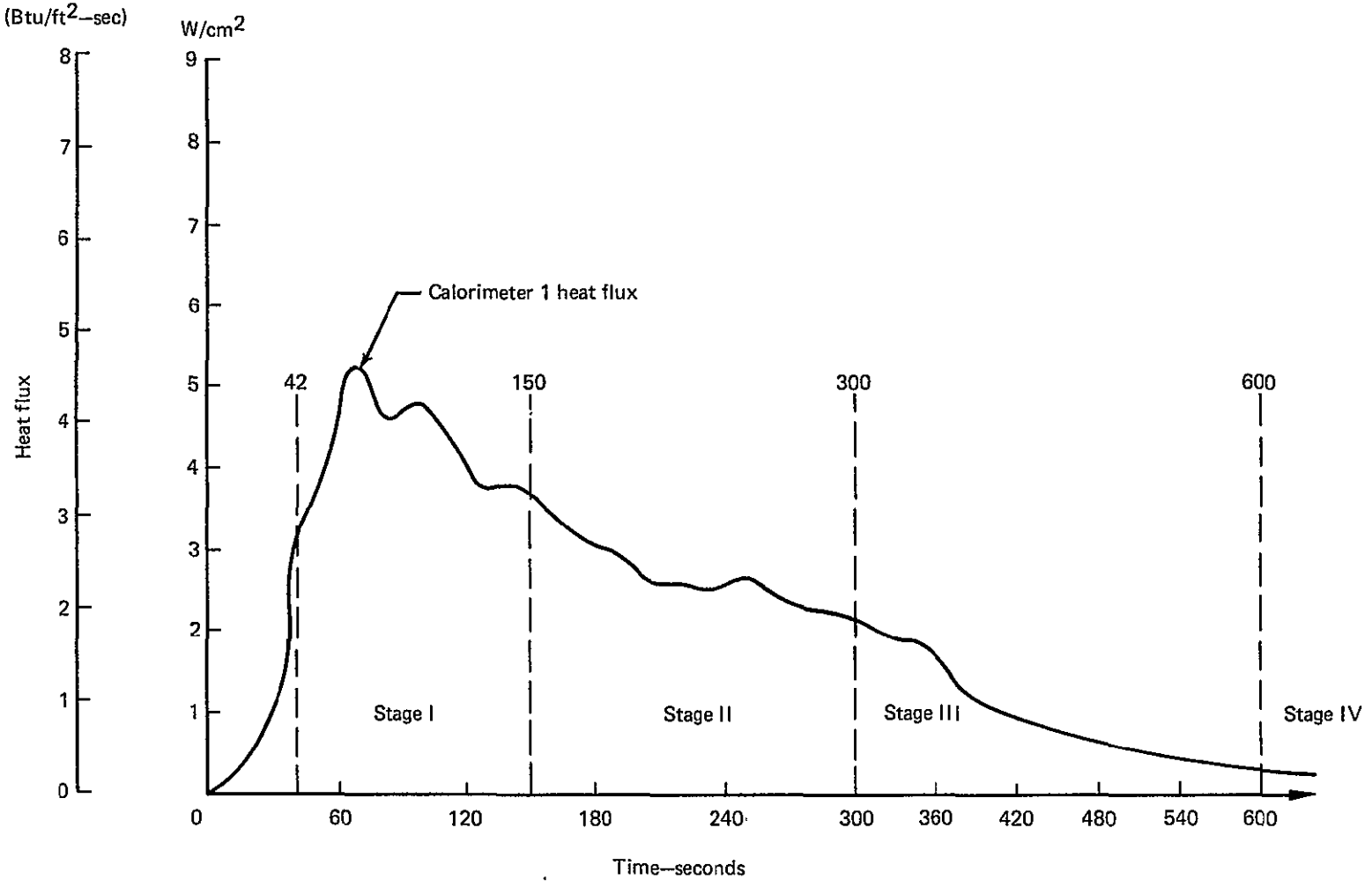

Figure 58.– Design In-flight Fire Source, Average Heat Flux at Calorimeter 1

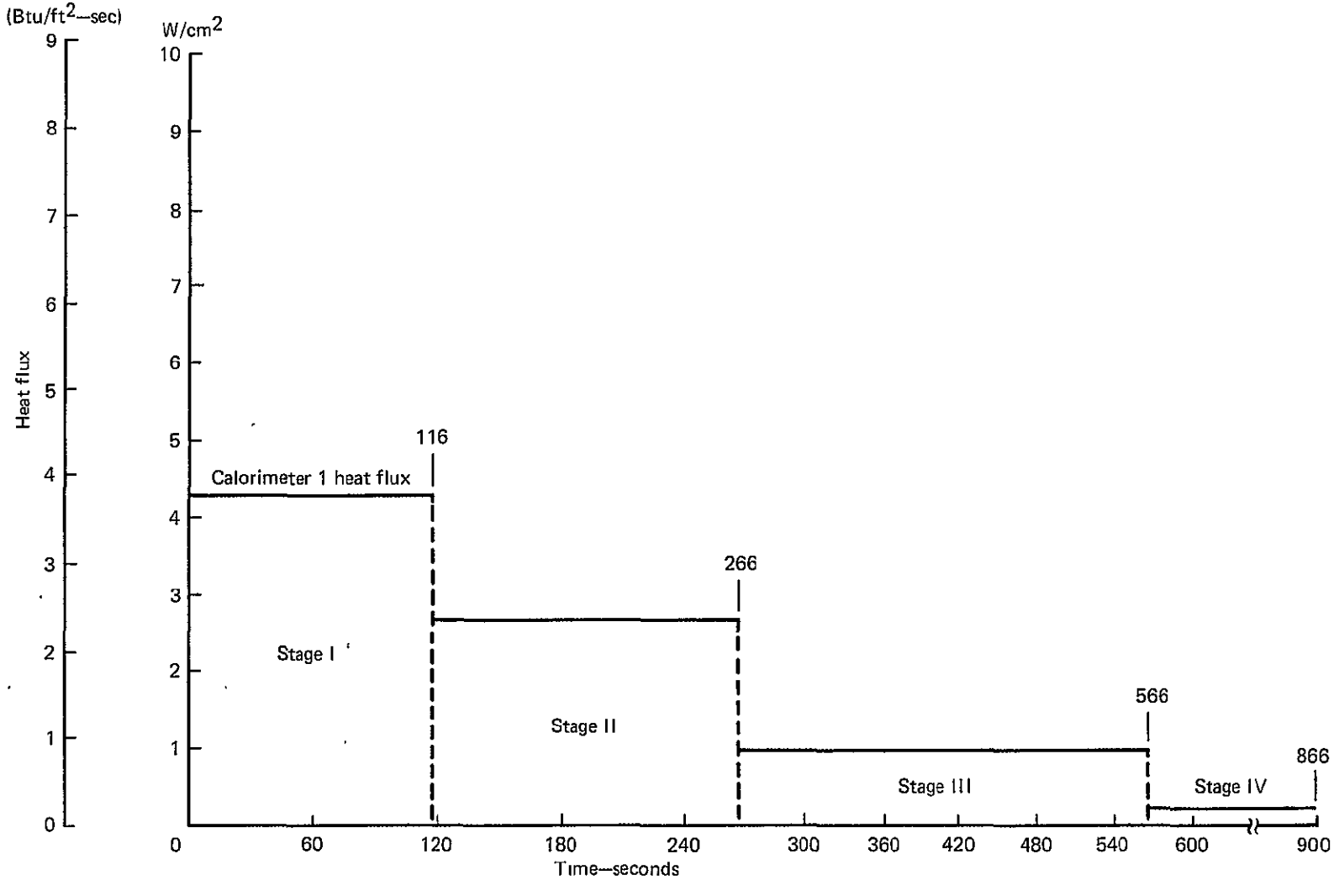

Figure 59.— Simulated Design In-flight Fire Source Heat Flux at Calorimeter 1

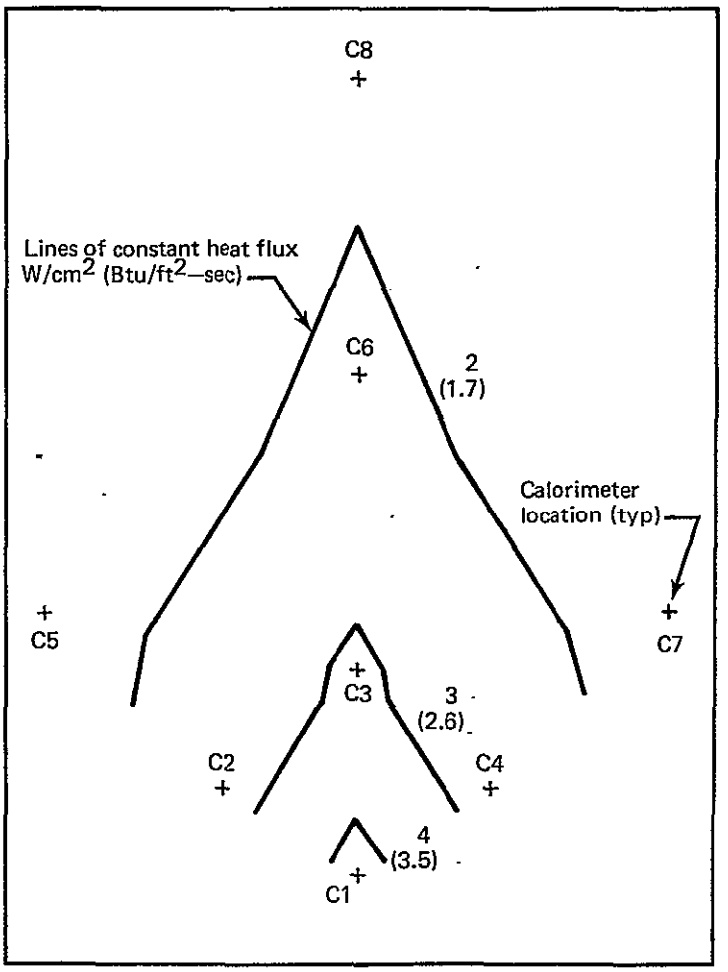

Figure 60.— Simulated Design In-flight Fire Calibration Panel Heat Flux Distribution—Stage I

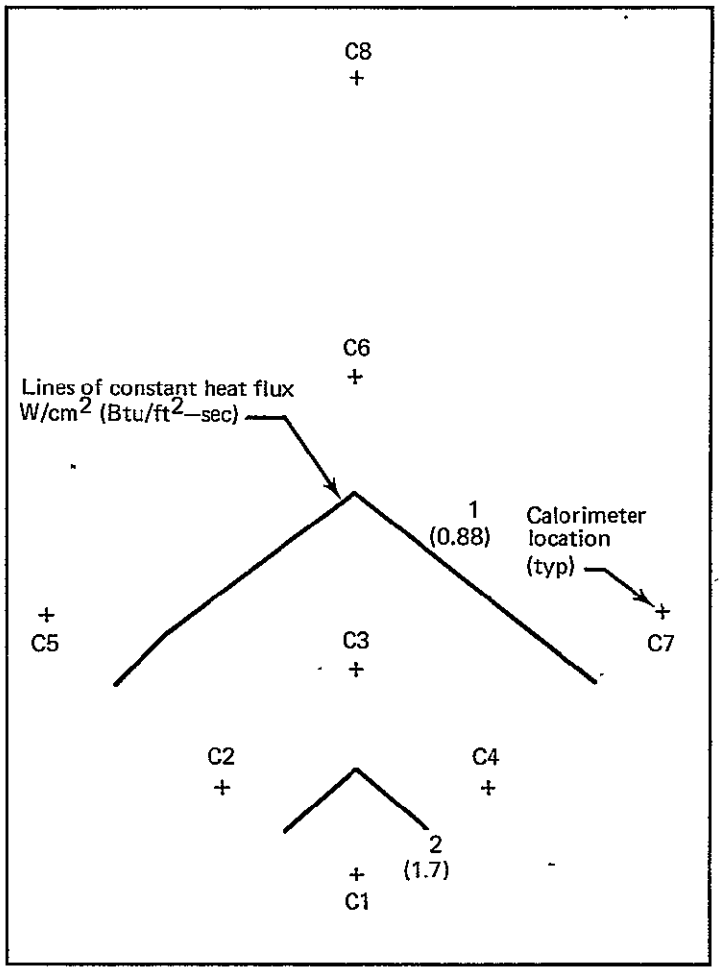

Figure 61.– Simulated Design In-flight Fire Calibration Panel Heat Flux Distribution–Stage II

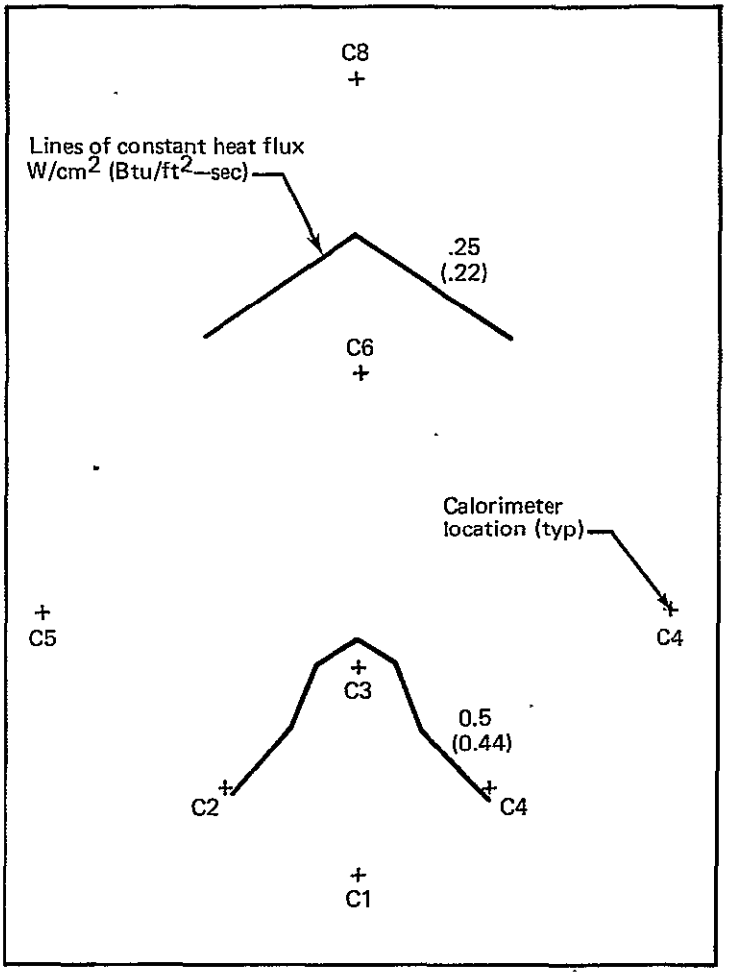

Figure 62.— Simulated Design In-flight Fire Calibration Panel Heat Flux Distribution—Stage III

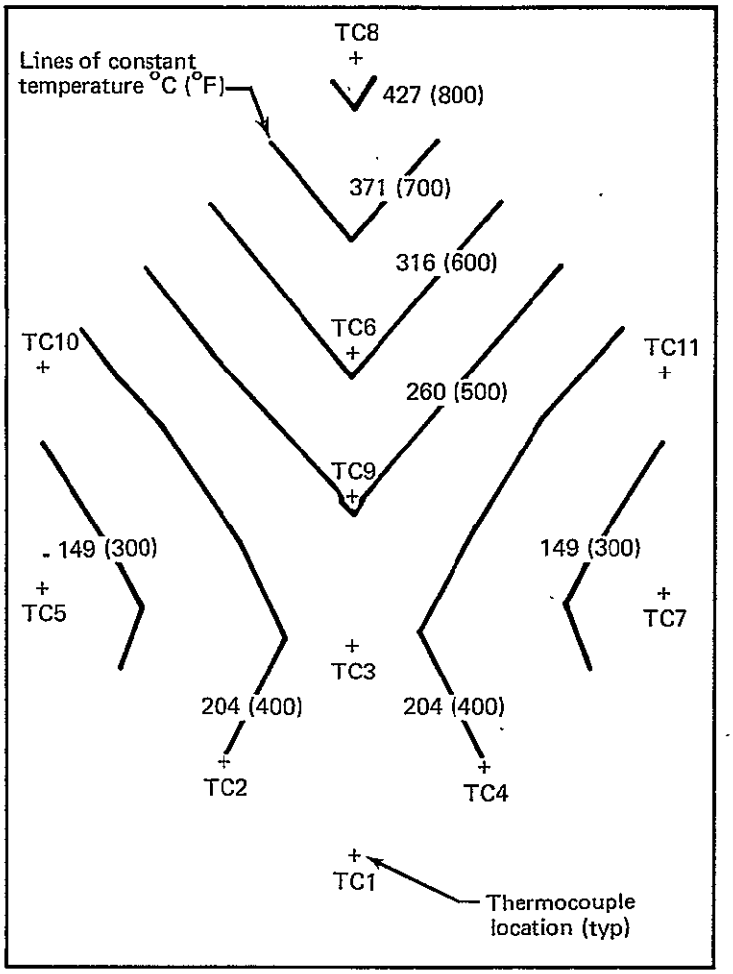

Figure 63.— Design In-flight Fire Calibration Panel Temperature Distribution—Stage I

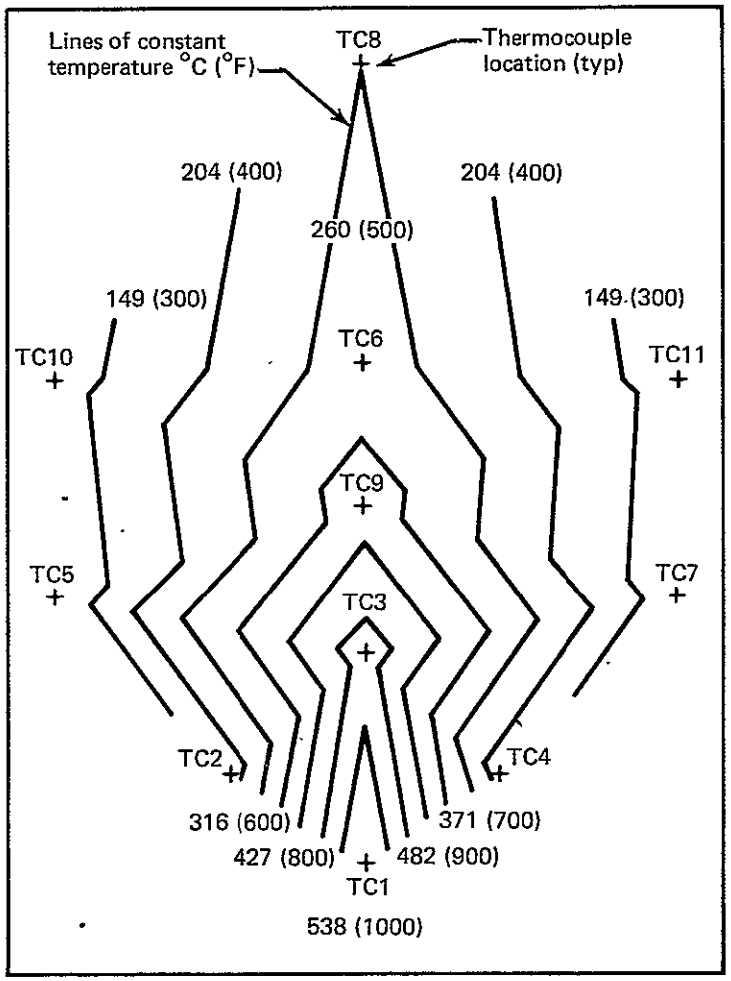

Figure 64.— Simulated Design In-flight Fire Calibration Panel Temperature Distribution—Stage I

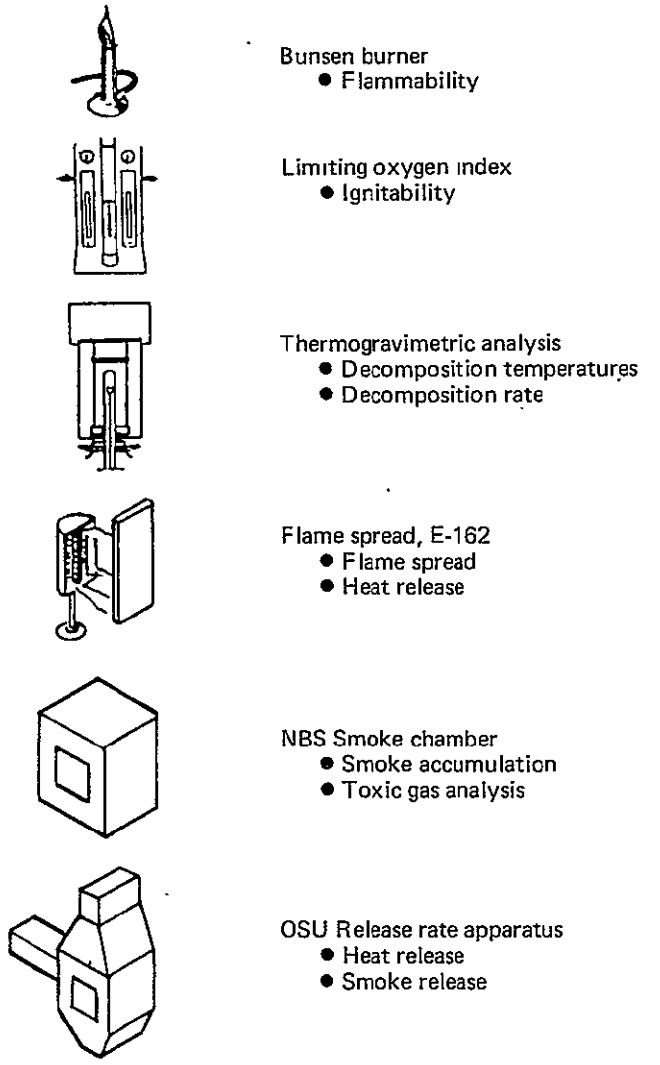

Figure 65.—Existing Laboratory Test Methods

Baseline material number①	Large scale heat release for 215 sec's Joules (Btu)	FAR 25.853 Bunsen burner —burn length— cm (in.) ②	ASTM E162-67 flame spread test		
			F_S	Q	I_S
N02/N03	4.54×10^6 (4300)	10.24 (4.03)	33.45	10.75	346.1
402/403	1.79×10^6 (1700)	9.91 (3.9)	24.86	1.88	49.62
412/413	4.85×10^6 (4600)	8.47 (3.3)	4.92	4.82	23.9
416/417	2.00×10^6 (1900)	11.85 (4.7)	9.39	3.02	28.10

① Large specimen no./laboratory specimen no. ② 60 second vertical ignition

Figure 66.—Evaluation by Laboratory Flammability Indices for Post-crash Condition

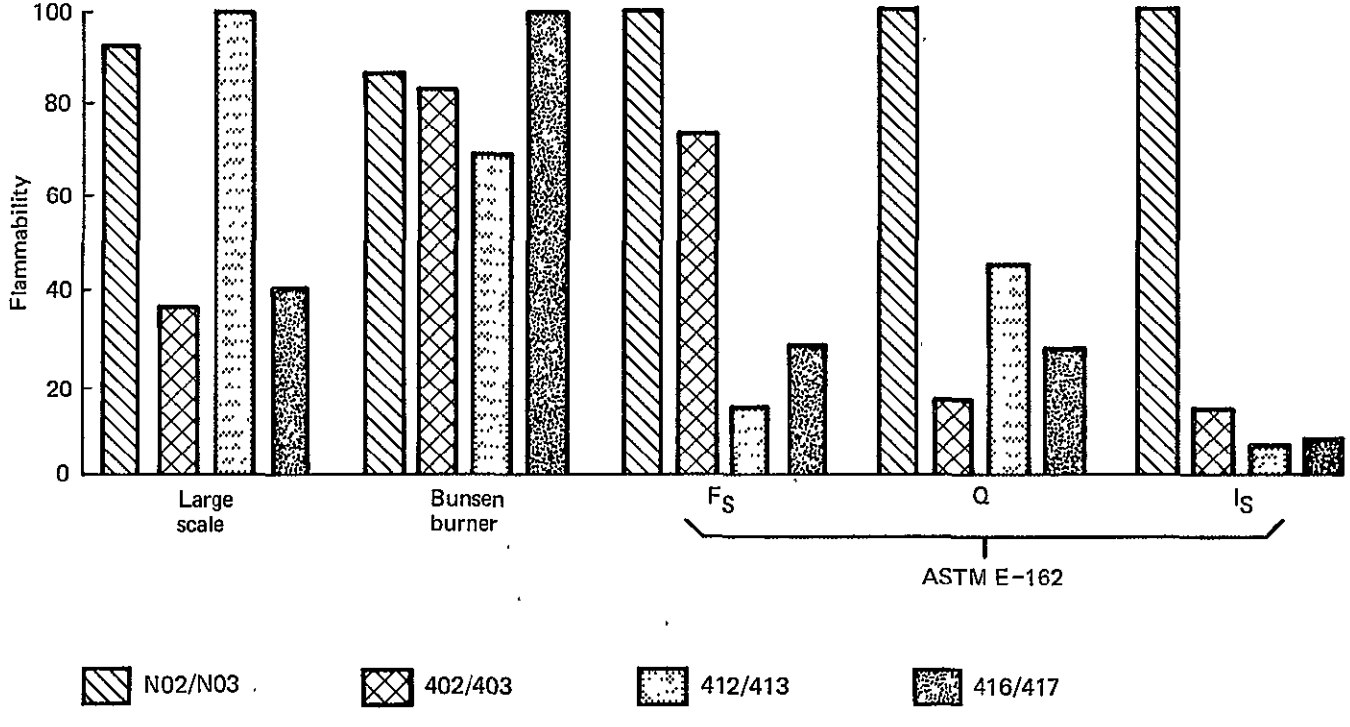

Figure 67.—Relative Flammability by Laboratory Indices for Post-crash Condition

Baseline material number ①	Large scale heat release for 215 sec Joules (Btu)	OSU ② release rate for 215 sec, J/cm^2 (Btu/ft^2)			
		1.5 (1.32) ③	2.5 (2.20)	3.5 (3.08)	5.0 (4.41)
N02/N03	4.54×10^6 (4300)	698 (615)	647 (570)	556 (490)	647 (570)
402/403	1.79×10^6 (1700)	74 (65)	250 (220)	409 (360)	698 (615)
412/413	4.85×10^6 (4600)	278 (245)	1055 (930)	1475 (1300)	1986 (1750)
416/417	2.00×10^6 (1900)	102 (90)	420 (370)	386 (340)	471 (415)

① Large specimen no./laboratory specimen no.

② Vertical, flaming, bottom-center ignition

③ W/cm^2 (Btu/ft^2-sec)

Figure 68.—Evaluation by OSU Heat Release for Post-crash Condition

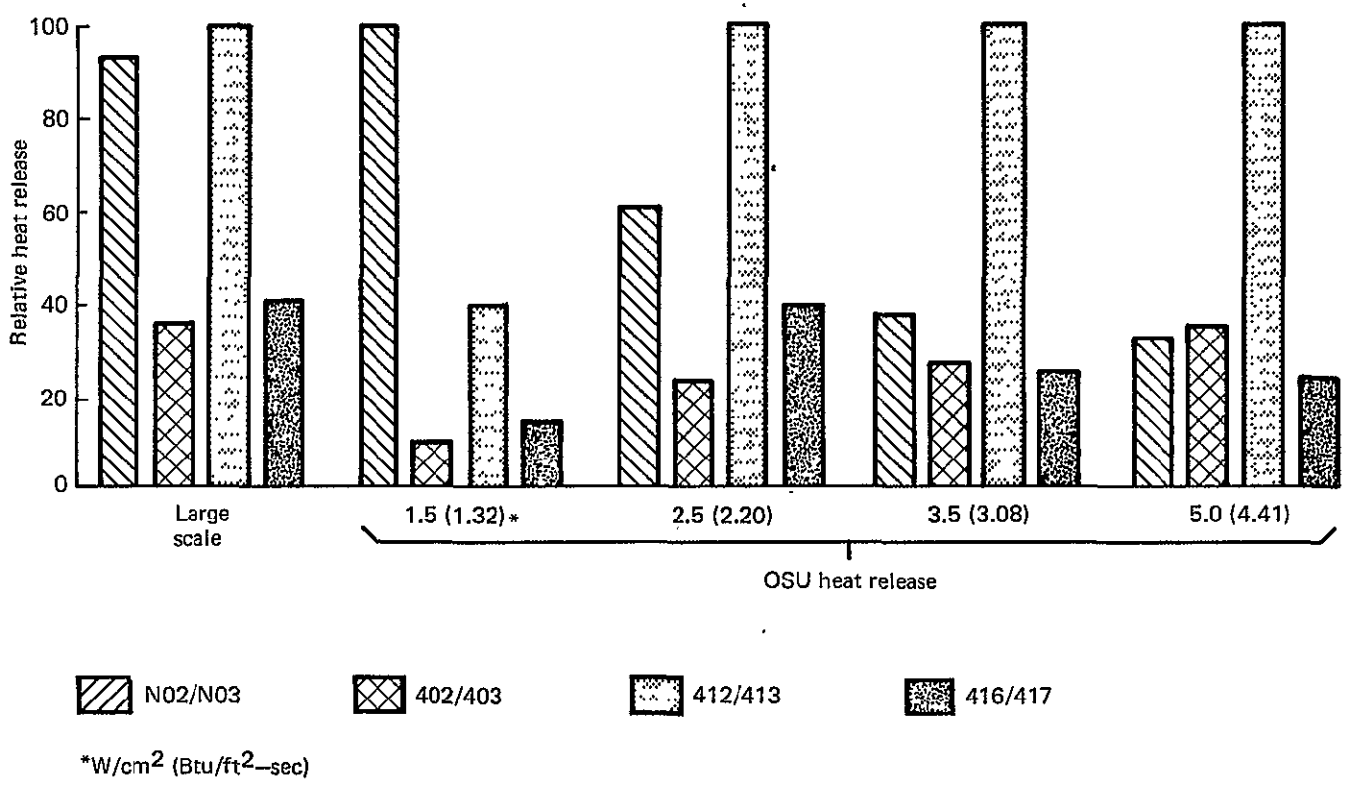

Figure 69.—Relative Heat Release by OSU Release Rate Apparatus for Post-crash Condition

Baseline material number①	Large scale smoke release for 90 seconds kilograms (pounds)	NBS smoke release for 90 sec, D_s②	
		at 2.5 (2.20)③	at 5.0 (4.41)③
N02/N03	1.50×10^{-1} (3.30×10^{-1})	300.0	350.0
402/403	1.14×10^{-1} (2.51×10^{-1})	75.0	105.0
412/413	8.30×10^{-2} (1.83×10^{-2})	0.0	210.0
416/417	7.71×10^{-2} (1.70×10^{-1})	3.0	15.0

① Large specimen no./laboratory specimen no.

② Flaming mode

③ W/cm^2 (Btu/ft^2-sec)

Figure 70.—Evaluation by NBS Smoke Chamber for Post-crash Condition

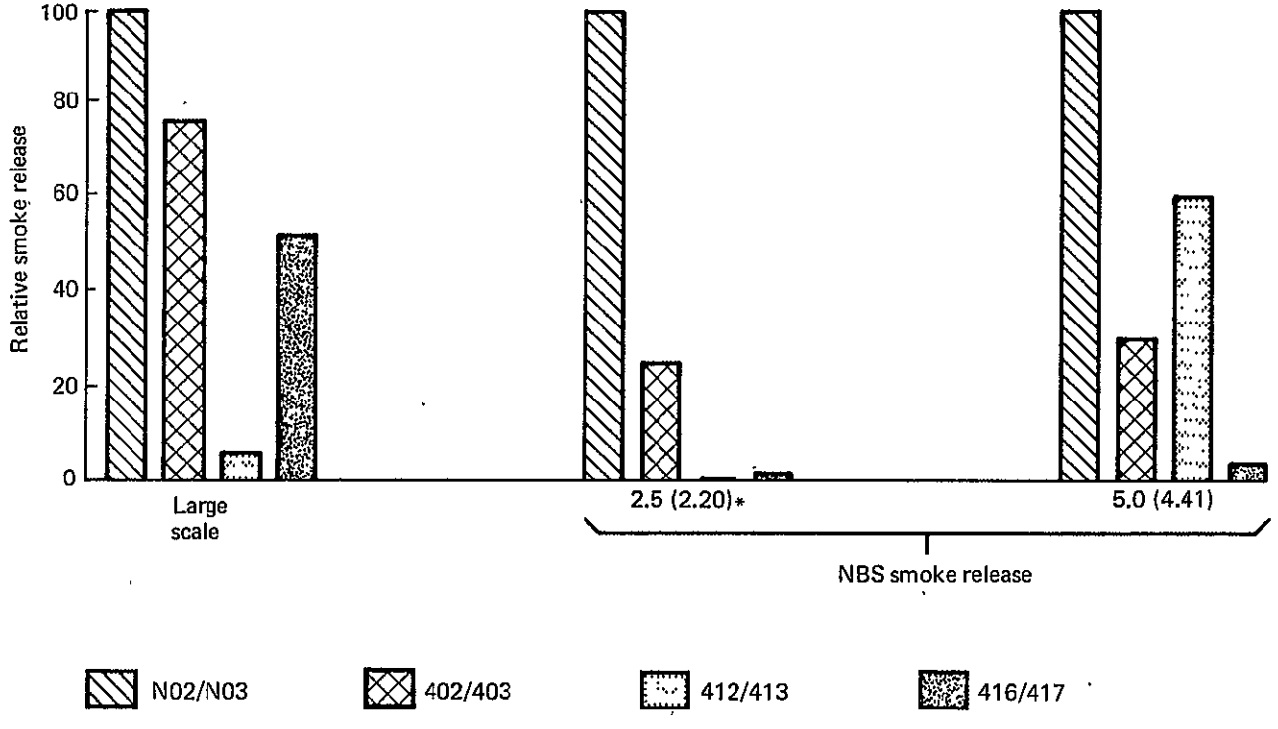

Figure 71.—Relative Smoke Release by NBS Chamber for Post-crash Conditions

Baseline material number①	Large scale smoke release for 90 seconds kilograms (pounds)	OSU smoke release for 90 seconds, D_s②			
		at 1.5 (1.32)③	at 2.5 (2.20)③	at 3.5 (3.08)③	at 5.0 (4.41)③
N02/N03	1.50×10^{-1} (3.31×10^{-1})	100.0	212.0	270.0	310.0
402/403	1.14×10^{-1} (2.51×10^{-1})	7.0	79.0	88.0	82.0
412/413	8.30×10^{-2} (1.83×10^{-1})	20.0	56.0	197.0	462.0
416/417	7.71×10^{-2} (1.70×10^{-1})	7.0	38.0	70.0	90.0

① Large specimen no./laboratory specimen no.

② Vertical, flaming, bottom-center ignition

③ W/cm^2 (Btu/ft^2-sec)

Figure 72.—Evaluation by OSU Smoke Release for Post-crash Condition

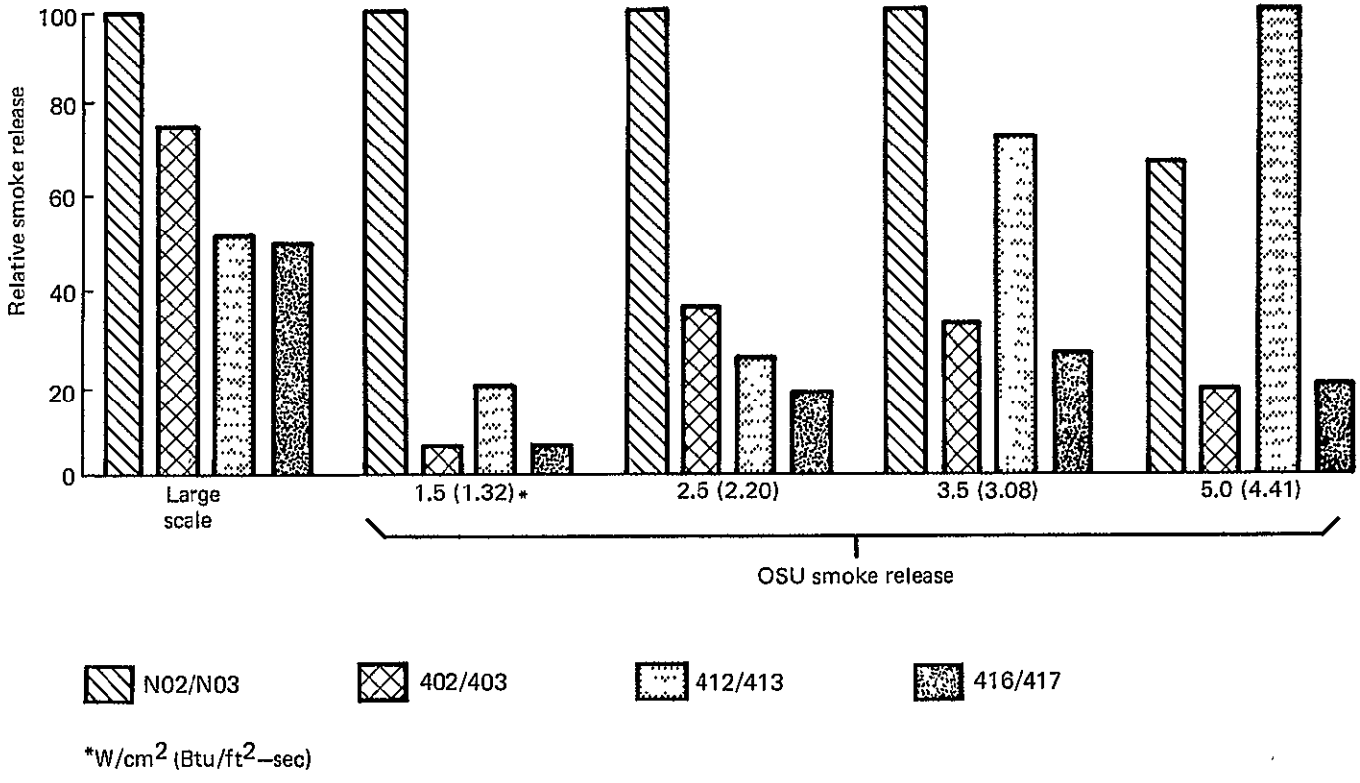

Figure 73.— Relative Smoke Release by OSU Release Rate Apparatus for Post-crash Condition

Baseline material number	Large scale toxic gas released at 300 sec—grams (10^{-2} lb)①				NBS chamber toxic gas released at 300 sec, at 2.5 and 5 W/cm^2—grams (10^{-2} lb)② ③			
	HF	HCL	HCN	CO	HF③	HCL③	HCN③	CO③
N02/N03	0 (0)	1.71 (0.376)	0.55 (0.121)	116.92 (25.777)				
at 2.5 W/cm^2					0	1.91 (0.421)	0	0.04 (0.008)
at 5.0 W/cm^2					0	0.73 (0.162)	0	0.44 (0.098)
402/403	18.77 (4.138)	63.07 (13.904)	0.41 (0.090)	24.39 (5.377)				
at 2.5 W/cm^2					0.027 (0.006)	0.044 (0.010)	0.0009 (0.0002)	0.156 (0.034)
at 5.0 W/cm^2					0.059 (0.013)	0.033 (0.007)	0.003 (0.0006)	0.209 (0.046)
412/413	0 (0)	0.86 (0.190)	0.38 (0.084)	58.93 (12.991)				
at 2.5 W/cm^2					0	0.031 (0.007)	0	0.158 (0.035)
at 5.0 W/cm^2					0	0.701 (0.154)	0	0.452 (0.0996)
416/417	5.94 (1.310)	45.99 (10.140)	0 (0)	30.00 (6.614)				
at 2.5 W/cm^2					0.010 (0.002)	0.253 (0.056)	0	0.058 (0.013)
at 5.0 W/cm^2					0.022 (0.005)	0.486 (0 107)	0	0.038 (0.008)

① Large scale volume = 39.64 M^3 (1400 ft^3)

② NBS chamber volume = 0.509 M^3 (18 ft^3)

③ Totals calculated at a constant temp. (35°C (95°F)) for the entire test

Figure 74.—Evaluation by NBS Chamber Toxicant Release for Post-crash Condition

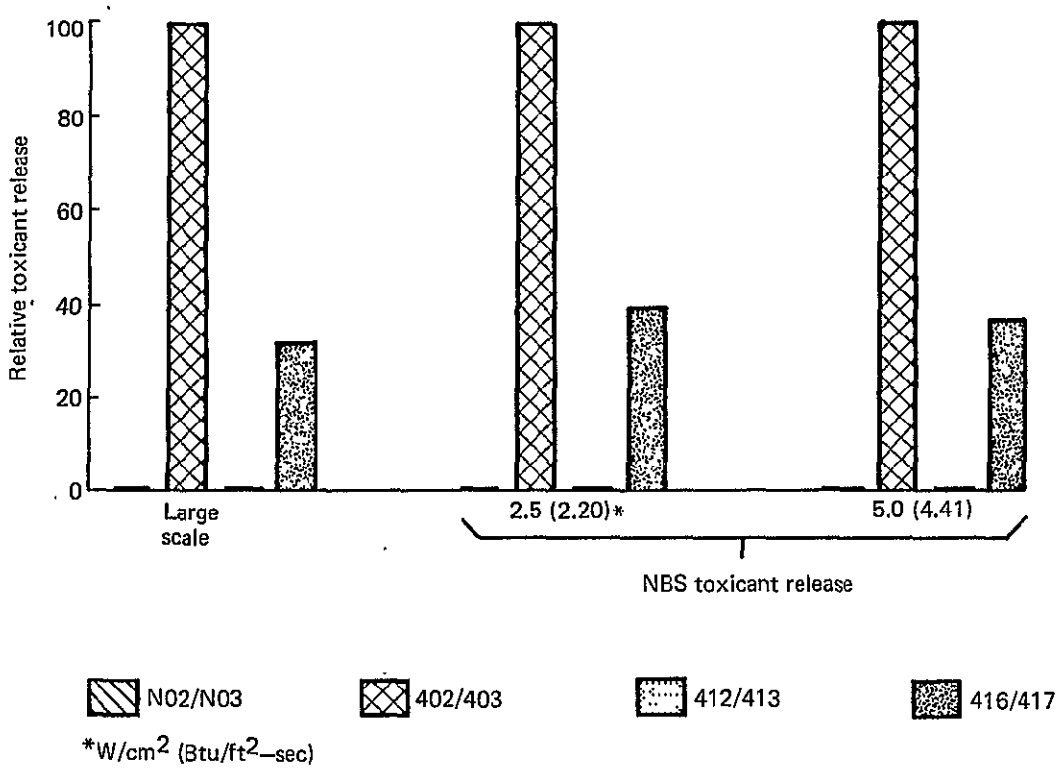

Figure 75.—Relative Toxicant Release by NBS Chamber for Post-crash Condition, Hydrogen Fluoride (HF)

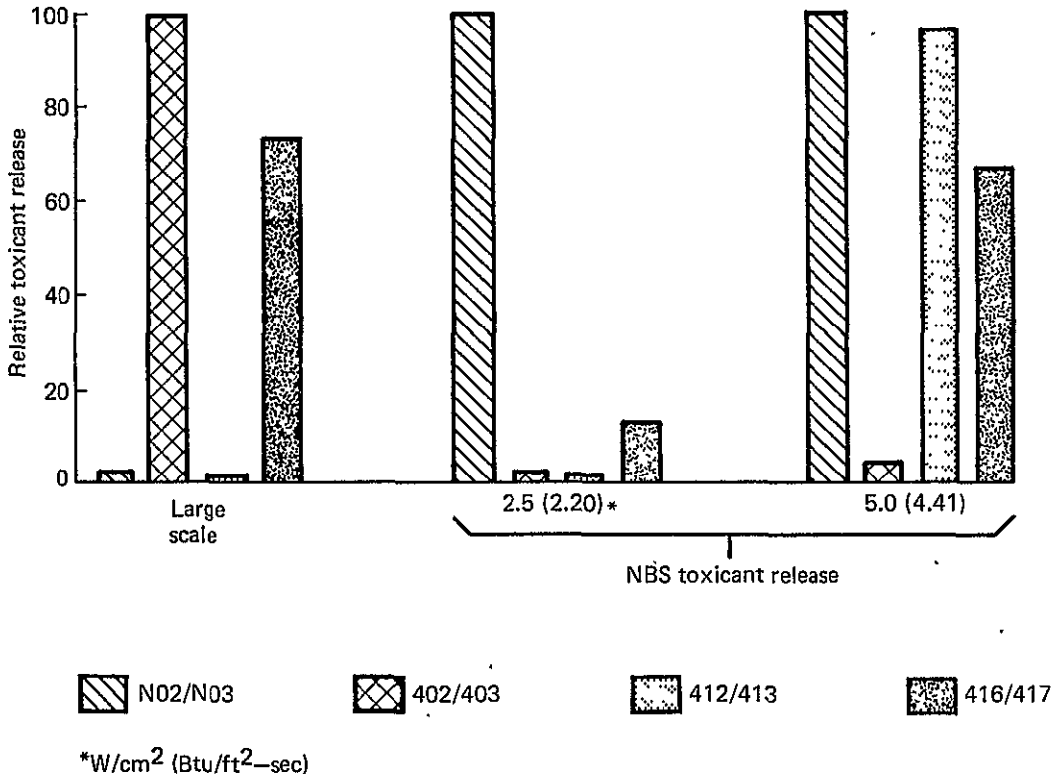

Figure 76.—Relative Toxicant Release by NBS Chamber for Post-crash Condition, Hydrogen Chloride (HCL)

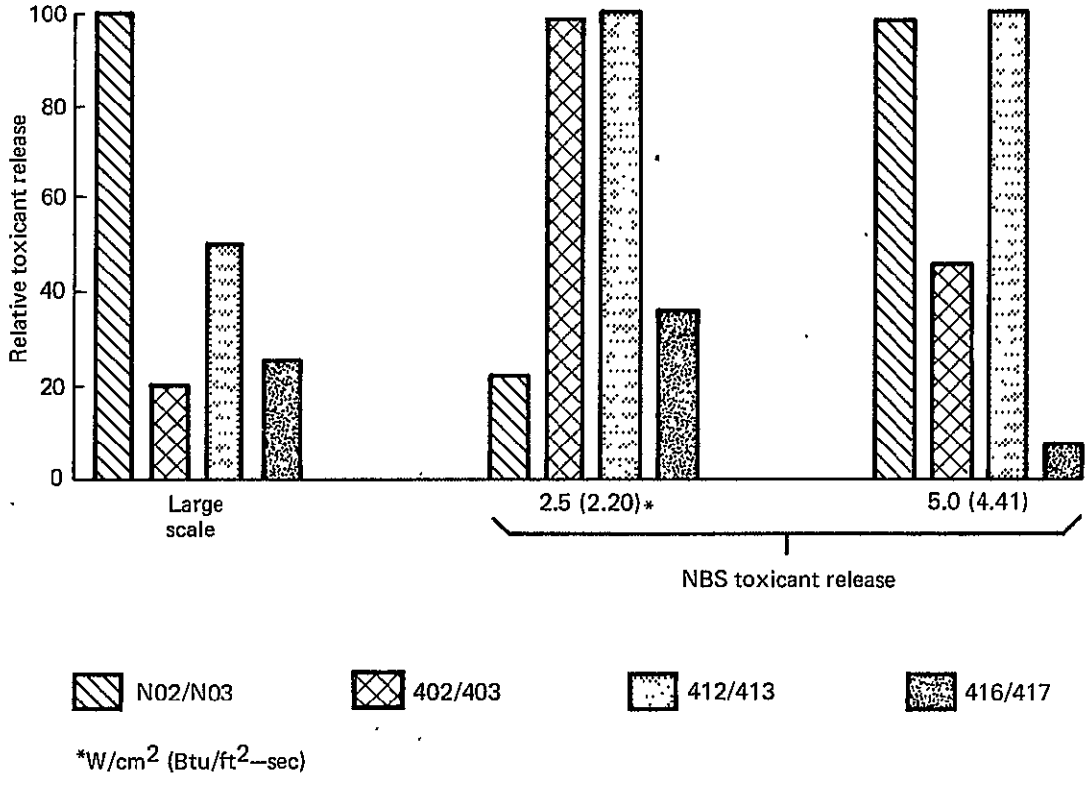

Figure 77.—Relative Toxicant Release by NBS Chamber for Post-crash Condition, Carbon Monoxide (CO)

Baseline material number①	Large scale heat release for 300 seconds Joules (Btu)	OSU② heat release for 300 seconds, J/cm^2 (Btu/ft^2)			
		at 1.5 (1.32)③	at 2.5 (2.20)③	at 3.5 (3.08)③	at 5.0 (4.41)③
NO2/NO3	5.75 x 10^6 (5450)	620 (547)	568 (501)	495 (437)	575 (507)
402/403	1.74 x 10^6 (1650)	88 (78)	248 (219)	420 (370)	765 (675)
412/413	9.28 x 10^5 (880)	432 (381)	1600 (1411)	1968 (1736)	2515 (2218)
416/417	2.11 x 10^6 (2000)	110 (97)	442 (390)	400 (358)	515 (454)

① Large specimen no./laboratory specimen no.

② Vertical, flaming, bottom-center ignition

③ W/cm^2 (Btu/ft^2-sec)

Figure 78.—Evaluation by OSU Heat Release for In-flight Condition

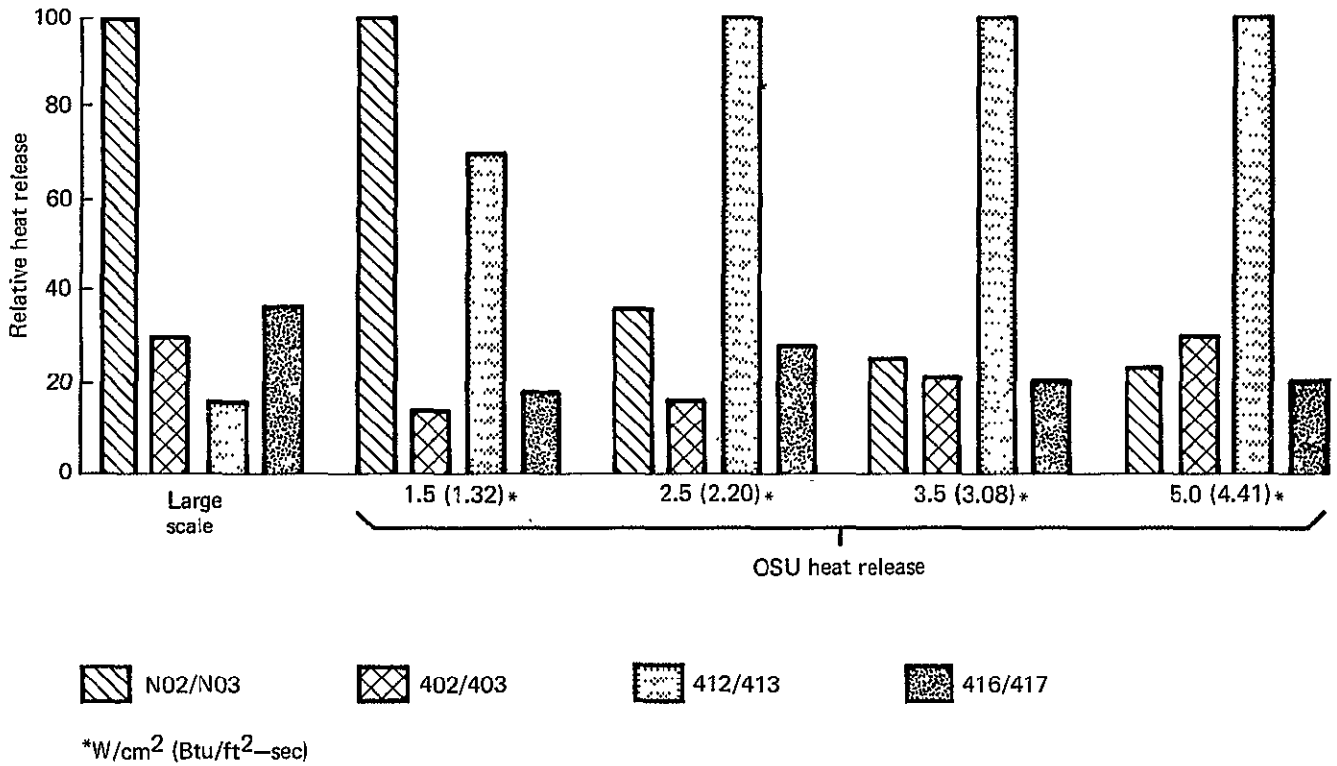

Figure 79.—Relative Heat Release by OSU Release Rate Apparatus for In-flight Condition

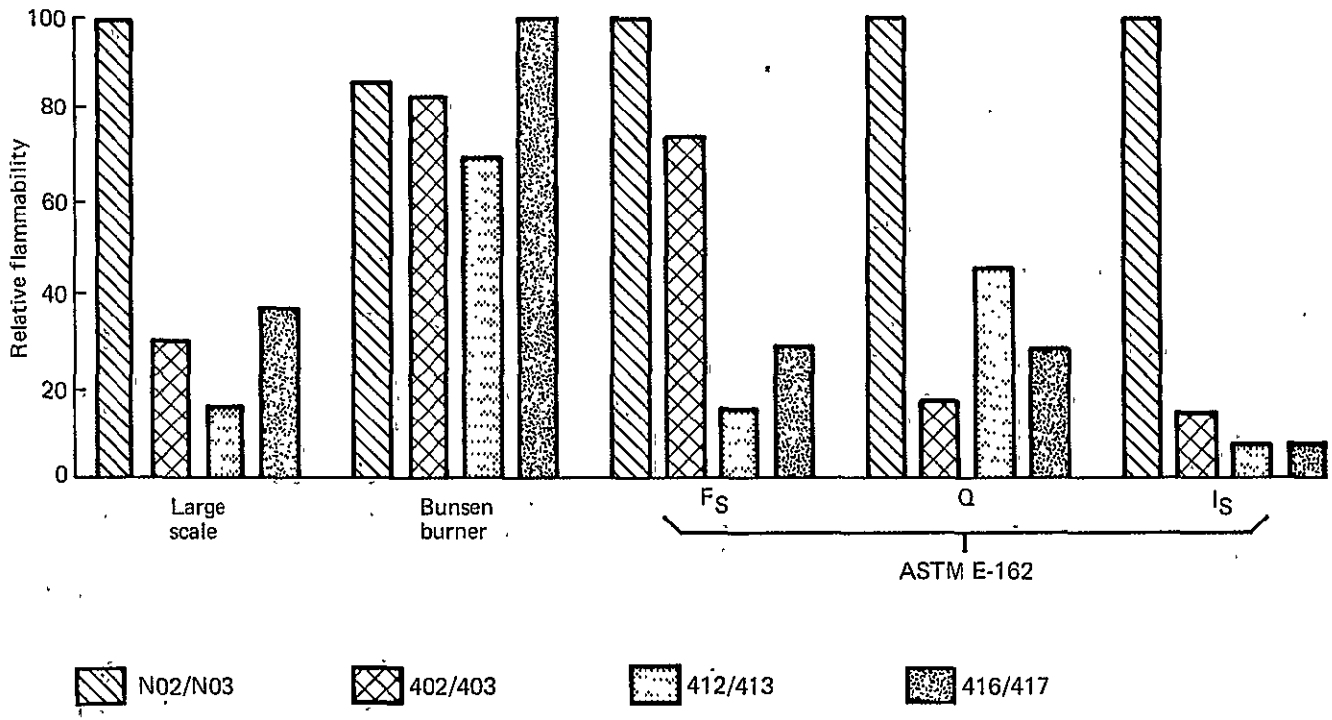

Figure 80.—Relative Flammability by Laboratory Indices for In-flight Condition

Baseline material number②	Large scale smoke release for 300 seconds kilograms (pounds)	OSU② smoke release for 300 seconds, D_s			
		at 1.5 (1.32)③	at 2.5 (2.20)③	at 3.5 (3.08)③	at 5.0 (4.41)③
N02/N03	1.75×10^{-1} (3.85×10^{-1})	122.0	215.0	270.0	310.0
402/403	6.67×10^{-2} (1.47×10^{-1})	7.0	70.0	85.0	90.0
412/413	1.46×10^{-2} (3.23×10^{-2})	168.0	576.0	1025.0	1450.0
416/417	8.62×10^{-2} (1.90×10^{-1})	10.0	40.0	70.0	90.0

① Large specimen no./laboratory specimen no.

② Vertical, flaming, bottom-center position

③ W/cm^2 (Btu/ft^2-sec)

Figure 81.—Evaluation by OSU Smoke Release for In-flight Condition

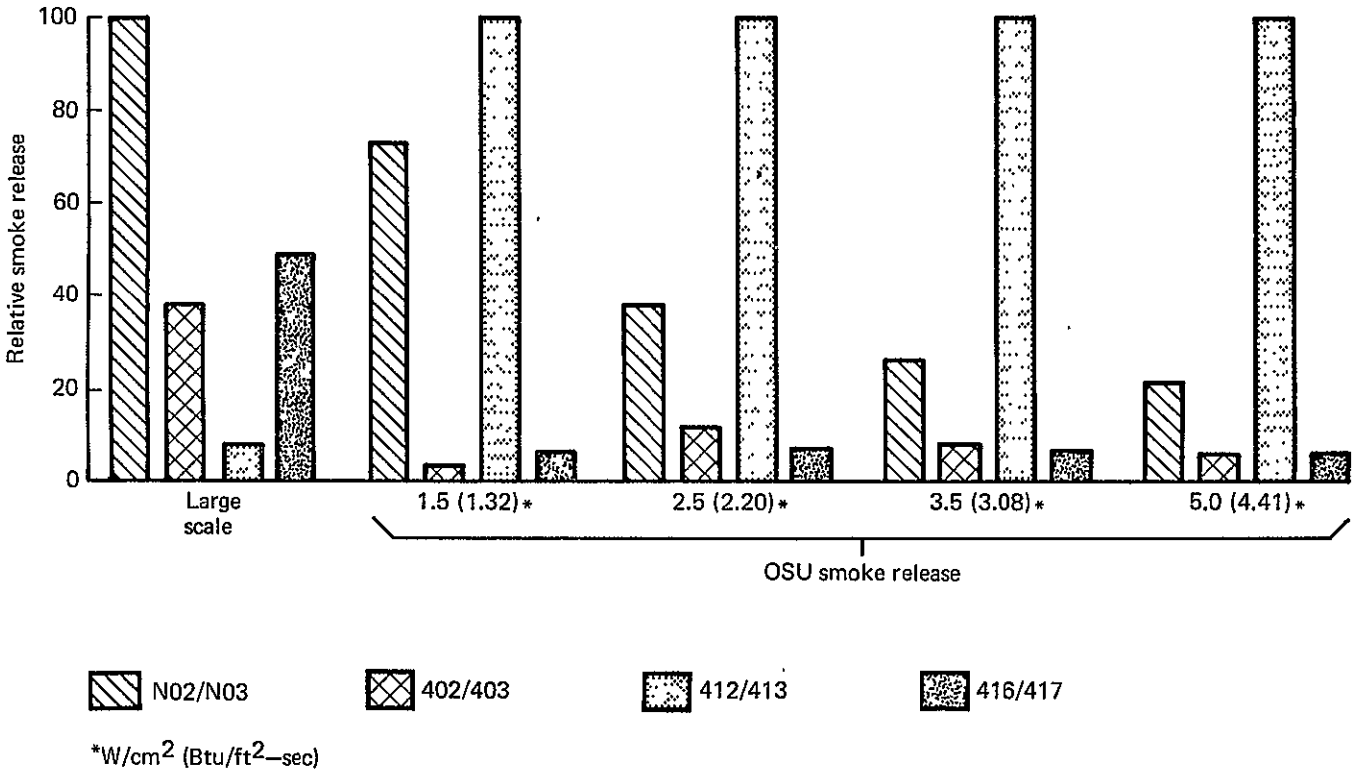

Figure 82.—Relative Smoke Release by OSU Release Rate Apparatus for In-flight Conditions

Baseline material number ①	Large scale smoke release for 300 seconds kilograms (pounds)	NBS smoke release for 300 seconds, D_s ②	
		at 2.5 (2.20) ③	at 5.0 (4.41) ③
N02/N03	1.75×10^{-1} (3.85×10^{-1})	480.0	350.0
402/403	6.67×10^{-2} (1.47×10^{-1})	70.0	110.0
412/413	1.46×10^{-2} (3.23×10^{-2})	315.0	640.0
416/417	8.62×10^{-2} (1.80×10^{-1})	110.0	140.0

① Large specimen no./labatory specimen no.

② Flaming mode

③ $W/cm^2/(Btu/ft^2\text{-sec})$

Figure 83.—Evaluation by NBS Smoke Chamber for In-flight Condition

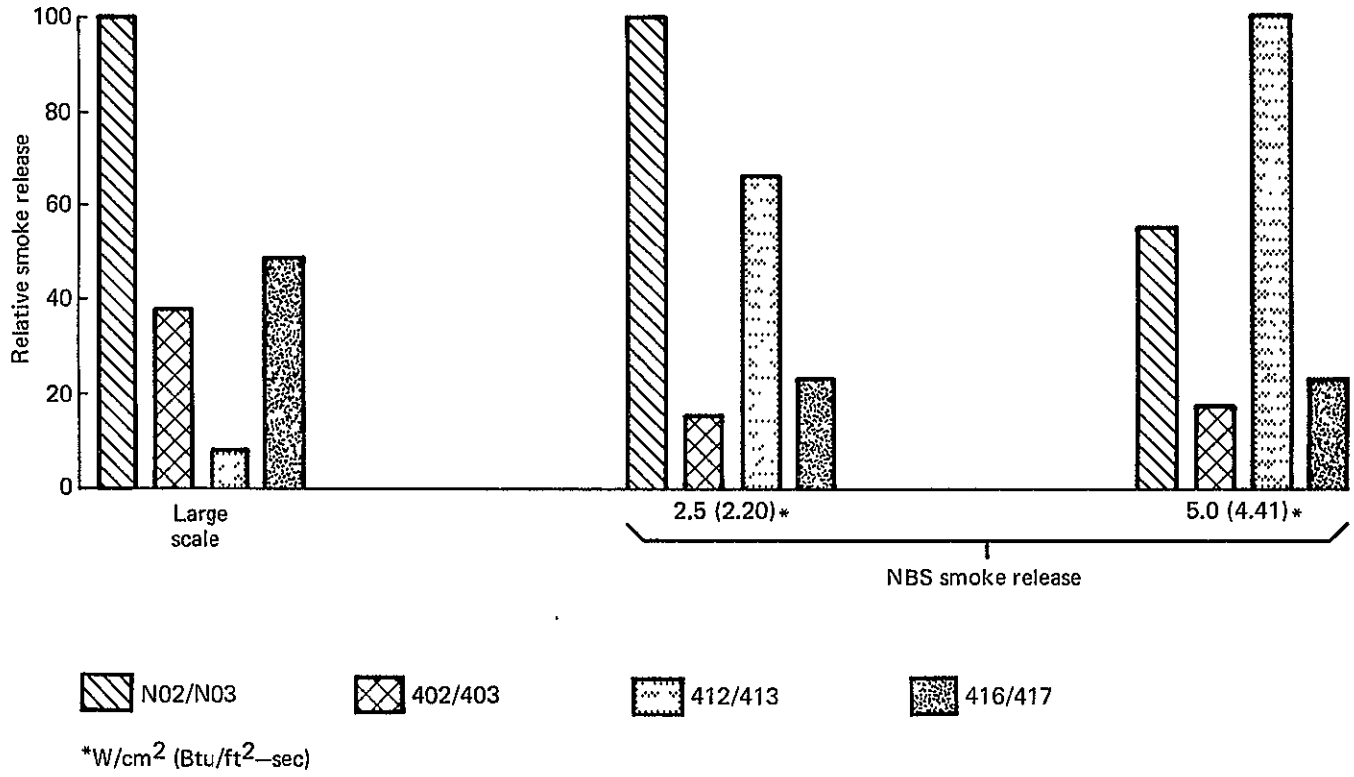

Figure 84.—Relative Smoke Release by NBS Smoke Chamber for In-flight Conditions

Baseline material number	Large scale toxic gas released at 300 sec, grams (10^{-2} lb) ①				NBS chamber toxic gas released at 300 sec, at 2.5 and 5 W/cm^2, grams (10^{-2} lb) ② ③			
	HF	HCL	HCN	CO	HF ③	HCL ③	HCN ③	CO ③
N02/N03	0 (0)	56.97 (12.559)	0.327 (0.072)	66.93 14.754				
at 2.5 W/cm^2					0	1.91 (0.421)	0	0.04 (0.008)
at 5.0 W/cm^2					0	0.73 (0.162)	0	0.44 (0.098)
402/403	11.922 (2.628)	17.776 (3.919)	Not tested for	28.789 (6.347)				
at 2.5 W/cm^2					0.027 (0.006)	0.044 (0.0098)	0.0009 (0.0002)	0.156 (0.035)
at 5.0 W/cm^2					0.059 (0.013)	0.033 (0.007)	0.003 (0.0006)	0.209 (0.046)
412/413	0 (0)	0 (0)	0 (0)	1.928 (0.425)				
at 2.5 W/cm^2					0	0.031 (0.007)	0	0.158 (0.035)
at 5.0 W/cm^2					0	0.701 (0.154)	0	0.452 (0.0996)
416/417	1.143 (0.252)	20.275 (4.4699)	0 (0)	32.663 (7.201)				
at 2.5 W/cm^2					0.010 (0.002)	0.253 (0.056)	0	0.058 (0.013)
at 5.0 W/cm^2					0.022 (0.005)	0.486 (0.107)	0	0.038 (0.008)

① Large scale volume = 39.64 M^3 (1400 ft^3)

② NBS chamber volume = 0.509 M^3 (18 ft^3)

③ Totals calculated at a constant temp. (35°C (95°F)) for entire test

Figure 85.—Evaluation by NBS Chamber, Toxicant Release for In-flight Condition

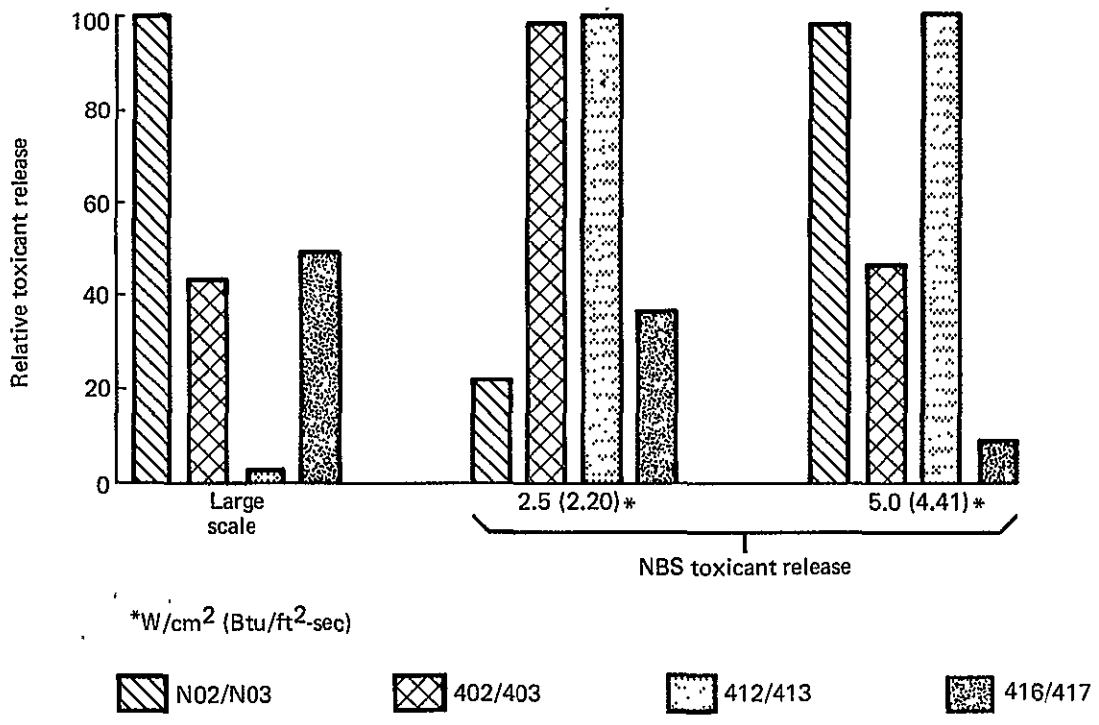

Figure 86.—Relative Toxicant Release by NBS Chamber for In-flight Condition, Carbon Monoxide (CO)

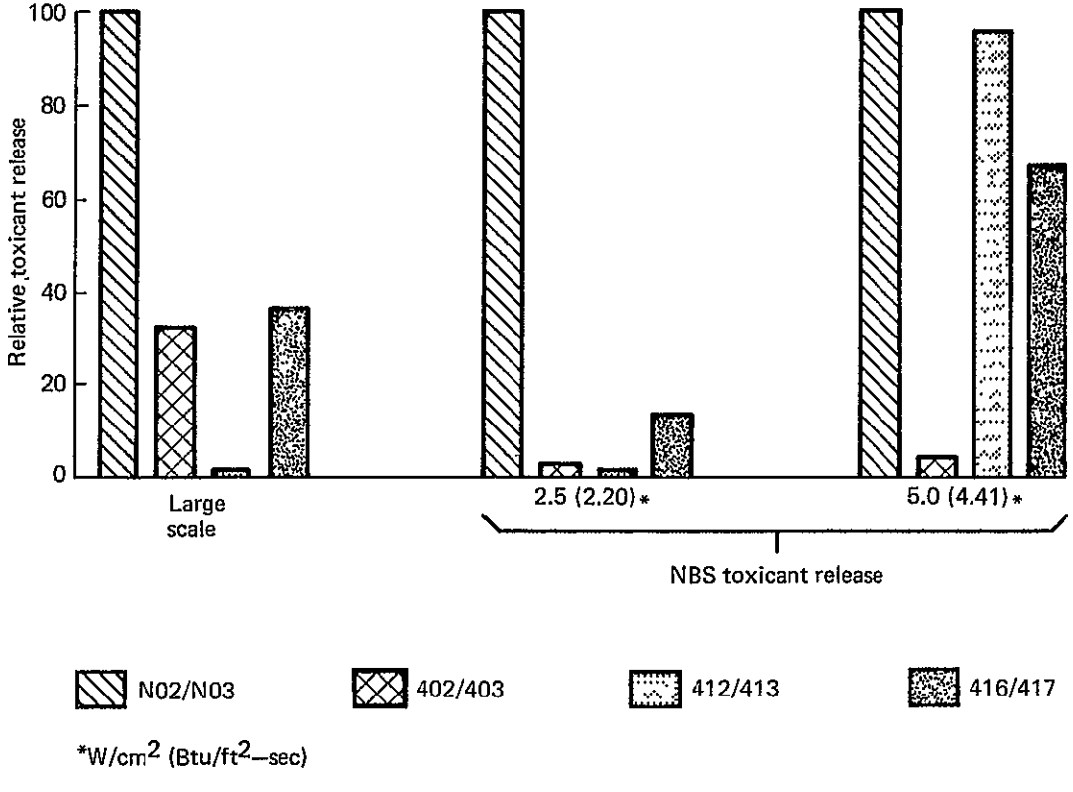

Figure 87.—Relative Toxicant Release by NBS Chamber for In-flight Condition, Hydrogen Chloride (HCL)

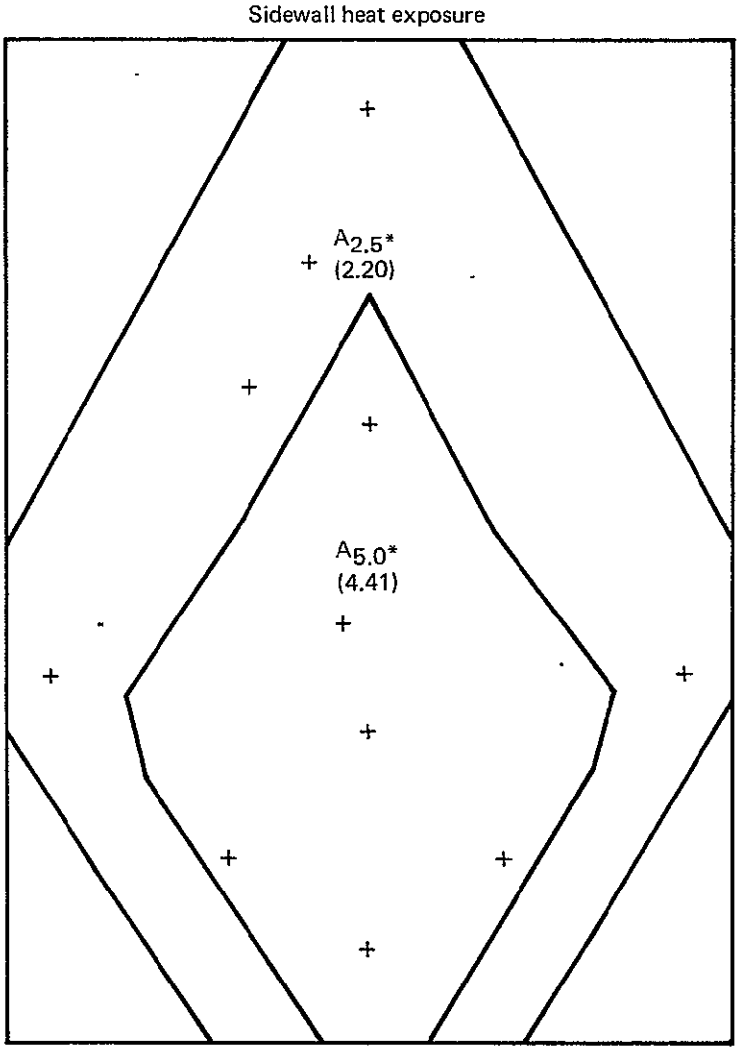

Correlation to OSU data

Total release = $A_{2.5}$ ($OSU_{2.5}$)
+ $A_{5.0}$ ($OSU_{5.0}$)

OSU - Release at subnoted heating rate in OSU apparatus

$A_{2.5}$ (2.20) * = 8289 (8.92) **
$A_{5.0}$ (4.41) = 5587 (6 01)

* W/cm^2 (Btu/ft^2-sec)
** cm^2 (ft^2)

Figure 89.— Correlation Assuming Two Heating Rates for Post-crash Condition

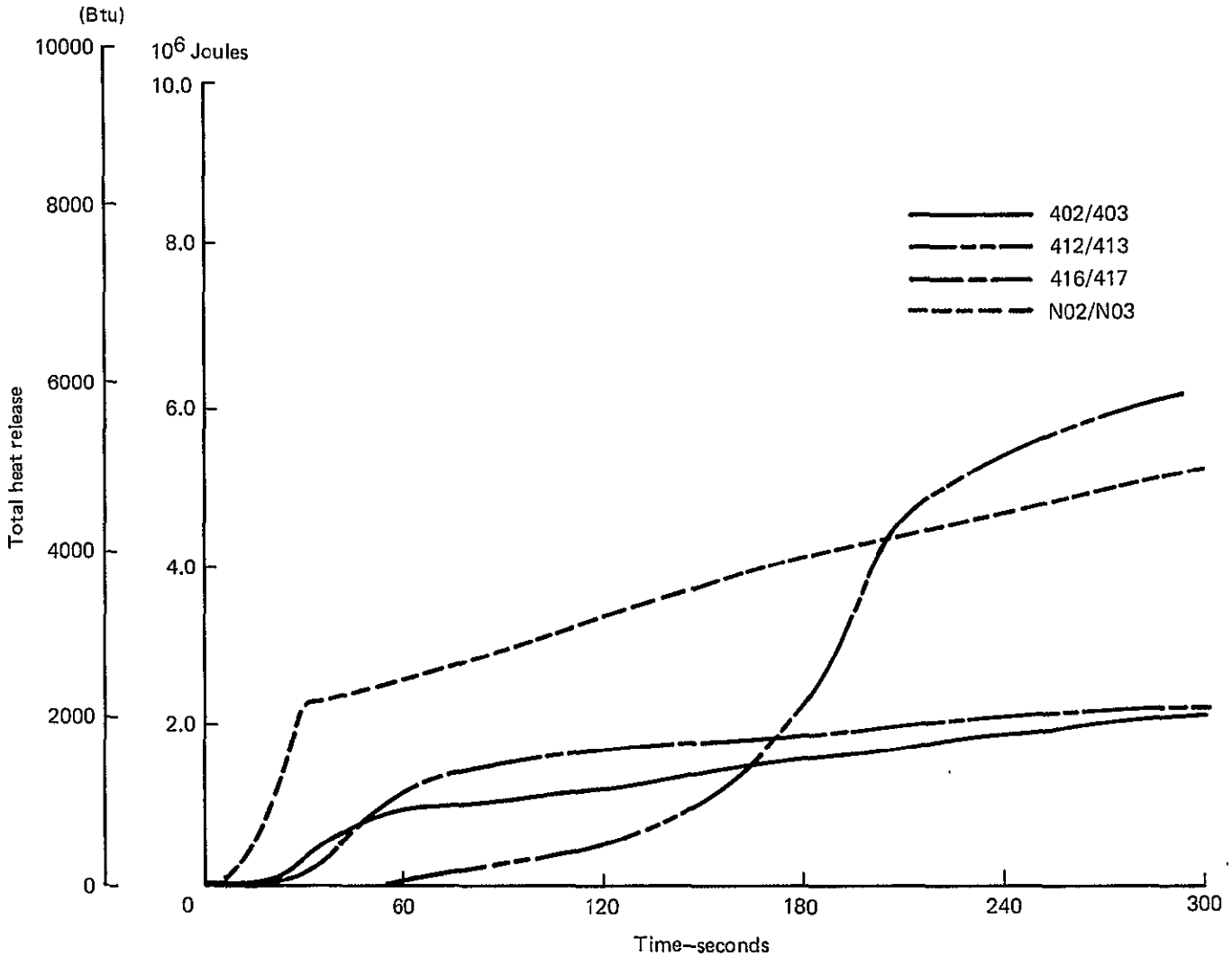

Figure 90.— Heat Release from Simulated Post-crash Fire Source Tests

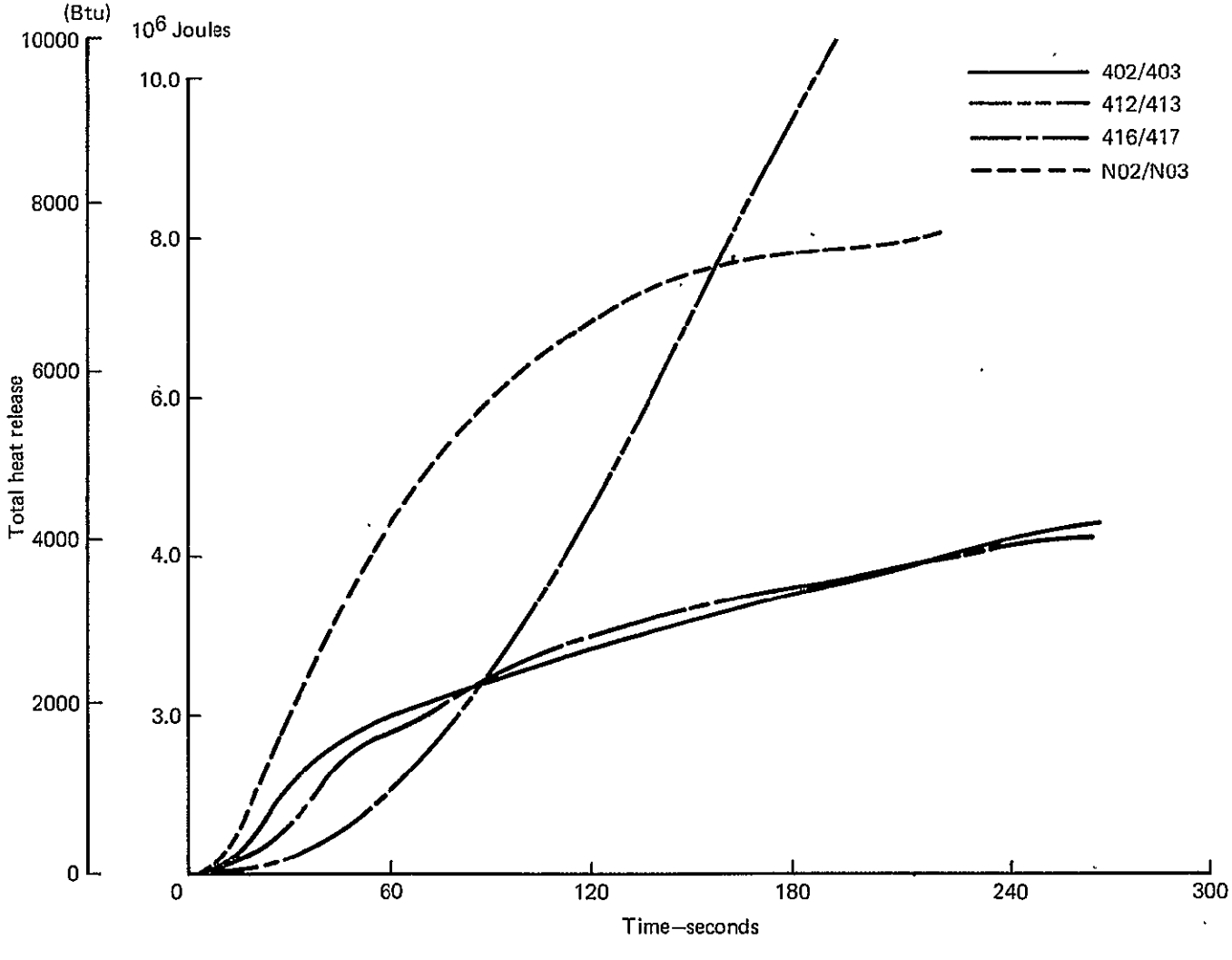

Figure 91.— Heat Release from Area Summation of OSU Data (Four Heating Rates) for Post-crash Fire Conditions

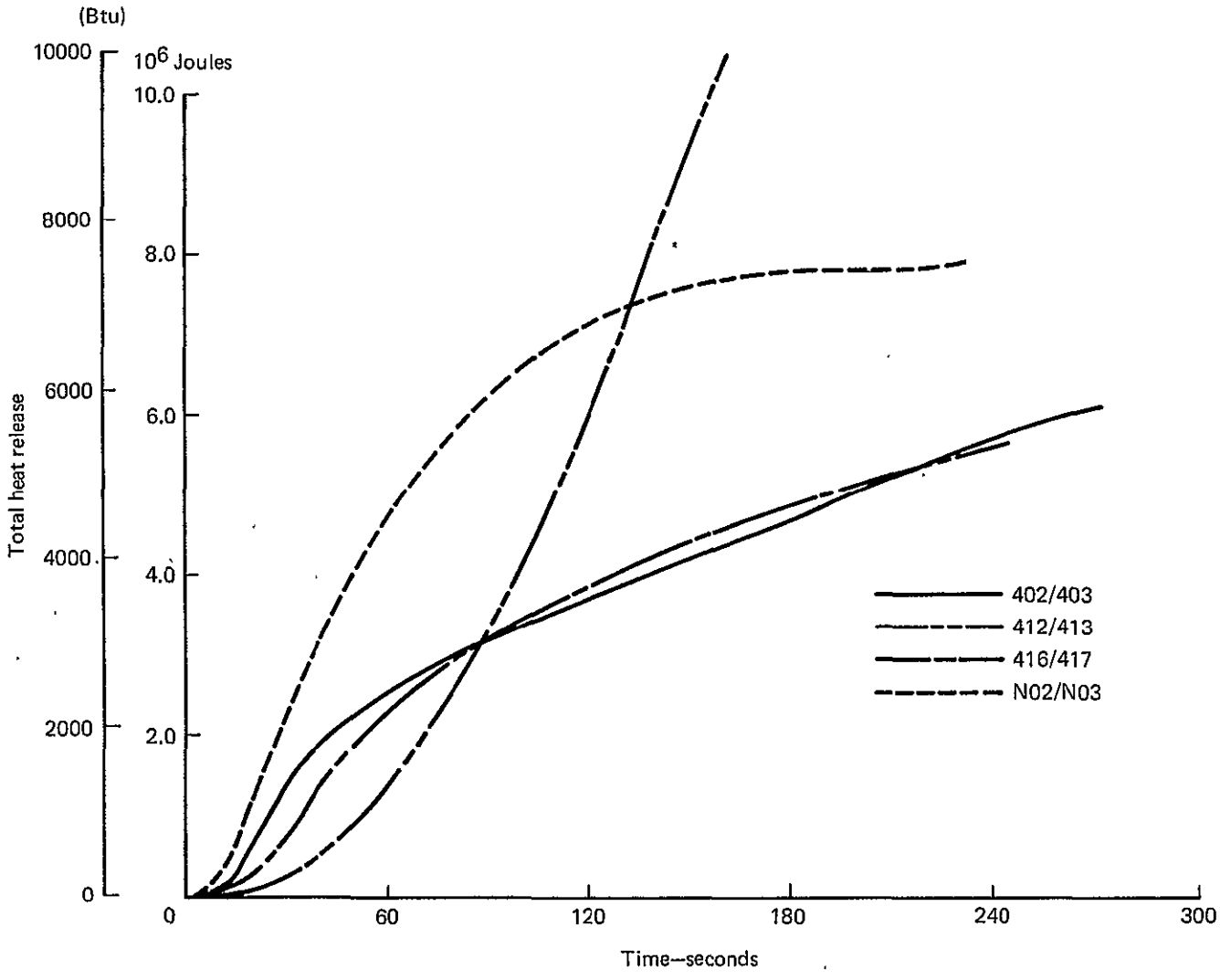

Figure 92.— Heat Release from Area Summation of OSU Data (Two Heating Rates) for Post-crash Fire Condition

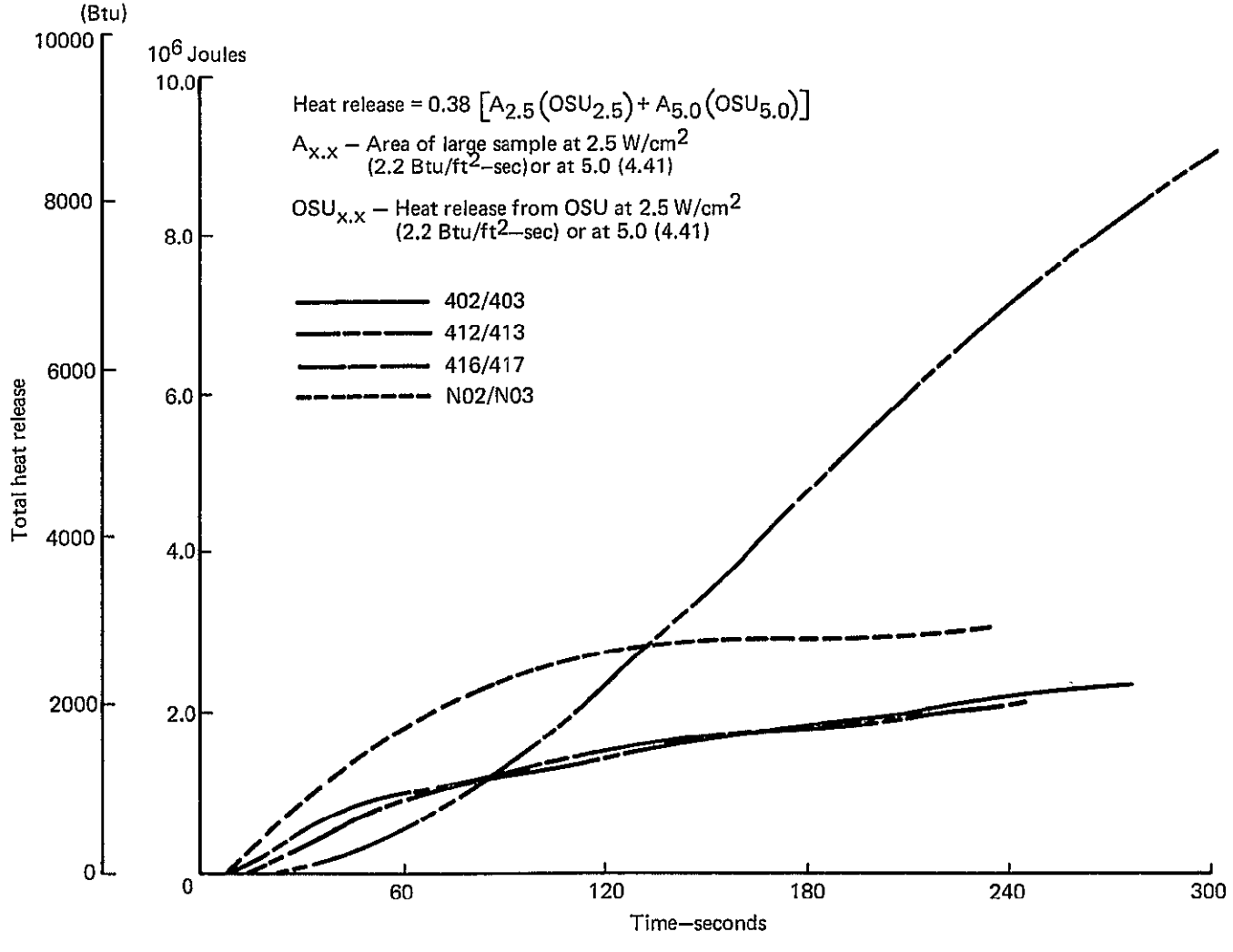

Figure 93.—Heat Release from Proportional Area Summation of OSU Data (Two Heating Rates) for Post-crash Fire Conditions

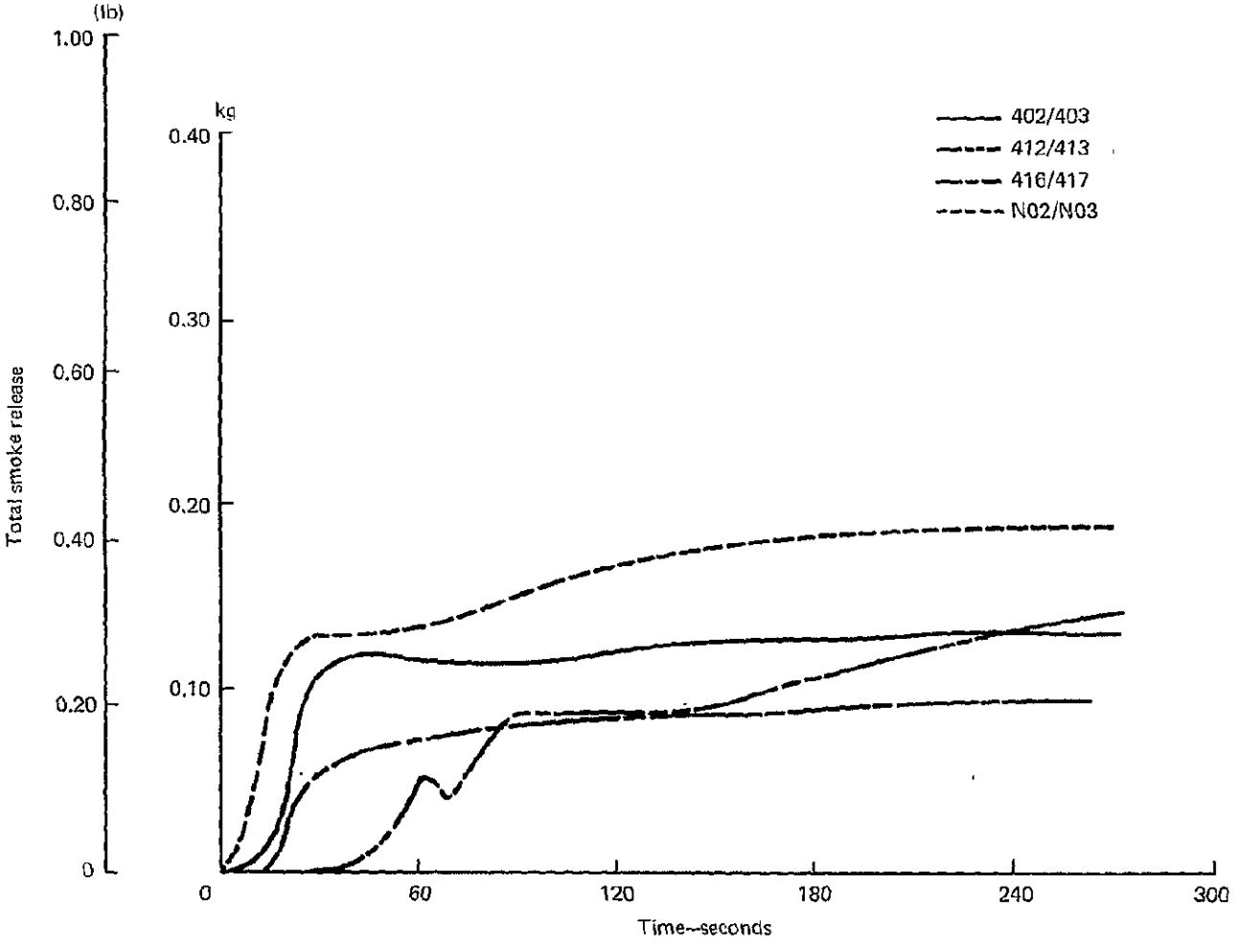

Figure 94.— Smoke Release from Simulated Post-crash Fire Source Tests

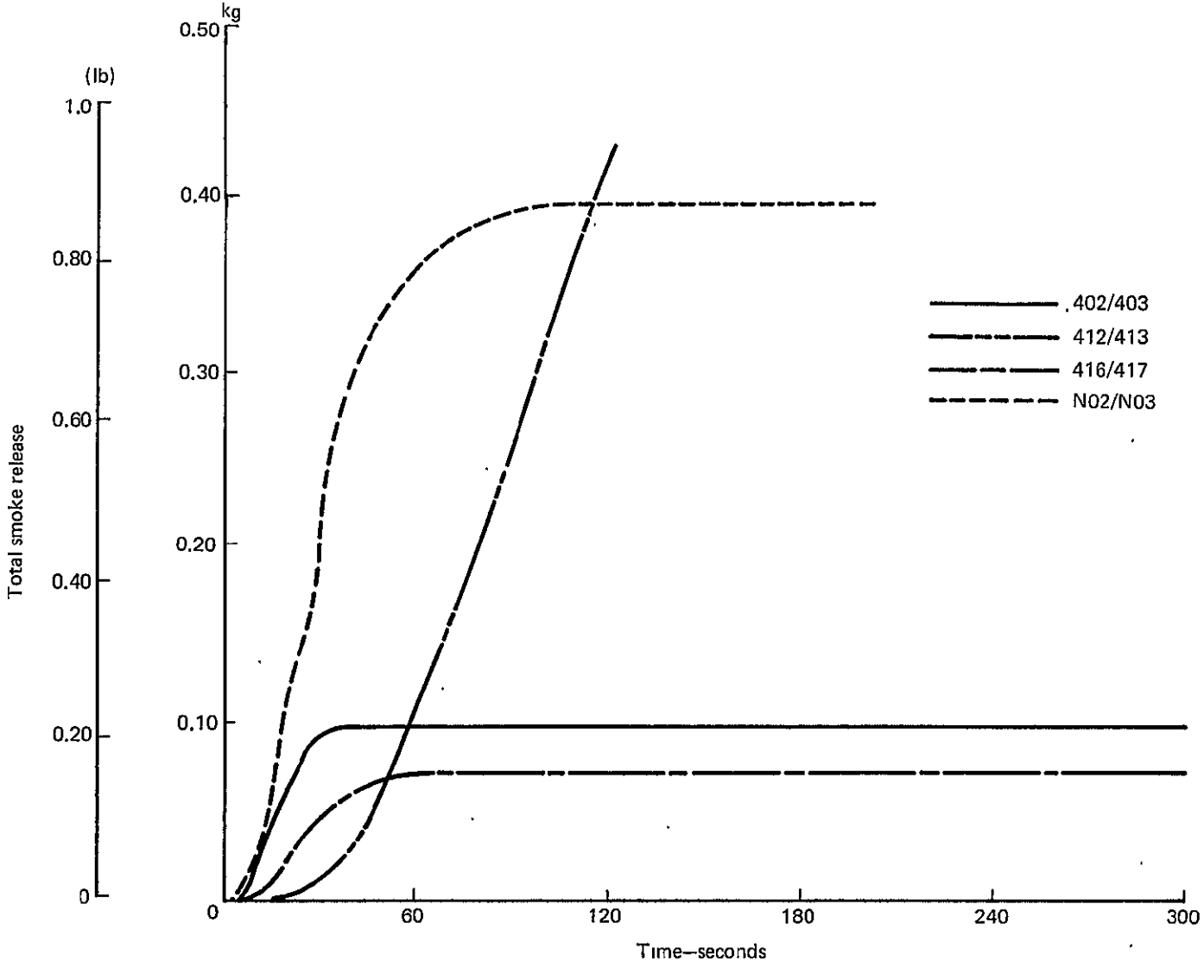

Figure 95.— Smoke Release from Area Summation of OSU Data (Four Heating Rates) for Post-crash Fire Condition

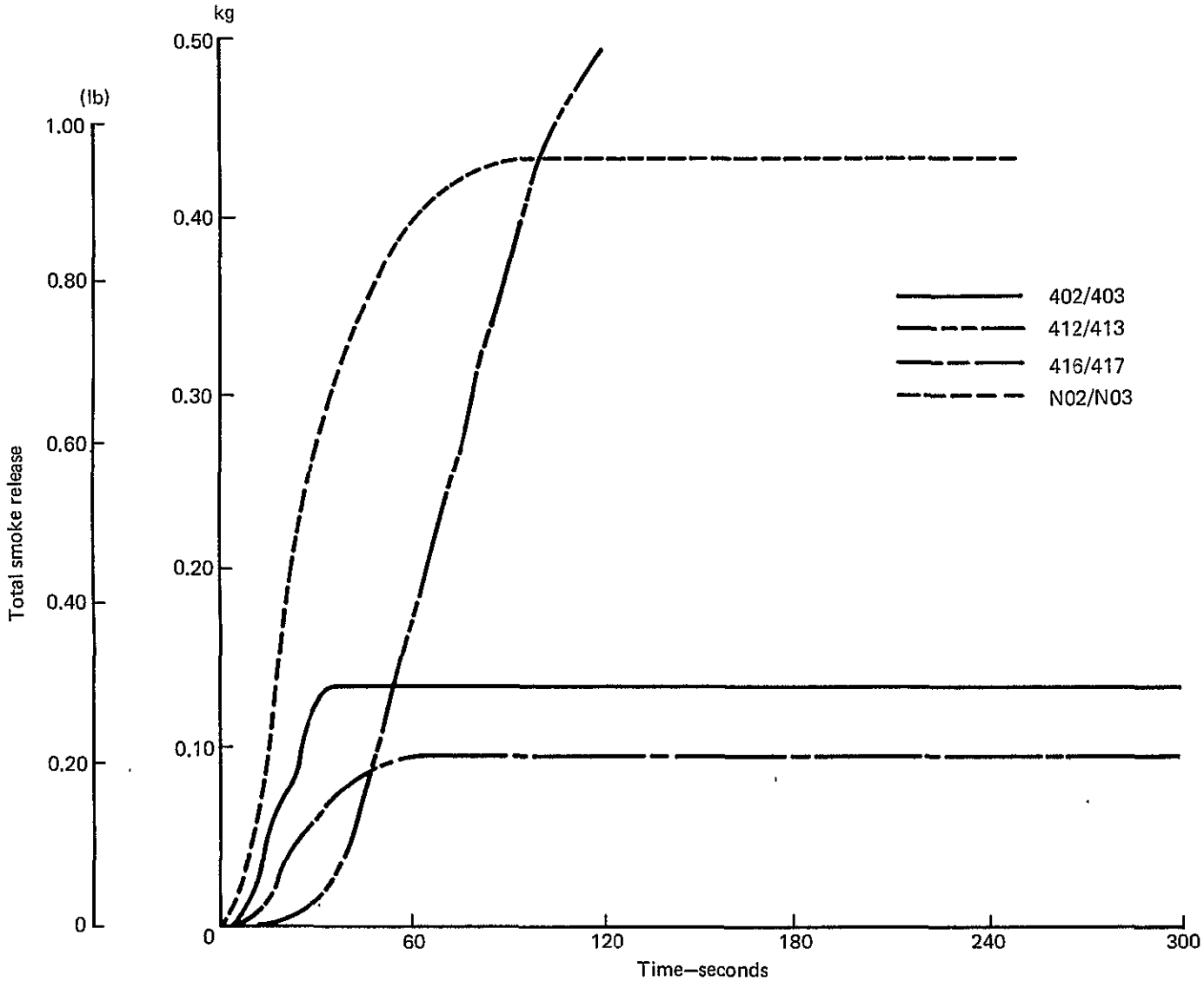

Figure 96.—Smoke Release From Area Summation of OSU Data (Two Heating Rates) for Post-crash Fire Condition

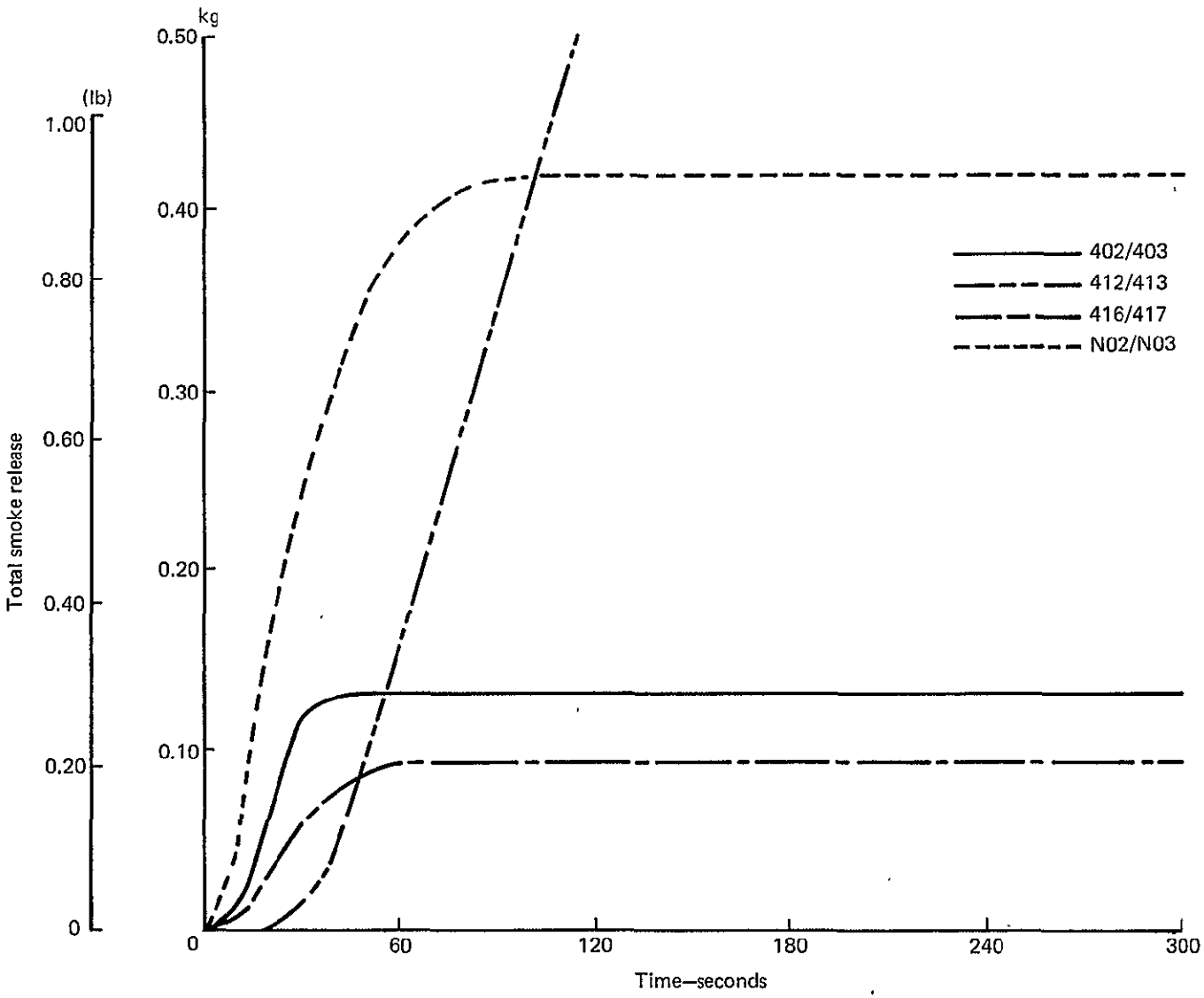

Figure 97.— Smoke Release from Proportional Area Summation of OSU Data (Two Heating Rates) for Post-crash Fire Conditions

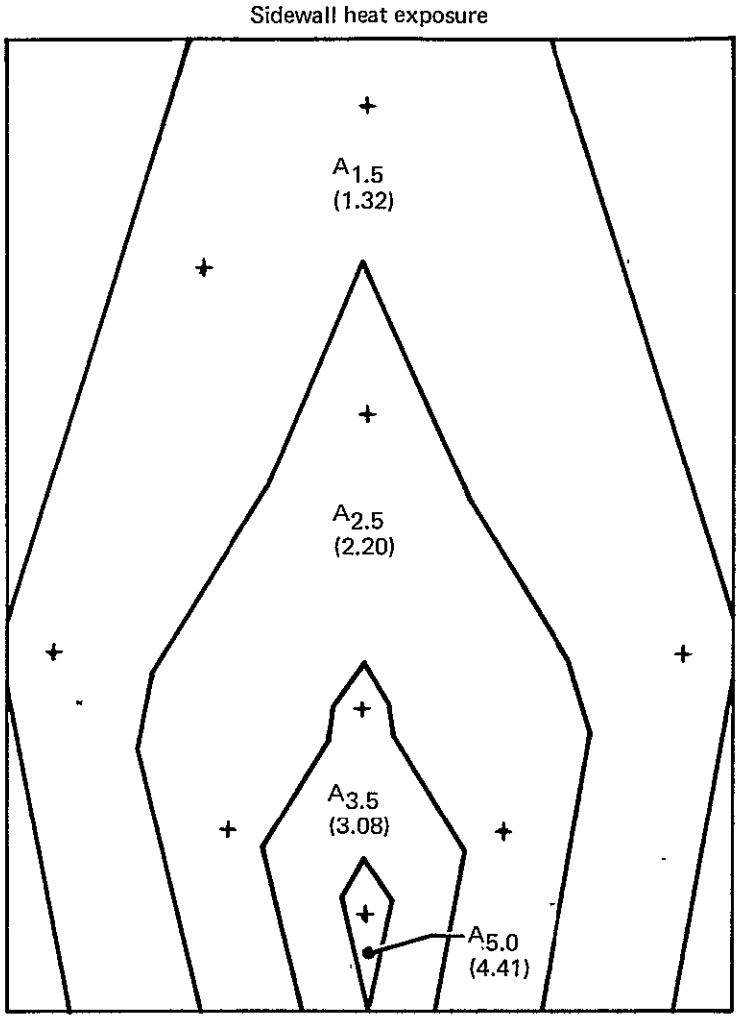

Stage I (0—120 sec)
Correlation to OSU data

Release total = $A_{1.5}$ ($OSU_{1.5}$) +
$A_{2.5}$ ($OSU_{2.5}$) + $A_{3.5}$ ($OSU_{3.5}$)+ $A_{5.0}$ ($OSU_{5.0}$)

OSU — Release at subnoted heating rate in OSU apparatus

$A_{1.5}$ (1.32)* = 8684 (9.35)**
$A_{2.5}$ (2.20) = 6682 (7.19)
$A_{3.5}$ (3.08) = 1135 (1.22)
$A_{5.0}$ (4.41) = 215 (0.23)

* W/cm^2 (Btu/ft^2-sec)
** $cm^2/(ft^2)$

Figure 98.— Correlation Assuming Four Heating Rates for Stage I In-flight Condition

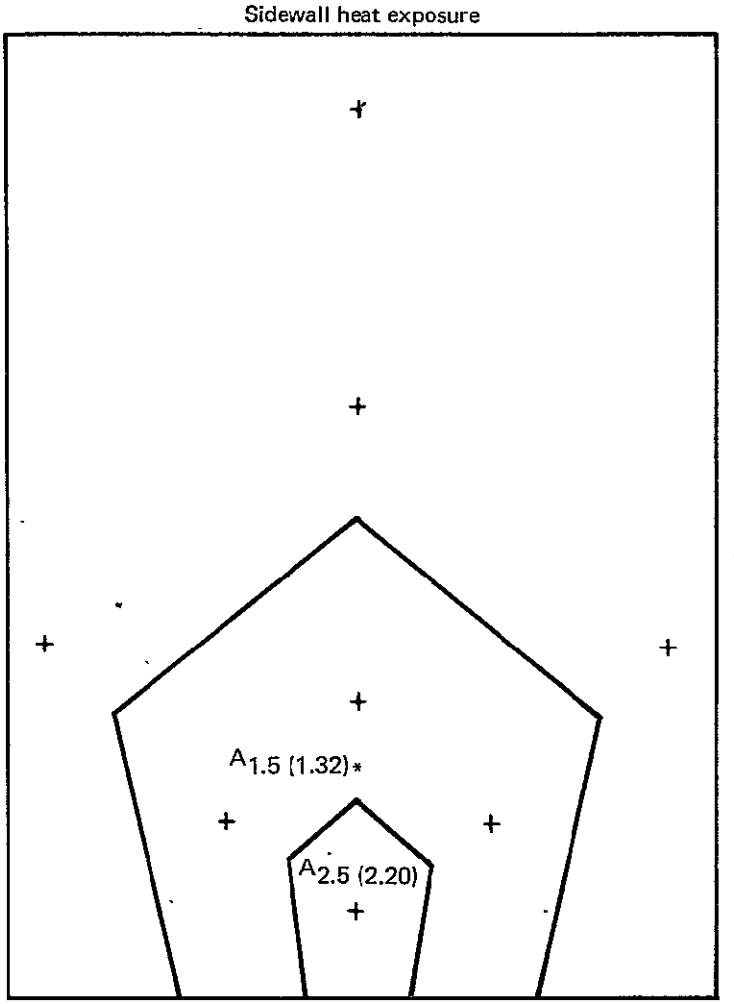

Stage II (120–270 sec)
Correlation to OSU data

Release total = $A_{1.5}$ ($OSU_{1.5}$)+
$A_{2.5}$ ($OSU_{2.5}$)

OSU — Release at subnoted heating rate in OSU apparatus

$A_{1.5}$ (1.32)* = 5723 (6.16)**

$A_{2.5}$ (2.20) = 784 (0.84)

* W/cm^2 (Btu/ft^2–sec)

** cm^2 (ft^2)

Figure 99.— Correlation Assuming Two Heating Rates for Stage II In-flight Condition

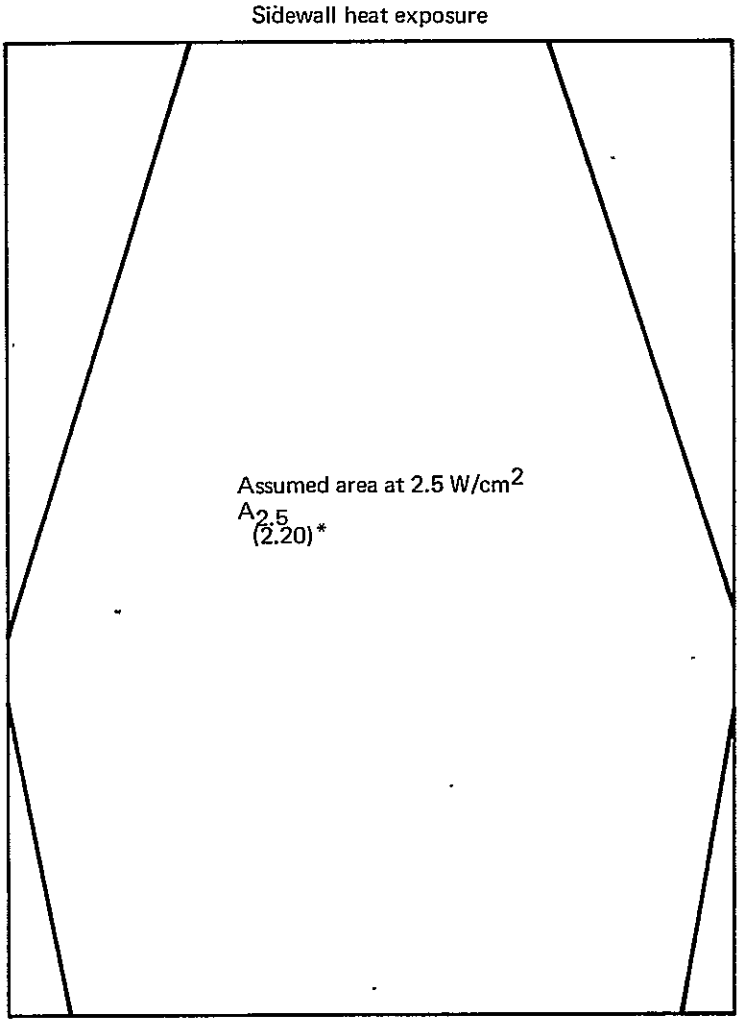

Stage I (0—120 sec)
Correlation to OSU data
Release total = $A_{2.5}$ ($OSU_{2.5}$)

$OSU_{2.5}$ = Release at subnoted heating rate in OSU apparatus

$A_{2.5}$ (2.20)* = 16716 (17.99)**

* W/cm^2 (Btu/ft^2—sec)

** cm^2 (ft^2)

Figure 100.—Correlation Assuming One Heating Rate for Stage I In-flight Condition

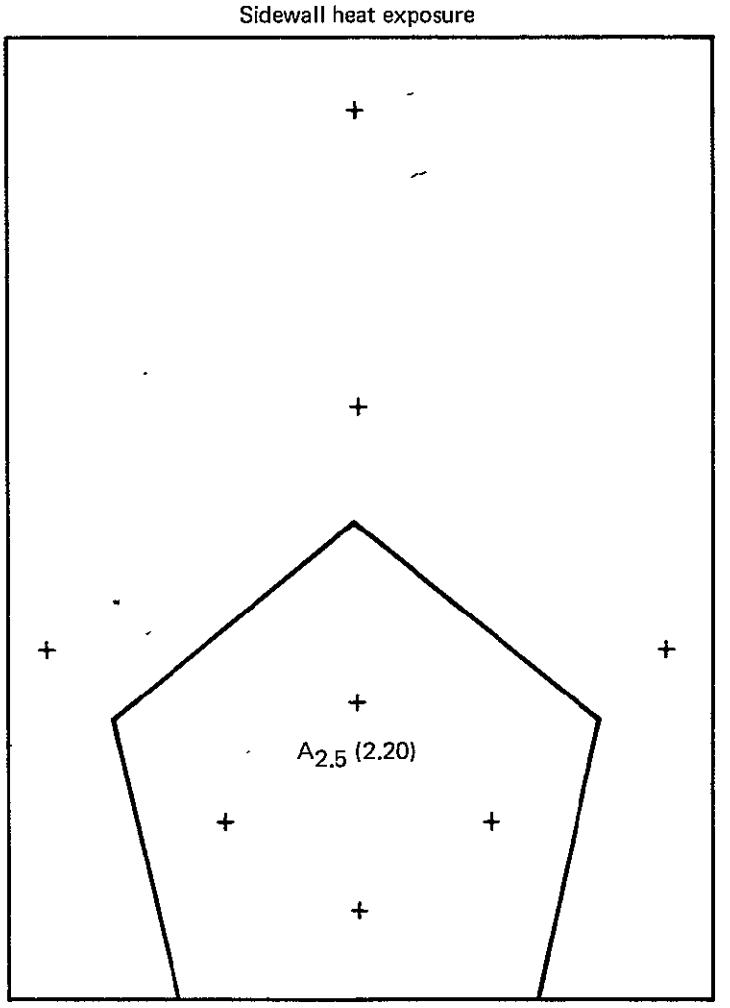

Stage II (120–270 sec)
Correlation to OSU data

Release = $A_{2.5}$ ($OSU_{2.5}$)

OSU – Release at subnoted heating rate in OSU apparatus

$A_{2.5}$ (2.20)* = 6507 (7.00)**

* W/cm^2 (Btu/ft^2–sec)

** cm^2 (ft^2)

Figure 101.—Correlation Assuming One Heating Rate for Stage II In-flight Condition

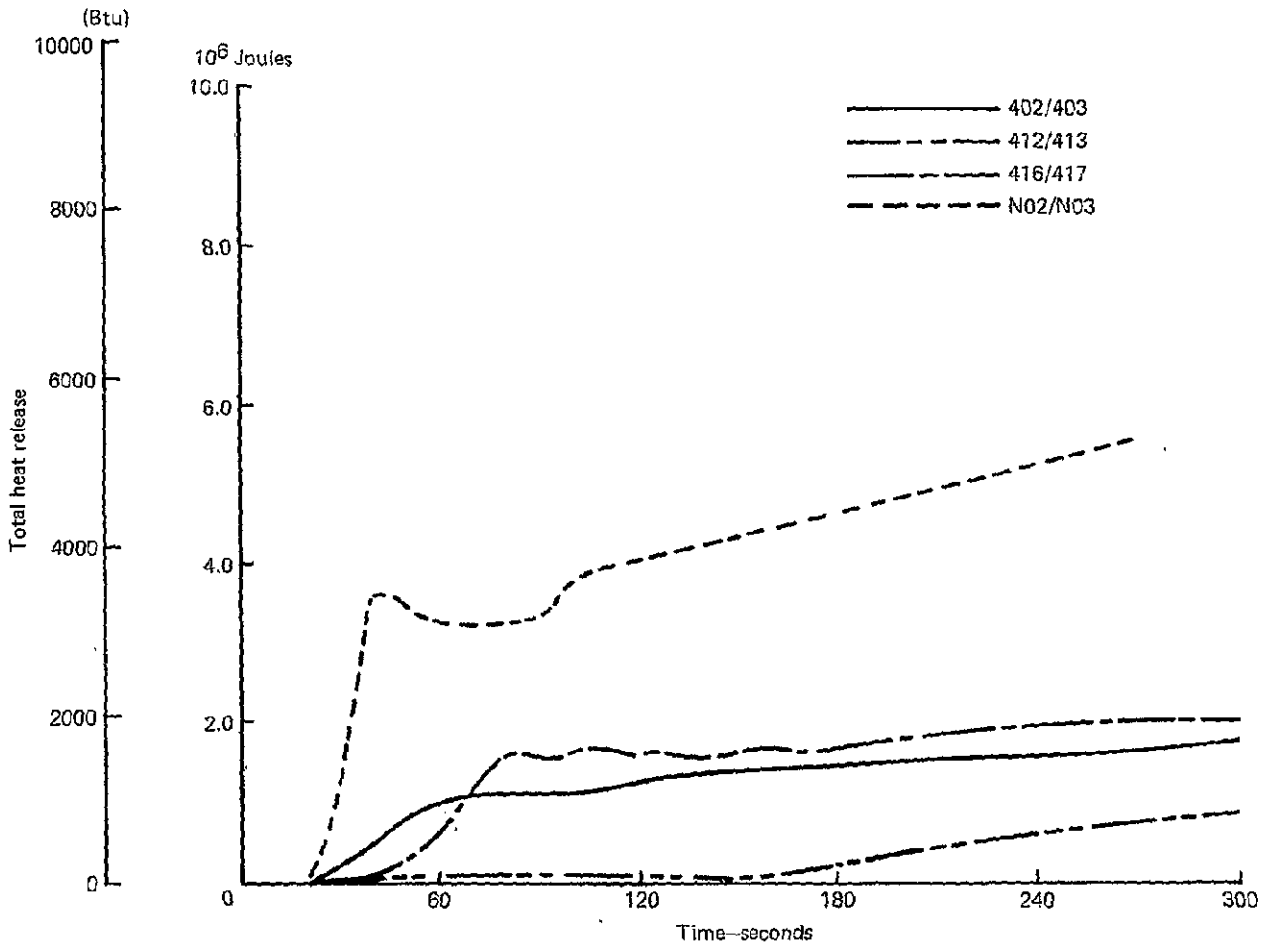

Figure 102.—Heat Release from Simulated In-flight Fire Source Tests

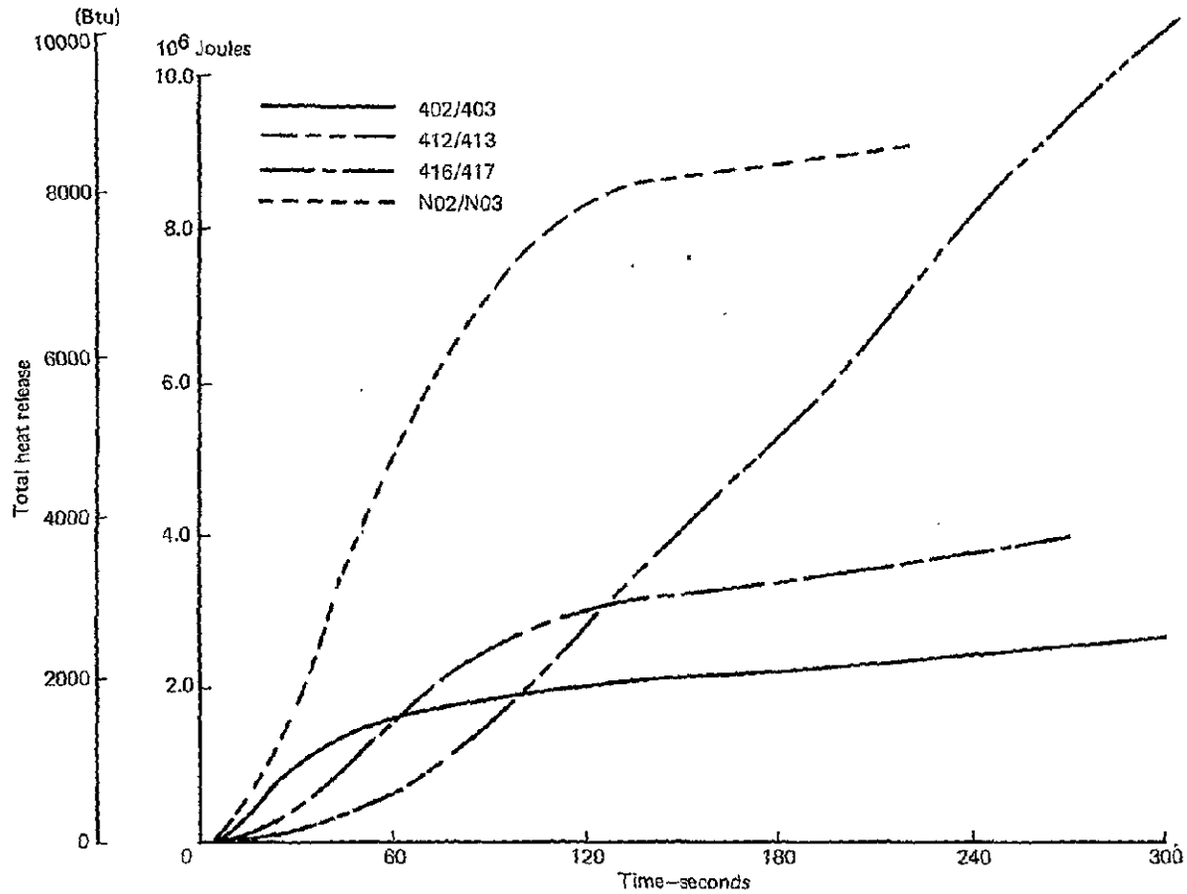

Figure 103.—Heat Release from Area Summation of OSU Data (Four Heating Rates) for In-flight Fire Conditions

Figure 104.—Heat Release from Area Summation of OSU Data (One Heating Rate) for In-flight Fire Conditions

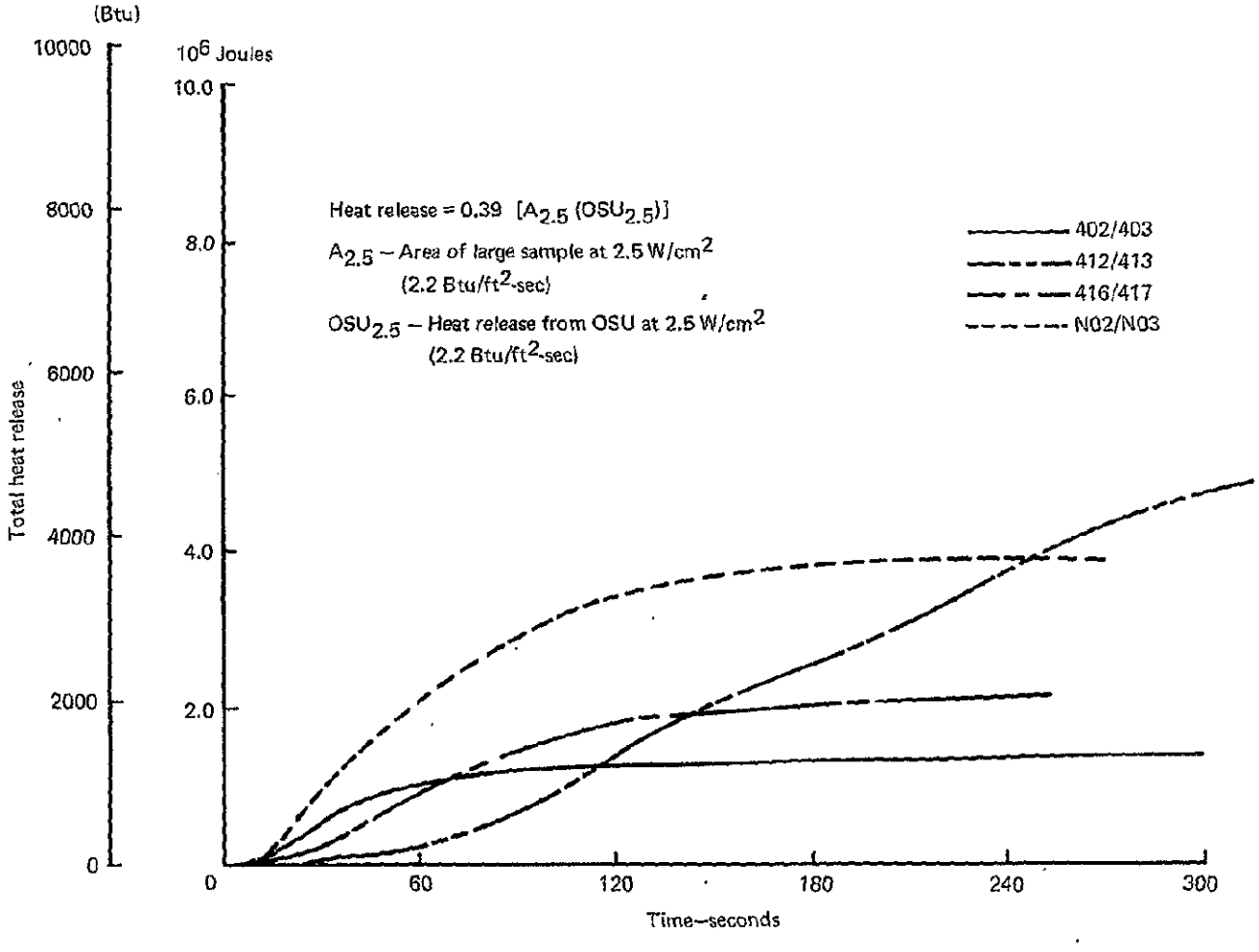

Figure 105.–Heat Release from Proportional Area Summation of OSU Data (One Heating Rate) from In-flight Fire Conditions

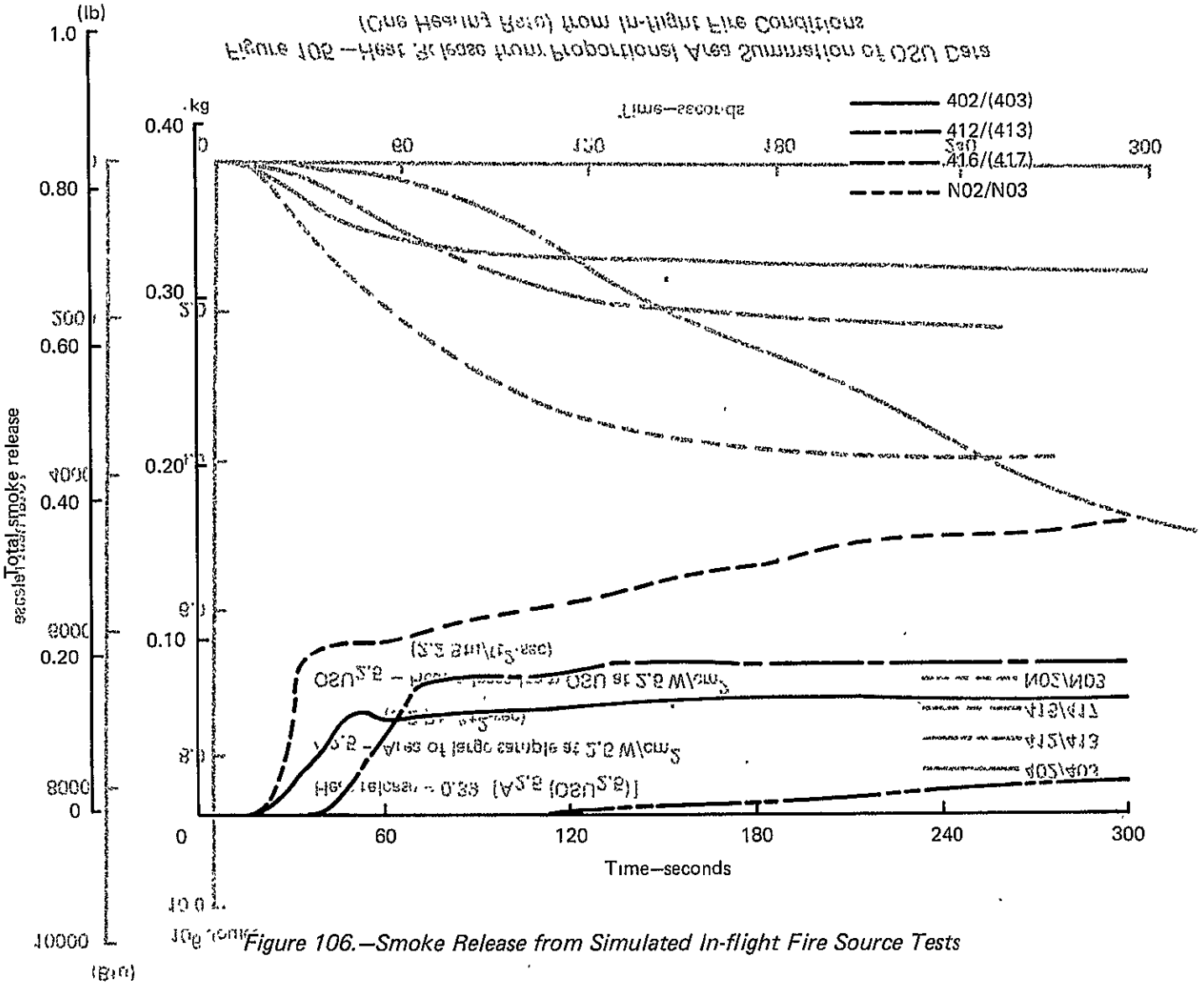

Figure 106.—Smoke Release from Simulated In-flight Fire Source Tests

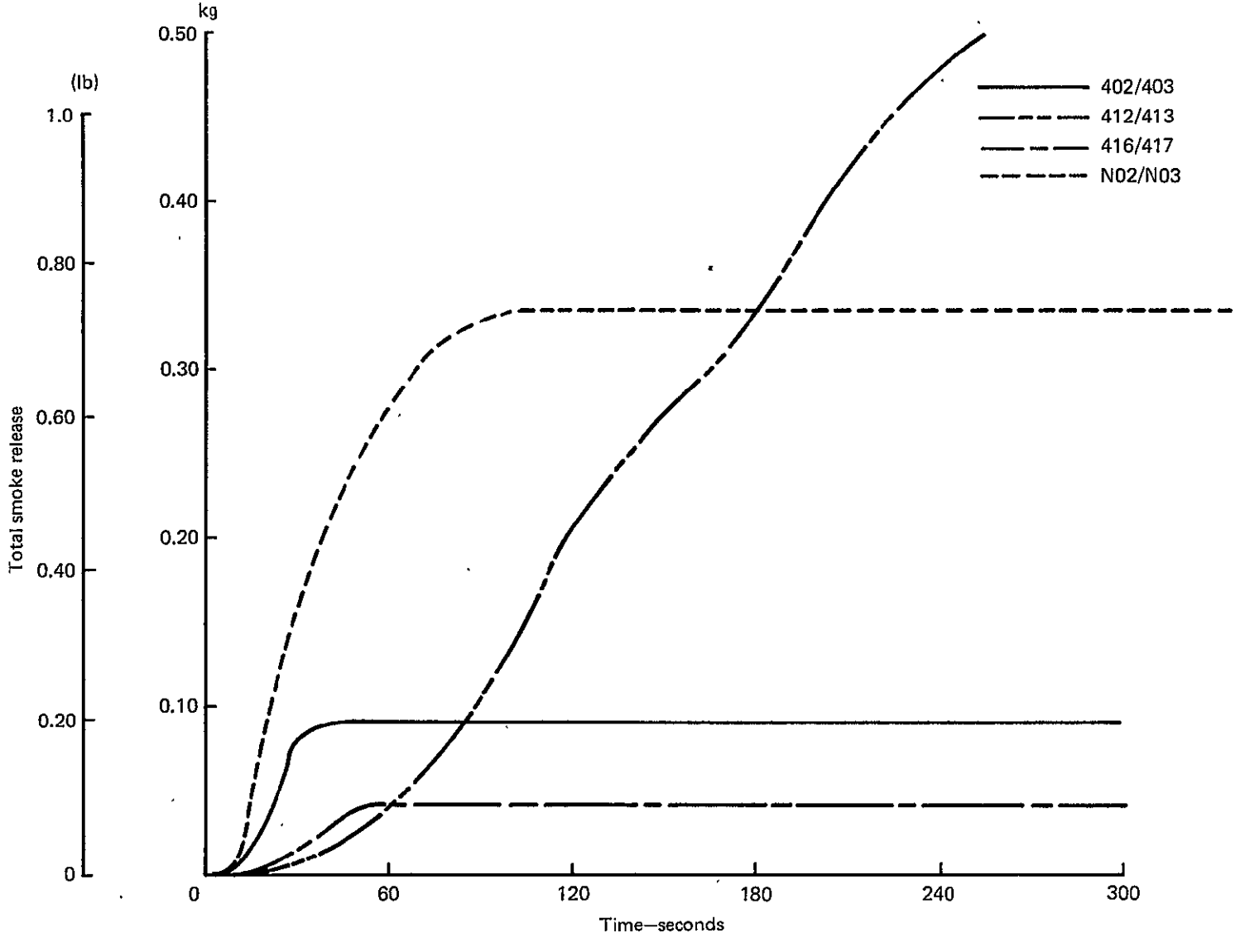

Figure 107.—Smoke Release from Area Summation of OSU Data (Four Heating Rates) for In-flight Fire Condition

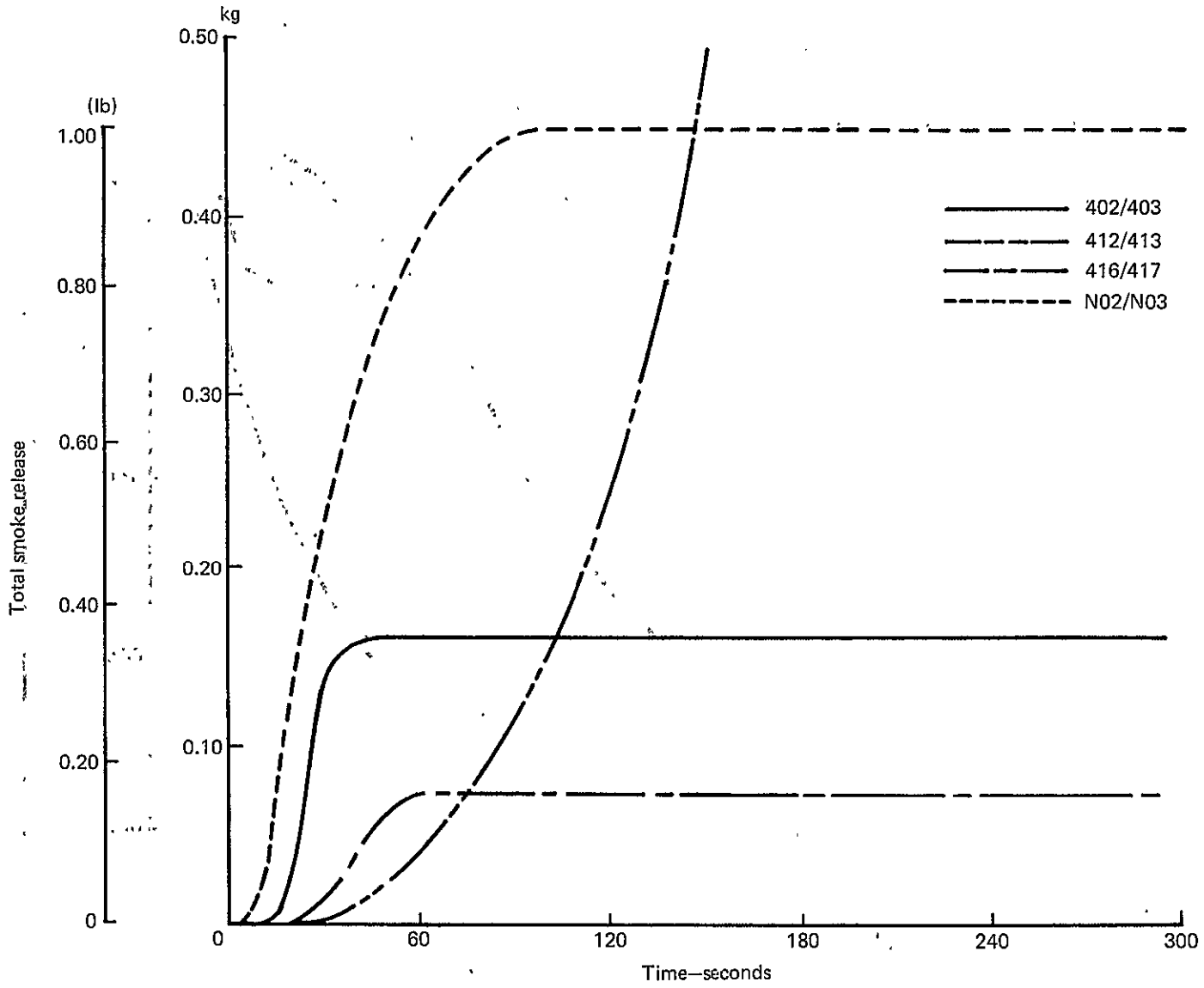

Figure 108.—Smoke Release from Area Summation of OSU Data (One Heating Rate) for In-flight Fire Condition

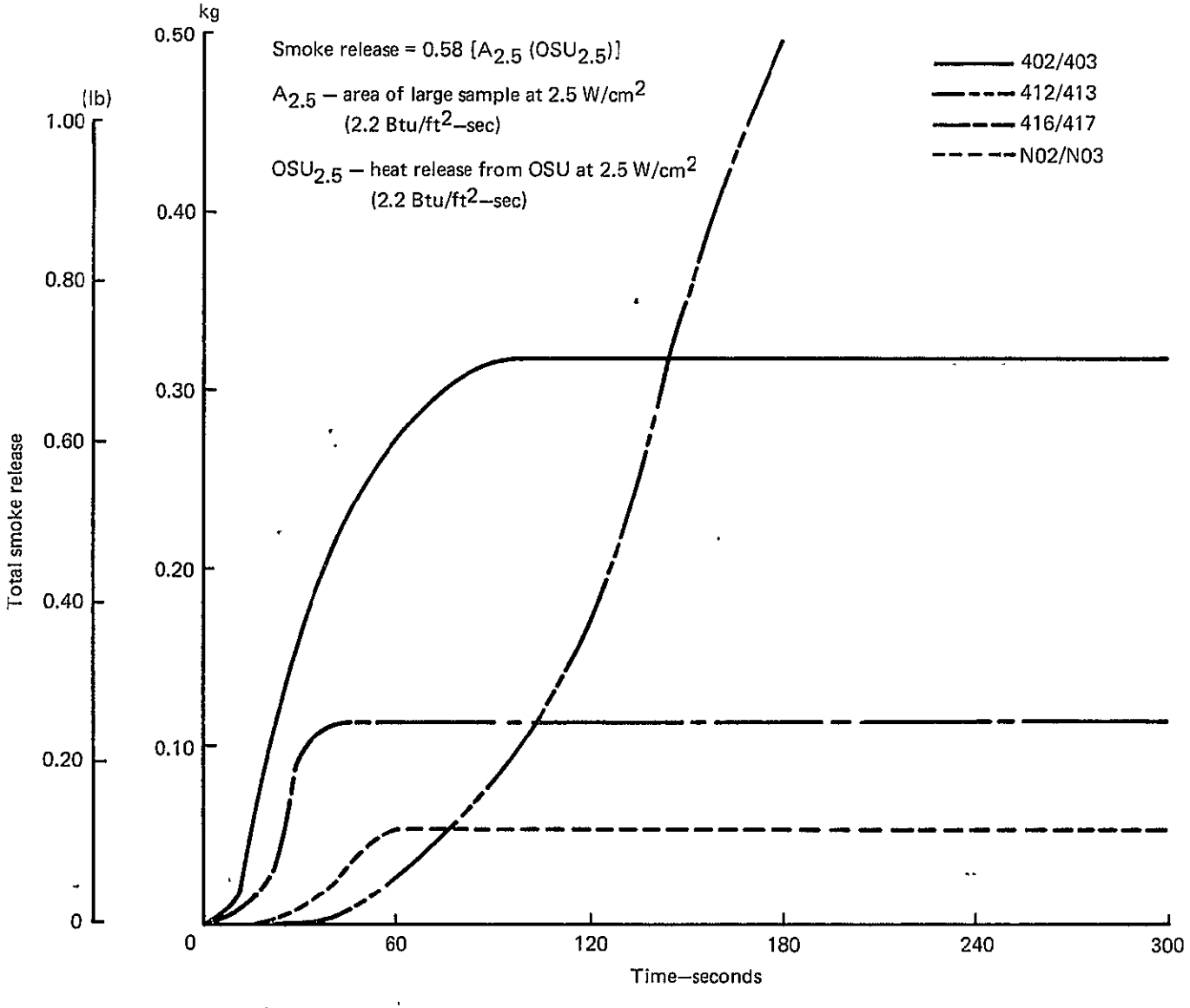

Figure 109.—Smoke Release from Proportional Area Summation of OSU Data (One Heating Rate) from In-flight Fire Conditions

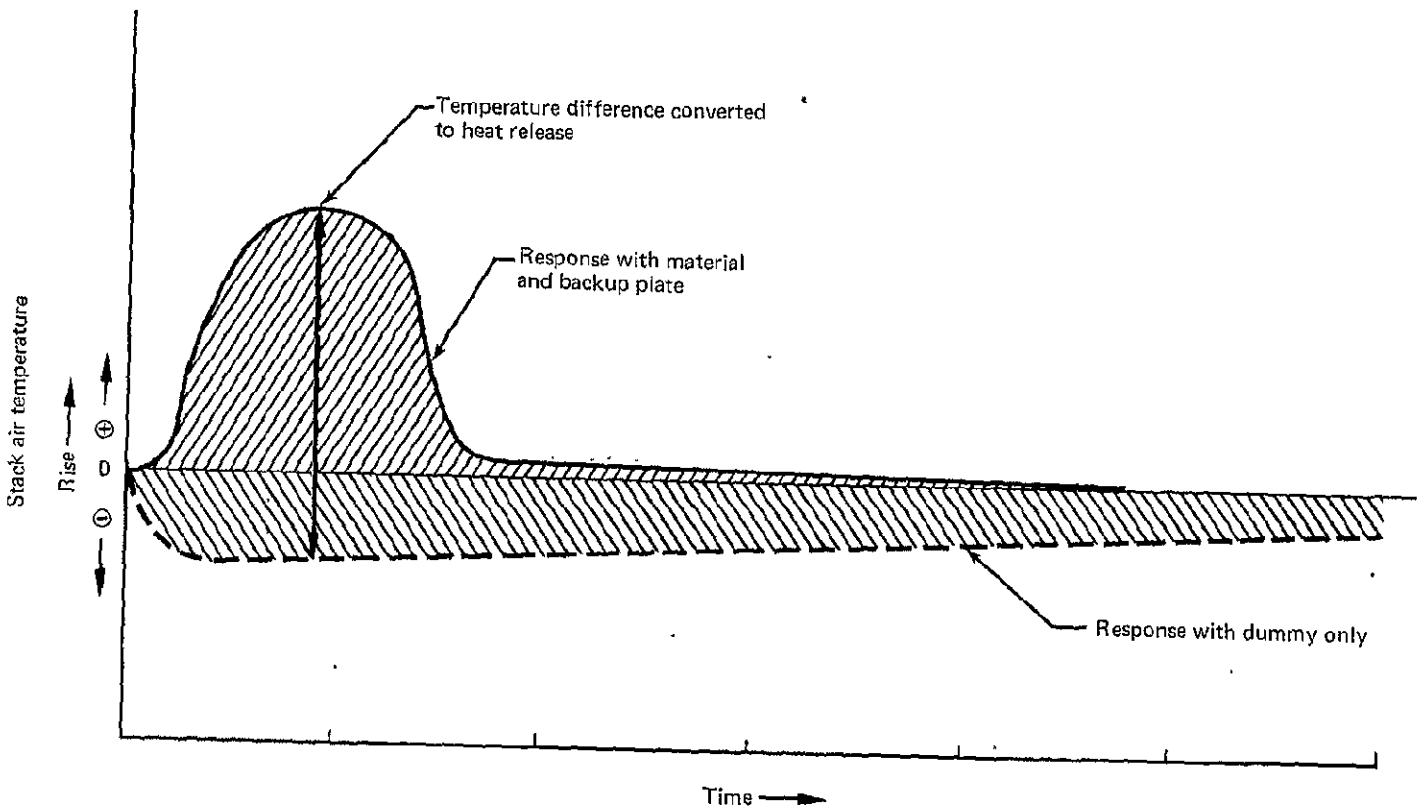

Figure 110.–Method of Heat Release Calculation from OSU

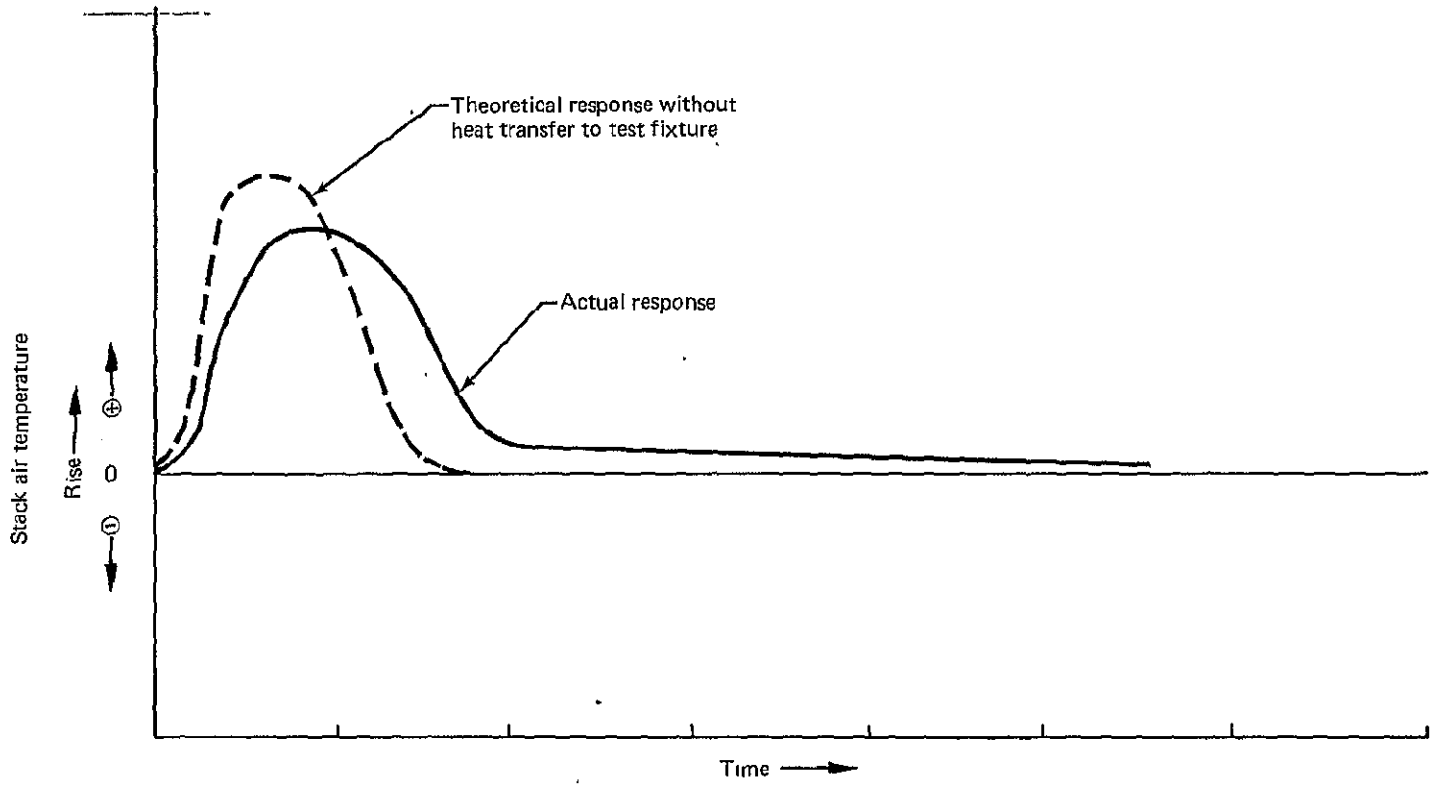

Figure 111.—Thermal Lag Characteristics of Heat Release Data from OSU Apparatus

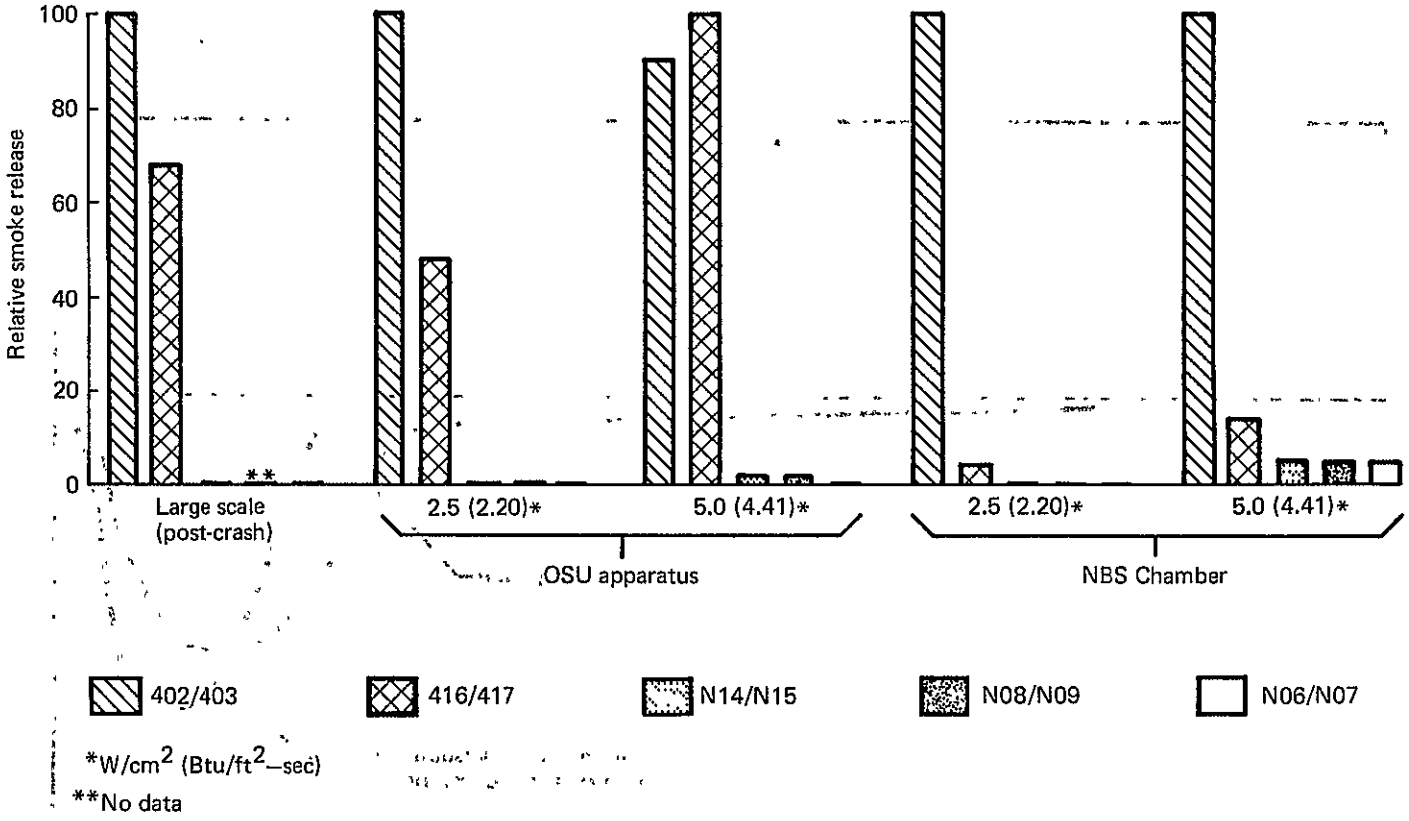

Figure 112.—Relative Smoke Release by Panel Materials at 90 Seconds

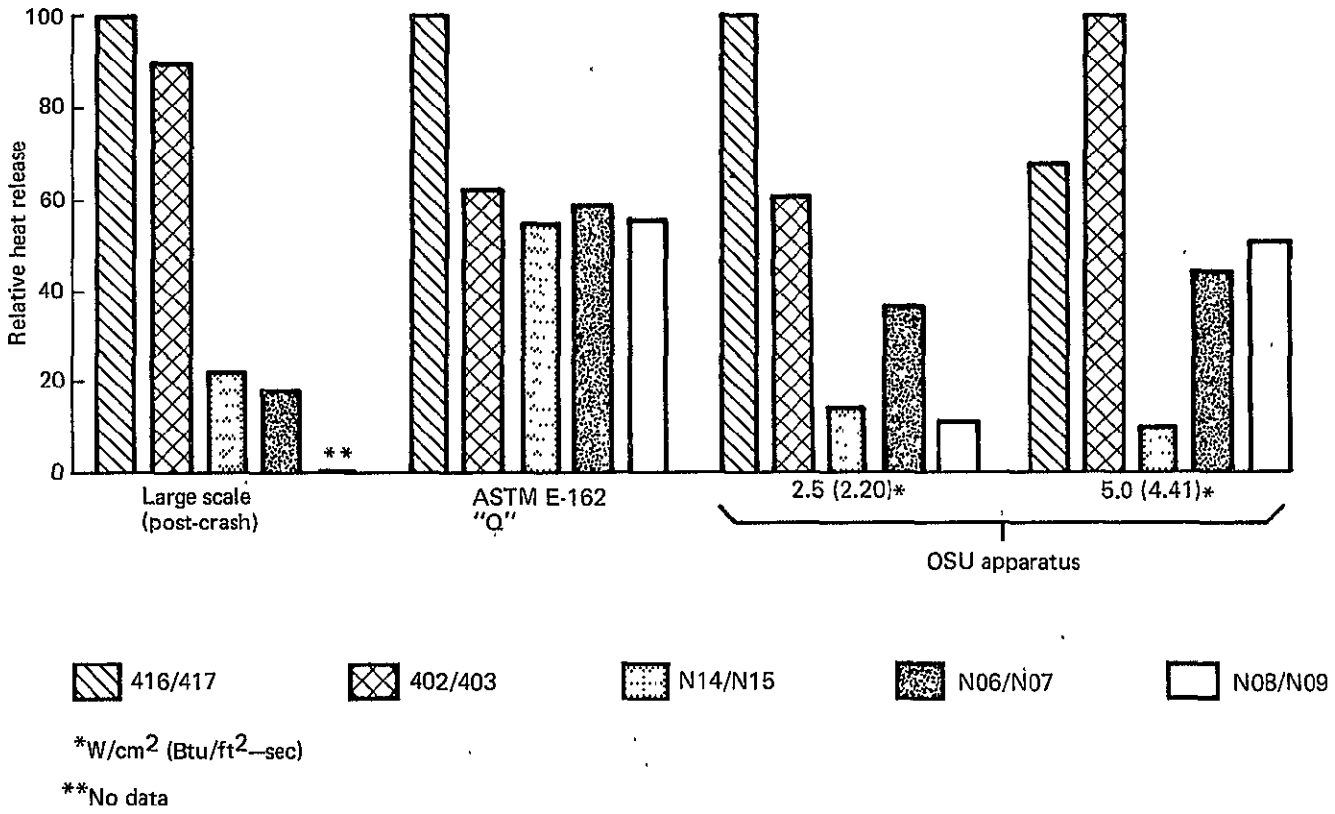

Figure 113.—Relative Heat Release by Panel Materials at 215 Seconds

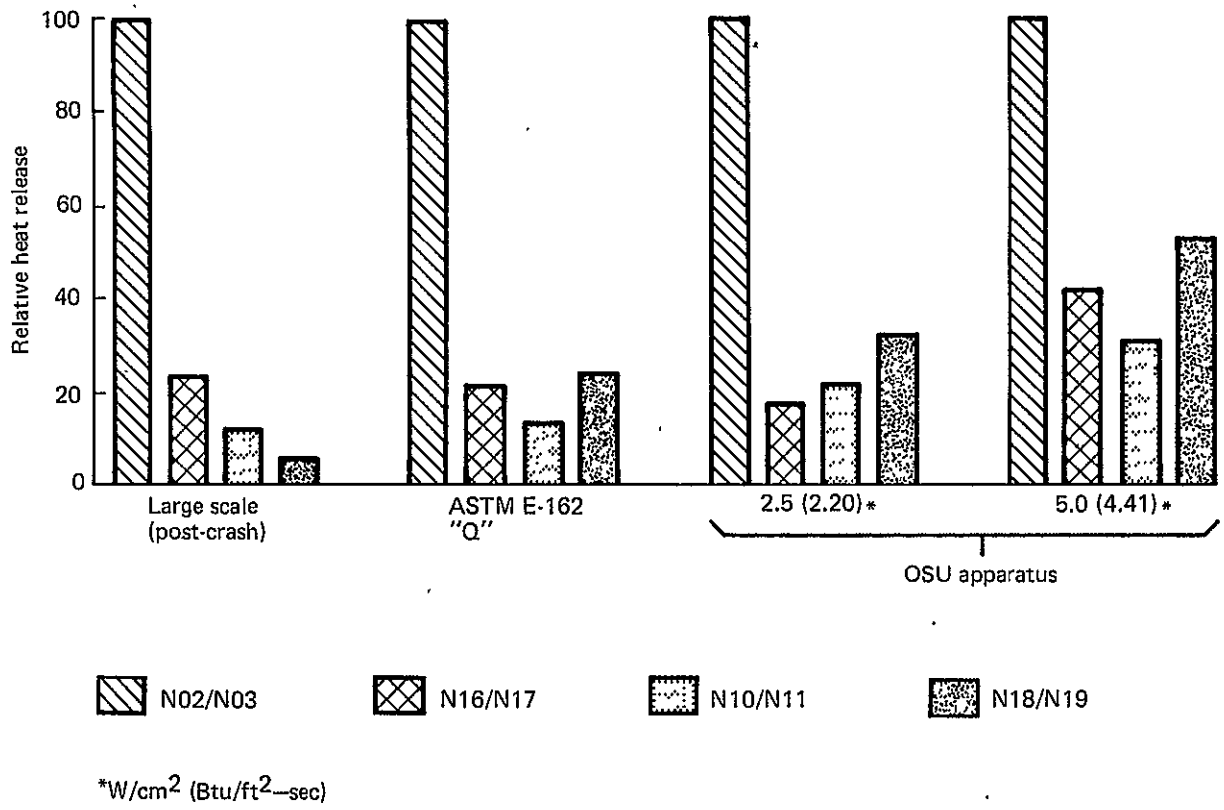

Figure 114.—Relative Heat Release by Laminates and Covering Material at 215 Seconds

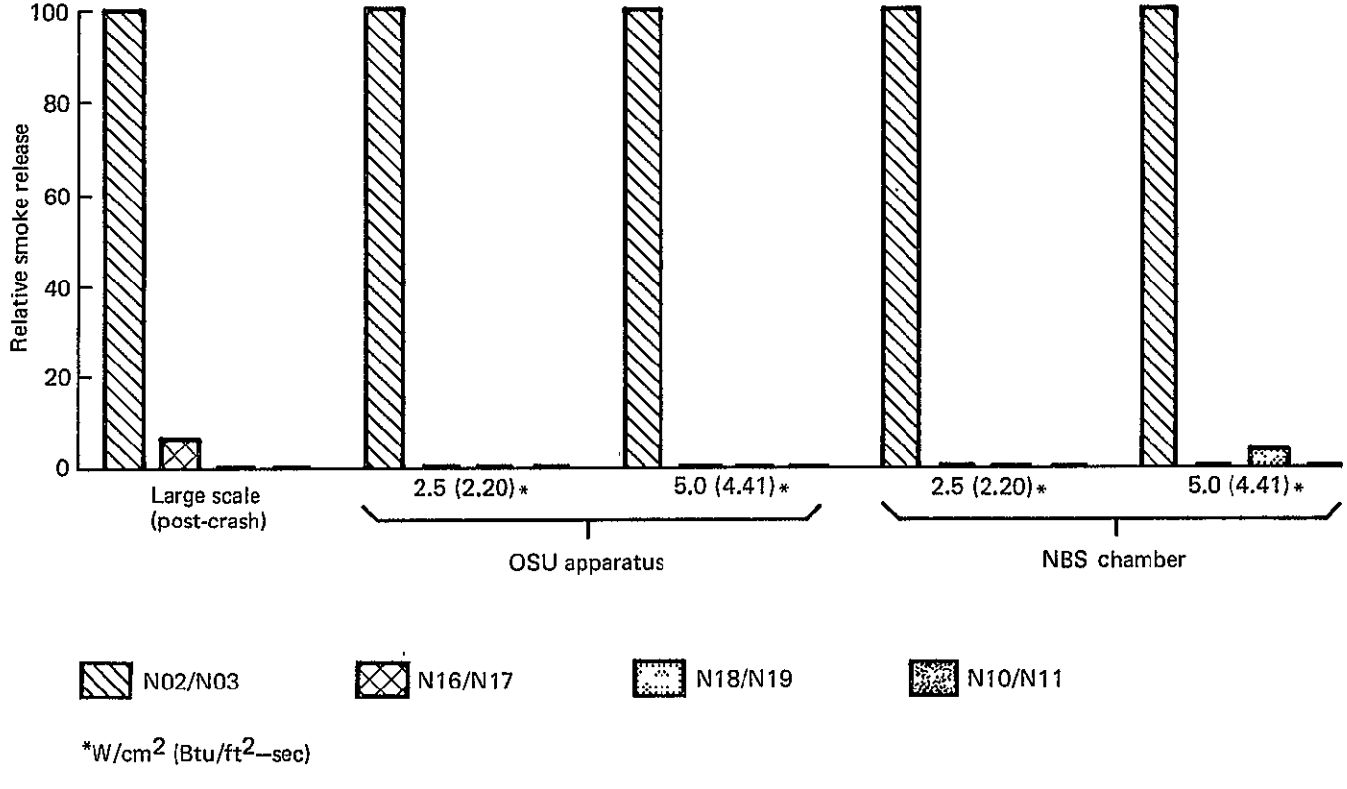

Figure 115.—Relative Smoke Release by Laminates and Covering Material at 90 Seconds

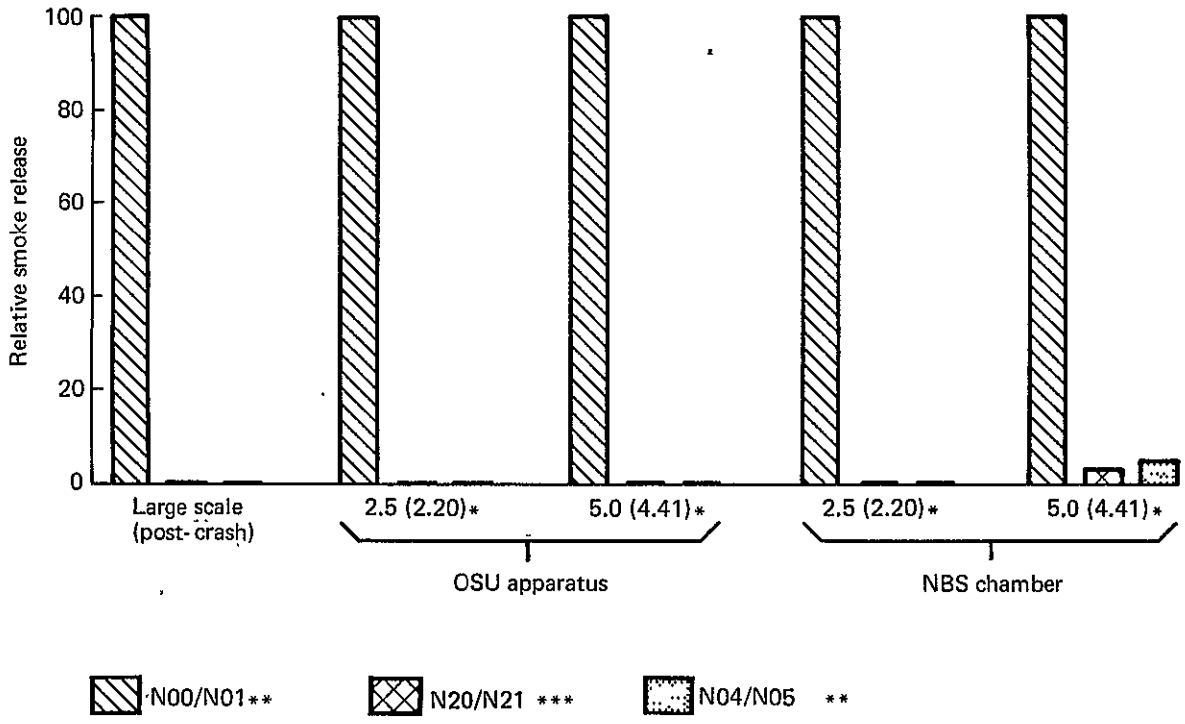

*W/cm^2 (Btu/ft^2–sec)

** Large scale samples 61 x 61 x 5.1 cm (24 x 24 x 2 in.) lab samples 2.54 cm (1 in.) thick

***Large scale samples 114.3 x 152.4 x 7.6 cm (45 x 60 x 3 in.) lab samples 2.54 cm (1 in.) thick

Figure 116.—Relative Smoke Release by Foams at 90 Seconds

C-4

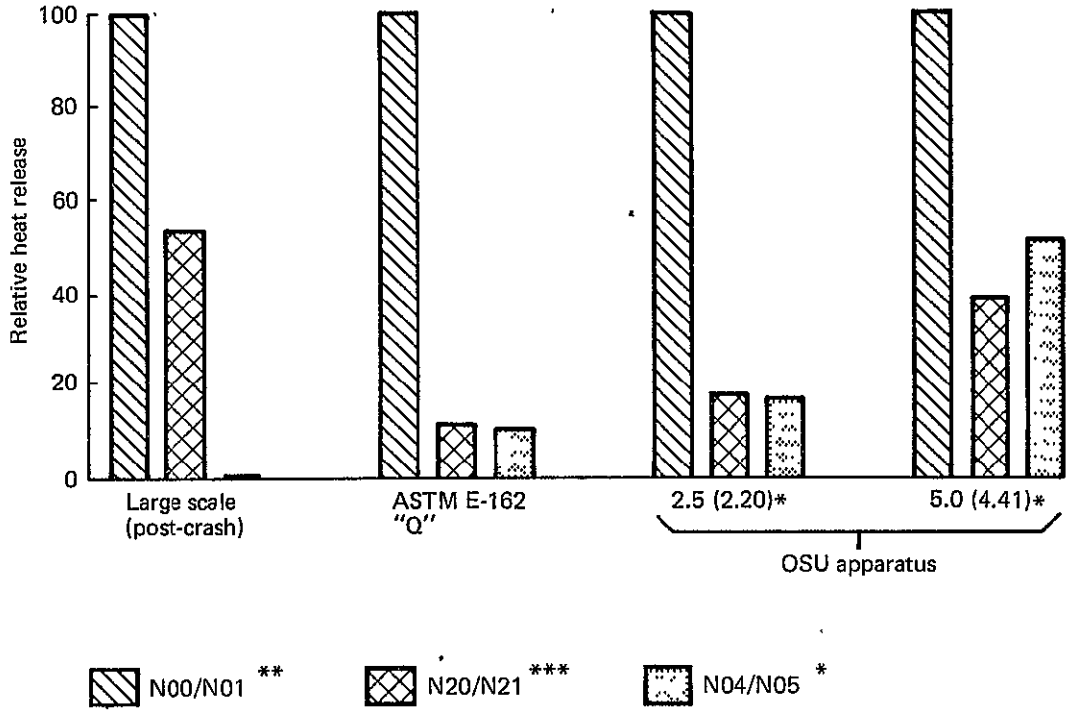

* W/cm^2 (Btu/ft^2–sec)

** Large scale sample 61 x 61 x 5.1 cm (24 x 24 x 2 in.); lab samples 2.54 cm (1 in.) thick

*** Large scale sample 114.3 x 152.4 x 7.6 cm (45 x 60 x 3 in.) lab samples 2.54 cm (1 in.) thick

Figure 117.—Relative Heat Release by Foams at 215 Seconds

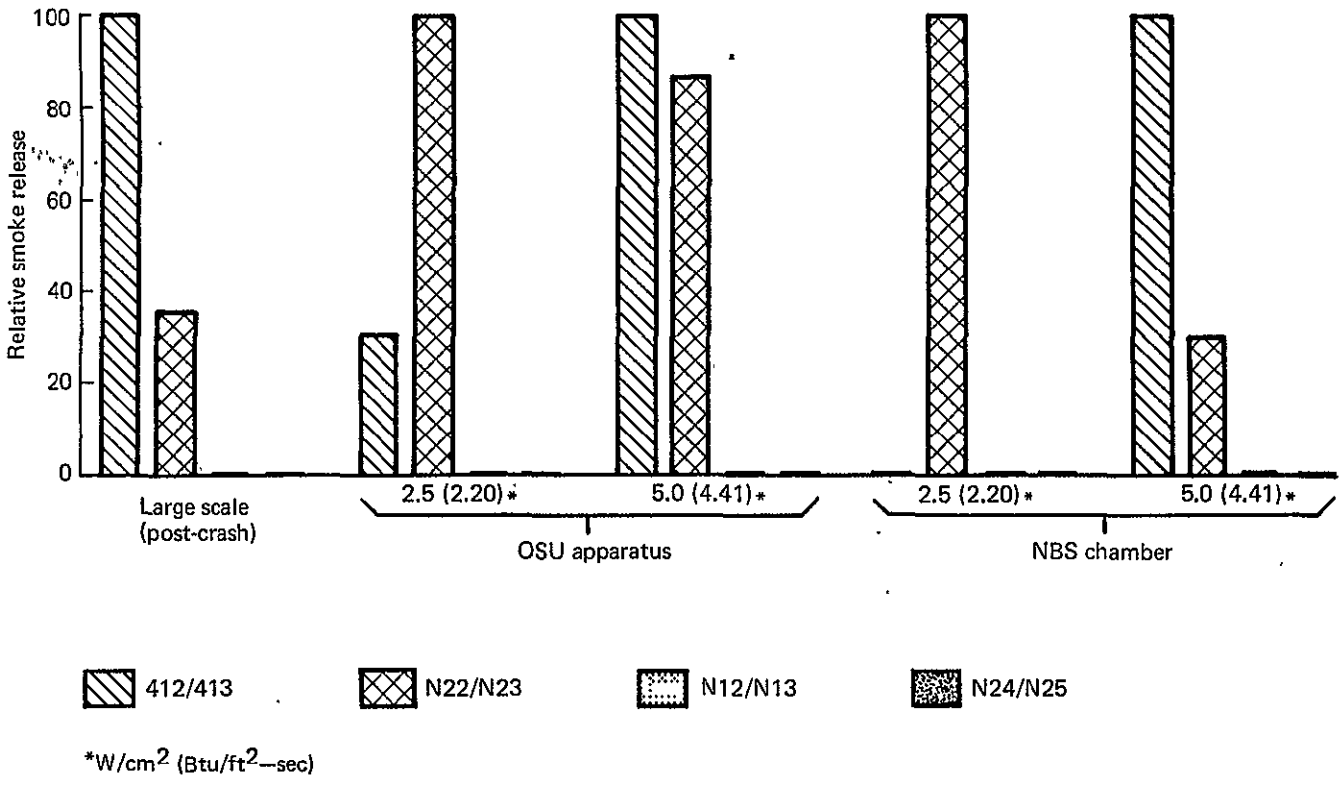

Figure 118.—Relative Smoke Release by Thermoplastics and Thermoplastic Replacements at 90 Seconds

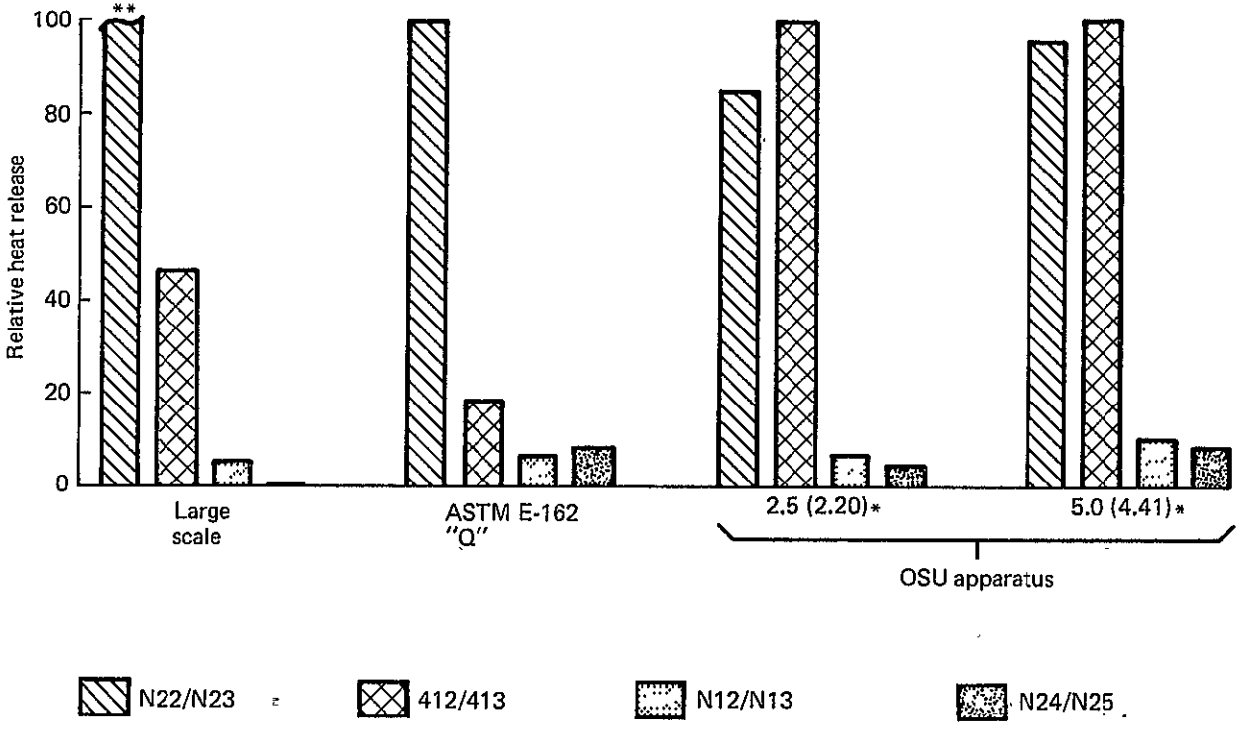

*W/cm^2 (Btu/ft^2–sec)

**Test aborted at 165 seconds to limit fixture damage; 165 second data used for this bar

Figure 119.—Relative Heat Release by Thermoplastics and Thermoplastic Replacements at 215 Seconds

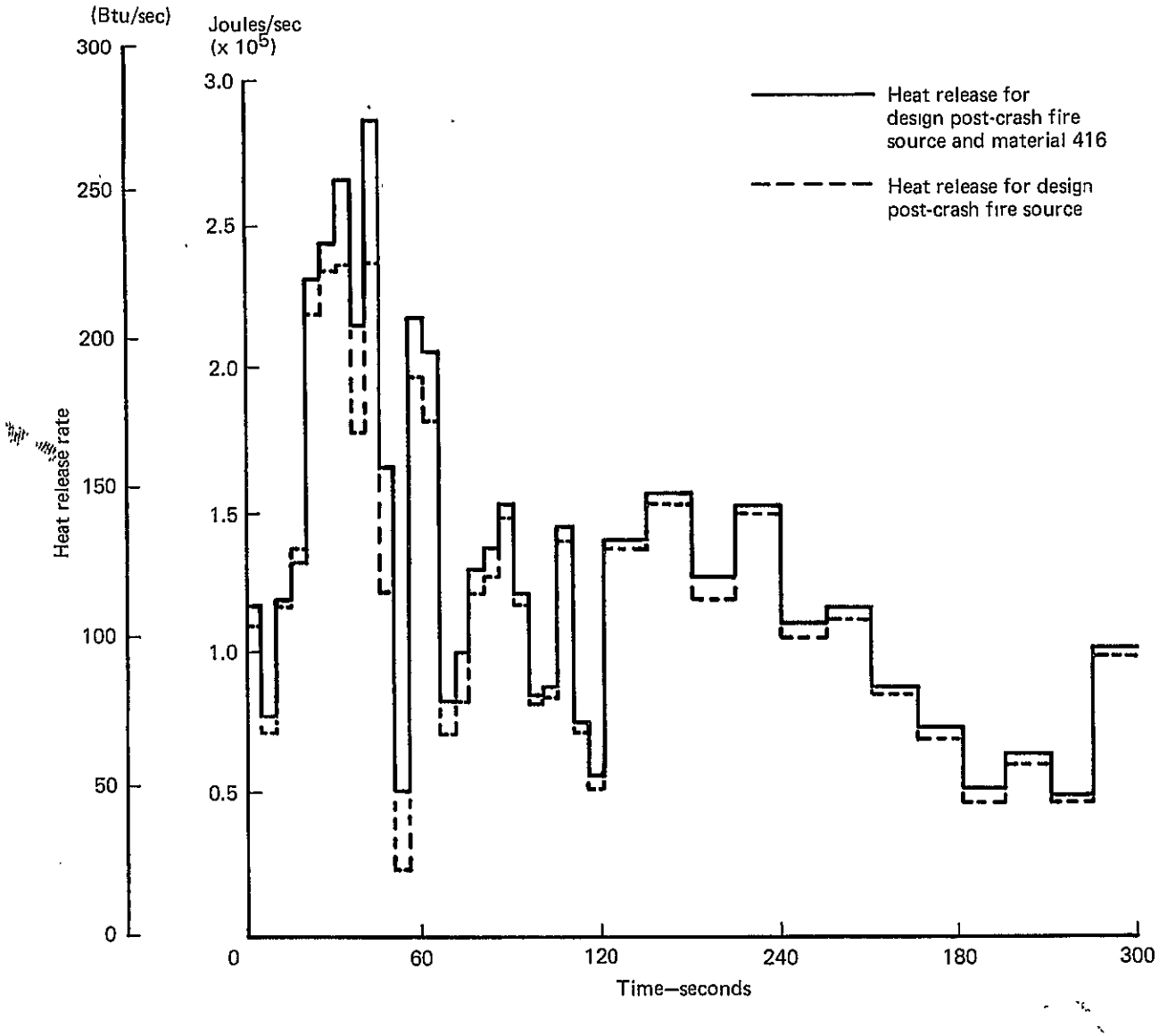

Figure 120.—Combining of Heat Release Rates for the Design Post-crash Fire Source and Material 416

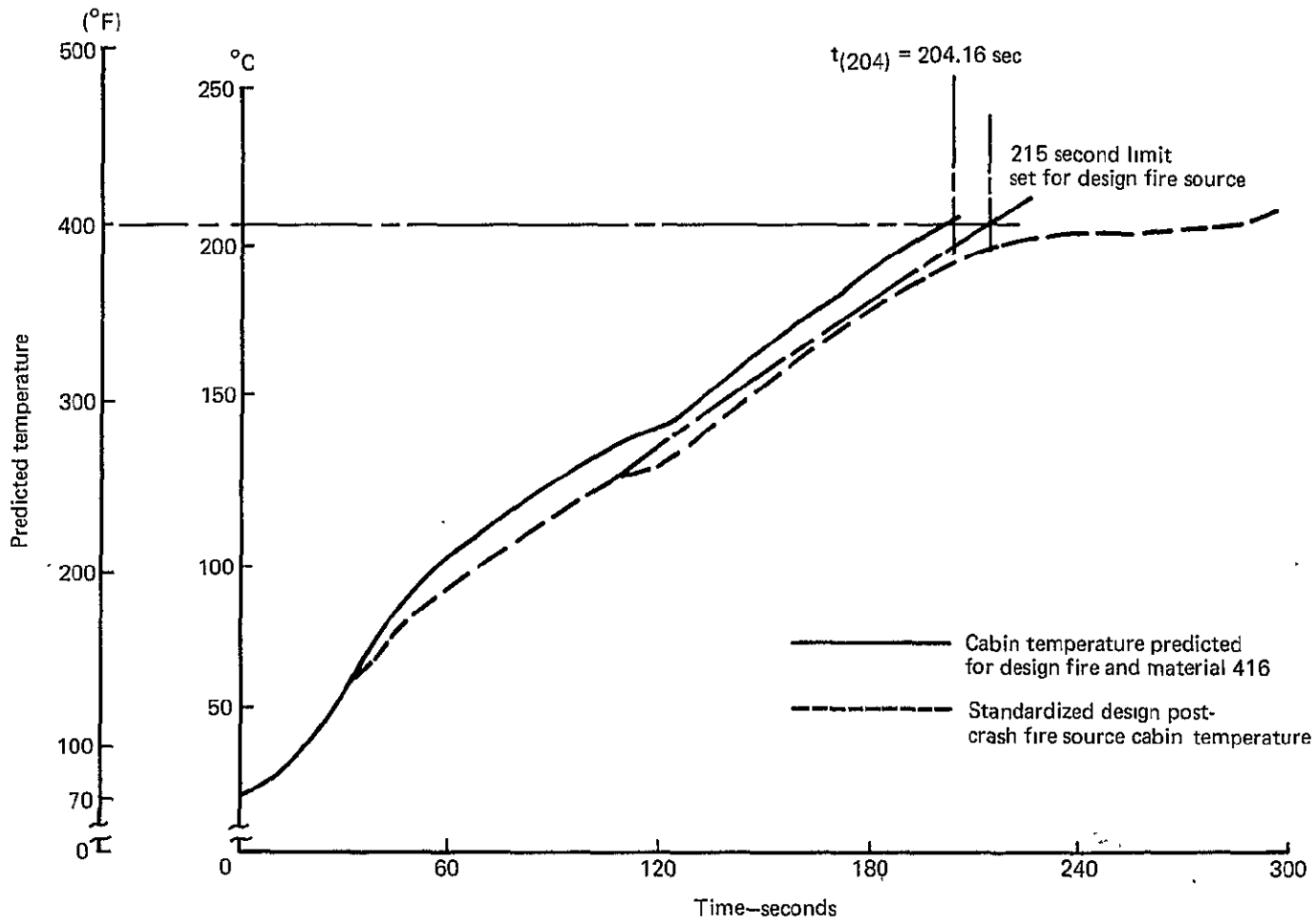

Figure 121.—Determining $t_{(204\,°C)}$ for Material 416 from Predicted Cabin Air Temperature

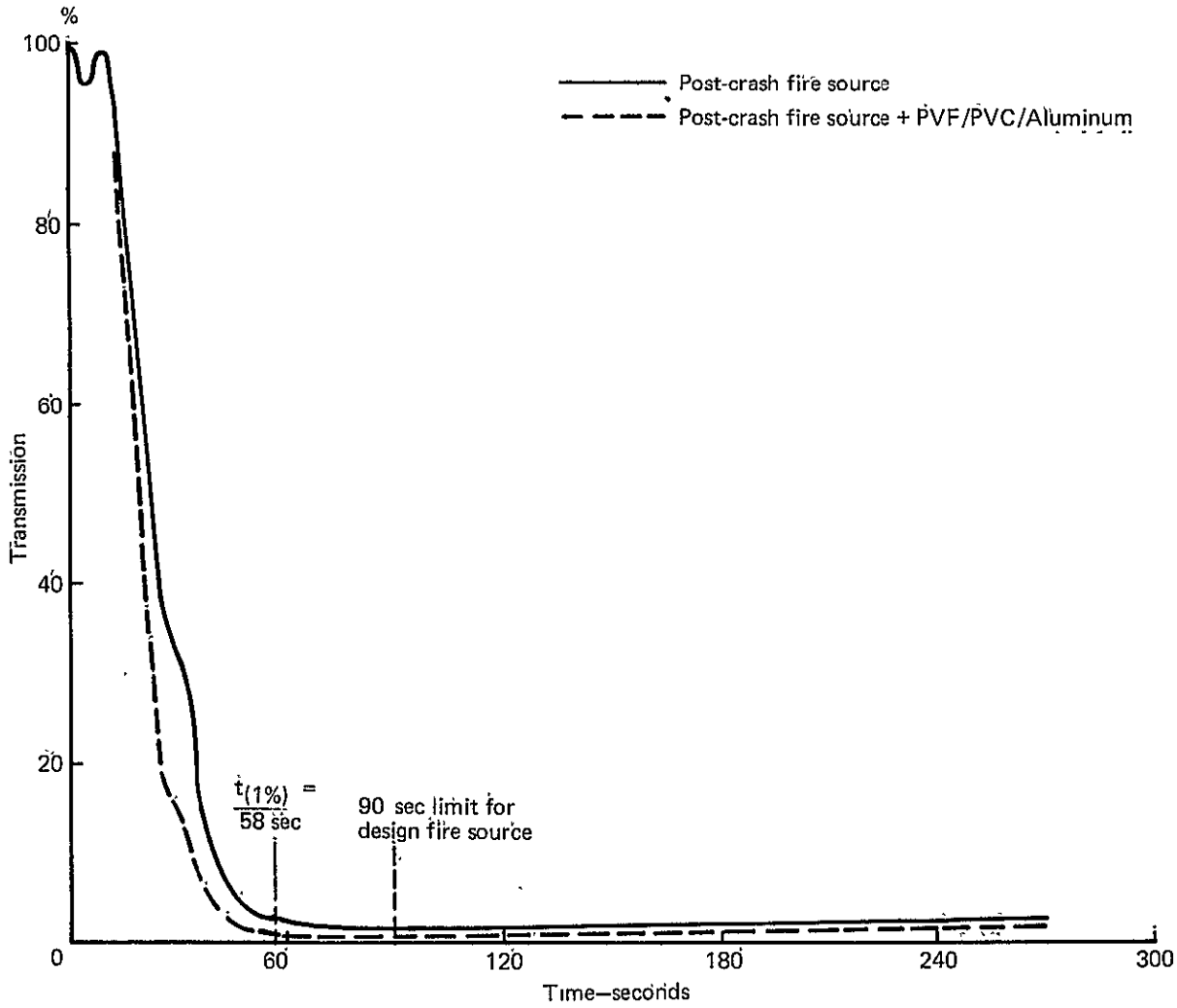

Figure 122.—Determining $t_{(1\%)}$ for Material 416 from Predicted Cabin Light Transmission